

Dissertation zur Erlangung des Doktorgrades
Fakultät für Biologie
der Ludwig-Maximilians-Universität München

Notch2 signalling in B cell activation, immune response and lymphomagenesis



vorgelegt von
Stefanie Ehrenberg

August 2014

Erklärung

Diese Dissertation wurde von Mai 2010 bis August 2014 in der Abteilung für Genvektoren des Helmholtz Zentrums München in der Arbeitsgruppe von PD Dr. Ursula Zimmer-Strobl erstellt und von PD Dr. Josef Mautner betreut.

Eidesstattliche Versicherung

Ich, Stefanie Ehrenberg, geboren am 16. Juni 1983 in München versichere hiermit ehrenwörtlich, dass ich die vorliegende Arbeit selbständig und nur unter Verwendung der angegebenen Hilfsmittel und Quellen angefertigt habe. Sämtliche Experimente wurden von mir selbst durchgeführt, sofern nicht explizit auf Dritte verwiesen wurde. Diese Dissertation wurde weder ganz, noch teilweise bei einer anderen Prüfungskommission vorgelegt und ich habe noch zu keinem früheren Zeitpunkt versucht, eine Dissertation einzureichen oder an einer Doktorprüfung teilzunehmen.

München, den 29.03.2015

Stefanie Ehrenberg

Erstgutachter: Herr PD Dr. Josef Mautner
Zweitgutachterin: Frau Prof. Dr. Elisabeth Weiß

Tag der Einreichung: 28.08.2014

Tag der mündlichen Prüfung: 05.02.2015

**Wenige wissen, wie viel man wissen muss,
um zu wissen, wie wenig man weiß.**

(Werner Heisenberg, Physiker)

Table of contents

Table of contents	i
List of figures	v
List of tables	vi
List of abbreviations	vii
1. Introduction	1
1.1 The immune system	1
1.2 Lymphocyte development	1
1.2.1 Early B cell development in the bone marrow	1
1.2.2 Late B cell development in the spleen	2
1.2.2.1 Splenic architecture	2
1.2.2.2 Development from an immature B cell population to mature B cells	3
1.2.2.3 Mature B cell populations	5
1.3 B cell activation and plasma cell development	6
1.3.1 T cell-dependent and T cell-independent immune reactions	6
1.3.1.1 Antigen capturing and presentation	7
1.3.1.2 T cell-independent immune response	8
1.3.1.3 T cell-dependent immune response	9
1.3.2 Fundamental molecular mechanisms in plasma cell differentiation	10
1.4 Notch receptor signalling	11
1.4.1 The structure and activation of Notch receptors	11
1.4.2 Notch signalling in lymphocytes	14
1.4.3 Notch in MZ B cell development	14
1.4.4 Notch signalling in lymphoma and other malignancies	15
1.5 Model systems	15
1.5.1 The Notch2IC-transgenic mouse strain	15
1.5.1.1 Generation	15
1.5.1.2 Phenotype	16
1.5.2 The Notch2-deficient mouse strain	16
1.5.2.1 Generation	16
1.5.2.2 Phenotype	17
2. Aim	18

3. Results	19
3.1 Comparison of gene expression profiles of Notch2IC-expressing MZ B and Notch2-deficient Fo B cells with wild type MZ B and Fo B cells	19
3.1.1 The experimental setting - Illumina BeadChip micorarrays	19
3.1.2 Gene expression profiles of Notch2IC-expressing MZ B as well as Notch2-deficient Fo B cells exhibit a close relationship to those of their respective wild type counterparts.....	23
3.1.3 Differences in B cell-specific gene expression profiles induced by constitutive Notch2IC expression or Notch2 deficiency	24
3.2 The impact of Notch2 signalling and the influence of the marginal zone environment on the MZ B cell phenotype.....	30
3.2.1 Notch2IC-expressing cells are able to maintain their MZ B cell phenotype in vitro..	30
3.2.2 Enhanced proliferation of Notch2IC-expressing B cells in response to α -CD40 or LPS stimulation can mainly be ascribed to their MZ B cell phenotype	31
3.2.3 Notch2IC-expressing B cells exhibit enhanced Erk, Jnk and PI3 kinase signalling even in the absence of a CD19 receptor.....	32
3.2.4 Notch2IC expression is not sufficient to sustain enhanced Erk, Jnk and Akt signalling outside the marginal zone environment.....	36
3.2.5 Notch2IC-expressing B cells spontaneously differentiate into CD138 ⁺ B220 ^{low} plasmablasts or plasma cells in vitro	39
3.2.6 Spontaneous plasmablast/plasma cell development of Notch2IC-expressing B cells in vitro is driven by Notch2IC expression	42
3.2.7 Notch2IC-expressing CD138 ⁺ B220 ^{low} cell populations spontaneously arising in vitro are functional antibody-secreting plasmablasts or plasma cells.....	43
3.2.8 Spontaneous plasmablast/plasma cell development of Notch2IC-expressing B cells in vitro correlates with increased Blimp-1 and Irf4 levels.....	45
3.3 The role of Notch2 signalling in immune responses.....	49
3.3.1 Notch2IC//CD19Cre ^{+/-} mice are impaired in their TI-2 immune response	49
3.3.2 Notch2IC//CD19Cre ^{+/-} mice are impaired in their immune response to the TI-1 antigen NP-LPS	50
3.3.3 Notch2IC//CD19Cre ^{+/-} mice exhibit defects in their SIGN-R1 ⁺ macrophage population and in antigen capturing	54
3.3.4 Notch2 ^{fl/fl} //CD19Cre ^{+/-} mice have a reduced TI-2 immune reponse, but functional antigen capturing and transport into the splenic follicle.....	55
3.4 The role of Notch2 in lymphomagenesis	59
3.4.1 Constitutive, B cell-specific Notch2 expression seems not to be sufficient to strongly drive B cell lymphomagenesis.....	59
3.4.2 Constitutive Notch2IC expression alters the phenotype of B cells in aging mice irrespective of tumor development.....	63

4. Discussion	66
4.1 Gene expression profiles of Notch2IC-expressing MZ B and Notch2-deficient Fo B cells resemble their wild type counterparts, yet still exhibiting clear differences.....	66
4.2 Notch2IC-expressing B cells show enhanced proliferation mainly due to their MZ B cell phenotype	68
4.3 Increased Erk, Jnk, Akt levels in Notch2IC-expressing MZ B cells in vivo.....	70
4.4 Notch2IC-expressing MZ B cells spontaneously differentiate to functional, antibody-secreting plasmablasts/plasma cells in vitro, but not in vivo	71
4.5 Notch2IC//CD19Cre ^{+/-} mice are impaired in their TI immune response, antigen capturing and the subsequent transport into the follicle.....	75
4.6 Notch2 ^{fl/fl} //CD19Cre ^{+/-} mice show reduced TI-2 immune response, despite intact antigen capturing and transport into the follicle	76
4.7 Constitutive Notch2 signalling is not acting as a strong oncogene in B cells, yet it alters the characteristic phenotype of B cells in aging mice.....	78
5. Summary	80
6. Zusammenfassung	82
7. Material	84
7.1 Mouse strains.....	84
7.2 Primer, enzymes and Southern blot DNA probe	84
7.3 Antibodies.....	85
7.4 Software	86
8. Methods	87
8.1 Mice-associated methods	87
8.1.1 Mouse breeding.....	87
8.1.2 Isolation of primary lymphocytes	87
8.1.3 Determination of cell numbers.....	88
8.1.4 Freezing of cells	88
8.1.5 In vitro culture of primary splenic mouse lymphocytes.....	88
8.1.5.1 In vitro culture with different stimuli.....	88
8.1.5.2 In vitro proliferation (CFSE) assay.....	88
8.1.6 Flow Cytometry.....	89
8.1.6.1 Analysis of murine lymphocytes by flow cytometry	89
8.1.6.2 Intracellular analysis of murine lymphocytes by flow cytometry.....	89
8.1.6.3 Fluorescence-associated cell sorting (FACS)	90
8.1.7 T cell-independent immunisation of mice.....	90
8.1.8 Enzyme-linked immunosorbent assay (ELISA).....	90

8.1.8.1 Preparation of serum from murine blood.....	91
8.1.8.2 Preparation of cell culture supernatant for ELISA.....	91
8.1.8.3 Detection of specific standard immunoglobulin titers	91
8.1.8.4 Detection of NP-specific immunoglobulin titers	91
8.1.9 Enzyme-linked immunosorbent spot (ELISPOT) assay	92
8.1.10 Immunohistochemistry and Immunofluorescence	92
8.2 DNA-related techniques.....	93
8.2.1 DNA isolation.....	93
8.2.1.1 Isolation of genomic DNA from murine tails	93
8.2.1.2 Isolation of genomic DNA from primary murine lymphocytes.....	93
8.2.2 DNA analysis.....	93
8.2.2.1 Polymerase Chain Reaction (PCR).....	93
8.2.2.2 Agarose gel electrophoresis of DNA.....	94
8.2.3 Southern blotting (Southern et al., 1997).....	94
8.2.3.1 Restriction digest of genomic DNA.....	94
8.2.3.2 Gelelectrophoresis and blotting	94
8.2.3.3 Hybridisation & detection.....	95
8.3 RNA-related techniques	95
8.3.1 Isolation & quantification of total RNA.....	95
8.3.2 cRNA synthesis	96
8.3.3 Micoarray-based gene expression profiling	98
8.4 Protein detection.....	101
8.4.1 Protein isolation & quantification	101
8.4.2 SDS polyacrylamide gel electrophoresis (PAGE).....	101
8.4.3 Western blotting	101
8.4.4 Immunostaining.....	102
8.4.5 Western blot quantification.....	102
8.5 Statistics	102
9. References.....	103
10. Appendix.....	120
Supplementary Data	120
Acknowledgements	143

List of figures

Figure 1: Schematic view of the microarchitecture of the spleen.....	3
Figure 2: Peripheral B cell maturation from the bone marrow.....	3
Figure 3: Cross section of the splenic white pulp illustrating the different ways of immune reactions.....	6
Figure 4: Expression of surface markers and transcription factors during plasma cell developmen.....	11
Figure 5: Notch receptors and their ligands.....	12
Figure 6: Notch receptor activation.....	13
Figure 7: Targeting strategy for the generation of Notch2IC-transgenic mice.....	16
Figure 8: Targeting strategy for the generation of B cell-specific Notch2-deficient mice.....	17
Figure 9: Schematic workflow of a whole mouse-genome gene expression profiling assay using Illumina BeadChip arrays.....	20
Figure 10: Sorted cell populations and experimental groups for gene expression profiling analyses.....	20
Figure 11: Exemplary dot plots from sorting experiments depicting splenic B cell populations before and after the FACS sorting procedure.....	20
Figure 12: Examples of Bioanalyzer graphs of total RNA and cRNA samples of high integrity and quality.....	21
Figure 13: Schematic workflow of Illumina BeadChip microarray data analyses.....	21
Figure 14: Quality controls revealed two outliers among all analysed cRNA samples.....	22
Figure 15: Box plots showing optimisations of microarray intensity distributions during data processing.....	22
Figure 16: Gene expression profiles of Notch2IC-expressing MZ B and Notch2-deficient Fo B cells resemble their wild type counterparts.....	23
Figure 17: Different amplification rounds result in a mild technical bias.....	24
Figure 18: Gene expression profiles of the two Fo B cell populations are more closely related then those of the two MZ B cell populations.....	25
Figure 19: Number of differentially regulated genes between the different B cell populations of the analysed mouse strains.....	26
Figure 20: Volcano plots depicting differentially regulated genes between the different B cell populations of the analysed mouse strains.....	27
Figure 21: In vitro cultured Notch2IC//CD19Cre ^{+/-} B cells maintain their MZ B cell phenotype.....	30
Figure 22: Notch2IC-expressing B cells are hyper-responsive to LPS and α -CD40 stimulation in vitro mainly due to their MZ B cell phenotype.....	32
Figure 23: Notch2IC-expressing B cells exhibit increased levels of pErk, pJnk and pAkt.....	33
Figure 24: Simplified scheme of the PI3 kinase pathway including members analysed by Western blot.....	33
Figure 25: Notch2IC-expressing B cells exhibit increased PI3K signalling in comparison to control B cells..	34
Figure 26: Western blot quantifications revealed increased basal and phosphorylated levels of Akt and p70 in Notch2IC-expressing B cells.....	35
Figure 27: Notch2IC-expressing and control MZ B cells have higher pErk, pJnk and pAkt levels than Fo B cells.....	36
Figure 28: Notch2IC expression is not sufficient to maintain enhanced pErk, pJnk or pAkt levels in vitro....	37
Figure 29: Control B cells exhibit greater activation in response to LPS and α -CD40 stimulation than Notch2IC-expressing B cells.....	38
Figure 30: No increased plasma cell population in unimmunised Notch2IC//CD19Cre ^{+/-} compared to CD19Cre ^{+/-} control mice.....	39
Figure 31: In vitro cultured Notch2IC//CD19Cre ^{+/-} B cells spontaneously differentiate into CD138 ⁺ B220 ^{low} plasmablasts/plasma cells.....	40
Figure 32: Only Notch2IC-expressing B cells spontaneously differentiate into CD138 ⁺ B220 ^{low} plasmablasts/plasma cells in vitro.....	41
Figure 33: Spontaneous differentiation of Notch2IC-expressing cells into CD138 ⁺ B220 ^{low} cells in vitro can be hampered by α -CD40 stimulation.....	42
Figure 34: Plasma cell differentiation is triggered by constitutive Notch2IC expression.....	43
Figure 35: IgM titers of in vitro cultured splenic B cells of Notch2IC//CD19Cre ^{+/-} and control mice.....	44
Figure 36: Unstimulated Notch2IC-expressing B cells are able to spontaneously differentiate to IgM-, IgG3- and IgG1-secreting plasmablasts/plasma cells in vitro.....	44
Figure 37: Notch2IC-expressing MZ B cells express higher Blimp-1 and Irf4 levels than wild type MZ B cells.....	45
Figure 38: Splenic Notch2IC-expressing B cells upregulate Blimp-1 and Irf4 expression with and without LPS stimulation.....	46

List of figures and tables

Figure 39: Notch2IC-expressing B cells cultured with or without LPS, exhibit an accelerated Blimp-1 and Irf4 induction compared to LPS-treated wild type B cells.....	47
Figure 40: LPS-stimulated non-plasma cells have higher Irf4 levels than unstimulated non-plasma cells.....	48
Figure 41: Notch2IC-expressing B cells cultured with α -CD40 have lower Blimp-1 levels than cells cultured with or without LPS.....	48
Figure 42: Notch2IC//CD19Cre ^{+/-} have reduced antigen-specific IgM and IgG3 serum titers after TI-2 immunisation.....	49
Figure 43: Notch2IC//CD19Cre ^{+/-} splenic B cells do not develop into antigen-specific IgG3-secreting plasma cells after TI-2 immunisation, yet they seem to carry polyreactive IgM receptors.....	50
Figure 44: Notch2IC//CD19Cre ^{+/-} mice are impaired in their TI-1 immune response to low NP-LPS concentrations.....	51
Figure 45: Notch2IC-expressing splenic B cells do not develop into antigen-specific IgG1- or IgG3-secreting plasma cells after TI-1 immunisation, yet they seem to be polyreactive.....	51
Figure 46: Marginal zone clearance after treatment with different NP-LPS concentrations.....	53
Figure 47: SIGN-R1 ⁺ macrophages seem reduced in Notch2IC//CD19Cre ^{+/-} mice.....	54
Figure 48: Notch2IC//CD19Cre ^{+/-} mice exhibit defects in antigen capturing and transport into the follicle.....	55
Figure 49: Notch2 ^{fl/fl} //CD19Cre ^{+/-} mice are devoid of MZ B cells.....	56
Figure 50: SIGN-R1 ⁺ macrophages are slightly reduced, but present in Notch2 ^{fl/fl} //CD19Cre ^{+/-} mice.....	56
Figure 51: Antigen capturing and transport into the follicle is similar in control and Notch2 ^{fl/fl} //CD19Cre ^{+/-} mice.....	57
Figure 52: Notch2 ^{fl/fl} //CD19Cre ^{+/-} have reduced antigen-specific IgM and IgG3 serum titers after TI-2 immunisation.....	58
Figure 53: Notch2 ^{fl/fl} //CD19Cre ^{+/-} mice have reduced numbers of antigen-specific IgM-, IgG1- and IgG3-secreting plasma cells after TI-2 immunisation.....	58
Figure 54: Splenic weight of aged and young Notch2IC//CD19Cre ^{+/-} and control mice.....	61
Figure 55: Correlation of splenic weight with age in Notch2IC//CD19Cre ^{+/-} and control mice.....	61
Figure 56: Total splenic cells as well as IgM ⁺ and IgM ⁺ hCD2 ⁺ splenic cell populations of aged Notch2IC//CD19Cre ^{+/-} and control mice.....	62
Figure 57: Southern blot analysis of aged Notch2IC//CD19Cre ^{+/-} and control mice.....	62
Figure 58: Results of representative FACS analyses, depicting splenic cells of aged Notch2IC//CD19Cre ^{+/-} and control mice.....	64

List of tables

Table 1-4: Fold changes of candidate genes from microarray analyses known to be up- or downregulated in MZ B cells or by Notch2 signalling.....	28
Table 5: Overview of all analysed aged Notch2IC//CD19Cre ^{+/-} and control mice.....	59
Table S1: Top 100 regulated genes between wild type MZ B and Fo B cells.....	120
Table S2: Top 100 regulated genes between Notch2-deficient Fo B and Notch2IC-expressing MZ B cells.....	122
Table S3: Top 100 regulated genes between wild type and Notch2IC-expressing MZ B cells.....	124
Table S4: Top 100 regulated genes between wild type and Notch2-deficient Fo B cells.....	127
Table S5: Some of the most significant functional annotation clusters comparing gene expression profiles of Notch2IC-expressing MZ B and Notch2-deficient Fo B cells.....	129
Table S6: Some of the most significant functional annotation clusters comparing gene expression profiles of wild type MZ B and Fo B cells.....	132
Table S7: Some of the most significant functional annotation clusters comparing gene expression profiles of wild type and Notch2IC-expressing MZ B cells.....	134
Table S8: Some of the most significant functional annotation clusters comparing gene expression profiles of wild type and Notch2-deficient Fo B cells.....	136
Table S9: Some of the most significant functional annotation clusters obtained with genes upregulated in wild type MZ B in comparison to wild type Fo B cells.....	138
Table S10: Some of the most significant functional annotation clusters obtained with genes upregulated in Notch2IC-expressing MZ B in comparison to wild type MZ B cells.....	140

List of abbreviations

%	percent
°C	degree Celcius
μCi	micro Curie
μg/μm/μl	microgram/micrometer/microliter
Aicda	activation-induced cytidine deaminase
ANK	ankryin repeats
ANOVA	analysis of variance
APC	allophycocyanin
APCs	antigen presenting cells
APRIL	a proliferation-inducing ligand
APS	ammonium persulfate
BAFF	B cell activating factor
Bcl6	B cell lymphoma 6
B-CLL	B cell chronic lymphocytic leukemia
BCM	B cell medium
BCR	B cell receptor
Blimp-1	B lymphocyte-induced maturation protein 1
BLNK	B cell linker
BM	bone marrow
BSA	bovine serum albumin
Btk	Bruton's tyrosine kinase
C-	carboxy
C	constant regions of the immunoglobulin chains
CAGGS	CMV early enhancer/chicken β-actin/rabbit globin promoter
CB2/Cnr2	cannabinoid receptor 2
CD40L	CD40 ligand
CFSE	carboxyfluorescein succinimidyl ester
CLP/CMP	common lymphoid progenitor/common myeloid progenitor
CMV	cytomegalovirus
CR	cysteine-rich domain
Cr2	complement receptor 2 (CD21)
Cre	Cre recombinase
cRNA/cDNA	copy ribonucleic acid/copy deoxyribonucleic acid
CSR	class switch recombination
Ctrl	control
DAB	3,3'-diaminobenzidine
DAPI	4',6-diamidin-2-phenylindol
DC	dendritic cell
D _H	diversity segments of the immunoglobulin heavy chains
DLBCL	diffuse large B cell lymphoma
ΔI	Delta-like
DMSO	dimethyl sulfoxide
DNA	deoxyribonucleic acid
dNTP	deoxyribonucleotide triphosphate
DSL	Delta, Serrate and Lag2 domain
DTT	dithiothreitol
EBF1	early B cell factor 1

List of abbreviations

EDTA	ethylene diamine tetra acetate
EGF	epidermal growth factor
ELISA	enzyme-linked immunosorbent assay
ELISPOT	enzyme-linked immuno spot assay
Erk	extracellular signal-regulated kinase
et al.	“et alii”
FACS	fluorescence-activated cell sorting
FCS	fetal calf serum
FcγRIIB	low-affinity receptor for IgG
FDC	follicular dendritic cell
Fig.	figure
Fitc	fluorescein isothiocyanate
fl	floxed, flanked by loxP sites
Fo	follicular
FoxO1	forkhead box protein O1
frt	flippase recognition target site
GC	germinal center
GS	γ-secretase
GSK-3	glykogen synthase kinase 3
h	hour
HD	heterodimerisation domain
HDAC1	histone deacetylase 1
Hes/Hey	hairy enhancer of split/ hairy related genes
HRP	horseradish peroxidase
HSC	hematopoietic stem cell
i.p.	intraperitoneal
ICAM1	intracellular adhesion molecule 1
Ig	immunoglobulin
IgH/IgL	immunoglobulin heavy/light chain
IL-7/IL-4	interleukin-7/-4
IRES	internal ribosomal entry site
Irf4	interferon regulatory factor 4
J _H /J _L	joining segments of the immunoglobulin heavy/light chains
Jnk	c-Jun N-terminal kinase
kb	kilobase
LFA1	lymphocyte function-associated antigen 1
LN	lymph node
LNR	LIN12-Notch repeats
loxP	locus of X-over P1
LPS	lipopolysaccharide
mA	milliampere
MAC1	macrophage receptor 1
MACS	magnetic cell separation
MAML	mastermind-like
MAPK	mitogen-activated protein kinase
MARCO	macrophage receptor with collagenous structure
MCL	mantel cell lymphoma
MHC	major histocompatibility complex
MIB1	mindbomb1
min	minute

MINT	Msx2-interacting nuclear target protein
Mitf	microphthalmia-associated transcription factor
ml	milliliter
mM/M	millimolar/molar
MMM	metallophilic marginal zone macrophages
MZ	marginal zone
MZBC	marginal zone bridging channel
MZM	marginal zone macrophages
MZP/MZBP	marginal zone B cell precursor
N-	amino
NF κ B	nuclear factor ‘kappa-light-chain-enhancer’ of activated B-cells
n.d./n.a.	not determined/not applicable
ng/nm	nanogram/nanometer
NLS	nuclear localisation signal
NotchEC/IC	extracellular/intracellular domain of the Notch receptor
NotchTM	transmembrane domain of the Notch receptor
NP	4-hydroxy-3-nitrophenylacetyl
o. n.	over night
PAGE	polyacrylamide gel electrophoresis
PALS	periarteriolar lymphoid sheath
Pax5	paired box 5
PBS	phosphate-buffered saline
PCA	Principal Component Analysis
pCAF	p300-associated factor
PCR	polymerase chain reaction
PCs	plasma cells
Pe	phycoerythrin
PerCP	peridinin chlorophyll protein
PEST	proline-glutamine-serine-threonine-rich domain
PFA	paraformaldehyde
PI	propidium iodide
PI3K	phosphatidylinositol-3-kinase
PTEN	phosphatase and tensin homologue
PVDF	polyvinylidene-fluoride
QC	quality control
RBP-J κ	Recombination signal binding protein for immunoglobulin kappa J region
RIN	RNA integrity number
RNA	ribonucleic acid
rpm	rounds per minute
RT	room temperature
S1P/ S1PR1/3	sphingosine-1-phosphate/sphingosine-1-phosphate receptor 1/3
SA-AP	streptavidin-coupled alkaline phosphatase
SD	standard deviation
SDS	sodium dodecyl sulfate
sec	second
SKIP	Ski-interacting protein
SLO	secondary lymphoid organs
SMZL	splenic marginal zone lymphoma
SP	spleen
SSC	saline sodium citrate

List of abbreviations

T1-3	transitional B cells type 1 to 3
TAD	transactivation domain
TAE	Tris acetate EDTA
T-ALL	T cell acute lymphoblastic leukemia
TAN1	translocation-associated Notch homologue
TBS	Tris-buffered saline
Tcl1B	T-cell leukemia/lymphoma protein 1B
TCR	T cell receptor
TD	T cell-dependent
TE	Tris EDTA
TEMED	N,N,N',N'-tetramethylene diamine
T _H	helper T cell
TI	T cell-independent
TLR	toll-like receptor
TNF/TNFR	tumor necrosis factor/ tumor necrosis factor receptor
TNP	2,4,6-trinitrophenyl
U	units
UV	ultraviolet
V	volt
v/v	volume per volume
VCAM1	vascular cell adhesion molecule 1
V _H /V _L	variable regions of the immunoglobulin heavy/light chains
VSN	Variance Stabilising Normalisation
w/v	weight per volume
WASP	Wiskott-Aldrich syndrom protein
wt	wild type
x g	x fold acceleration of gravity
Xbp1	X-box binding protein 1
α	anti

1. Introduction

1.1 The immune system

Animals are constantly exposed to a vast range of infectious agents able to enter their bodies at different sites causing various diseases. Thus, a well coordinated, adequate and specific reaction of the immune system is a prerequisite to be able to cope with such possibly life-endangering threats. In mammals, the immune system can grossly be classified into an innate and adaptive branch. All immune cells develop from pluripotent hematopoietic stem cells (HSC) produced in the fetal liver or the bone marrow (BM) after birth, further differentiating into common myeloid or common lymphoid progenitor cells (CMP, CLP). Amongst others CMPs give rise to granulocytes and macrophages, important players of the innate immune response. CLPs on the other hand can further differentiate into B and T or natural killer cells, of which the latter are considered to be part of innate immunity. B and T cells belong to the adaptive arm of the immune system resuming essential functions there. The innate immune response represents the first rapid, yet relatively unspecific line of defence against pathogens with macrophages and neutrophils, both phagocytic cells as key players. The adaptive immune response on the other hand, often also designated as acquired immunity, features high antigen specificities, self-non-self discrimination and immunological longterm memory to pathogens, though at the expense of time as it takes four to seven days before first effects become noticeable. The adaptive immune reaction can further be subdivided into humoral and cell-mediated immunity. The decision which path needs to be taken is mainly determined by the cytokine profile prevailing at that time. Cell-mediated immunity involves the activation of phagocytes as well as cytotoxic T cells and is risen against intracellular pathogens, virally infected cells, as well as against abnormal cells of the body. Humoral immune response is based on the effect mediated by antibodies specific for the prevailing antigen, secreted by antigen-activated B cells. Innate and adaptive immune responses are permanently being executed involving repeated expansion and deletion cycles of antigen-specific cell populations. Thus, thorough control mechanisms are needed to prevent dangerous developments such as autoimmunity, cellular transformation or overreactions eventually resulting in allergies (Janeway et al., 2012).

1.2 Lymphocyte development

1.2.1 Early B cell development in the bone marrow

The BM provides a highly appropriate microenvironment for early B cell development with non-lymphoid stromal cells furnishing essential survival, proliferation and differentiation factors (Janeway et al., 2012). Early B cell development implies several sequential differentiation steps in the end aiming at producing immature B cells expressing a functional, non-self-reactive B cell receptor (BCR). Commitment to the B cell lineage is driven by the controlled interplay of the interleukin 7 (IL-7) cytokine receptor, the transcription factors Ikaros, E2A (including its products E12 and E47), PU.1, Paired Box 5 (Pax5) and early B cell factor 1 (EBF1) (Ramirez et al., 2010). Thereby, EBF1 seems to be the master regulator in promoting B cell differentiation (Northrup and Allman, 2008). The BCR is made up of two identical immunoglobulin heavy (IgH) and light chains (IgL), associated with two

invariant accessory proteins, one Ig α and one Ig β . Both heavy and light chains are composed of variable and constant (C) regions, with variable regions (V_H and V_L) providing antigen binding and specificity. Ig α and Ig β on the other hand take over intracellular signalling after receptor binding as they represent the only noteworthy cytoplasmic domains of the BCR. To ensure the recognition of all possible antigens, a highly diverse repertoire of antigen specificities must be obtained during B cell development. To achieve this, the V_H region is encoded in numerous, different copies of three DNA segments, called the variable (V_H), diversity (D_H) and joining (J_H) segments. The same is true for the light chains except that there are only two variable and joining (V_L and J_L) and no D gene segments. The random selection and recombination of one gene segment of each type with each other to form the variable region is called somatic V(D)J recombination and accounts by sheer combinatorial diversity already for a substantial part of the great diversity of the BCR (Janeway et al., 2012; Jung et al., 2006; Edry and Melamed, 2004). After successful V(D)J recombination, immature B cells expressing a functional BCR are subsequently tested for the reactivity of their receptor. If strongly self-reactive BCRs - hence possible elicitors of autoimmunity - are detected within the BM, either clonal deletion ensures that cell development is stopped at this stage via apoptosis of these cells or receptor editing is induced, trying to change the current “self-specificity” of the BCR by further rearrangements (Edry and Melamed, 2004). B cells that recognise self-antigens can also become anergic, a state which comes along with short half-life as well as the downregulation of IgM and the BCR signalling pathway hence inhibiting further activation (Goodnow et al., 1988). In the end, each B cell carries a unique, non self-reactive antigen receptor of a single specificity. Hence, B cell development results in the generation of millions of different B cell receptors displaying different antigen specificities.

1.2.2 Late B cell development in the spleen

1.2.2.1 Splenic architecture

The spleen (SP) is the largest secondary lymphoid organ (SLO) harbouring about one-fourth of the body's lymphocytes. It is comprised of two compartments known as red and white pulp, which differ in their function and morphology. The red pulp constantly filters blood thereby removing old and damaged erythrocytes as well as foreign material, whereas the white pulp is in charge of the initiation of immune responses. Most of the splenic lymphocytes can be found in the white pulp, next to macrophages and dendritic cells (DC). It can be subdivided into three sub-compartments: the periarteriolar lymphoid sheath (PALS) harbouring mainly T cells, the follicles containing primarily follicular (Fo) B as well as follicular dendritic cells (FDCs) and the marginal zone (MZ). The latter has extensive vasculature and comprises MZ B cells, stromal cells and marginal zone macrophages (MZMs), which are interspersed within the MZ. Lining the marginal sinus are furthermore marginal metallophilic macrophages (MMMs). The different types of macrophages can be distinguished from one another by surface expression of MOMA-1 (MMMs) or the C-type lectin SIGN-R1 and the macrophage receptor with collagenous structure (MARCO) (MZMs). Together with the marginal sinus the MZ builds the border between the red and the white pulp (Mebius and Kraal, 2005; Cesta, 2006). Lymphocytes are thought to leave the follicle via the marginal zone bridging channels (MZBCs),

which are extensions of the white pulp through the MZ into the red pulp. It is also the place where antigen-activated B cells become plasmablasts (Balasz et al., 2002) and from where they directly gain access to the red pulp (for detail see chapter 1.3.1.2). In these regions T cells are adjacent to the MZ (Mebius and Kraal, 2005). A detailed scheme of the splenic microarchitecture is depicted in figure 1.

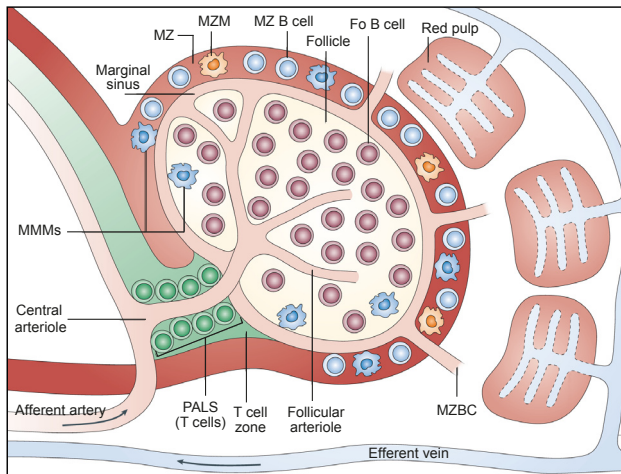


Figure 1: Schematic view of the microarchitecture of the spleen (from Pillai and Cariappa, 2009). Blood arrives at the spleen through the afferent splenic artery, which branches into central arterioles sheathed by the white-pulp. It reaches the marginal sinus from where it flows to the red pulp through the marginal zone (MZ) or to the white pulp through the conduit network. From the red pulp the blood runs into venous sinuses, which collect into the efferent splenic vein. The white pulp of the spleen consists of a T cell zone, also called periarteriolar lymphoid sheath (PALS), B cell follicles mainly harboring follicular (Fo) B cells, marginal metallophilic macrophages (MMM) lining the marginal sinus and the marginal zone (MZ) with its marginal zone macrophages (MZM) and marginal zone B cells. Marginal zone bridging channels (MZBCs) are extensions of the white pulp through the MZ into the red pulp.

1.2.2.2 Development from an immature B cell population to mature B cells

Most immature B cells exit the BM to migrate to the spleen, where they finish their maturation (Fig. 2). These cells are called “transitional” B cells as they are “in transit” from one organ to another. Although immature B cells can also at least to a certain degree continue their maturation in the BM (Fig. 2) (Allman and Pillai, 2008; Cariappa et al., 2007b; Lindsley et al., 2007), MZ B cells only develop in the splenic environment (Tan et al., 2009; Pillai and Cariappa, 2009). B cell maturation in the periphery involves three stages of transitional B cell populations (T1-3), from which follicular or MZ B cells can

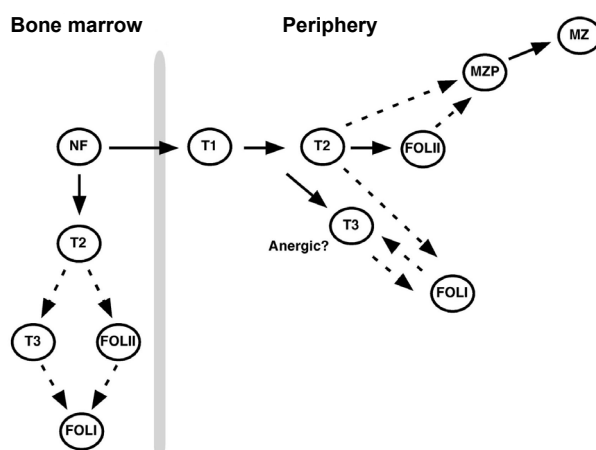


Figure 2: Peripheral B cell maturation from the bone marrow (taken from Allman and Pillai, 2008). Current model for peripheral B cell maturation from the bone marrow. T1-3 (transitional B cell stages), NF (newly formed, immature B cells), FOLI-II (follicular B cells), MZ (marginal zone B cells), MZP (marginal zone B cell precursors).

develop. Transitional B cells are characterised by the expression of AA4.1⁺, CD24⁺, higher IgM and lower CD22 and B220 levels than mature B cells (Chung et al., 2003; Yeramilli and Knight, 2011). BCR expression is essential for the survival of the transitional B cell population (Lam et al., 1997; Kraus et al., 2004; Tze et al., 2005), but from the T2 stage on, in addition to tonic BCR signalling, signals from the B cell activating factor (BAFF) receptor are needed for B cell survival (Batten et al., 2000; Cancro, 2009; Chung et al., 2003; Gross et al., 2001; Schiemann et al., 2001). Transitional B cells can either develop into splenic Fo B or MZ B cells and an interplay of multiple different signalling

pathways as well as factors involved in B cell migration and retention are assumed to influence this decision. Concerning signalling pathways, the BCR with its co-receptor CD19 were a long time among the most prominent factors believed to impact on the Fo B versus MZ B cell decision, with strong BCR signalling involving the Bruton's tyrosine kinase (Btk) favouring the formation of Fo B cells (Hardy et al., 1983; Hikida et al., 2003; Wen et al., 2003; Pillai and Cariappa, 2009) and a weak one the development of MZ B cells precursors (MZBPs) and ultimately MZ B cells (Samardzic et al., 2002; Cariappa et al., 2001; Pillai et al., 2005). Yet, recently we could show that Notch2 signalling is essential and the key pathway in regulating MZ B versus Fo B cell development (discussed in detail in chapter 1.4.3), as constitutive Notch2 signalling could rescue MZ B cell development in CD19-deficient mice, which had been shown to be devoid of MZ B cells (Hampel et al., 2011; Martin and Kearney, 2000). Apart from that, the nuclear factor "kappa-light-chain-enhancer" of activated B cells (NF κ B) signalling pathway is also implicated in Fo B and MZ B cell differentiation. BAFF, which can be found at high concentrations in the lymphoid follicles (Hase et al., 2004; Suzuki et al., 2010) and which mainly induces non-canonical NF κ B signalling is primarily needed by T2 and Fo B cells (Pillai and Cariappa, 2009). The MZ B cell fate on the other hand seems mainly triggered via the canonical NF κ B pathway (Sasaki et al., 2006), as mice lacking p50, I κ Ba or p65 - all members of the canonical NF κ B pathway - show defects in MZ B cell development (Cariappa et al., 2000). However, Weih and colleagues could show that in addition the non-canonical NF κ B pathway also impacts on MZ B cell development (Weih et al., 2001). In addition, deficiencies in the phosphatase SHIP (Helgason et al., 1998), or the phosphatidylinositide-3-kinases delta isoform (PI3K δ) (Okkenhaug et al., 2002), have been shown to result in reduced MZ B cell numbers (Clayton et al., 2002; Jou et al., 2002), whereas mice deficient for the phosphatase and tensin homologue (PTEN), a negative regulator of PI3K signalling, display increased MZ B cell numbers (Suzuki et al., 2003). These data suggest that PI3K signalling positively regulates MZ B cell development. Besides the just described signalling pathways various factors mediating B cell migration, retention and positioning are crucial for MZ B cell development, as it is still believed that transitional B cells need to migrate into the MZ environment to be able to fully mature to MZ B cells (Pillai and Cariappa, 2009). During peripheral maturation chemokine receptor CXCR5-expressing T1 B cells (IgM^{high} IgD⁻ CD21⁻ CD23⁻) enter the splenic white pulp via the marginal sinus, where they migrate into the splenic follicles in response to a CXCL13 gradient created by FDCs (Lo et al., 2003). There they further differentiate into T2 (IgM^{high} IgD⁺ CD21⁺ CD23⁺) and T3 (IgM^{low} IgD⁺ CD21⁺ CD23⁺) transitional B cells, which are now able to recirculate (Chung et al., 2003; Allman et al., 2001b; Pillai and Cariappa, 2009). The sphingosine-1-phosphate receptors 1 and 3 (S1PR1/3) are already highly expressed on MZ B cell precursors and participate in MZ B cell homing to as well as retention in the sphingosine-1-phosphate (S1P) rich MZ. They are essential for overcoming the just described attraction to the follicle by CXCL13. Next to its indispensable role in MZ B cell commitment, Notch2 signalling could potentially also be implicated in supplying MZ B cells and their precursors with MZ localisation signals (Saito et al., 2003; Cinamon et al., 2008; Cinamon et al., 2004; Simonetti et al., 2013). Other players that engage in MZ B cell migration and localisation are for example the Wiskott-Aldrich syndrome protein (WASP), a cytoskeletal protein, which if missing causes a disruption of the actin polymerisation in MZ B cells so that they are no longer able to migrate in response to the S1P

gradient (Thrasher, 2002; Westerberg et al., 2008) or SWAP-70, a RhoGTPase-interacting and F-actin-binding protein, which regulates MZ B cell adhesion (Chopin et al., 2010). MZ B cells are furthermore positioned to the MZ by the interaction of the two integrins lymphocyte function-associated antigen 1 (LFA1) and $\alpha 4\beta 1$ on their surface with the intracellular adhesion molecule 1 (ICAM1) and the vascular cell adhesion molecule 1 (VCAM1), respectively (Lu and Cyster, 2002). And last but not least, MZ B cells may also receive further MZ retention signals from MARCO⁺ macrophages (Karlsson et al., 2003) that are localised in the MZ. However, besides all this knowledge, until today it is not completely clear if there is a specific B cell stage from which MZ B and Fo B cells branch from each other or where MZ B cell precursors reside within the spleen. There are interesting studies showing that MZ B cells can also develop from mature Fo B cells in rats (Dammers et al., 1999) implicating that MZ B cells could potentially also arise from later transitional stages or even mature Fo B cells. Apart from that, the role of T3 transitional B cells in B cell development is still not completely clear, although it is currently under discussion if these cells represent anergic B cells (Teague et al., 2007; Liubchenko et al., 2012). So, in summary, an integrated model out of differentiation and migration factors cooperating at the same time rather than in a chronological order mediate this important cell fate decision.

1.2.2.3 Mature B cell populations

Fo B cells represent the majority of mature B cells (~75 %) mainly homing to B cell follicles in the spleen and lymph nodes (LN). They continually recirculate via the (blood) circulation through the BM and peripheral lymphoid organs. They typically are IgD^{high} IgM^{low} CD23⁺ and CD21^{Int}. Follicular B cell zones are always adjacent to T cell areas, allowing a rapid interaction of antigen-activated Fo B and T cells if necessary. Therefore, Fo B cells are well suited for and hence key players of T cell-dependent (TD) immune responses where B and T cells need to interact (details in 1.3.1.3). With ~5 %, MZ B cells are less abundant and in contrast to Fo B cells sessile within the spleen (Srivastava et al., 2005). They express high levels of IgM, CD21, CD1d, CD25, CD9, CD80, CD86 and integrins as well as low levels of IgD and CD23 (Pillai et al., 2005). They reside in the MZ which is constantly exposed to large amounts of blood exiting the circulation via the marginal sinus. There they are perfectly positioned to fulfill their main and very important function, namely to rapidly trap and react to blood-borne pathogens (for detail see 1.3.1.2) (Zandvoort and Timens, 2002). To fulfill this important role a large fraction of MZ B cells carry polyreactive BCRs and express high levels of toll-like receptors (TLR) for a quick recognition of conserved microbial molecular patterns (Bendelac et al., 2001; Martin and Kearney, 2002; Trembl et al., 2007; Gururajan et al., 2007). In addition, they are described to have a pre-activated phenotype (Gunn and Brewer, 2006; Oliver et al., 1999b), the capacity to self-renew (Tarakhovskiy, 1997) and to survive the whole life-span of the host (Hao and Rajewsky, 2001; Pillai et al., 2005; Martin and Kearney, 2002), although it is currently under discussion if their pool is constantly being refilled via their self-renewing capacity or by precursors (Pillai et al., 2005). Next to Fo B and MZ B cells, which represent B-2 cells, another naïve mature B cell population exists in the periphery, referred to as B-1 cells. B-1 B cells, which can further be sub-divided into B-1a and B-1b B cells, are believed to arise early in life and are thought to be mainly derived from fetal liver stem cells (Allman and Pillai, 2008; Dorshkind and Montecino-Rodriguez, 2007). B-1 B cells represent the main

B cell population in the peritoneal and pleural cavities (Allman and Pillai, 2008) and are $CD19^{\text{high}}$, $B220^{\text{low}}$, IgM^{high} , $CD43^+$. Furthermore they express the myeloid marker $CD11b$, yet they lack $CD23$. The two subpopulations B-1a and B-1b can be differentiated by means of their $CD5$ expression. While B-1a cells are positive for $CD5$, B-1b cells are not (Dorshkind and Montecino-Rodriguez, 2007). B-1 cells have like MZ B cells the potential to self-renew (Tarakhovsky, 1997) and both cell types often cooperate with each other in T cell-independent (TI) immune responses (Martin et al., 2001). B-1a and MZ B cells are major sources of natural, mostly IgM^+ , polyreactive antibodies arising without the stimulation by environmental antigens, providing instantaneous protection against for example microbial antigens. These antibodies play a crucial part in protecting the organism in the early phase of infection (Holodick et al., 2014; Casali and Schettino, 1996; Cerutti et al., 2013). Hence, B-1 and MZ B cells are two cell populations playing a pivotal role during the transition from innate to adaptive immune response (more details about this in 1.3.1.2).

1.3 B cell activation and plasma cell development

1.3.1 T cell-dependent and T cell-independent immune reactions

B cells and their ability to differentiate into plasma cells (PCs) producing antigen-specific antibodies, which in turn are able to identify and neutralise invading bacteria or viruses are a crucial mechanism of the humoral arm of adaptive immunity. Depending on the type of antigen, where antigen encounter takes place and which B cell subset and accessory cells are involved, the outcome of the immune reaction differs. B cell activation is generally divided into two different routes: T cell-dependent and T cell-independent immune response. Figure 3 illustrates schematically the different ways of immune reactions described in this chapter.

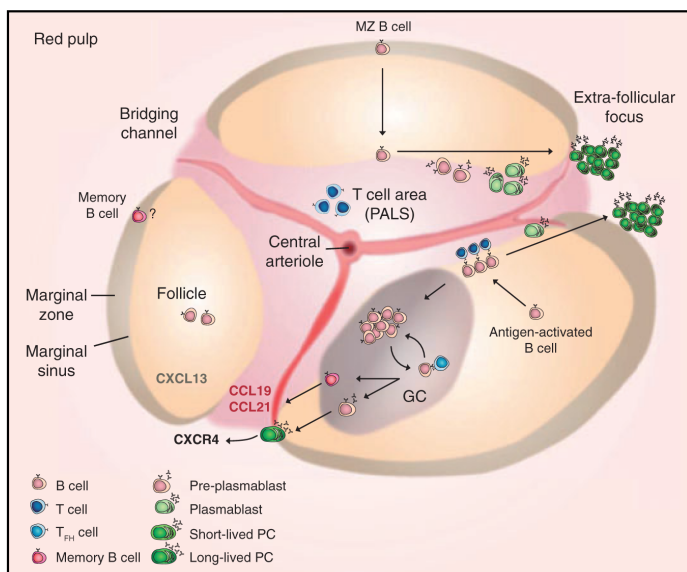


Figure 3: Cross section of the splenic white pulp illustrating the different ways of immune reactions (from Oracki et al., 2010). Antigens entering via the blood circulation activate Fo B and/or MZ B cells, causing their migration towards the T cell area and a subsequent burst of proliferation. MZ B cells - now plasmablasts - then exit the white pulp via the bridging channels and further differentiate into short-lived plasma cells in extra-follicular foci. Fo B cells carrying a BCR with high antigen-affinity continue migrating towards the red pulp, where they also form extra-follicular foci. Fo B cells with a low-affinity BCR re-enter the follicle and form germinal centers (GC), where they undergo further affinity maturation. PALS (periarteriolar lymphoid sheath), PC (plasma cell), T_{FH} cell (T follicular helper T cell).

1.3.1.1 Antigen capturing and presentation

Mature, naïve B cells whose antigen receptor is able to bind an antigen are activated, start to proliferate (clonal expansion) and finally differentiate to plasma cells secreting antigen-specific antibodies (Janeway et al., 2012). B cells bind antigens, when these are tethered to the surface of specialised antigen-presenting cells (APC). Yet, in contrast to T cells, B cells recognise antigens only in their unprocessed native state (Bergtold et al., 2005; Huang et al., 2005). **This means that APCs must either be able to stably immobilise and display antigen on their surface for a longer time or internalise them into non-degrading intracellular compartments for subsequent presentation.** The most important cell populations implicated in antigen capturing and presentation are macrophages, granulocytes (especially neutrophils), DCs and FDCs. They are constantly monitoring the blood and lymphatic fluids for foreign antigens. Most of these antigens are either directly trapped and ingested within SLOs such as the spleen, lymph nodes, Peyer's patches or are captured in the circulation, ingested and then transported to SLOs, where they are presented to B cells (Batista and Harwood, 2009). Macrophages express different receptors enabling them to present unprocessed antigen: MAC1 (macrophage receptor 1), the FcγRIIB (low-affinity receptor for IgG) and SIGN-R1 for example have been shown to be implicated in the internalisation and/or retention of antigen on the cell surface (Phan et al., 2007; Bergtold et al., 2005; Koppel et al., 2005). **The same receptors (SIGN-R1 and FcγRIIB receptor) have been shown to be expressed by DCs (Batista and Harwood, 2009).** Due to technical limitations, antigen presentation to B cells has predominantly been studied in lymph nodes. However, as the spleen exhibits a similar core organisation, mechanisms might resemble each other in both tissues. In lymph nodes, a CD169⁺ macrophage population resides within the follicle just beneath the subcapsular sinus, with processes extending into lymphatic vessels. In this way, antigens can be captured out of the lymphatics and subsequently presented and transferred to Fo B cells. It is conceivable that CD169⁺ macrophages have a similar role in the spleen (Batista and Harwood, 2009; Cyster, 2010). Furthermore, DCs of the lymph nodes have been shown to localise outside the follicle near high endothelial venules, where they can present antigen to passing, circulating Fo B cells entering the lymph nodes (Qi et al., 2006). **In the spleen, mainly MZ macrophages and circulating CD11c⁺ DCs interact with MZ B cells, thereby transferring captured antigen (Balazs et al., 2002; Chen et al., 2005; Kang et al., 2006).** MZ B cells whose BCR is able to bind the antigen can now initiate TI antibody responses and in addition transport the antigens into the follicle, where they are further transferred to FDCs (Chorny et al., 2012; Cinamon et al., 2008). **FDCs are subsequently able to keep these antigens on their surface for longer periods to ensure an efficient encounter of the presented antigen with a cognate Fo B cell (Suzuki et al., 2009).** However, also non-cognate MZ B cells can bind antigens on APCs and due to a constant up- and downregulation of the S1PR1, MZ B cells are continuously shuttling between the MZ and the follicle (Arnon et al., 2013), thereby permanently transferred antigens onto FDCs. Thus, the probability that the antigen is recognised by a cognate Fo B cell is strongly increased. This antigen transfer between MZ B cells and FDCs however is dependent on complement receptors, which are highly expressed on both cell types (Batista and Harwood, 2009). Antigen-activated splenic neutrophils, which localise in peri-MZ regions, can also interact with MZ B cells and thereby trigger antibody production as well as class switch recombination (CSR) and

somatic hypermutation (SHM) involving BAFF and a proliferation-inducing ligand (APRIL) (Puga et al., 2012). Last but not least, within lymph nodes small soluble antigens are believed to be able to gain access to Fo B cells and FDCs by directly entering the follicle via small pores within the subcapsular sinus without the help of any antigen-presenting cell (Pape et al., 2007). Fo B cells subsequently are able to capture antigens directly and in turn present them. However, whether a similar mechanism exists in the spleen is not known so far.

1.3.1.2 T cell-independent immune response

The TI immune response links innate and adaptive immunity and bridges the temporal gap until the production of high-affinity antibodies is initiated by Fo B cells (Martin et al., 2001). **Therefore, it is the first and more rapid, hence still rather unspecific, reaction of the adaptive immune system in response to infectious agents.** It is in large parts accomplished by “innate-like” B-1 and MZ B cells, without the help of T cells and is therefore known as T cell-independent immune response (Martin et al., 2001; MacLennan et al., 2003; Zandvoort and Timens, 2002; Hsu et al., 2006; Haas et al., 2005; Alugupalli et al., 2004). **In contrast to TD immune reactions (see next chapter), it does not involve affinity maturation of the BCR and has a minor role in creating long-lived memory B cells.** TI antigens are further split into TI type 1 and TI type 2 antigens. The typical example for a TI-1 antigen is the cell wall component lipopolysaccharide (LPS) of gram-negative bacteria. TI-1 antigens are mitogens that bind to TLRs and BCRs irrespective of their antigen specificity, thus activating B cells in a polyclonal fashion, thereby inducing proliferation and subsequent differentiation to antibody-secreting plasma cells (Bekeredjian-Ding and Jegou, 2009; Peng, 2005; Minguet et al., 2008). **Type 2 antigens are highly repetitive molecules such as polysaccharides from the cell wall of encapsulated bacteria, viral capsids or polymeric proteins, thereby leading to an extensive cross-linking of antigen-specific BCRs, delivering a persistent signal via Btk (Mond et al., 1995). Artificial TI-2 antigens are typically haptens coupled to ficoll, dextran or acrylamide (Oracki et al., 2010; Elgert, 2009). Activation by these type of antigens triggers the maintenance or upregulation of CXCR4 as well as the downregulation of S1PR1, CXCR5, CCR7 and probably also integrin adhesiveness on B cells (Cinamon et al., 2004; Hargreaves et al., 2001; Lu and Cyster, 2002) enabling them to move to the outer PALS, where they become B cell blasts and undergo clonal expansion, steps involving proliferation and the increase in size. A proportion of this proliferating population will start to secrete antigen-specific antibodies and is then defined as plasmablasts. During all this time, these cells continue to migrate towards the bridging channels following a gradient of the CXCR4 ligand CXCL12 (highly concentrated in the red pulp) to gain access to the red pulp, where they cluster into extra-follicular foci (Wehrli et al., 2001; Hargreaves et al., 2001). Within these foci cells further differentiate into mature plasma cells, which have stopped proliferating and mostly secrete low-affinity IgM and IgG3 (Martin et al., 2001; Ellyard et al., 2005). CD11c^{high} DCs, macrophages or stromal cells secrete the tumor necrosis factor (TNF) receptor ligands BAFF and APRIL, which are essential for the survival and continuous differentiation of plasmablasts and plasma cells (Balazs et al., 2002; Garcia, V et al., 1999a; Garcia, V et al., 1999b). However, these extra-follicular foci soon disperse and thus barely contribute to the long-lasting plasma cell pool (Smith et al., 1996).**

1.3.1.3 T cell-dependent immune response

TD antigens consist of whole cells, viruses, parasites or soluble proteins and do not induce antibody production without T cell help (Stein, 1992). Key players in TD immune responses are Fo B cells, although they have also been shown to respond to TI antigens and to enhance TI immune responses (Swanson et al., 2010). Fo B cells are constantly recirculating through SLOs, where they screen for antigens on the surface of APCs. Those cells that are able to bind antigens with their antigen-specific BCR, ingest, process and present them on major histocompatibility complex (MHC) class II proteins on their surface (Avalos and Ploegh, 2014; Lanzavecchia, 1990; Carrasco and Batista, 2007). This initial antigen induced activation further leads to an upregulation of the ICOS ligand, a co-stimulatory molecule for T cells and the chemokine receptor CCR7 (Pereira et al., 2010; Mak et al., 2003; Tafuri et al., 2001). The latter draws Fo B cells to and makes them align along the B-T cell boundary within the splenic follicle (Reif et al., 2002). Simultaneously, naïve CD4⁺ T cells located within the T cell zone are primed by parts of the same antigen presented by APCs, making them so called armed CD4⁺ helper T (T_H) cells. An upregulation of the chemokine receptor CXCR5 is directing them in the direction of the B cell follicle (Haynes et al., 2007). This orchestrated movement of B and T cells, specific for the same antigen towards each other from different positions greatly enhances the likelihood of their encounter and thus the induction of an adequate immune response (Oracki et al., 2010). The MHC II:peptide complex on the B cell surface can now be recognised by the antigen-specific T cell receptor (TCR) on armed CD4⁺ helper T cells, thereby forming the so called immunological synapse (Duchez et al., 2011). This interaction entails the further production of surface-bound and secreted cues, enabling T_H cells and B cells to activate each other, in the end triggering B cell proliferation and subsequent plasma cell differentiation (Janeway et al., 2012). The most common and important activating molecules expressed by activated T cells are the CD40 ligand (CD40L), a member of the TNF receptor (TNFR) family, which is membrane-bound and binds to the CD40 receptor on B cells (van and Banchereau, 2000; Basso et al., 2004) as well as the secreted cytokine IL-4 (Nelms et al., 1999). At the B-T cell boundary, both B and T cells will proliferate for several days. Subsequently, dependent on the strength of BCR-antigen interaction, Fo B cells can now either enter a germinal center (GC) or form extra-follicular foci (Paus et al., 2006; MacLennan et al., 2003). Fo B cells with a high-affinity BCR will continue proliferating and develop into plasmablasts while migrating towards the red pulp via the bridging channels, where they will form extra-follicular foci. After some days proliferation ceases and the plasmablasts become short-lived plasma cells (MacLennan et al., 2003). Those cells with a low-affinity binding re-enter the follicle to initiate the GC reaction, which is a hallmark of TD immune responses. GCs arise within follicles of SLOs and consist of proliferating B cells, forming a sort of secluded appropriate microenvironment in which they can undergo further proliferation, Ig class switch recombination as well as affinity maturation via somatic hypermutation to ultimately produce antibody-secreting B cells with greater affinity and specificity for the cognate antigen as well as memory B cells (Shlomchik and Weisel, 2012; Honjo et al., 2002). The GC reaction has a pivotal role in contributing to the immunological memory, as the majority of memory B cells and long-lived BM plasma cells are germinal center-derived (Shlomchik and Weisel, 2012; Oracki et al., 2010). In both TD and TI immune responses long-lived plasma cells need to gain access to specialised

niches within the BM, providing them with essential survival signals. Otherwise they would undergo apoptosis within some days (Radbruch et al., 2006).

1.3.2 Fundamental molecular mechanisms in plasma cell differentiation

Two groups of transcription factors antagonising and able to repress each other in their function regulate plasma cell differentiation. Key players of the first group, suppressing plasma cell development are Pax5 and B cell lymphoma 6 protein (Bcl6), whereas members of the second group such as B lymphocyte-induced maturation protein 1 (Blimp-1), interferon regulatory factor 4 (Irf4) and X-box binding protein 1 (Xbp1) drive plasma cell development (Shapiro-Shelef and Calame, 2005). Pax5 has a major role in establishing and maintaining B cell identity, and its target genes are associated with important B cell functions such as immunoglobulin gene rearrangement and BCR signalling (CD19, CD79a and B-cell linker (BLNK)) (Schebesta et al., 2007). **At the same time it inhibits gene transcription essential for plasma cell development (Oracki et al., 2010; Nutt et al., 2001; Nera and Lassila, 2006). Bcl6 has been shown to be necessary for GC formation and its crucial function in this context consists in inhibiting further differentiation of B cells to low-affinity, short-lived plasma cells by repressing Blimp-1 (Shaffer et al., 2000; Reljic et al., 2000). So, for efficient and productive plasma cell development it is not sufficient to upregulate plasma cell-specific genes, but concomitantly the B cell gene expression program needs to be downregulated. Blimp-1 fulfills both roles as it represses mature B cell genes such as *pax5*, *spiB*, *CIITA* as well as genes of the GC program such as *bcl6* and activation-induced cytidine deaminase (*aiida*) (Lin et al., 2002; Lin et al., 1997; Martins and Calame, 2008; Sciammas and Davis, 2004; Shaffer et al., 2002). At the same time it induces a gene which is also pivotal for plasma cell development and especially for later antibody secretion, namely *xbp1*, which activates genes of the secretory pathway (Shaffer et al., 2002; Shaffer et al., 2004). Beyond this, Blimp-1 leads to the upregulation of CXCR4, which guides plasmablasts to the red pulp where they can further develop to fully mature plasma cells (Sciammas and Davis, 2004). MZ B and B-1 cells express higher Blimp-1 levels than Fo B cells, which allows them to develop into plasma cells and hence react to pathogens more rapidly (Fairfax et al., 2007). However, although Blimp-1 is indispensable for the full differentiation of plasma cells and their longterm maintenance, it is not needed for its initiation (Kallies et al., 2004; Shapiro-Shelef and Calame, 2005; Kallies et al., 2007). Irf4 is, like Blimp-1, highly expressed in plasma cells and necessary for their development. Yet, in contrast to Blimp-1, Irf4 is quite likely to play a critical part in the initiation phase of plasma cell development and to precede Blimp-1 expression, as it has been shown to induce Blimp-1, and Irf4-deficient B cells are devoid of the entire Blimp-1-dependent plasma cell program (Klein et al., 2006; Sciammas et al., 2006). Transient Irf4 expression is known to induce the GC reaction, whereas sustained and higher Irf4 concentrations lead to plasma cell differentiation at the expense of GC formation (Ochiai et al., 2013). Another factor possibly implicated in the initiation of the plasma cell program is the microphthalmia-associated transcription factor (Mitf), which negatively regulates Irf4, as Mitf knockout mice exhibit spontaneous plasma cell formation, which can be reverted by an Irf4 knockdown (Lin et al., 2004). Next to these key players there are various other factors known to be implicated in the regulation of plasma cell differentiation (reviewed in Oracki et al., 2010; Shapiro-Shelef and Calame, 2005).**

There are different steps in plasma cell development characterised by varying levels of specific surface markers and changes in transcription factor activity (Fig. 4). Yet, mature plasma cells typically have low levels of CD19, B220, MHC class II, CD79, CD5, CD86, CD21, CD22 as well as surface Ig and increased levels of Syndecan-1 (CD138), CD9, CD43 and CD93 (Smith et al., 1996; Lalor et al., 1992; Fairfax et al., 2008).

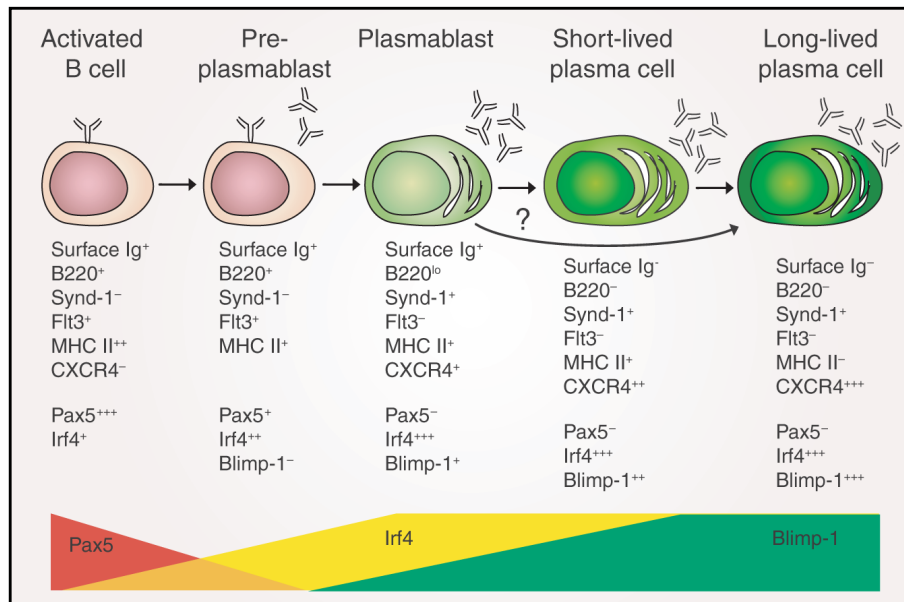


Figure 4: Expression of surface markers and transcription factors during plasma cell development (taken from Oracki et al., 2010). The different stages of plasma cell development can be identified according to the expression of some specific surface markers. Depending on the differentiation stage, the levels of the transcription factors Pax5, Irf4 and Blimp-1 may change considerably.

1.4 Notch receptor signalling

1.4.1 The structure and activation of Notch receptors

The Notch signalling pathway is evolutionary highly conserved and can be found in most multicellular organisms as diverse as nematodes and mammals (Radtke et al., 2010). It is named after the Notch receptor gene, which was first discovered 1917 by Thomas Hunt Morgan due to an altered, “notched” phenotype in the wings of fruit flies (Morgan, 1917). Later on, a loss of function of the *Drosophila Notch* gene, which was cloned in the mid eighties, was found to be responsible for that phenotype (Kidd et al., 1986; Wharton et al., 1985). Notch signalling plays amongst others an important role in the regulation of cell survival and proliferation, cell fate decisions and cell differentiation in a wide variety of biological systems from embryonic to adult life (Alberi et al., 2013; Fortini et al., 2014; Zanotti and Canalis, 2013; Koch et al., 2013; Noah and Shroyer, 2013; Fouillade et al., 2012; Perrimon et al., 2012). Mammals possess four different members (Notch1, 2, 3, 4) of the Notch family of transmembrane receptors and five different ligands of the Delta-like (Dll) or Jagged family (Dll1, 3, 4, and Jagged1, 2) (Fig. 5). Receptors and ligands of adjacent cells are able to interact with each other, thereby inducing the Notch signalling cascade (Bray, 2006). Notch receptors are heterodimers that belong to the group of single-pass type I transmembrane receptors. They consist of an extracellular domain (NotchEC) at the N-terminus containing epidermal growth factor (EGF)-like repeats that mediate ligand

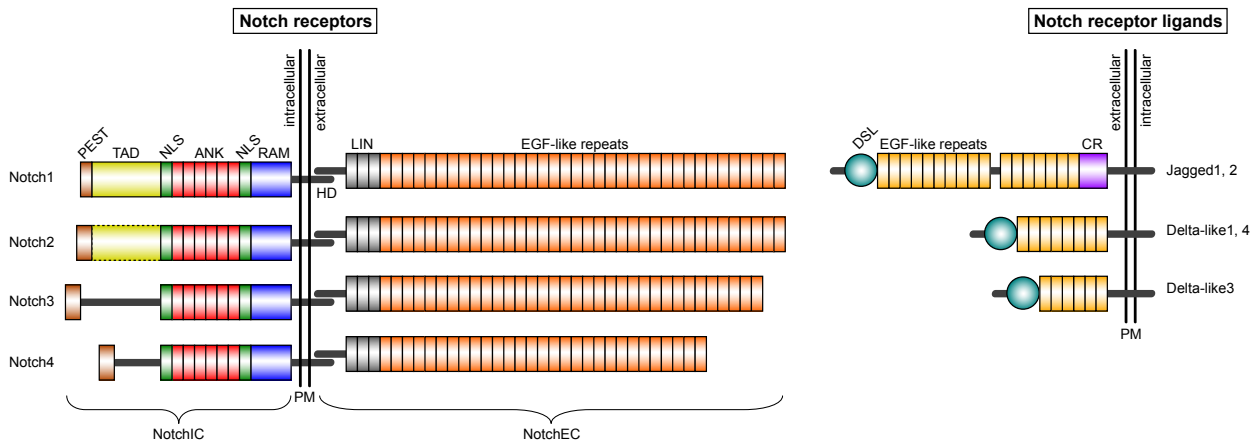


Figure 5: Notch receptors and their ligands (adapted from Radtke et al., 2010). Mammals have four Notch receptors (Notch1-4) and five different ligands: Jagged1, 2 and Delta-like (DII) 1, 3 and 4. All ligands typically carry an amino-terminal domain called DSL (Delta, Serrate and Lag2), responsible for receptor binding followed by epidermal growth factor (EGF)-like repeats. In Jagged1 and 2, a cysteine-rich domain (CR) is located close to the plasma membrane (PM) downstream of the EGF-like repeats. The receptors also carry EGF-like repeats in their extracellular domains (NotchEC, mediating ligand-binding), followed by three cysteine-rich LIN domains - inhibiting ligand-independent activation - and the heterodimerisation domain (HD). The cytoplasmic part (NotchIC) consists of a RAM domain, six ankyrin repeats (ANK), which bind to the transcription factor RBP-J κ , two nuclear localisation signals (NLS), a transactivation domain (TAD, only in Notch1 and 2) and a proline-glutamine-serine-threonine-rich (PEST) sequence regulating protein stability.

binding, three cysteine rich LIN12-Notch repeats (LNR) that prevent ligand-independent activation and the heterodimerisation domain made of a hydrophobic stretch of amino acids (Fig. 5) (Kopan and Ilagan, 2009). This NotchEC is non-covalently conjoined to the C-terminal part of the Notch receptor consisting of an extracellular heterodimerisation (HD), a transmembrane (NotchTM) and a cytoplasmic intracellular domain (NotchIC) (Blau Mueller et al., 1997; Logeat et al., 1998; Kopan and Ilagan, 2009). The cytoplasmic, intracellular part NotchIC mediates signal transduction and comprises a RAM domain, six ankyrin repeats (ANK) necessary for the binding to the transcription factor CSL/RBP-J κ (CBF in human, *Suppressor of Hairless* in *Drosophila*, *Lag1* in *C. elegans*, RBP-J κ in mice), two nuclear localisation signals (NLS), a transactivation domain (TAD) as well as a proline-glutamine-serine-threonine-rich (PEST) domain, which is implicated in protein stability (Fig. 5) (Gordon et al., 2008; Radtke et al., 2010). When Notch signalling is triggered by receptor-ligand interaction between neighbouring cells (Fig. 6), two proteolytic cleavage steps are induced. At first, metalloproteases of the ADAM family, probably ADAM10 or 17, cleave Notch extracellularly, thereby leaving the shedded NotchEC to endocytosis by the ligand-expressing cell. The second cleavage step is effected within the transmembrane domain, thus liberating the intracellular part of the Notch receptor (NotchIC) and is mediated by the γ -secretase (GS) activity of a multiprotein complex (Fig. 6). NotchIC can now translocate into the nucleus, where it interacts with the DNA binding protein and transcriptional repressor CSL/RBP-J κ . Subsequently other co-activators are recruited such as mastermind proteins (MAML1-3) and the MED8-mediator transcription activation complex thereby abolishing repression and inducing the transcription of Notch target genes (Fig. 6) (Radtke et al., 2010). A great number of genes can directly be regulated by Notch (Palomero et al., 2006; Hamidi et al., 2011; Weng et al., 2006) amongst which the most prominent target genes are members of the hairy enhancer of split (*Hes*) or hairy related genes (*Hey*). Notch signalling is regulated at multiple levels (reviewed in Bray, 2006;

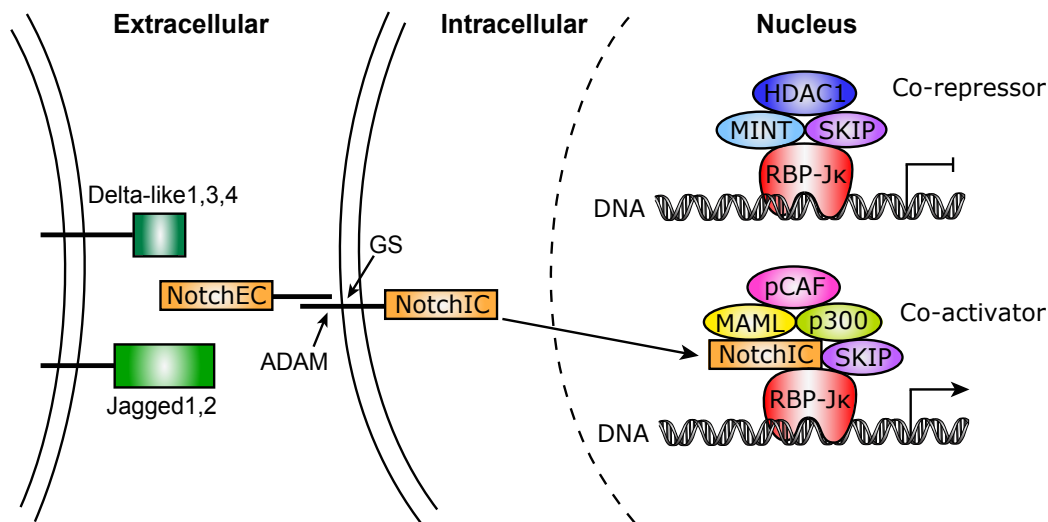


Figure 6: Notch receptor activation. The interaction of Notch-specific ligands with the extracellular part of the Notch receptors on neighbouring cells induces two sequential proteolytic cleavage steps. First, Notch is cleaved extracellularly by metalloproteases of the ADAM family, while the γ -secretase (GS) cleaves it within the transmembrane domain. The now freed intracellular part of the receptor (NotchIC) can translocate into the nucleus, where it displaces the co-repressor complex consisting of SKIP (Ski-interacting protein), MINT (Msx2-interacting nuclear target protein) and HDAC1 (histone deacetylase 1) by interacting with the transcription factor RBP-Jk and further recruiting a co-activator complex consisting of MAML (mastermind-like), p300, pCAF (p300-associated factor) and SKIP. In this manner the transcription of Notch target genes is induced.

Kopan and Ilagan, 2009). Restricting the expression of Notch receptors or their ligands to a specific cell-type or in a spatial or temporal manner represents one of them (Besseyrias et al., 2007; Santos et al., 2007; Radtke et al., 2004). Furthermore, ligand-receptor interaction is regulated by posttranslational modification. The Fringe glycosyltransferase for example facilitates Notch signalling induced by Delta ligands, while simultaneously inhibiting Jagged-mediated signalling by adding *N*-acetylglucosamine to some EGF-like repeats (Haines and Irvine, 2003; Moloney et al., 2000; Besseyrias et al., 2007). Another way of controlling Notch signalling is by regulating its half-life. Once NotchIC is released into the nucleus, it is quite rapidly subjected to ubiquitin-dependent proteasomal degradation executed via its PEST domain, thereby stopping further transcription of Notch regulated genes (O'Neil and Look, 2007; Deimling et al., 2007). Furthermore, Notch signalling can be negatively regulated, for example via the MINT (Msx2-interacting nuclear target) repressor protein, which competes with NotchIC for the interaction with CSL/RBP-Jk (Kuroda et al., 2003). Notch belongs to the rare group of genes in diploid organisms that display haploinsufficiency, meaning that one copy of the gene is not enough to generate sufficient gene product. Hence, the organism is quite sensitive to changes in gene dosage. Haploinsufficiency of Notch2 or Jagged1 for example has been shown to lead to Alagille's syndrome (Oda et al., 1997; McDaniell et al., 2006), whereas reduced Notch1 signalling is associated with a special type of aortic disease (Garg et al., 2005). Amplification or overexpression of Notch on the other hand is mainly cancerogenic (for detail see 1.4.4) Thus, it seems that not only the type of receptor-ligand interaction determines the outcome of Notch signalling, but also the cellular context and the signalling strength.

1.4.2 Notch signalling in lymphocytes

In lymphocytes, predominantly Notch1 and Notch2 are expressed, where they fulfill non-redundant functions. Nevertheless, the implication of Notch, especially Notch1 in T cell lineage commitment and development is the best-characterised function of these receptors in hematopoiesis. Inactivation of Notch1 or RBP-J κ in early lymphocyte progenitors of the BM leads to a block in T cell development and at the same time to the emergence of an ectopic B cell population in the thymus (Han et al., 2002; Radtke et al., 1999). Overexpression of Notch1 in these progenitors on the other hand culminates in ectopic T cell development in the BM accompanied by a block in B cell development at the pro-/pre-B cell stage (Pui et al., 1999). This data clearly demonstrates that Notch1 is necessary and sufficient to induce T cell development. Furthermore, Notch1 is continuously required for $\alpha\beta$ T cells development up to the double negative stage 3, whereas it seems dispensable for $\gamma\delta$ T cells (Wolfer et al., 2002). Together with the signalling via the pre-TCR it is essential for successful β -selection, after which it is downregulated (Ciofani et al., 2006; Maillard et al., 2006; Allman et al., 2001a). Early B lymphocytes in the BM express both Notch1 and Notch2, whereas Notch2 is the predominant receptor on mature B cells, with highest expression levels in MZ B cells and their precursors. Notch2 is expendable for T cell development, yet it is crucial for MZ B cell development (Walker et al., 2001; Saito et al., 2003; Witt et al., 2003; Tan et al., 2009). Expression of different levels of a constitutively active Notch2 receptor in hematopoietic stem cells by means of a retrovirus revealed that high Notch2 levels led to the development of a strongly proliferating T cell population in the BM, while lower Notch2 expression levels blocked B-2 B cell development at the large pre-B cell stage and enhanced splenic B-1 B cell differentiation (Witt et al., 2003).

1.4.3 Notch in MZ B cell development

Notch2 is an indispensable key player in MZ B cell development and this has clearly been confirmed by analysing various different mouse models. Mice with B cell-specific ablations of Notch2 or RBP-J κ (Saito et al., 2003; Tanigaki et al., 2002) as well as mice with deletions of Mastermind-like 1 (MAML1) (Wu et al., 2007; Oyama et al., 2007), ADAM10 (Gibb et al., 2010) or Delta-like 1 (Hozumi et al., 2004) all reveal defects in MZ B cell development, while the generation of Fo B cells is not affected. Constitutively active Notch2 signalling shifts nearly all B cells to the MZ B cell compartment even in the absence of CD19 (Hampel et al., 2011). Furthermore, inactivation of MINT, a suppressor of Notch, results in an increase in MZ B cells (Kuroda et al., 2003). The ligand which is crucial for MZ B cell differentiation is Dll1, mainly found on endothelial cells of the splenic red pulp and in the MZ. T2 B cells with a strong Notch2 signalling are believed to be guided to the MZ, where the initially rather weak binding between Notch2 and Dll1 is strengthened by the two glycosyltransferases lunatic and manic fringe inducing them to differentiate into MZBPs (IgM^{high} IgD^{high} CD21^{high} CD1d^{high} CD23⁺) and hence into MZ B cells (Tan et al., 2009; Allman and Calamito, 2009). Furthermore, it seems necessary that Dll1 is endocytosed by the ligand-expressing cell after binding, as deficiencies in the E3 ubiquitin ligase Mindbomb1 (MIB1) also impair MZ B cell development (Song et al., 2008). Although Notch2 is clearly an essential part during MZ B cell differentiation, its interplay with other signalling pathways is probably a prerequisite for the generation of mature, functional MZ B cells correctly located in the MZ.

1.4.4 Notch signalling in lymphoma and other malignancies

The oncogenic potential of mammalian Notch was for the first time discovered in 1991, when in a subset of T cell acute lymphoblastic leukemia (T-ALL) patients a chromosomal translocation - later named TAN1 (translocation-associated Notch homologue) - was revealed resulting in an overexpressed constitutively active Notch1 receptor (Ellisen et al., 1991). Subsequent studies disclosed that within the hematopoietic system, deregulated Notch signalling seems particularly oncogenic for T cells (Pear et al., 1996). Weng and colleagues as well as Aster and colleagues could show that 50 % of all human T-ALLs and 55 % of pediatric primary T-ALL tumors had activating mutations of the Notch1 gene (Weng et al., 2006; Aster et al., 2008). In addition, not only constitutive active Notch1, but also Notch2 and 3 have been shown to lead to T cell leukemias (Tzoneva and Ferrando, 2012; Pui et al., 1999; Bellavia et al., 2000; Rohn et al., 1996). Apart from that, altered Notch signalling has up to now also been associated with different B cell malignancies such as mantle cell lymphoma (MCL) (Kridel et al., 2012), diffuse large B cell lymphoma (DLBCL) (Lee et al., 2009), splenic marginal zone lymphoma (SMZL) (Troen et al., 2008; Kiel et al., 2012; Rossi et al., 2012), Hodgkin lymphoma (Jundt et al., 2002; Jundt et al., 2004) and B cell chronic lymphocytic leukemia (B-CLL) (Hubmann et al., 2002; Gianfelici, 2012; Rosati et al., 2009) and reviewed in (Rossi et al., 2012; South et al., 2012; Roy et al., 2007; Koch and Radtke, 2007; Bolos et al., 2007; Hopfer et al., 2005). In these B cell malignancies, most types of defects in Notch signalling in some way affected the PEST domain of the receptors itself or inhibitory interaction partners of Notch, thereby leading to impaired degradation or inhibition and hence to sustained or enhanced Notch signalling. However, it is also known that Notch can, depending on the cellular context, also act as a tumor suppressor. In the skin, for example, Notch clearly has a tumor suppressive role, as various skin cancers are linked to a knockout of the *notch1* gene (Nicolas et al., 2003) and reviewed in (South et al., 2012). Yet in summary, it seems that the interplay between Notch and other signalling cascades as well as the cellular context, determine the outcome and effect of Notch signalling with regard to cellular differentiation, induction of apoptosis or rather proliferation and hence possibly tumor formation.

1.5 Model systems

In this work the Notch2IC-transgenic mouse line (Hampel et al., 2011) and a mouse strain carrying a truncated Notch2 receptor (Besseyrias et al., 2007) were used. The following section will give a brief overview of the generation of these mice and results that are already published.

1.5.1 The Notch2IC-transgenic mouse strain

1.5.1.1 Generation

To investigate the influence of constitutive Notch2 signalling on B cell development, activation and lymphomagenesis in vivo, the conditional transgenic mouse strain Notch2IC^{fSTOP} was generated in our research group. By using the *Cre/loxP* system a ligand-independent, thus constitutively active expression of the intracellular part of the Notch2 receptor (Notch2IC) could be achieved. The details of the targeting strategy are described in (Hampel et al., 2011). A schematic illustration is depicted in figure 7.

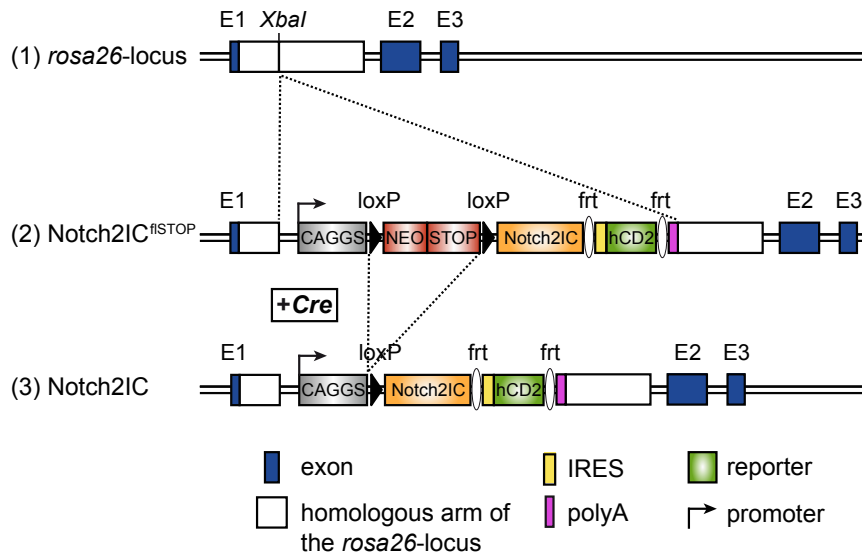


Figure 7: Targeting strategy for the generation of Notch2IC-transgenic mice. The conditional *notch2IC* allele (*notch2IC^{fSTOP}*) and an *IRES-hCD2* coding sequence as a reporter were both inserted into the murine *rosa26*-locus. A loxP-flanked transcription and translation termination sequence (STOP cassette) was placed upstream of the *notch2IC* coding sequence. (1) Wild type *rosa26*-locus with its three exons and the *XbaI* restriction site within the first intron, where the transgene was inserted; (2) the *rosa26*-locus after successful homologous recombination, now harbouring the targeting construct (*Notch2IC^{fSTOP}*); (3) the *rosa26*-locus after successful homologous recombination and deletion of the STOP cassette via *Cre*-mediated recombination (*Notch2IC*), leading to the expression of *notch2IC* under the control of the constitutive active CAGGS promoter. The dotted lines represent homologous and *Cre*-mediated recombination events. CAGGS (CMV early enhancer/chicken β -actin/rabbit globin promoter); STOP (STOP cassette); hCD2 (truncated human CD2); NEO (neomycin-geneticin resistance gene); *Cre* (*Cre* recombinase) loxP (locus of X-over P1); frt (flippase recognition target sites).

1.5.1.2 Phenotype

The detailed phenotypical characterisation of the *Notch2IC*-transgenic mouse line has already been described (Hampel et al., 2011). In brief, B cell-specific expression was achieved by breeding *Notch2IC^{fSTOP}* mice to *CD19-Cre^{+/-}* mice. Expression of the *Cre*-recombinase controlled by the endogenous CD19 promoter led to a deletion efficiency of 17 % in B cells of the bone marrow and of 79 % in splenic B cell populations (Hampel et al., 2011). *CD19-Cre*-induced conditional expression of *Notch2IC* resulted in a slight splenomegaly (1.5-fold), with normal T and B cell numbers in these animals. However, the most obvious phenotype was an induction of a strong differentiation towards MZ B cells at the expense of the Fo B cell population. *Notch2IC*-expressing MZ B cells thereby reflected the phenotype and biological behaviour of wild type (wt) MZ B cells with respect to their localisation in the MZ, expression of characteristic surface markers and their pre-activated state. For simplicity, mice carrying one *notch2IC* and one *CD19-Cre* allele will be referred to as *Notch2IC//CD19Cre^{+/-}*, whereas mice with two *CD19-Cre* alleles will be referred to as *Notch2IC//CD19Cre^{+/+}*.

1.5.2 The Notch2-deficient mouse strain

1.5.2.1 Generation

Another approach to clarify the role of *Notch2* signalling in MZ B cell development and immune response was the generation of a mouse strain enabling a conditional ablation of *Notch2* signalling specifically in B cells. To this end, a targeting vector based on the genomic DNA fragment of the murine

notch2-locus including exons b to h and the 5'-part of exon i (according to the nomenclature described in Hamada et al., 1999; coding for the transmembrane and intracellular part of the Notch2 receptor) was used. The two endogenous exons d and e (coding for the C-terminal part of the RAM23 domain and the nuclear localisation sequence) were flanked by loxP sites, allowing a *Cre*-mediated excision of this functional intracellular part of the Notch2 receptor. Figure 8 shows a schematic illustration of the targeting strategy.

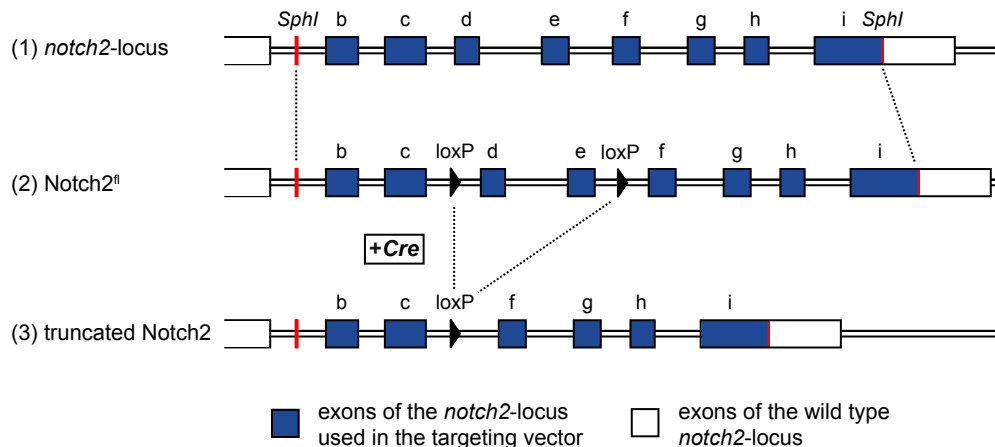


Figure 8: Targeting strategy for the generation of B cell-specific Notch2-deficient mice. A targeting vector based on a genomic DNA fragment of the murine *notch2*-locus including exons b to h and the 5'-part of exon i (coding for the transmembrane and intracellular part of Notch2) were inserted into the murine wild type *notch2*-locus. Within the construct, exons d and e (coding for the C-terminal part of the RAM23 domain and the nuclear localisation sequence) were flanked by loxP sites. (1) Wild type *notch2*-locus with its exons and the *SphI* restriction sites before exon b and within exon i, where the transgene was inserted; (2) the *notch2*-locus after successful homologous recombination, now harbouring the targeting construct (*Notch2^{fl}*); (3) the *notch2*-locus after successful homologous recombination and deletion of exons d and e via *Cre*-mediated recombination (*Notch2^Δ*), leading to the expression of a truncated, non-functional Notch2 receptor. The dotted lines represent homologous and *Cre*-mediated recombination events. Exons marked in blue belong to the targeting vector, whereas white exons belong to the wild type locus. *Cre* (*Cre* recombinase), loxP (locus of X-over P1).

1.5.2.2 Phenotype

The B cell-specific ablation of Notch2 signalling was achieved by breeding *Notch2^{fl/fl}* mice to *CD19-Cre^{+/-}* mice. Mice carrying two *notch2^{fl}* transgenes and one *CD19-Cre* allele will be referred to as *Notch2^{fl/fl}/CD19Cre^{+/-}*. *Cre*-mediated deletion of the two exons d and e of the *notch2* gene led to the expression of a truncated Notch2 protein, lacking the functional, intracellular part. B cell-specific truncation of the Notch2 receptor resulted in the ablation of MZ B cell development. As *notch2* belongs to the genes displaying haploinsufficiency heterozygous *Notch2^{wt/fl}/CD19Cre^{+/-}* mice already exhibited the typical phenotype, characterised by a lack in MZ B cells (see chapter 3.3.4). In accordance, in immunohistological analyses no IgM⁺ MZ B cells could be detected outside of the marginal sinus lined by MOMA-1⁺ macrophages (see chapter 3.3.4).

2. Aim

Notch2 signalling is critical for MZ B cell differentiation, and increased Notch activity has been implicated in the development of various types of lymphomas. To investigate the influence of a constitutively active Notch2 signal or a constitutive Notch2 ablation on B cell development, activation and lymphomagenesis *in vivo*, two transgenic mouse strains were generated in our research group expressing either conditionally a constitutively active or a truncated Notch2 receptor dependent on the *Cre/loxP* system. B cell-specific expression of the intracellular part of the Notch2 receptor (Notch2IC) resulted in an expansion of MZ B cells, whereas truncation of the Notch2 receptor resulted in a lack of the MZ B cell population, underlining the central role of Notch2 in the development of MZ B cells.

To learn more about the contribution of Notch2 signalling to the biology of MZ B cells on a large scale, differences and similarities between wild type and Notch2IC-expressing MZ B cells as well as between wild type and Notch2-deficient Fo B cells were to be investigated by whole mouse-genome gene expression profiling analyses. By this approach we intended to distinguish Notch2-regulated genes from those influenced by the cell-type identity or cellular environment.

Compared to control B cells, Notch2IC-expressing cells exhibited enhanced proliferation after LPS or α -CD40 stimulation and enhanced Akt, Erk, Jnk signalling. As MZ B cells are known to exhibit an activated phenotype and an increased proliferation potential compared to other B cell types, we aimed at figuring out whether enhanced proliferation and signalling of Notch2IC-expressing cells is an MZ B cell intrinsic phenotype or further increased by constitutive Notch2IC expression. Furthermore, we planned to investigate whether the MZ B cell phenotype and the increased activity of signalling pathways is induced by constitutive Notch2 expression or the MZ environment.

MZ B cells are key players in T cell-independent immune responses. Yet, it is still unknown if and how Notch2 signalling is implicated in this type of immune reaction. To get deeper insights into the role of Notch2 in B cell activation and its regulation during immune responses, the TI immune reaction was to be explored in Notch2IC//CD19Cre^{+/-} and Notch2-deficient mice.

Activating mutations in the Notch signalling pathway have been described in several B cell lymphomas, in particular in splenic marginal zone lymphomas. Notch2IC-expressing B cells displayed increased activation and c-Myc expression as well as enhanced proliferation in comparison to control B cells. Hence, we suspected that these mice might develop MZ B cell lymphomas due to the strong Notch2 activity and hence expansion of MZ B cells. To investigate this, cohorts of Notch2IC//CD19Cre^{+/-} and control mice were to be aged and analysed for lymphoma development.

3. Results

3.1 Comparison of gene expression profiles of Notch2IC-expressing MZ B and Notch2-deficient Fo B cells with wild type MZ B and Fo B cells

The spleen comprises two main, mature B cell populations, MZ B and Fo B cells, which are distinct in their function, frequency, localisation, the expression of characteristic surface markers as well as in their activation state (for detail see chapter 1). Notch2 signalling plays a pivotal role regarding the decision whether Fo B or MZ B cells develop (see 1.4.3). Mice carrying a B cell-specific Notch2 ablation have no MZ B cells, whereas other B cell populations are not affected (Saito et al., 2003; Besseyrias et al., 2007). On the other hand, constitutive, ligand-independent, B cell-specific expression of the intracellular part of Notch2 (Notch2IC) leads to a strong expansion of the MZ B cell population at the expense of Fo B cells (Hampel et al., 2011). In addition to MZ B cell differentiation, Notch2 signalling is presumably also implicated in positioning MZ B cells and their precursors in the MZ and it is assumed that MZ B cell precursors need to reside at least a certain time in the MZ to become mature MZ B cells (Tan et al., 2009; Simonetti et al., 2013). To learn more about Notch target genes in B cells, we aimed to investigate which genes are differentially regulated in Notch2IC-expressing B cells in contrast to Notch2-deficient B cells and how closely related they are to their respective wild type counterparts. By this approach we also aimed at differentiating between genes controlled by Notch2, from genes that are regulated by the cell-type identity and hence possibly by the environment surrounding Fo B or MZ B cell populations.

3.1.1 The experimental setting - Illumina BeadChip micorarrays

As our research group has the Notch2^{fl/fl}//CD19Cre^{+/-} and Notch2IC//CD19Cre^{+/-} mouse strains as well as wild type mice at hands, we were able to generate and assess whole mouse-genome gene expression profiles of Fo B cells from Notch2^{fl/fl}//CD19Cre^{+/-} mice, Notch2IC-expressing MZ B cells as well as wild type Fo B and MZ B cells using Illumina BeadChip microarrays. A schematic outline of the experimental workflow of the conducted microarray hybridisation experiments using Illumina BeadChips is depicted in figure 9. In total, splenic B cells of six Notch2^{fl/fl}//CD19Cre^{+/-} and five Notch2IC//CD19Cre^{+/-} mice were sorted for Fo B cells and MZ B cells respectively (Fig. 10). In addition splenic B cells of 21 control mice were sorted for both cell populations (Fig. 10). To this end, splenic B cells were stained and sorted according to their CD21 and CD23 expression, with MZ B cells being CD21^{high} CD23^{low} and Fo B cells CD21^{low} CD23^{high} (Fig. 11). Notch2IC//CD19Cre^{+/-} cells were additionally gated on hCD2⁺ lymphocytes. Sorted cell populations were recovered with an average purity of 97 to 98 % of lymphocyte-gated cells. Figure 11 shows exemplary dot plots displaying frequencies of both B cell populations, gating and purity before and after the sorting procedures. Total RNA of just purified cell populations was isolated after sorting. Its quality and quantity was assessed and only samples exhibiting an intact ribosomal RNA species of good quality (Fig. 12A) were used in cRNA amplifications.

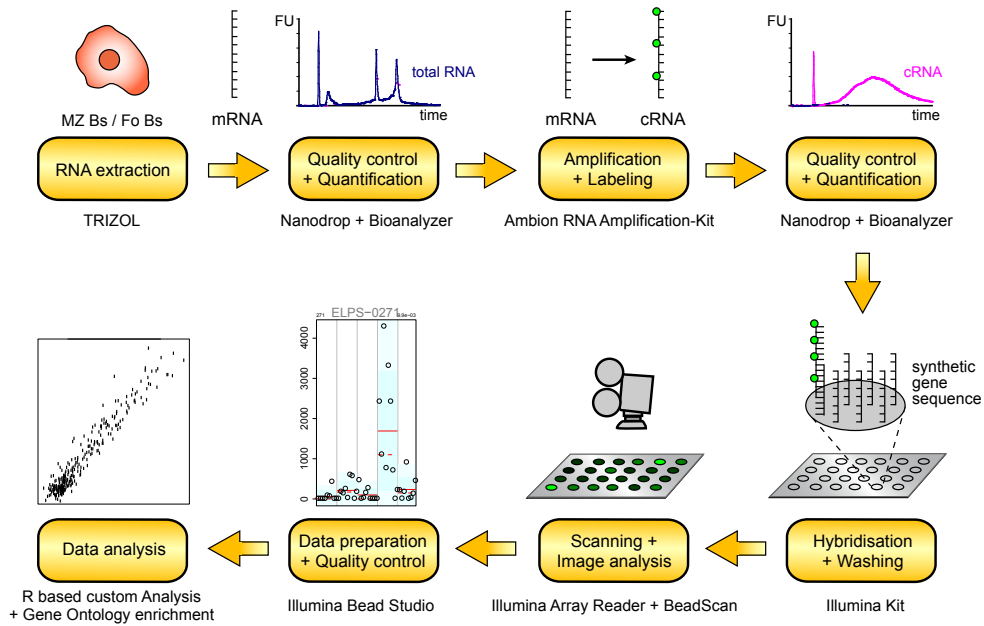


Figure 9: Schematic workflow of a whole mouse-genome gene expression profiling assay using Illumina BeadChip arrays. Desired B cell populations were sort-purified using fluorescence-activated cell sorting (FACS) and total RNA was subsequently extracted. The quality, integrity and quantity of the gained RNA was examined utilising a Nanodrop 2000 and an Agilent 2100 Bioanalyzer. Total RNA was then amplified and at the same time labeled with biotinylated nucleoside triphosphates (NTP) for later detection. Similar as before the generated so called biotinylated copy RNA (cRNA) underwent quality control and quantification. cRNAs were then hybridised onto Illumina BeadChip arrays and finally signal detection and subsequent data analyses were performed.

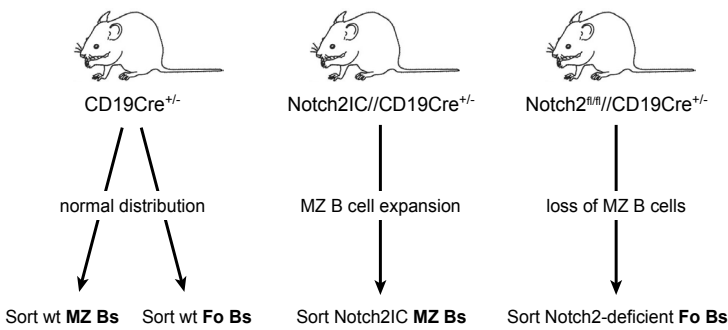


Figure 10: Sorted cell populations and experimental groups for gene expression profiling analyses. MZ B and/or Fo B cells were sort-purified from Notch2IC//CD19Cre^{+/-}, Notch2^{fl/fl}//CD19Cre^{+/-} and CD19Cre^{+/-} mice. Subsequently samples exhibiting the best quality and highest RNA amounts were placed on Illumina BeadChip arrays for the comparison of whole mouse-genome gene expression profiles.

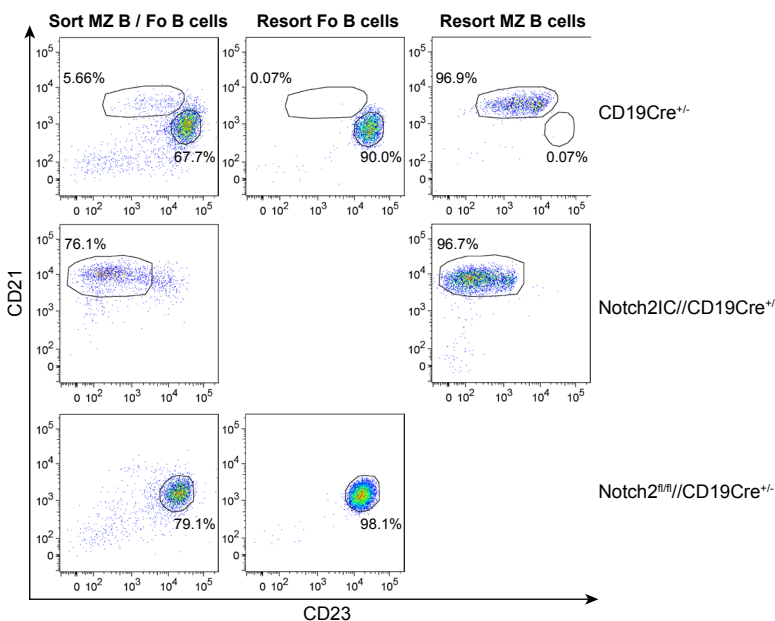


Figure 11: Exemplary dot plots from sorting experiments depicting splenic B cell populations before and after the FACS sorting procedure. Splenic cells from CD19Cre^{+/-} control mice, Notch2IC//CD19Cre^{+/-} and Notch2^{fl/fl}//CD19Cre^{+/-} mice were sorted for MZ B and/or Fo B cell populations via CD21 and CD23 expression. Depicted dot plots are pre-gated on Thy1.2⁺, B220⁺, and in the case of Notch2IC-expressing cells, additionally on hCD2⁺ lymphocytes. During sorting either CD21^{high} CD23^{low} MZ B cells and/or CD21^{low} CD23^{high} Fo B cells were sort-purified. Sorting was performed with an average purity of 97 to 98 % of lymphocyte-gated cells.

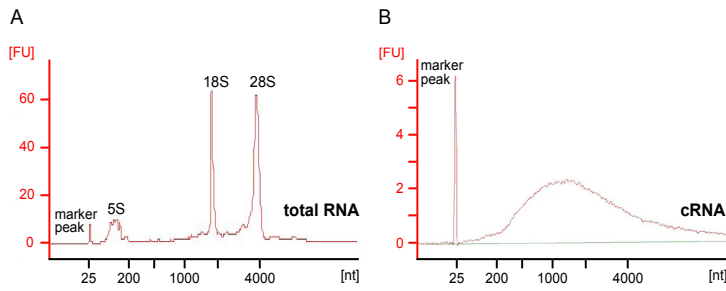


Figure 12: Examples of Bioanalyzer graphs of total RNA and cRNA samples of high integrity and quality. MZ B cells from a Notch2IC//CD19Cre^{+/-} mouse were sort-purified. Total RNA was subsequently isolated and subjected to cRNA amplification. RNA quality and integrity was measured on a Bioanalyzer before (A) and after amplification (B). 5S, 18S and 28S peaks represent the subunits of eukaryotic ribosomal RNA.

RNA samples of six Notch2^{fl/fl}//CD19Cre^{+/-}, five Notch2IC//CD19Cre^{+/-} and 15 control mice were subjected to two independent cRNA amplification rounds. To minimise technical bias introduced by the different amplification batches, which might later on influence the identified differences in gene expressions, samples from the four different cell populations were equally distributed between both amplification rounds. In the end, the 24 best cRNA samples (based on amplification-yield and quantity, Fig. 12B) were placed on the Illumina BeadChip arrays, comprising five samples of sorted Notch2-deficient Fo B cells, five samples of sorted Notch2IC-expressing MZ B cells as well as seven samples of wild type MZ B cells and Fo B cells respectively. Here again, sample randomisation and alternating processing between the experimental groups was applied in order to avoid technical bias and hence falsifying subsequent gene expression profiles gained by group comparisons. Scanning of the Illumina BeadChip arrays and subsequent quality control (QC) analyses, background removal, Variance Stabilising Normalisation (VSN), scatterplots, hierarchical clustering and Principal Component Analyses (PCA) as well as statistical analyses were performed by or in cooperation with Dr. Peter Weber from the MPI of Psychiatry. Figure 13 gives an schematic outline of the analytical workflow performed on microarray data.

Quality controls, which were directly performed after BeadChip scanning yielded overall good results. Yet two outliers (one CD19Cre^{+/-} MZ B cell sample and one Notch2IC//CD19Cre^{+/-} MZ B cell sample) could be detected, which had to be removed from all subsequent analyses (Fig. 14). For all the remaining samples fulfilling QC criteria a threshold was set (p -detection < 0.05 in at

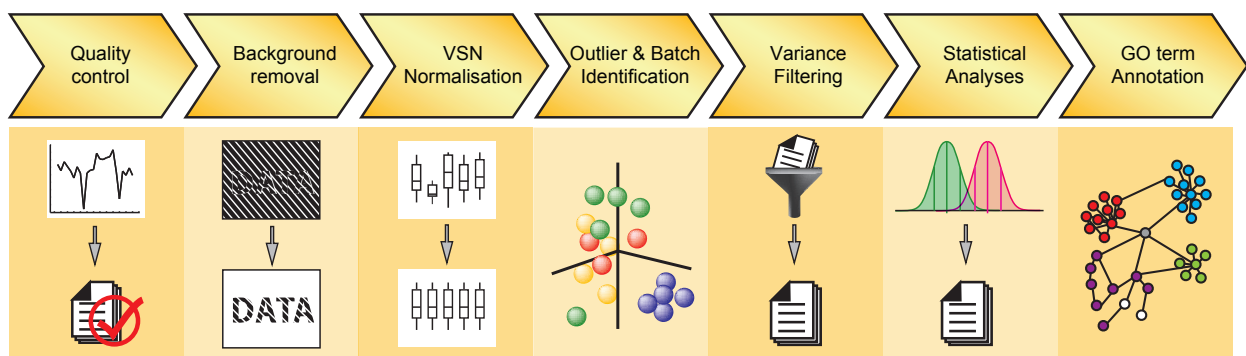


Figure 13: Schematic workflow of Illumina BeadChip microarray data analyses (performed by or in cooperation with Dr. Peter Weber). Microarray data were initially subjected to platform-specific quality controls. Subsequently background removal was performed (threshold: p -detection < 0.05 in at least three samples of whole data set), followed by a Variance Stabilising Normalisation (VSN). Via hierarchical clustering and Principal Component Analyses (PCA) outliers and sample patterns (batch) were identified. In the end a variance filter (variance > 0.05) was applied and remaining probes were subjected to statistical analysis of variance (ANOVA). To identify biologically enriched terms Annotation Cluster Analyses were performed on final gene lists using the DAVID online platform.

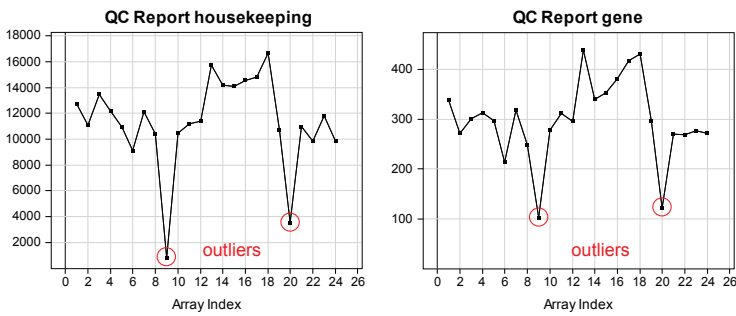


Figure 14: Quality controls revealed two outliers among all analysed cRNA samples. Intensity plots showing the microarray mean intensity of each analysed sample. Thereby y-axes represent mean signal intensities of each individual sample; x-axes represent each of the 24 analysed samples (array index). The intensity plot on the left depicts mean signal intensities of housekeeping genes on the array; the intensity plot on the right mean intensities of all expressed genes.

least three samples in the whole data set) allowing us to separate significant gene expression from background noise, leaving us with 20242 variables (genes) above background for further analyses. To adjust signal intensities between samples, a Variance Stabilising Normalisation was performed. This type of adjustment normalises data, while concomitantly performing a transformation, resulting in approximately constant variances between samples. This homogeneity of variance (homoscedasticity) is a prerequisite for subsequent statistical tests. The combined background removal and VSN normalisation in the end resulted in the assimilation of the different data distribution of each sample to each other. Thereby technical variance is diminished while biological variances are preserved, thus making data more comparable. Figure 15 depicts exemplary boxplots showing the distribution of raw data (Fig. 15A), data after background removal (Fig. 15B) and data after background removal and VSN normalisation (Fig. 15C). The depicted boxplots illustrate how background removal and VSN normalisation assimilate the data, leading to almost normal distributions.

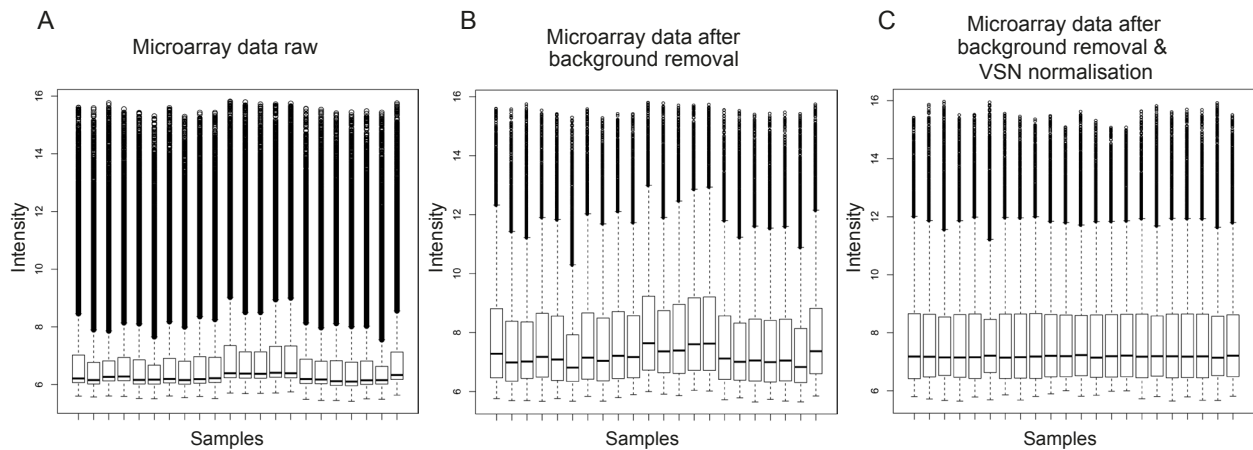


Figure 15: Box plots showing optimisations of microarray intensity distributions during data processing. (A) Depicted box plots represent unprocessed microarray data directly after scanning of Illumina BeadChips. (B) Box plots of microarray data after background removal. Data above background: p-detection < 0.05 in at least three samples in the whole data set. (C) Box plots of microarray data after background removal and VSN normalisation. Black lines within box plots represent the median values. Any data not within the range of the whiskers are plotted as individual dots.

3.1.2 Gene expression profiles of Notch2IC-expressing MZ B as well as Notch2-deficient Fo B cells exhibit a close relationship to those of their respective wild type counterparts

As additional quality control and to receive a first impression of similarities and differences between gene expression profiles of Notch2-deficient Fo B cells, Notch2IC-expressing MZ B cells and wild type Fo B and MZ B cells, VSN normalised data were subjected to a hierarchical clustering analysis. This method aims at building cluster hierarchies based on a dissimilarity metrics, which can then be displayed as a dendrogram. Thus, gene expression profiles that show pronounced overall similarity will be displayed in greater proximity than samples that are highly different. However, one should keep in mind that hierarchical clustering analyses comprise both, technically and biologically induced, differences in gene expression. Analysis of the dendrogram revealed that samples clustered in the first place according to their cell-type identity. Regardless of constitutive Notch2 signalling or an ablation of the Notch2 signal, MZ B cell populations and Fo B cells constituted two big clusters (Fig. 16). However, within these two main clusters, cell populations grouped again into two and three subgroups, clearly separating Notch2-expressing MZ B cells and Notch2-deficient Fo B cells from their respective wild type counterparts. Yet, “cluster 2” branched up much earlier into its subcluster 2.1 and 2.2 than “cluster 1” into its respective subclusters, suggesting that Notch2-deficient Fo B cells are presumably more closely related to wild type Fo B cells than MZ B cell populations among each other. The third “subcluster 1.2” among Fo B cells is most likely the result of a mild technical bias induced by the two different amplification rounds (for detailed explanation see below).

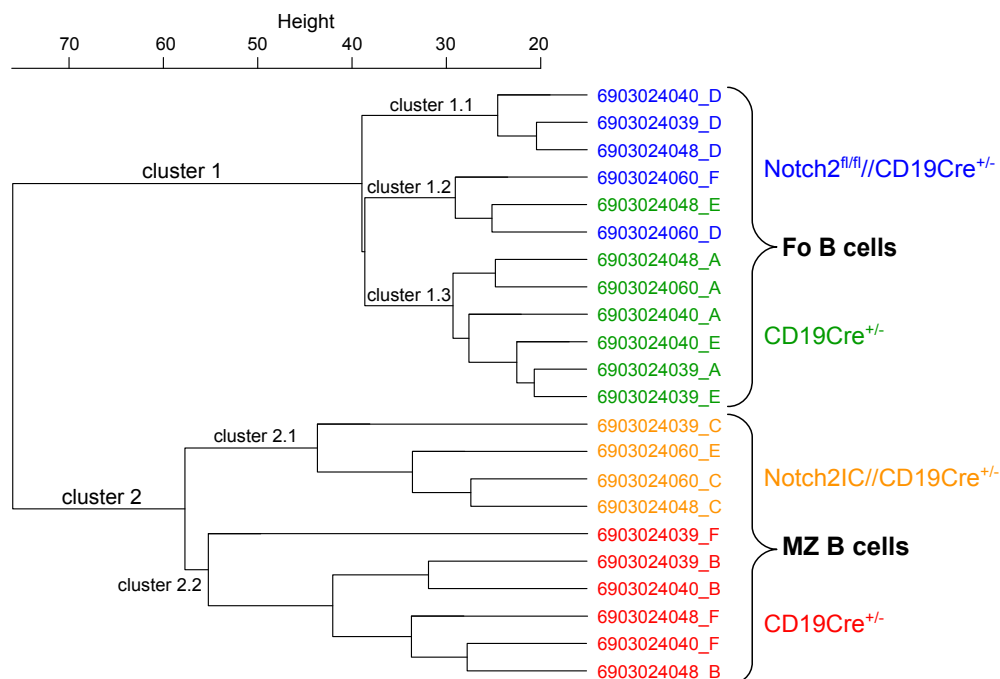


Figure 16: Gene expression profiles of Notch2IC-expressing MZ B and Notch2-deficient Fo B cells resemble their wild type counterparts. Dendrogram of unsupervised, agglomerative hierarchical clustering analysis of VSN normalised Illumina BeadChip microarray data from sort-purified Notch2-deficient Fo B cells (blue) and Notch2IC-expressing MZ B cells (orange) as well as control MZ B (red) and Fo B cells (green). The degree of relationship between the samples is illustrated by the dendrogram, whereas the height of each branch represents the distance between the two samples or clusters being connected. Numbers (e.g. 6903024040_D) are Illumina internal sample identifiers.

For a deeper and more detailed analysis of the acquired data and to differentiate between biological and technical effects, Principal Component Analyses (PCA) were performed. PCA is a common multivariate technique for finding patterns in data sets comprising high dimensions. The central idea of a PCA is to reduce the dimensionality of a data set consisting of a large number of interrelated variables (in our case genes), while retaining as much of the existing information and variation as possible. In the following PCA graphs, each dot depicts the sum of all expressed genes of one sort-purified B cell population and the three axes represent the three main principal components displaying the main differences between the analysed B cell populations.

As different cRNA amplification rounds often result in a technical bias eventually masking “real” biological effects (Dr. Peter Weber, personal communication; Leek et al., 2010), data was checked for such a possible, technically induced bias. Figure 17 clearly shows that in spite of taking precautions by applying sample randomisation, there was still some mild amplification round induced bias detectable. Hence, subsequent PCA analyses and lists of differentially regulated genes were generated by including the amplification rounds as a co-variate - so called “eliminated factor” - in regression based statistics.

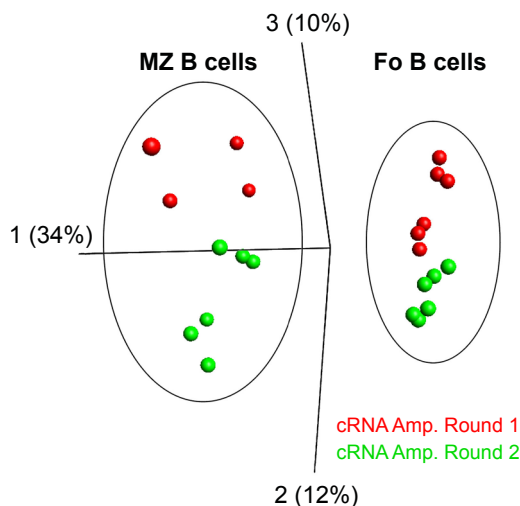


Figure 17: Different amplification rounds result in a mild technical bias. Principal Component Analysis of VSN normalised Illumina BeadChip microarray data from sort-purified Notch2-deficient Fo B cells and Notch2IC-expressing MZ B cells as well as control MZ B and Fo B cells. Red spheres are samples processed during the first amplification round, while green spheres represent all samples of the second amplification round. Percents represent the percentages of variance explained by each of the depicted main principal components one to three.

Further PCA analyses now focusing only on the biological differences between the four different sample types (experimental groups) again clearly revealed that Fo B and MZ B cell populations were separate from each other (Fig. 18A, B). Greater differences were again detectable between wild type and Notch2IC-expressing MZ B cells (Fig. 18A, B) than among the wild type and Notch2-deficient Fo B cells (Fig. 18C, D). However, the similarity between the two Fo B cell populations was even more pronounced now after removal of the amplification round-induced bias.

3.1.3 Differences in B cell-specific gene expression profiles induced by constitutive Notch2IC expression or Notch2 deficiency

After PCA analyses, lists comprising differentially regulated genes were generated (GlucoRe Omics Explorer). Data was first filtered by variance (variance > 0.05) and subsequently an analysis of variance (ANOVA) with the amplification round as co-variate (eliminated factor) was conducted. For comparison of CD19Cre^{+/-} MZ B and Fo B cells, paired tests were applied as both cell populations

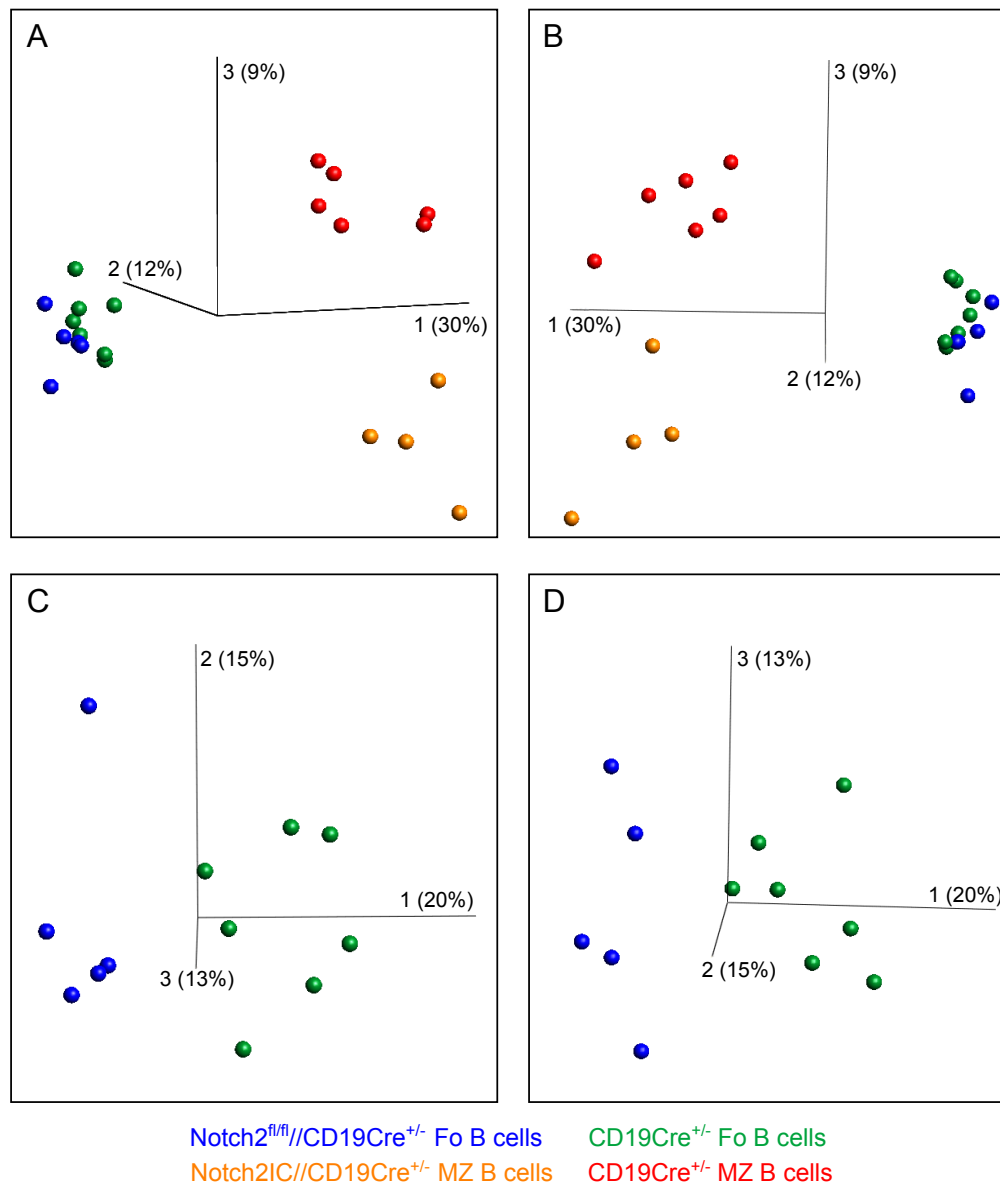


Figure 18: Gene expression profiles of the two Fo B cell populations are more closely related than those of the two MZ B cell populations. (A-B) Principal Component Analysis of VSN normalised Illumina BeadChip microarray data from sort-purified Notch2-deficient Fo B cells and Notch2IC-expressing MZ B cells, as well as control MZ B and Fo B cells including the amplification round as co-variate (eliminated factor). **(C-D)** Principal Component Analysis of VSN normalised Illumina BeadChip microarray data comparing sort-purified Notch2-deficient Fo B cells with control Fo B cells including the amplification round as co-variate (eliminated factor). Notch2IC-expressing MZ B cells (orange); CD19Cre^{+/-} MZ B cells (red); CD19Cre^{+/-} Fo B cells (green); Notch2-deficient Fo B cells (blue). The percentages of variance explained by each of the depicted main principal components one to three are given.

had always been isolated from one individual wild type mouse and are thus biologically related to each other. For the other comparisons unpaired tests were performed. To control for false positive rates due to multiple testing the Benjamini-Hochberg procedure was used for correction of the p-values, thereby obtaining the so called q-values. Final gene lists comprise only data with a q-value < 0.05 (see CD in the appendix). For convenience, the top 100 most strongly regulated genes of these final gene lists were included in the appendix (Tables S1 - S4). The following scheme (Fig. 19) shall give a first impression of the varying numbers of regulated genes among the analysed samples. With only 44 differentially regulated genes, wild type Fo B cells are closely related to Notch2-deficient Fo B cells, followed by wild

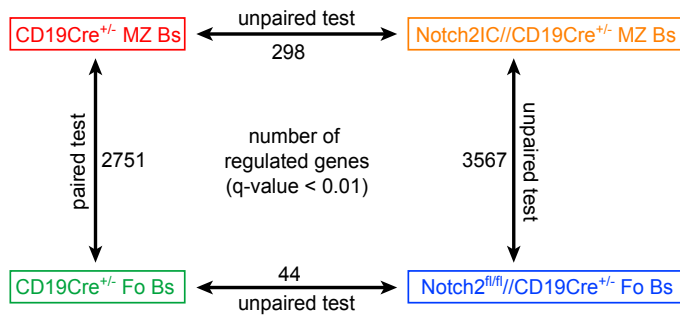


Figure 19: Number of differentially regulated genes between the different B cell populations of the analysed mouse strains. VSN normalised Illumina BeadChip microarray data from sort-purified Notch2-deficient Fo B and Notch2IC-expressing MZ B cells as well as control MZ B and Fo B cells was filtered by variance (> 0.05). Subsequently, an ANOVA was conducted including the amplification round as co-variate (eliminated factor). The scheme depicts numbers of regulated genes with a q-value < 0.01 .

type and Notch2IC-expressing MZ B cells with 298 genes. The greatest difference could be observed when comparing two different cell-types with each other. Still, comparing Notch2IC-expressing B cells with Notch2-deficient cells yielded the strongest gene regulation with 3567 differentially regulated genes. To visualise and to get an overview of the extracted lists of differentially regulated genes, so called Volcano plots were generated, in which the statistical significance (q-value) is plotted against the fold change. In contrast to multivariate PCA analyses, Volcano plots are univariate analyses based on the individual gene expression level. Hence, every single gene is depicted as spot, whereas in PCA analyses a spot represents the combinations of all genes of one B cell population. Labeled genes highlighted by filled, coloured circles within Volcano plots represent the top 25 most significant and most strongly regulated genes of the respective comparisons. As analyses before, they showed that comparisons of different cell types (Fo Bs versus MZ Bs) yielded more significantly regulated genes (Fig. 20A, B) than comparisons of similar cell populations (Fig. 20C, D). Interestingly, among the top 25 regulated genes between control and Notch2-deficient Fo B cell populations, a large proportion was only regulated two-fold or less (Fig. 20D), whereas in the other three comparisons more of the top 25 regulated genes were regulated more than two-fold (Fig. 20A, B, C). Furthermore, these plots revealed that more of the most strongly regulated genes were upregulated in those cell populations that had presumably more Notch2 signalling in the respective comparisons, suggesting that Notch2 might be responsible for these upregulations. In detail, when comparing Notch2IC-expressing MZ B cells to other B cell populations with less Notch2 signalling, more of the top regulated genes were upregulated in Notch2IC-expressing cells (Fig. 20A, C). A similar effect could be observed for wild type MZ B cells versus Fo B cells (Fig. 20B), with MZ B cells being the ones with more Notch2 signalling, and for the comparison of Notch2-deficient B cells with wild type Fo B cells (Fig. 20D), in which wild type Fo B cells have more Notch2 signalling. These results demonstrate that a constitutive Notch2 signal or an ablation of Notch2 signalling leads to additional gene regulations beyond those defining the cell-type identity, although these differences are smaller when comparing Fo B cell populations among each other. However, it still suggests that wild type Fo B cells get at least sporadic Notch2 signalling from time to time, possibly explaining some of the differentially regulated genes between wild type and Notch2-deficient Fo B cells.

To get a first notion in what range obtained fold regulations and statistical significances on our lists of regulated gene lists are and to have some reference values to be able to differentiate between “strong” and “weak” regulations, obtained gene lists were at first sorted by statistical significance and checked for candidate genes already well known to be up- or downregulated in MZ B cells or directly by Notch2

Notch2IC was constitutively expressed, whereas a fraction of them were further downregulated in the absence of Notch2 signalling in Fo B cells. Typical MZ B cell surface markers such as CD9, CD1d and CD38 as well as the typical activation marker CD86 (Pillai et al., 2005; Vences-Catalan and Santos-Argumedo, 2011; Oliver et al., 1999a), which already showed upregulation in the wild type MZ B versus Fo B cell populations on our arrays had similar or even further enhanced levels in Notch2IC-expressing cells. CD23 on the other hand is highly expressed on Fo B cells and downregulated in MZ B cells (Pillai and Cariappa, 2009). Notch2IC expression even further decreased CD23 expression, whereas Notch2 deficiency enhanced its expression. MZ B cells have been shown to express higher levels of toll-like receptors on their surface (Gururajan et al., 2007; Martin and Kearney, 2002). This again matched with differences in expression in our gene expression profile analyses, as TLR7, TLR3 and TLR4 were upregulated in MZ B cells compared to Fo B cells and TLR3 also in Notch2IC-expressing cells versus wild type MZ B cells. The sphingosine-1-phosphate receptor 3 (S1PR3), the cannabinoid receptor 2 (Cnr2, CB2), and ICAM1, which are implicated in the migration of MZ B cells or retaining them within the MZ, were upregulated in MZ B versus Fo B cells and apart from ICAM1 further upregulated by Notch2IC expression. Genes which were already described to be Notch target genes or upregulated in MZ B cell populations such as Deltex1, Hes1, CD1d, CD21, CD27, CB2, CD38 and CD23 clearly displayed differences in their expression strength between control and Notch2-deficient Fo B cells,

Tables 1-4: Fold changes of candidate genes from microarray analyses known to be up- or downregulated in MZ B cells or by Notch2 signalling.

Table 1

N2IC MZ B cells vs. N2KO Fo B cells	
Gene symbol	Fold change
CD9	13.8
Deltex1	13.6
Hes5	5.3
CD1d	4.8
Hes1	4.8
CD27	4.2
TLR7	2.7
Hey3	2.5
CD21	2.5
PD-L1	2.5
TLR3	2.4
CD38	2.3
S1PR3	2.2
Notch1	2.1
CB2	2.0
CXCR7	1.8
CD86	1.5
Icam-1	1.5
Notch2	1.5
Deltex4	1.4
Hey2	1.3
CD23	-25.8

Table 2

CD19 MZ B cells vs. CD19 Fo B cells	
Gene symbol	Fold change
CD9	5.3
Deltex1	5.0
CD1d	4.5
Hes1	3.1
CXCR7	2.8
TLR7	2.7
CD21	2.4
PD-L1	2.2
CD86	2.0
S1PR3	1.6
CD27	1.4
Deltex4	1.4
CD38	1.3
TLR3	1.3
Icam-1	1.3
CB2	1.2
Hey2	1.1
Hes5	1.2
CD23	-7.3

Table 3

CD19 Fo B cells vs. N2KO Fo B cells	
Gene symbol	Fold change
Deltex1	2.1
Hes1	1.6
CD21	1.5
Notch1	1.3
CD27	1.2
CB2	1.2
Icam-1	1.2
ADAM17	1.2
CD1d	1.2
CD38	1.2
Deltex2	1.2
TLR7	1.2
S1PR3	-1.1
CXCR7	-1.1
TLR3	-1.1
TLR4	-1.3
CD23	-1.4

Table 4

N2IC MZ B cells vs. CD19 MZ B cells	
Gene symbol	Fold change
Hes5	5.3
CD9	3.4
CD27	2.9
Hey3	2.6
TLR3	2.1
CD38	1.8
Notch1	1.7
Deltex1	1.7
S1PR3	1.6
CB2	1.4
Notch2	1.4
PD-L1	1.3
Hes1	1.2
Hey2	1.2
CD1d	1.1
CD21	-1.2
CXCR7	-1.3
CD23	-3.6

Final lists of differentially regulated genes obtained by comparing Notch2IC-expressing (N2IC) and Notch2-deficient (N2KO) B cells among each other and with their respective wild type counterparts (CD19) were sorted by significance and checked for candidate genes known to be up- or downregulated in MZ B cells or by Notch2 signalling. Genes with a positive fold change value are upregulated in the respective population named first. TLR (toll-like receptor), S1PR3 (sphingosine-1-phosphate receptor 3), CB2 (cannabinoid receptor 2).

indicating that there may at least be some Notch2 signalling left in wild type Fo B cells.

The Annotation Cluster Tool of the bioinformatics Database for Annotation, Visualisation and Integrated Discovery (DAVID) was used to identify enriched biological terms, functionally related groups, or other clusters among the lists of differentially regulated genes. For this type of analysis, gene lists were sorted by q-values and as the DAVID software is limited in the number of genes it can analyse at a time, only genes with a q-value below a certain threshold were analysed. For comparisons of wild type Fo B versus MZ B cells and Notch2IC-expressing B cells with Notch2-deficient B cells only genes with a q-value < 0.0149 were chosen. For the comparison of wild type Fo B with Notch2-deficient Fo B cells and wild type MZ B versus Notch2IC-expressing MZ B cells genes with a q-value < 0.0549 were analysed. Hence, the following remaining gene numbers were subjected to analyses with the DAVID software: 3471 genes for wild type Fo B versus MZ B cells, 4099 for Notch2-deficient versus Notch2IC-expressing B cells, 1262 for wild type MZ B versus Notch2IC-expressing MZ B cells and 385 genes for the comparison of the two Fo B cell populations. The top most significant and relevant annotation clusters found for the four comparisons are summarised in the tables S5 - S8 (appendix). In addition, for comparisons between wild type MZ B with Fo B cells as well as with Notch2IC-expressing MZ B cells additional annotation cluster analyses were performed using only the subsets of genes upregulated in MZ B versus Fo B cells or in Notch2IC-expressing versus wild type MZ B cells respectively, to be able to discriminate enriched terms based on an induction

of Notch2 signalling (Tables S9, S10; appendix). Some of these enriched biological terms found by annotation clustering were in accordance with data obtained from experiments described in the following chapters and in addition further strengthened them and will therefore be discussed in the respective context.

3.2 The impact of Notch2 signalling and the influence of the marginal zone environment on the MZ B cell phenotype

3.2.1 Notch2IC-expressing cells are able to maintain their MZ B cell phenotype in vitro

Our previous investigations revealed that Notch2IC-expressing MZ B cells share a lot of similarities with wild type MZ B cells. Especially typical MZ B cell surface markers were upregulated in wild type and Notch2IC-expressing MZ B cells versus Fo B cells. As in contrast to wild type MZ B cells, Notch2 signalling is continuously active in Notch2IC-expressing MZ B cells even in the absence of specific ligands, we wanted to investigate whether Notch2IC expression is sufficient to maintain a MZ B cell phenotype when cells are taken out of their MZ environment, which normally provides the Notch2 ligand (Tan et al., 2009). To this end, splenic B cells from control and Notch2IC//CD19Cre^{+/-} mice were isolated and cultured for up to two days without stimulation (Fig. 21). The expression of typical

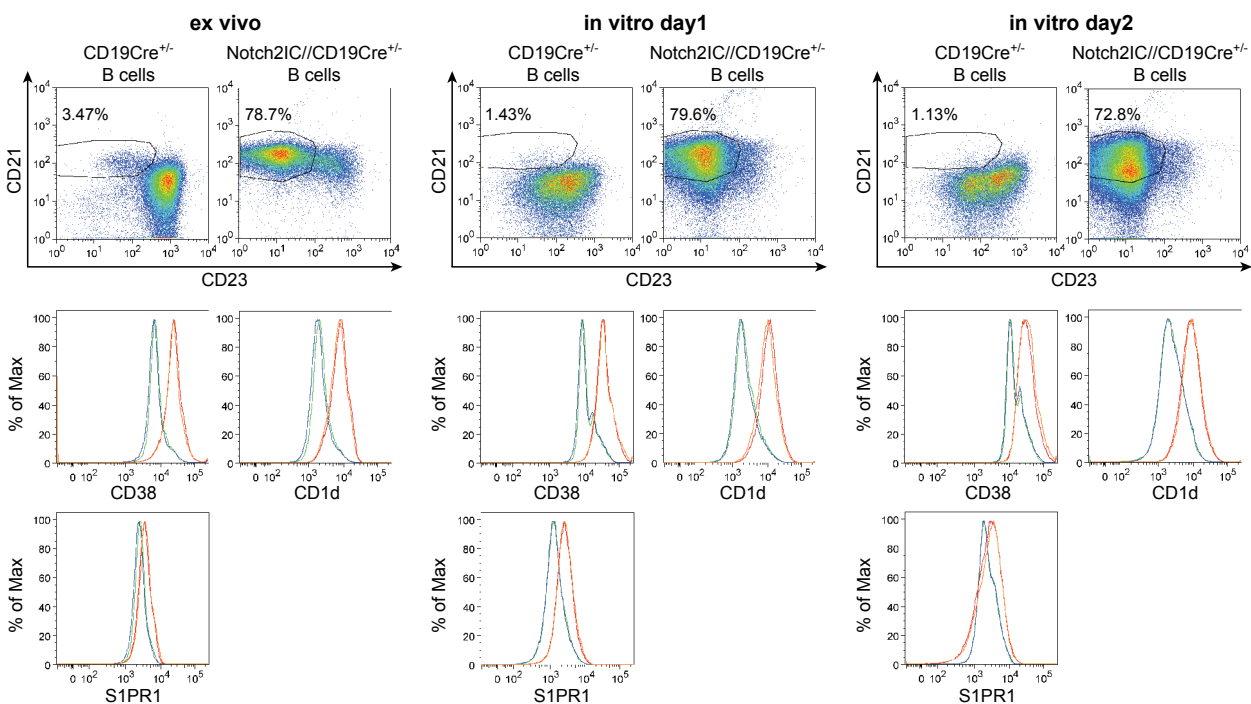


Figure 21: In vitro cultured Notch2IC//CD19Cre^{+/-} B cells maintain their MZ B cell phenotype. Splenic B cells were isolated from Notch2IC//CD19Cre^{+/-} and CD19Cre^{+/-} mice and cultured for up to two days without stimulation. Expression of CD21, CD23, CD38, CD1d and S1PR1 was analysed by flow cytometry ex vivo and after one or two days of in vitro culture. Exemplary dot plots and histograms of control B cells are gated on lymphocytes (ex vivo) or living cells (in vitro) positive for B220. Exemplary dot plots and histograms of Notch2IC-expressing B cells are gated on lymphocytes (ex vivo) or living cells (in vitro) positive for hCD2. Histograms depict overlays of the abundance of indicated molecules in control B cells (blue and green lines) and Notch2IC-expressing B cells (red and orange lines). Numbers indicate percentages of CD21^{high} MZ B cells. Data is representative of two independent experiments.

MZ B cell surface markers such as CD21, CD23, CD1d, CD38 and S1PR1 were analysed daily. Ex vivo isolated Notch2IC-expressing B cells exhibited the already described expansion of the CD21^{high} CD23^{low} MZ B cell population at the expense of Fo B cells. Furthermore, Notch2IC-expressing cells displayed higher CD38, CD1d and S1PR1 levels than control B cells. On day one and two in vitro, in control B cells no CD21^{high} MZ B cells could be detected anymore, whereas Notch2IC-expressing cells were always able to maintain higher CD21 levels than control B cells. In addition, CD38, CD1d and S1PR1 levels stayed increased compared to control B cells. These results suggest indeed that constitutive Notch2 signalling is sufficient to sustain the MZ B cell phenotype outside of the MZ, however, further experiments need to be performed to affirm that other relevant MZ B cell markers and thus a “complete” MZ B cell phenotype can really be maintained.

3.2.2 Enhanced proliferation of Notch2IC-expressing B cells in response to α -CD40 or LPS stimulation can mainly be ascribed to their MZ B cell phenotype

First experiments performed by F. Hampel, a former laboratory member, showed that splenic B cells from Notch2IC//CD19Cre^{+/-} mice displayed highly enhanced proliferative behaviour compared to B cells from control mice when treated with LPS or α -CD40 in in vitro cultures. As it is known that specifically MZ B cell populations exhibit increased proliferation in response to LPS or α -CD40 stimulation (Gunn and Brewer, 2006; Thomas et al., 2007; Oliver et al., 1999b), these findings further affirmed the MZ B cell phenotype of Notch2IC-expressing B cells. Yet, as splenic B cells from Notch2IC//CD19Cre^{+/-} mice comprise ~80 % MZ B cells compared to ~5 % in B cell populations of control mice, the question remained if the enhanced proliferative behaviour of Notch2IC-expressing B cells can only be attributed to their MZ B cell phenotype or if constitutive Notch2 signalling is additionally intensifying the proliferation rate especially after stimulation. This question was particularly interesting as the search for enriched biological terms among our Illumina BeadChip microarray data comparing Notch2IC-expressing with wild type MZ B cells, using the ‘Annotation Cluster Tool’, already pointed out that constitutive Notch2IC expression might additionally increase cell division rates in MZ B cell populations (Table S7, S10). To finally clarify this question, proliferation rates of sort-purified wild type MZ B cells were compared to those of MZ B cells from Notch2IC//CD19Cre^{+/-} mice. Wild type MZ B cells and Notch2IC-expressing MZ B cells were recovered with a purity of ~97 % respectively. Sort-purified MZ B cells were labelled with carboxyfluorescein succinimidyl ester (CFSE) and cultured for three days without any stimuli or with LPS, α -CD40 or α -CD40+IL-4. CFSE is a green fluorescent dye, which binds inner cell membrane proteins and hence is incorporated into the cell. Due to its progressive decrease within daughter cells after each cell division, proliferation can easily be monitored. On the basis of the resting peak on day three (the population of undivided B cells, thus exhibiting highest CFSE intensity) the percents of divided cells (% divided) as well as the proliferation index (number of divisions of cells that underwent at least one division) and division index (average number of cell divisions in total, including cells that never divided) were determined. These analyses, now comparing only MZ B cell populations with each other, revealed that

the enhanced proliferation rate of Notch2IC-expressing cells seen in former experiments can mainly be ascribed to their MZ B cell phenotype. Still, Notch2IC-expressing cells showed slightly better proliferation rates after α -CD40 stimulation (Fig. 22).

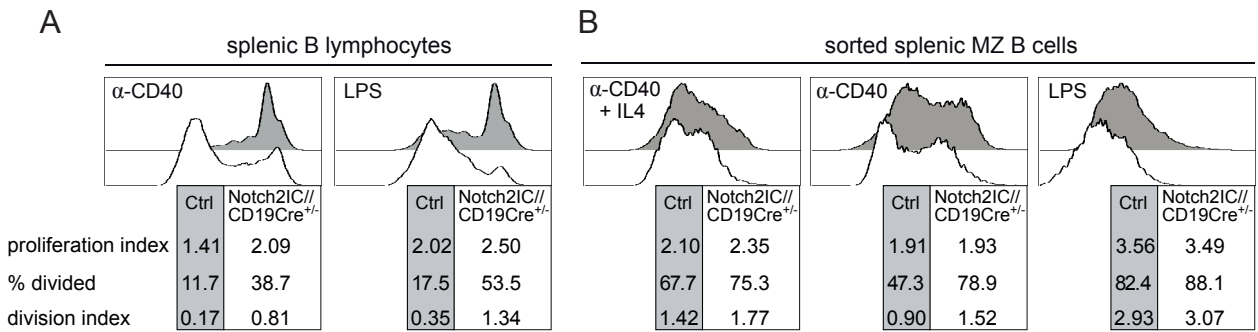


Figure 22: Notch2IC-expressing B cells are hyper-responsive to LPS and α -CD40 stimulation in vitro mainly due to their MZ B cell phenotype. (A) Splenic B cells of control and Notch2IC//CD19Cre^{+/-} mice were enriched by depletion of CD43⁺ non-B cells. They were subsequently labeled with CFSE and cultured with the indicated stimuli (LPS concentration: 50 μ g/ml, α -CD40 concentration: 2.5 μ g/ml). After three days, proliferation profiles of propidium iodide-negative cells were assessed by flow cytometric analysis and are displayed in the histogram overlays as grey (control B cells) and white (Notch2IC-expressing B cells) graphs. Data is representative of four independent experiments. (B) Splenic MZ B cells of control and Notch2IC//CD19Cre^{+/-} mice were enriched by depletion of CD23⁺ and/or CD43⁺ cells and further sort-purified for B220⁺, CD21^{high}, CD23^{low} cells and in the case of Notch2IC-expressing cells additionally for hCD2⁺ cells. To be able to gain enough MZ B cells for an in vitro culture after FACS sorting, splenic cell populations from 12 CD19Cre^{+/-} mice and 3 Notch2IC//CD19Cre^{+/-} mice were pooled. Sorted MZ B cells were labeled with CFSE and cultured with the indicated stimuli (LPS concentration: 50 μ g/ml, α -CD40 concentration: 2.5 μ g/ml, IL-4 concentration: 10 ng/ml). After 2.5 days, proliferation profiles of propidium iodide-negative cells were assessed by flow cytometric analysis and are displayed in the histogram overlays as grey (control MZ B cells) and white (Notch2IC-expressing MZ B cells) graphs. Data is representative of three independent experiments. Proliferation index: average number of divisions of cells that underwent at least one division; % divided: percentage of cells that initially start to divide, also called precursor frequency; division index: average number of cell divisions in total.

3.2.3 Notch2IC-expressing B cells exhibit enhanced Erk, Jnk and PI3 kinase signalling even in the absence of a CD19 receptor

It is widely accepted that MZ B cells have a pre-activated phenotype in comparison to Fo B cells (Gunn and Brewer, 2006; Oliver et al., 1999b). In accordance, we could show that Notch2IC-expressing cells resemble wild type MZ B cells regarding this pre-activation, as Notch2IC-expressing MZ B cells had increased CD80, CD86, CD25 and ICAM1 levels compared to wild type splenic B cells (mainly Fo B cells) (Hampel et al., 2011). As already briefly described before (3.1.3), our microarray experiments also revealed that expression levels of CD80, CD86 and ICAM1 were increased in wild type and Notch2IC-expressing MZ B versus Fo B cells. Beyond that, Annotation Cluster Analyses performed on our microarray data with genes differentially upregulated in wild type MZ B versus Fo B cells and in Notch2IC-expressing B cells versus wild type MZ B cells revealed enriched terms such as “regulation of B cell/lymphocyte activation” and “positive regulation of B cell/lymphocyte activation”, possibly also indicating that Notch2IC is additionally enhancing the natural pre-activated state of MZ B cells. Apart from that enriched terms such as “protein serine/threonine kinase activity” and “positive regulation of MAPKKK cascade” could also be found. Consequently, we were interested in which signalling pathways would possibly be involved in the activated MZ B cell phenotype. Up to now

it was not really possible to analyse the activity of signalling pathways in MZ B cells in detail, since only low amounts of this cell population can be isolated by sort-purification from wild type splenic cell suspensions. Notch2IC//CD19Cre^{+/-} mice allowed us to perform Western blot analyses, as huge amounts of Notch2IC-expressing B cells closely resembling wild type MZ B cells with respect to the pre-activated state could be isolated. F. Hampel previously showed and I could confirm that Notch2IC-expressing B cells exhibited enhanced phosphorylation of the MAP kinases Erk and Jnk as well as of the Akt kinase (Fig. 23 and Hampel et al., 2011). F. Hampel could also demonstrate that constitutive Notch2 signalling is able to rescue MZ B cell development in Notch2IC//CD19Cre^{+/-} mice, which lack the CD19 receptor. Respective B cells also kept their enhanced phosphorylation of the MAP kinases Erk and Jnk (Hampel et al., 2011). This was unexpected since CD19 has been shown to be essential for MZ B cell development as CD19-deficient mice are devoid of this cell population (Pezzutto et al., 1987; Rickert et al., 1995; Engel et al., 1995). The CD19 receptor is quite important regarding the induction of PI3K/Akt signalling (Otero et al., 2001). Therefore, we wondered if this specific pathway is still active even in the absence of CD19. Beyond this we were further interested in investigating whether other members of the PI3K pathway would be affected in Notch2IC//CD19Cre animals, apart from Akt. Figure 24 shows a simplified scheme of the PI3K pathway containing analysed members. In brief, BCR cross-linking leads to a rapid phosphorylation of the CD19 co-receptor,

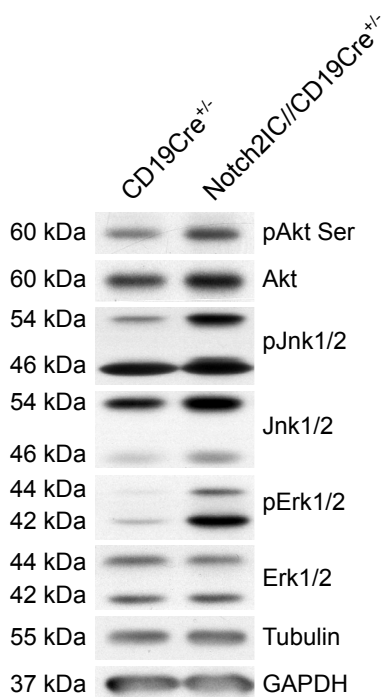


Figure 23: Notch2IC-expressing B cells exhibit increased levels of pErk, pJnk and pAkt. Splenic B cells were purified from Notch2IC//CD19Cre^{+/-} and control mice. Whole-cell extracts were subjected to immunoblot analyses using antibodies specific for pAkt (pS473), pJnk, pErk and the corresponding non-phosphorylated forms. Equal protein loading was controlled by an α -tubulin and α -GAPDH staining. Results are representative of three independent experiments, further confirming experiments and results performed and obtained by F. Hampel.

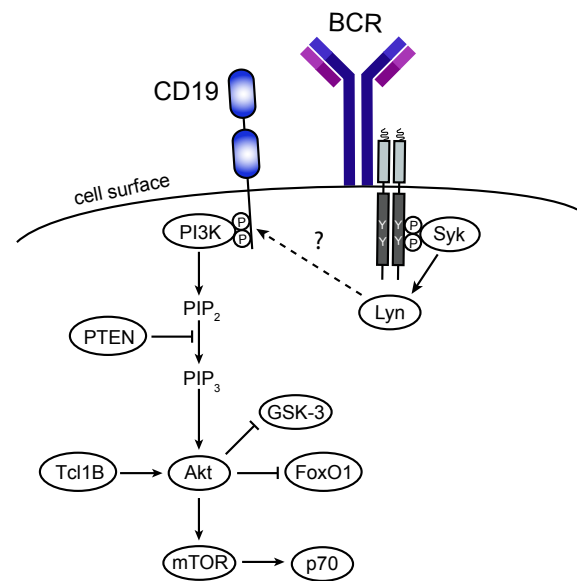


Figure 24: Simplified scheme of the PI3 kinase pathway including members analysed by Western blot. The CD19 receptor is rapidly phosphorylated upon BCR engagement, leading to the recruitment and binding of the PI3 kinase. PIP₂ is now converted to PIP₃ thereby activating Akt and hence mTOR and the S6 kinase (p70). GSK-3 and FoxO1 are phosphorylated and thereby inhibited by Akt signalling. Tcl1B functions as an Akt co-activator. PTEN is a 3'-phosphoinositide phosphatase and inhibits the PI3K/Akt signalling pathway by converting PIP₃ back to PIP₂.

which in turn recruits the PI3 kinase, which can now convert phosphatidylinositol-4,5 bisphosphate (PIP₂) to phosphatidylinositol-3,4,5 trisphosphate (PIP₃) (Otero et al., 2001). Subsequently, the serine/threonine kinase Akt is recruited to the plasma membrane and phosphorylated at position serine 473 (S473) and threonine 308 (T308), leading to the activation of mTOR and the S6 kinase (S6K/p70). Moreover, Akt phosphorylates and thereby inhibits the glycogen synthase kinase 3 (GSK-3) and the forkhead box protein O1 (FoxO1) (Porta et al., 2014). Phosphorylated FoxO1 is translocated from the nucleus to the cytoplasm, where it is degraded (Tzivion et al., 2011). The T-cell leukemia/lymphoma protein 1B (Tcl1B) functions as an Akt co-activator (Laine et al., 2000; Auguin et al., 2004). PTEN is a 3'-phosphoinositide phosphatase and inhibits the PI3K/Akt signalling pathway by converting PIP₃ back to PIP₂ (Porta et al., 2014).

Expression levels of pAkt, Akt, pp70, p70, pGSK-3, GSK-3, FoxO1, PTEN and Tcl1B1/5 were examined by Western blot analyses. An α -tubulin staining was used as a control for equal protein loading. B cells from Notch2IC//CD19Cre^{+/-} as well as from Notch2IC//CD19Cre^{+/+} (CD19-deficient) mice exhibited increased levels of pAkt, pp70, Tcl1B1/5 as well as pGSK-3 (Fig. 25), indicating that Notch2IC-expressing cells indeed have an increased activity of the PI3K/Akt signalling pathway regardless of their CD19 deficiency. As basal levels of Akt and p70 were also already quite strongly induced in Notch2IC-expressing cells, we wanted to check whether increased expression levels of the phosphorylated, active forms of the two proteins were only based on the elevated basal levels. For this, pAkt, Akt, pp70 and p70 levels were quantified using densitometry. Respective GSK-3 expression levels were used as reference as these exhibited the lowest variations among samples. Quantifications suggest that although basal Akt and p70 levels were already elevated due to Notch2IC expression the increase in expression levels of the phosphorylated forms was even greater (Fig. 26). Expression of PTEN, which is known to negatively regulate PI3K signalling by reversing the

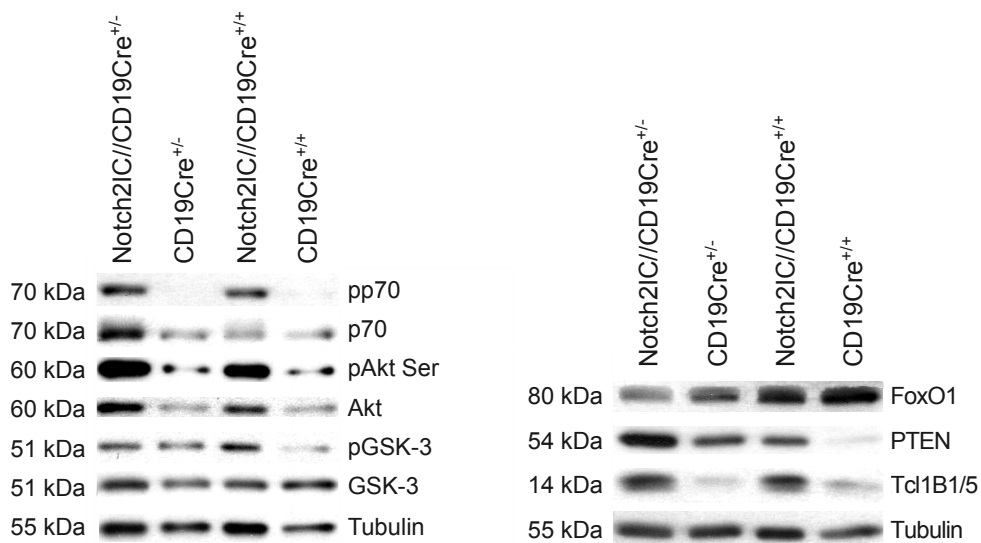


Figure 25: Notch2IC-expressing B cells exhibit increased PI3K signalling in comparison to control B cells. Splenic B cells were purified from Notch2IC//CD19Cre^{+/-}, Notch2IC//CD19Cre^{+/+} and corresponding control mice. Whole-cell extracts were subjected to immunoblot analyses using antibodies specific for pAkt (pS473), pp70/pS6K, pGSK-3, FoxO1, PTEN as well as Tcl1B1/5 and the corresponding non-phosphorylated forms. Equal protein loading was controlled by an α -tubulin staining. The results are representative of three to five independent experiments for Notch2IC//CD19Cre^{+/+} and CD19Cre^{+/+} animals and 7-13 for Notch2IC//CD19Cre^{+/-} and CD19Cre^{+/-} animals.

phosphorylation of PIP₃ to PIP₂ and thereby antagonising further downstream signalling (Iwanami et al., 2009) was also increased in Notch2IC-expressing cells (Fig. 25). Yet, these enhanced PTEN levels were in accordance with increased PI3K/Akt signalling, as activation of this pathway also entails that more PIP₃ is available and probably needs to be converted back into PIP₂, representing a mechanism continuously counterregulating increased PI3K/Akt signalling. In addition, CD19-deficient B cells displayed reduced PTEN and increased FoxO1 levels compared to CD19Cre^{+/-} control B cells, affirming the important role of CD19 regarding the induction of PI3K signalling. Still, Notch2IC-expressing B cells exhibited increased PTEN and decreased FoxO1 expression than their respective controls (CD19Cre^{+/-} or CD19Cre^{+/+}). This shows that constitutive Notch2 signalling can at least partially rescue CD19 defects regarding the PI3K pathway.

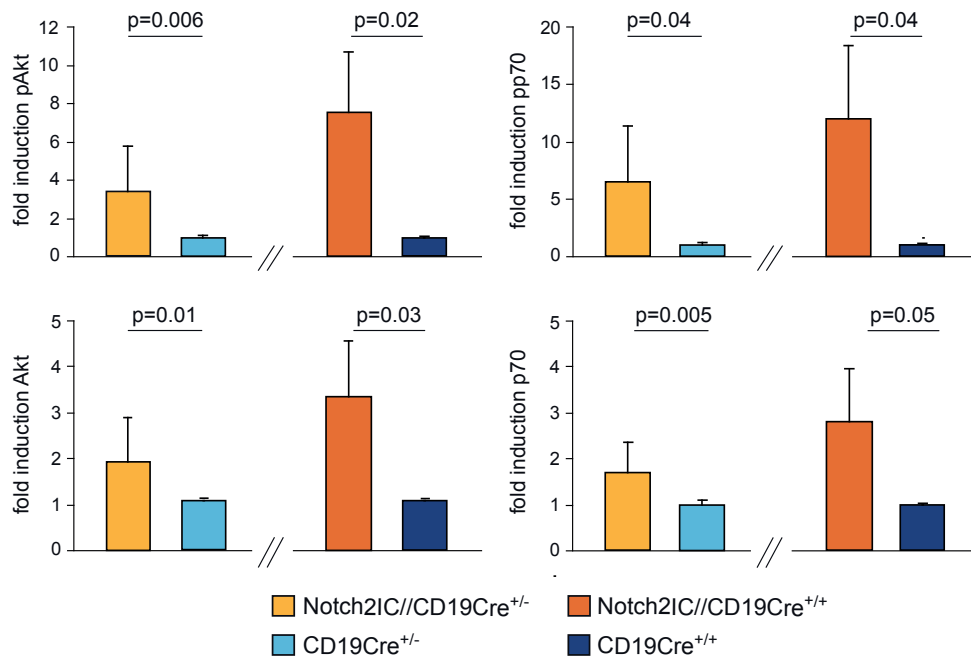


Figure 26: Western blot quantifications revealed increased basal and phosphorylated levels of Akt and p70 in Notch2IC-expressing B cells. Splenic B cells were purified from Notch2IC//CD19Cre^{+/-}, Notch2IC//CD19Cre^{+/+} and corresponding control mice. Whole-cell extracts were subjected to immunoblot analyses using antibodies specific for pAkt (pS473), pp70/pS6K and the respective non-phosphorylated forms. Expression levels were quantified by densitometry measurement of Western blot films. The results are representative of three to five independent experiments for Notch2IC//CD19Cre^{+/+} and CD19Cre^{+/+} animals and 7-13 for Notch2IC//CD19Cre^{+/-} and CD19Cre^{+/-} animals

Although immunoblot experiments demonstrated that in Notch2IC-expressing MZ B cells the MAP kinases pErk and pJnk as well as the PI3K/Akt signalling were strongly induced, the question remained whether this increase is an intrinsic phenotype of MZ B cells or if it is specifically triggered by the expression of the Notch2IC transgene. To this end, intracellular flow cytometrical analyses were performed, allowing to compare the amounts of pErk, pJnk and pAkt in wild type MZ B with those in Notch2IC-expressing MZ B cells and in addition to differentiate between expression levels in MZ B and Fo B cells. CD21^{high} control MZ B cells displayed clearly elevated pErk, pJnk as well as pAkt levels in contrast to CD21^{low} Fo B cells (Fig. 27, left panels). In accordance with previous Western blot experiments, Notch2IC-expressing B cells had higher expression levels than control B cells (Fig. 27, center panels). Yet, histogram overlays exhibited that Notch2IC-expressing MZ B cell populations had

similar levels than control MZ B cells (Fig. 27, right panels), thereby implicating that higher pErk, pJnk and pAkt levels are mainly induced by the MZ B cell phenotype or the localisation of MZ B cells in the MZ and not by Notch2IC expression.

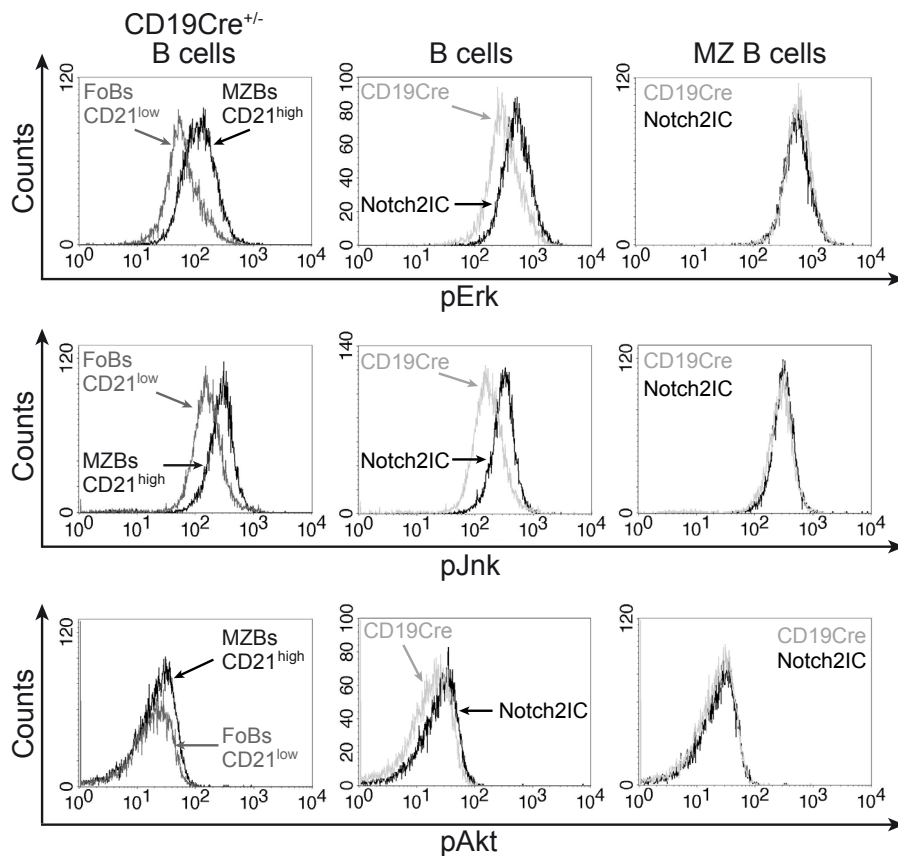


Figure 27: Notch2IC-expressing and control MZ B cells have higher pErk, pJnk and pAkt levels than Fo B cells. Splenic B cells were isolated from Notch2IC//CD19Cre^{+/-} and CD19Cre^{+/-} mice, stained for surface markers, fixed, permeabilised and subsequently stained and analysed for the indicated phosphorylated signalling molecules by intracellular flow cytometry. Histograms are lymphocyte-gated and depict overlays of the indicated molecules. Histograms on the left depict control lymphocytes gated on B220⁺, CD21^{high} MZ B cells (black line) and CD21^{low} Fo B cells (dark gray line), histograms in the center show B220⁺ hCD2⁺ Notch2IC-expressing (black line) versus B220⁺ control cells (light gray line) and histograms on the right display B220⁺ hCD2⁺ CD21^{high} Notch2IC-expressing (black line) and B220⁺ CD21^{high} control MZ B cells (light gray line). Data is representative of four independent experiments.

3.2.4 Notch2IC expression is not sufficient to sustain enhanced Erk, Jnk and Akt signalling outside the marginal zone environment

As shown in the chapter before, wild type as well as Notch2IC-expressing MZ B cells exhibit similarly increased pErk, pJnk and pAkt expression levels suggesting that the increased activity of these signalling pathways is rather mediated by the MZ environment than by Notch2IC expression itself. Therefore we assumed that constitutive Notch2 signalling is not sufficient to maintain enhanced MAP kinase and PI3K/Akt signalling outside this natural environment. To test this hypothesis, B cells were isolated from spleens of CD19Cre^{+/-} as well as Notch2IC//CD19Cre^{+/-} mice and taken into in vitro culture without stimulation. After day one and two, protein expression levels of pErk, pJnk, pAkt and the corresponding non-phosphorylated forms were analysed by subjecting whole-cell extracts of these cultured cells to Western blot analyses. As results were similar for day one and two, only day

one is depicted here. After in vitro culture, protein levels of pErk, pJnk and pAkt were decreased in Notch2IC-expressing B cells in comparison to ex vivo isolated B cells (Fig. 28 and data not shown). Phosphorylations of Erk and Jnk2 were completely abrogated, whereas pAkt and pJnk1 levels were partially maintained. Control B cells also showed reductions in pErk, pJnk and pAkt levels, however tubulin and GAPDH levels were also drastically reduced, possibly implicating that more of the unstimulated control B cells died, hence making it difficult to judge if the downregulation in control B cells was specific. Since constitutive Notch2 signalling was not able to maintain increased Erk and Jnk2

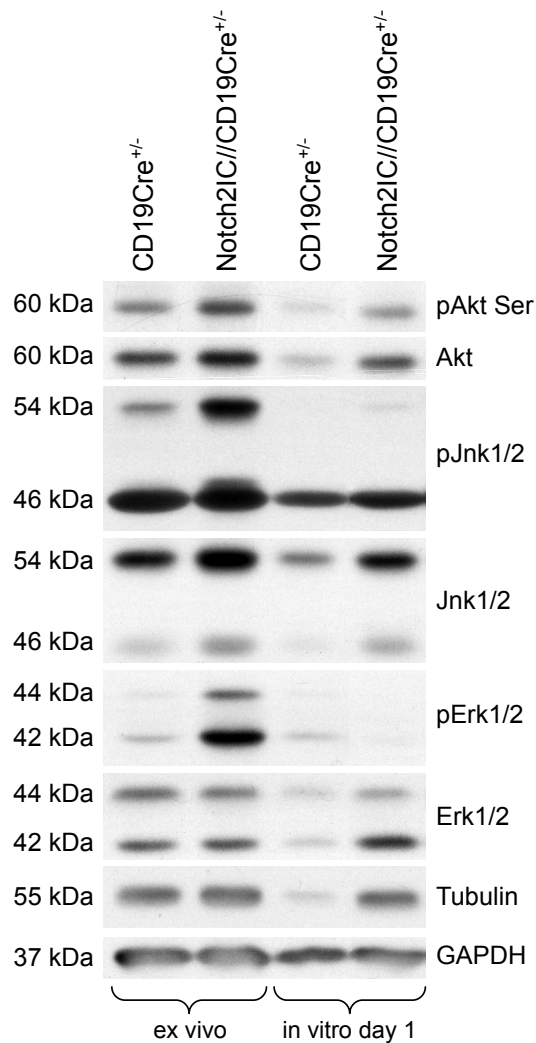


Figure 28: Notch2IC expression is not sufficient to maintain enhanced pErk, pJnk or pAkt levels in vitro. Splenic B cells were purified from Notch2IC//CD19Cre^{+/-} and CD19Cre^{+/-} control mice and directly analysed ex vivo and in addition cultured for up to two days without any stimuli. Subsequently, whole-cell extracts were subjected to Western blot analyses using antibodies specific for pAkt (pS473), pErk, pJnk and the corresponding non-phosphorylated forms. Equal protein loading was controlled by an α -tubulin and α -GAPDH staining. The results are representative of two independent experiments for B cells cultured for two days and one experiment for B cells cultured only one day. The depicted Western blot was performed with one set of animals.

phosphorylation after ex vivo isolation, it is likely that these signalling pathways are rather activated by the MZ environment than by Notch2 signalling. In contrast, Notch2 might at least partially contribute to the phosphorylation of Akt since in contrast to control B cells this phosphorylation was maintained to some extent. In summary, these results suggest that enhanced Erk and Jnk2 phosphorylation detectable in Notch2IC-expressing MZ B cells is to a great part induced by the localisation within the MZ, while the expression of typical MZ B cell surface markers seems to be directly regulated by Notch2 signalling as they are sustained outside of this environment.

As shown in 3.2.2, α -CD40 and LPS are potent inducers of MZ B cell activation and proliferation and Notch2IC-expressing cells exhibit a similar or even slightly enhanced proliferation compared to wild type MZ B cells in the presence of these stimuli. Hence, we wanted to compare MAP kinase and PI3K signalling of control and Notch2IC-expressing B cells under these stimulatory conditions in vitro. B cells were isolated from spleens of CD19Cre^{+/-} and Notch2IC//CD19Cre^{+/-} mice and taken into in vitro culture with or without α -CD40 or LPS. After one and two days, protein expression levels of pErk, pJnk, pAkt and the corresponding non-phosphorylated forms were analysed by subjecting whole-cell extracts of these cultured cells to Western blot analyses (Fig. 29). In control B cells, both, LPS and α -CD40 stimulation enhanced Erk and Akt phosphorylation. Yet, α -CD40 treatment resulted

in a faster upregulation, as pAkt and pErk levels were already drastically increased after one day, while in LPS-treated cells expression was highest on day two. α -CD40 was also able to enhance pJnk expression peaking at day one, however after LPS treatment pJnk was slightly reduced compared to ex vivo levels. In contrast to control B cells, Erk signalling in Notch2IC-expressing B cells dropped despite α -CD40 or LPS stimulation. However, a slight rescue seems to be detectable on day two of in vitro culture. Similar to control cells, pJnk and pAkt levels of Notch2IC-expressing cells were increased by α -CD40 stimulation, while LPS treatment led to a reduction of pJnk and no change in pAkt. However, compared to ex vivo levels, α -CD40-induced increases in Erk and Akt signalling were more pronounced in control B cells than in Notch2IC-expressing cells. These findings indicate that control B cells respond better to LPS and α -CD40 stimulation than Notch2IC-expressing B cells most likely due to the pre-activated state of the latter cell population.

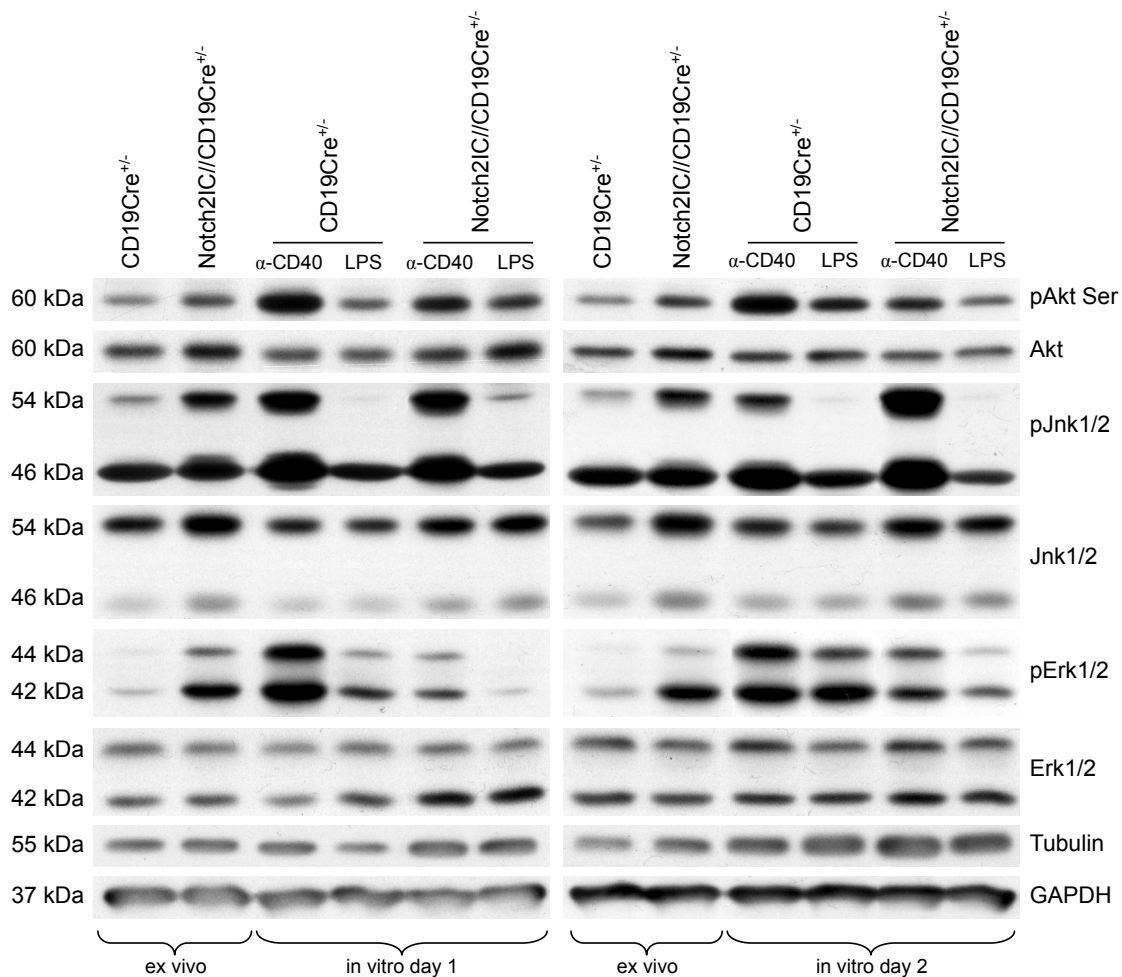


Figure 29: Control B cells exhibit greater activation in response to LPS and α -CD40 stimulation than Notch2IC-expressing B cells. Splenic B cells were purified from Notch2IC//CD19Cre^{+/+} and CD19Cre^{+/+} control mice and directly analysed ex vivo and in addition cultured for up to two days with α -CD40 or LPS stimulation. Subsequently, whole-cell extracts were subjected to Western blot analyses using antibodies specific for pAkt (pS473), pErk, pJnk and the corresponding non-phosphorylated forms. Equal protein loading was controlled by α -tubulin and α -GAPDH staining. The results are representative of two independent experiments for B cells cultured for two days and one experiment for B cells cultured only one day. The Western blot on the left, depicting results from the time points “ex vivo” and “in vitro day 1”, was performed with one set of animals. The Western blot on the right was performed with another independent set of mice.

3.2.5 Notch2IC-expressing B cells spontaneously differentiate into CD138⁺

B220^{low} plasmablasts or plasma cells in vitro

The experiments and results described in the chapters before clearly showed that Notch2IC-expressing B cells exhibit an activated phenotype in vivo, including increased proliferation potential and enhanced activity of the Erk, Jnk as well as the PI3K/Akt signalling pathways. Due to their pre-activated phenotype, MZ B cells are known to be able to rapidly differentiate into CD138⁺ B220^{low} antibody-secreting plasma cells (Zandvoort and Timens, 2002). To investigate whether the increased frequency of MZ B cells in Notch2IC-expressing mice could lead to the (spontaneous) appearance of an increased frequency of plasmablasts or plasma cells, splenic B cells were isolated from Notch2IC//CD19Cre^{+/-} and CD19Cre^{+/-} control mice and analysed by flow cytometry. As plasma cells exhibit high CD138 and low B220 levels, B cells were stained with a mixture of CD138, B220 and hCD2 antibodies. Percentages of plasma cells were low in both control and Notch2IC-expressing B cell populations (Fig. 30), suggesting that constitutive Notch2IC expression does not drive spontaneous plasma cell differentiation in vivo, although Notch2IC/CD19Cre^{+/-} mice have a strongly increased proportion of pre-activated MZ B cells. Next we wanted to know if plasma cell development was inducible and subsequently possibly enhanced in in vitro cultures of Notch2IC-expressing MZ B cells in comparison to control B cells, when triggered with the right stimuli. As LPS is known to be a potent inducer of plasma cell differentiation in wild type B cells, Notch2IC-expressing and control B cells were isolated from spleens and cultured for up to three days with or without LPS stimulation. Development of plasmablasts or plasma cells was checked daily by staining B cells with a mixture of CD138, B220, hCD2 antibodies and a marker for dead cells and subsequently analysing them by flow cytometry (Fig. 31). As expected, during these three days of in vitro culture unstimulated control B cells showed no signs of plasma cell development, whereas in LPS-stimulated control B cells, CD138⁺ B220^{low} plasma cells were clearly distinguishable on day two and three. In great contrast to this, in cultures of Notch2IC-expressing B cells this CD138⁺ B220^{low} population already appeared spontaneously at day one without adding any stimuli and strongly augmented on day two. LPS stimulation did not further increase proportions of CD138⁺ B220^{low} cells, but rather seemed to slightly hamper spontaneous

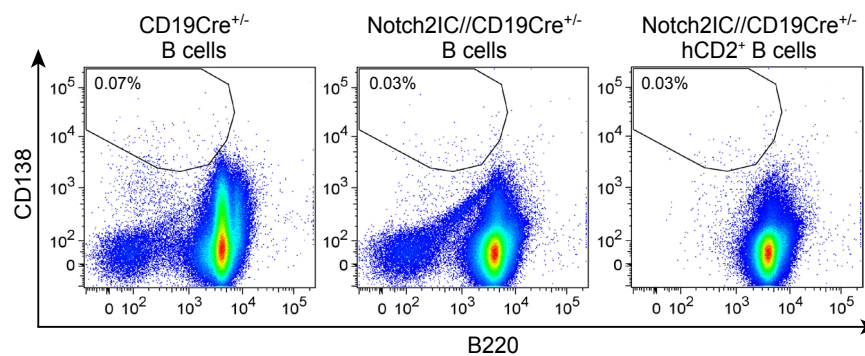


Figure 30: No increased plasma cell population in unimmunised Notch2IC//CD19Cre^{+/-} compared to CD19Cre^{+/-} control mice. Splenic B cells were isolated from Notch2IC//CD19Cre^{+/-} and CD19Cre^{+/-} mice and analysed for their CD138 and B220 expression by flow cytometry. Exemplary dot plots are gated on living cells (left and center panel) and in the case of Notch2IC-expressing cells additionally also on hCD2⁺ populations (right panel). Data is representative of five independent experiments.

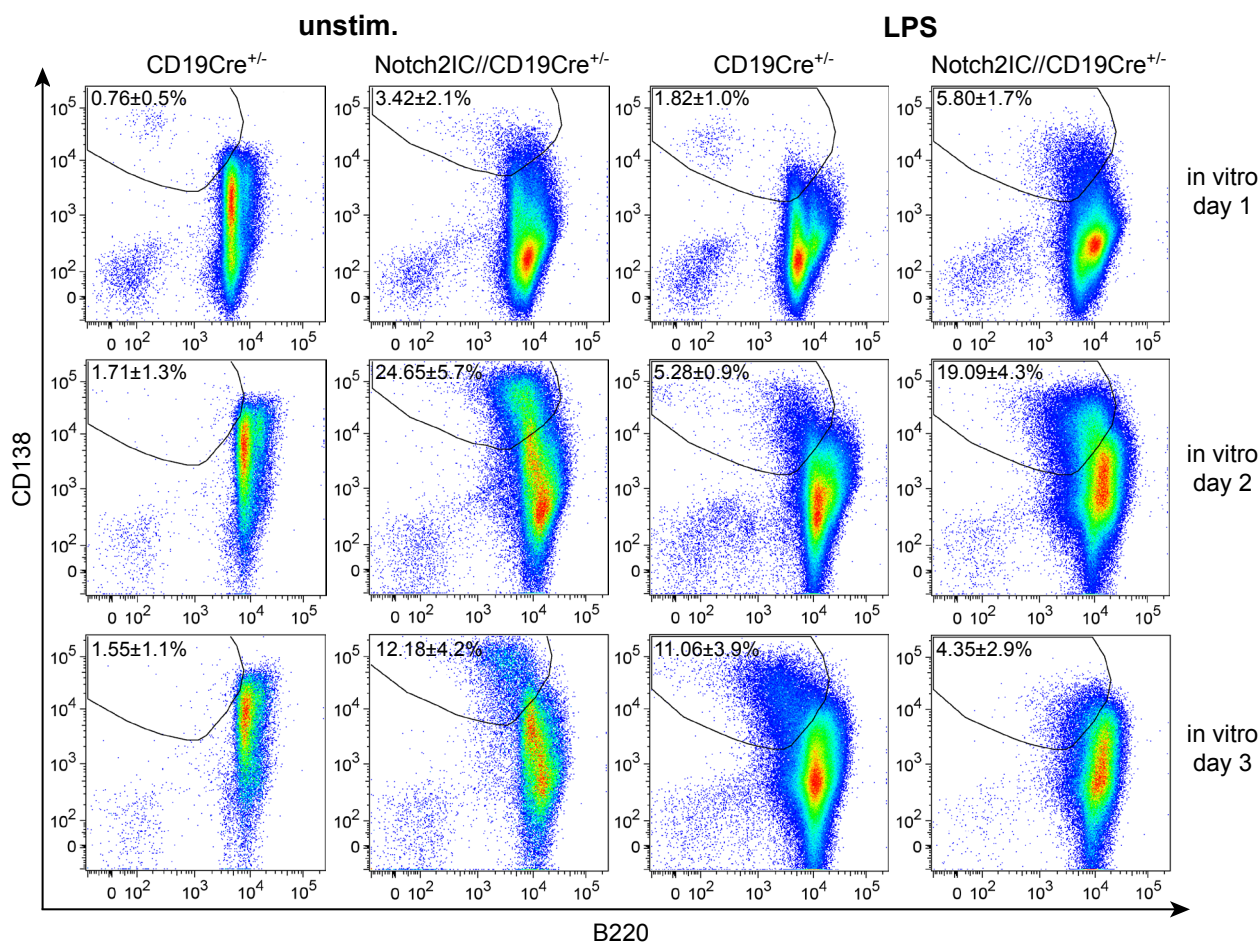


Figure 31: In vitro cultured Notch2IC//CD19Cre^{+/-} B cells spontaneously differentiate into CD138⁺ B220^{low} plasmablast/plasma cells. Splenic B cells were isolated from Notch2IC//CD19Cre^{+/-} and CD19Cre^{+/-} mice, cultured for up to three days with or without LPS stimulation and analysed for CD138 and B220 expression by flow cytometry. Dot plots are gated on living cells. Numbers indicate mean percentages and SD of CD138⁺ B220^{low} cell populations. Calculations are based on three to five independent experiments for CD19Cre^{+/-} mice and four to ten independent experiments for Notch2IC//CD19Cre^{+/-} animals.

plasmablast/plasma cell formation, as on day two and three percentages of CD138⁺ B220^{low} cells were slightly lower after LPS stimulation than in unstimulated Notch2IC-expressing cells. Still, we noticed that on day one, frequencies of CD138⁺ B220^{low} cells in LPS-treated Notch2IC-expressing cells were higher than those in unstimulated cells. Nevertheless, highest percentages of CD138⁺ B220^{low} cells obtained in cultures of unstimulated or LPS-stimulated Notch2IC-expressing B cells were always higher than the highest amounts of CD138⁺ B220^{low} cells obtained in LPS-treated control B cells. Additional gating on hCD2⁺ cells revealed that only cells expressing the Notch2IC transgene exhibited this differentiation potential, which was the case for all the results described in this chapter (Fig. 32). B cells that did not express hCD2 behaved like control B cells except that even after LPS stimulation no plasma cell development could be detected (Fig. 32).

α -CD40 stimulation is known to enhance proliferation and survival of in vitro cultured wild type B cells and to induce IgG switching. Beyond this, CD40 ligation on B cells has been shown to inhibit plasma cell differentiation (Satpathy et al., 2010; Randall et al., 1998). Therefore, we were interested in what effect α -CD40 stimulation would have on in vitro cultured Notch2IC-expressing B cells and whether it would be able to inhibit spontaneous plasma cell development. Experiments were

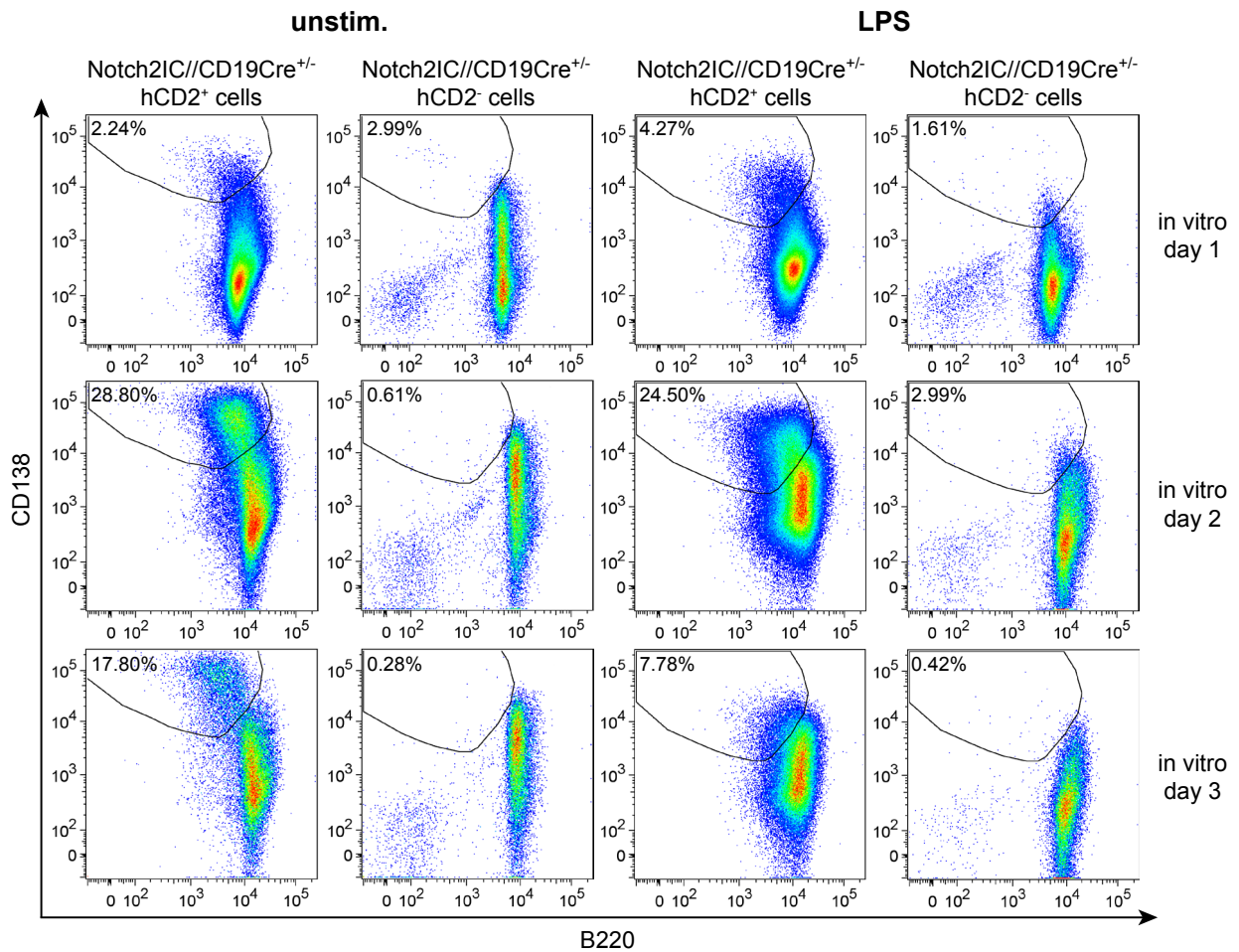


Figure 32: Only Notch2IC-expressing B cells spontaneously differentiate into CD138⁺ B220^{low} plasmablasts/plasma cells in vitro. Splenic B cells were isolated from Notch2IC//CD19Cre^{+/-} mice, cultured for up to three days with or without LPS stimulation and analysed for CD138 and B220 expression by flow cytometry. Exemplary dot plots are gated on living cells, positive or negative for hCD2. Numbers indicate percentages of CD138⁺ B220^{low} cell populations. Data is representative of four to ten independent experiments.

performed as previously described, except that B cells were now cultured in the presence of α -CD40 or α -CD40+LPS stimuli (Fig. 33). Indeed, stimulation with α -CD40 strongly diminished spontaneous plasmablast/plasma cell differentiation of Notch2IC-expressing B cells in the absence of LPS or even completely abolished the formation of a CD138⁺ B220^{low} population in LPS-treated control as well as in Notch2IC-expressing cells. Yet, percentages of CD138⁺ B220^{low} cells were still higher in α -CD40-treated Notch2IC-expressing than in α -CD40 or α -CD40+LPS-treated control B cells, again peaking at day two of in vitro culture. On day three of α -CD40+LPS treatment almost all Notch2IC-expressing B cells were dead, possibly due to overstimulation of already pre-activated MZ B cells. These experiments suggest that Notch2IC-expressing B cells still have an intrinsic potential to spontaneously differentiate into plasmablasts/plasma cells, which is somehow inhibited in vivo and can also be hampered by α -CD40 stimulation.

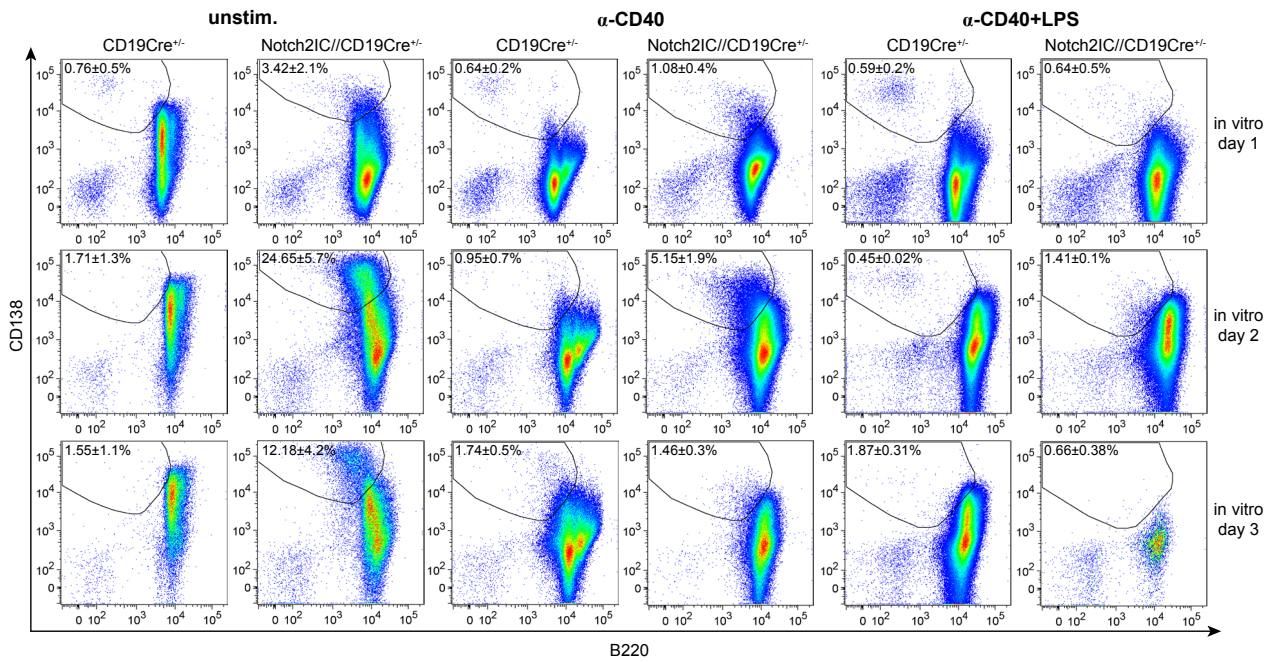


Figure 33: Spontaneous differentiation of Notch2IC-expressing cells into CD138⁺ B220^{low} cells in vitro can be hampered by α-CD40 stimulation. Splenic B cells were isolated from Notch2IC//CD19Cre^{+/-} and CD19Cre^{+/-} mice, cultured for up to three days with or without α-CD40 or α-CD40+LPS stimulation and analysed for CD138 and B220 expression by flow cytometry. Dot plots are gated on living cells. Numbers indicate mean percentages and SD of CD138⁺ B220^{low} cell populations. Calculations are based on two to five independent experiments for CD19Cre^{+/-} mice and two to ten independent experiments for Notch2IC//CD19Cre^{+/-} animals.

3.2.6 Spontaneous plasmablast/plasma cell development of Notch2IC-expressing B cells in vitro is driven by Notch2IC expression

To investigate whether the spontaneous differentiation of Notch2IC-expressing B cells to plasmablasts or plasma cells in vitro was an intrinsic effect of MZ B cells or induced by constitutive Notch2 expression, we compared sort-purified wild type MZ B and Fo B cells with Notch2IC-expressing MZ B cells. To this end, splenic B cell populations were sorted according to their CD21 and CD23 expression, with MZ B cells being CD21^{high} CD23^{low} and Notch2IC-expressing cells additionally hCD2⁺ and Fo B cells being CD21^{low} CD23^{high}. Subsequently, sort-purified cell populations were cultured for two days with or without LPS. Plasmablast/plasma cell differentiation was checked by a hCD2, CD138, B220 staining. Wild type Fo B cells did not show any signs of plasma cell differentiation neither with LPS nor without stimulation (Fig. 34, left panel). An expected amount of MZ B cells from control mice developed to CD138⁺ B220^{low} cells, yet only after LPS stimulation (Fig. 34, central panel), whereas Notch2IC-expressing B cells displayed plasmablast/plasma cell formation with and without LPS stimulation (Fig. 34, right panel). In contrast to experiments performed with total, splenic B cells (see previous chapter), LPS-stimulated, sort-purified Notch2IC-expressing MZ B cells exhibited increased frequencies of CD138⁺ B220^{low} cells compared to unstimulated Notch2IC-expressing cells. A possible explanation for this difference could be that LPS accelerates plasma cell differentiation. Thus, the optimal time points exhibiting maximal plasmablast/plasma cell frequencies in LPS-treated Notch2IC-expressing B cells might have been missed in previous experiments with unsorted B cells. In experiments with sort-purified cells, peaks of plasmablast/plasma cell differentiation are possibly

shifted to a later time point, as cells need a certain time to recover from the sort procedure, before starting to proliferate or differentiate. Still, these results suggest that constitutive Notch2 signalling further enhances spontaneous plasma cell formation in MZ B cells as soon as cells are taken out of their natural environment.

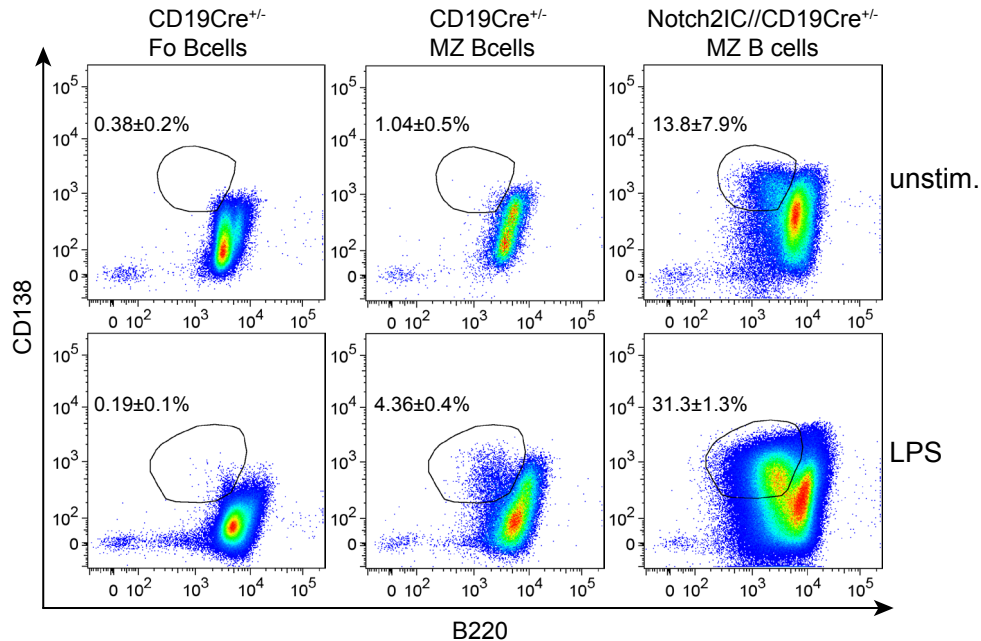


Figure 34: Plasma cell differentiation is triggered by constitutive Notch2IC expression. Splenic cells of CD19Cre^{+/-} and Notch2IC//CD19Cre^{+/-} were sort-purified for Thy1.2⁺, B220⁺, CD21^{high} CD23^{low} MZ B and CD21^{low} CD23^{high} Fo B cells and in the case of Notch2IC-expressing cells also for hCD2⁺. Purified cell populations were subsequently cultured for two days with or without LPS in similar cell densities. On day two, plasma cell development was analysed by flow cytometry. Dot plots are gated on living cells and in the case of Notch2IC-expressing cells on hCD2⁺ populations. Data is representative of two independent experiment.

3.2.7 Notch2IC-expressing CD138⁺ B220^{low} cell populations spontaneously arising in vitro are functional antibody-secreting plasmablasts or plasma cells

Next we tested, whether in vitro cultured Notch2IC-expressing B cells indeed developed to functional, antibody-secreting plasmablasts/plasma cells. Firstly, we assessed antibody titers in the supernatant of in vitro cultures. For this, splenic B cells from Notch2IC//CD19Cre^{+/-} and control mice were cultured for eight days with or without LPS, α -CD40 and α -CD40+LPS stimulation. On the last day, cell culture supernatants were collected and concentrations of total IgM titers were determined by ELISA (Fig. 35). In accordance with former experiments, IgM secretion could be detected in cultures of unstimulated Notch2IC-expressing B cells, but not in those of control B cells. LPS treatment clearly increased IgM secretion in cultures of control B cells, but not significantly in those of Notch2IC-expressing B cells. In line with previous flow cytometrical analyses, α -CD40 stimulation decreased spontaneous IgM secretion in Notch2IC-expressing B cells as well as in LPS-treated control and Notch2IC-expressing B cells. However, regardless of the stimulus Notch2IC-expressing B cells were always secreting greater amounts of IgM compared to control B cells, which might at least partly be due to their MZ B cell

phenotype. Concentrations of other antibody isotypes were below the detection limit. Secondly, we determined the number of IgM-, IgG1- and IgG3-secreting plasma cells by ELISPOT analyses (Fig. 36). To this end, splenic B cells from Notch2IC//CD19Cre^{+/-} and CD19Cre^{+/-} control mice were isolated and cultured for one day without stimulation. On day one, frequencies of living cells were determined. Subsequently, living cells were transferred onto ELISPOT plates in specific cell densities, culturing them for additional two days. Then the frequencies of antibody-secreting plasma cells were visualised and determined. Unstimulated Notch2IC-expressing B cells displayed increased numbers of IgG3-, IgM- and IgG1-secreting plasma cells. Even among 8x10³ Notch2IC-expressing B cells were a lot more IgM-secreting cells than in cultures containing 1x10⁵ control B cells. Together with the results from ELISA experiments above, these analyses prove that the CD138⁺ B220^{low} cells arising in Notch2IC-expressing B cells even without stimulation at day two of in vitro culture are indeed antibody-secreting plasma cells or plasmablasts.

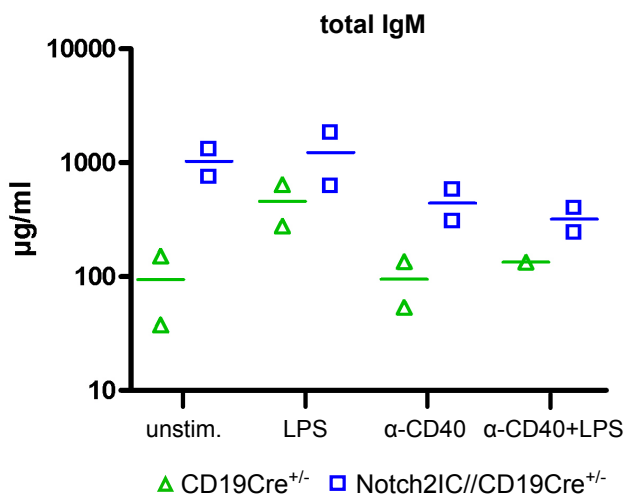


Figure 35: IgM titers of in vitro cultured splenic B cells of Notch2IC//CD19Cre^{+/-} and control mice. Splenic B cells were isolated from Notch2IC//CD19Cre^{+/-} and control mice and taken into culture with or without LPS, α-CD40 or α-CD40+LPS stimulation. After eight days, cell culture supernatants were collected and concentrations of total IgM titers were determined by ELISA. Two mice were analysed per group.

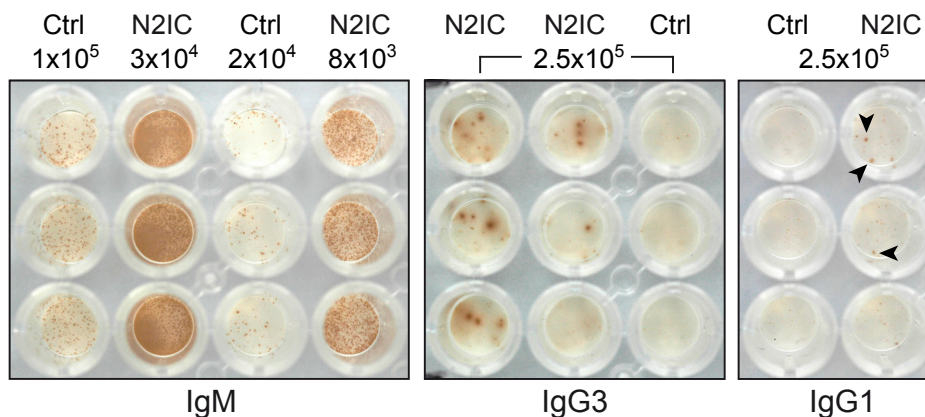


Figure 36: Unstimulated Notch2IC-expressing B cells are able to spontaneously differentiate to IgM-, IgG3- and IgG1-secreting plasmablasts/plasma cells in vitro. Splenic B cells were isolated from Notch2IC//CD19Cre^{+/-} (N2IC) and control mice (Ctrl) and taken into in vitro culture. After one day, amounts of living cells were determined and subsequently cells were plated and cultured onto ELISPOT plates in the depicted densities. After additional two days antibody-secreting plasma cells were visualised as brown spots by staining with 3,3'-diaminobenzidine (DAB). Two mice were analysed per group.

3.2.8 Spontaneous plasmablast/plasma cell development of Notch2IC-expressing B cells in vitro correlates with increased Blimp-1 and Irf4 levels

Plasma cells and their precursors are known to specifically upregulate the two transcription factors Irf4 and Blimp-1 (Shapiro-Shelef and Calame, 2005). Therefore, we analysed by intracellular FACS analyses whether these two transcription factors are already elevated in Notch2IC-expressing MZ B cells in comparison to control B cells ex vivo. Splenic B cells were stained for CD21 and CD23 expression on their surface and subsequently intracellularly for one of the two transcription factors (Fig. 37). Ex vivo analyses revealed only very slightly increased Blimp-1 levels in wild type MZ B cells versus Fo B cells. Still, Blimp-1 expression was significantly higher in Notch2IC-expressing cells compared to wild type Fo B cells and compared to control MZ B cells (Fig. 37). Results obtained for Irf4 levels were more definite. MZ B cells exhibited higher Irf4 levels than Fo B cells and Notch2IC-expressing cells enhanced expression levels compared to wild type MZ B cells (Fig. 37).

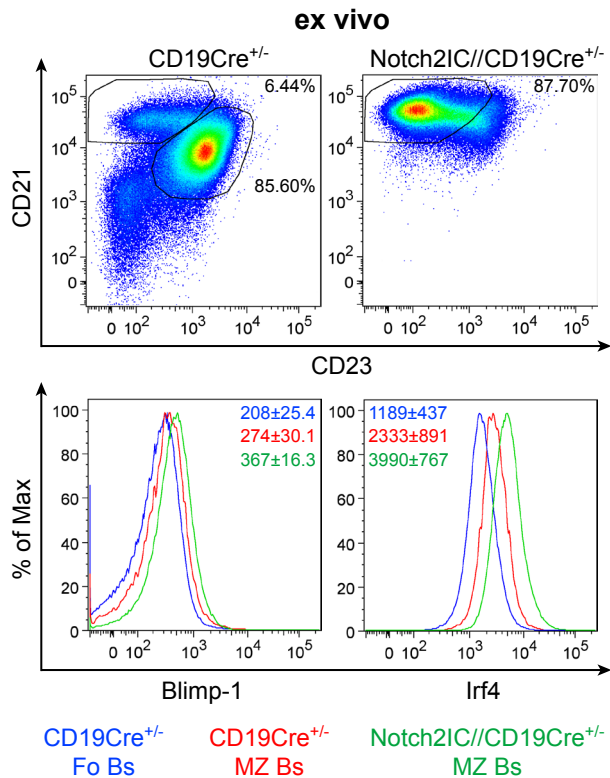


Figure 37: Notch2IC-expressing MZ B cells express higher Blimp-1 and Irf4 levels than wild type MZ B cells. Splenic B cells were isolated from Notch2IC//CD19Cre^{+/-} and CD19Cre^{+/-} mice, stained for CD21 and CD23 surface markers, fixed, permeabilised and subsequently stained and analysed for the indicated transcription factors by intracellular flow cytometry. Exemplary dot plots are gated on B220⁺ lymphocytes, Notch2IC-expressing cells additionally on hCD2⁺ cells. They depict CD21^{high} CD23^{low} wild type MZ B and CD21^{low} CD23^{high} wild type Fo B cells as well as CD21^{high} CD23^{low} Notch2IC-expressing MZ B cells. Histograms depict overlays of the abundance of the indicated molecules. They are gated on living, B220⁺, CD21^{high} CD23^{low} wild type MZ B cells (red line), CD21^{low} CD23^{high} wild type Fo B cells (blue line) and living, B220⁺ and hCD2⁺ CD21^{high} CD23^{low} Notch2IC-expressing MZ B cells (green line). Numbers represent means of medians and SD. Data is representative of three independent experiments.

Secondly, we compared the regulation of Blimp-1 and Irf4 induction in Notch2IC-expressing and control B cells in the presence and absence of stimulation during in vitro culture. Splenic B cells of Notch2IC//CD19Cre^{+/-} and control mice were isolated and cultured for up to three days with or without LPS stimulation and Blimp-1 and Irf4 levels were monitored on daily basis (Fig. 38). In cultures of unstimulated control B cells no changes in Blimp-1 and Irf4 levels could be detected, whereas, unstimulated Notch2IC-expressing cells exhibited a clear upregulation of Blimp-1 and an increase in the proportion of Irf4^{high} cells, both peaking at day two. In control cells, increases in Blimp-1 and Irf4 could only be detected when cultured with LPS. Under these circumstances, two distinct

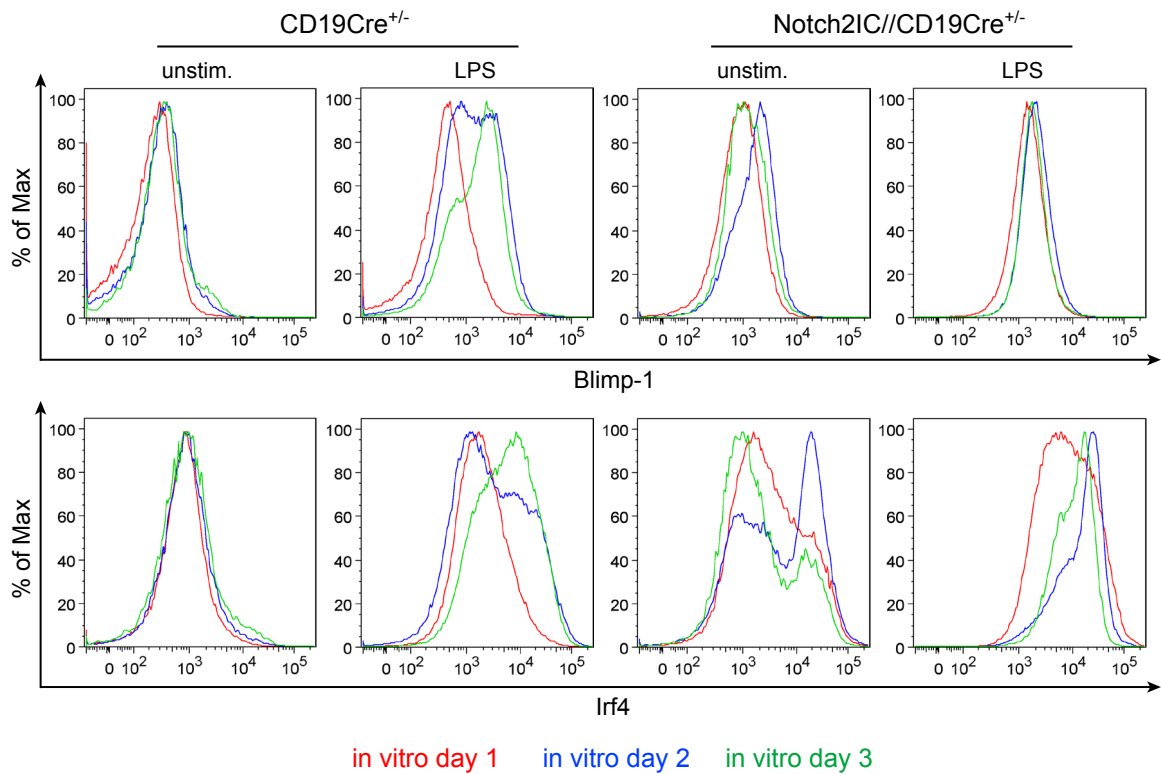


Figure 38: Splenic Notch2IC-expressing B cells upregulate Blimp-1 and Irf4 expression with and without LPS stimulation. Splenic B cells were isolated from Notch2IC//CD19Cre^{+/-} and CD19Cre^{+/-} mice and cultured for one to three days with or without LPS. On days one to three, cells were stained for the surface marker B220, fixed, permeabilised and subsequently stained and analysed for the indicated transcription factors by intracellular flow cytometry. Exemplary histograms are gated on living, B220⁺ cells and depict overlays of the abundance of the indicated molecules. Data is representative of three independent experiments.

populations varying in their Blimp-1 and Irf4 expression strength (Blimp-1^{high} Irf4^{high} and Blimp-1^{low} Irf4^{low}) could be distinguished on day two, with a nearly complete shift towards the Blimp-1^{high} Irf4^{high} population observable on day three. In LPS-treated Notch2IC-expressing cells, only small increases in Blimp-1 levels peaking at day two could be detected, suggesting that at day one maximal Blimp-1 expression was already reached. Similar to unstimulated Notch2IC-expressing cells, LPS treatment induced a strong increase in Irf4^{high} cells already on day one, peaking at day two and slightly decreasing on day three. However, in contrast to unstimulated Notch2IC-expressing cells, on day two nearly all LPS-treated Notch2IC-expressing cells were already Irf4^{high}. These data underline our finding that Notch2IC-expressing B cells quickly differentiate to plasmablasts/plasma cells without stimulation. Moreover, these data implicate that LPS stimulation further accelerates plasma cell differentiation in Notch2IC-expressing B cells. To directly compare overall courses of Blimp-1 and Irf4 expression of unstimulated and LPS-treated Notch2IC-expressing and control B cells over three days, we depicted Blimp-1 and Irf4 levels of these cells in histogram overlays (Fig. 39). On day one and two, LPS-treated Notch2IC-expressing cells exhibited highest Blimp-1 levels and highest frequencies of Irf4^{high} cells, followed by unstimulated Notch2IC-expressing cells and LPS-treated control cells (Fig. 39, left column). These findings confirmed our hypothesis that Notch2IC-expressing cells are faster in upregulating Blimp-1 and Irf4 compared to LPS-stimulated controls and that this upregulation can further be accelerated by LPS treatment. In addition, these overlays affirmed that with LPS treatment, highest Blimp-1 levels were already reached on day one in Notch2IC-expressing cells and do not further

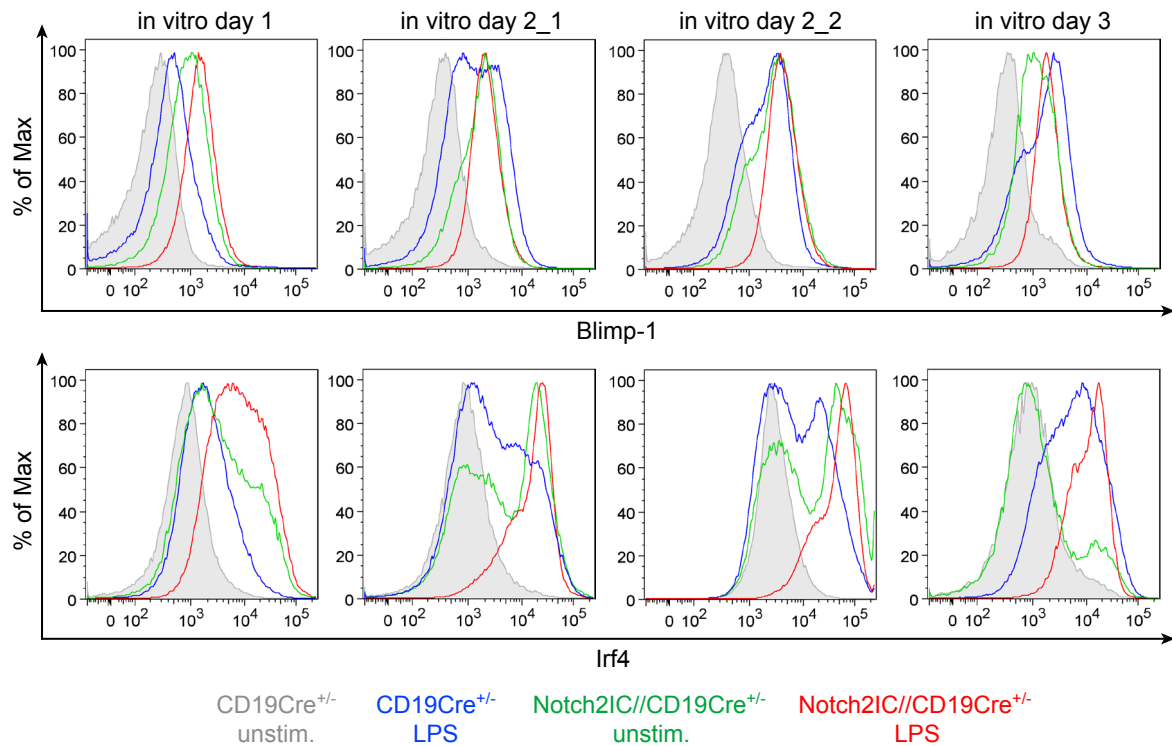


Figure 39: Notch2IC-expressing B cells cultured with or without LPS, exhibit an accelerated Blimp-1 and Irf4 induction compared to LPS-treated wild type B cells. Splenic B cells were isolated from Notch2IC//CD19Cre^{+/-} and CD19Cre^{+/-} mice and cultured with or without LPS. On day one to three, cells were stained for B220, fixed, permeabilised and subsequently stained and analysed for the indicated transcription factors by intracellular flow cytometry. Exemplary histograms depict overlays of the abundance of the indicated molecules. They are gated on living, B220⁺ B cells and in the case of Notch2IC-expressing B cells on living, hCD2⁺ cells. To illustrate the fast dynamics in expression levels, histograms of two different experiments are depicted for day two. Data is representative of two independent experiments.

increase over time. While on day three Blimp-1 levels and the amount of Irf4^{high} cells started to drop in unstimulated Notch2IC-expressing cells, both transcription factors were still highly expressed in LPS-treated Notch2IC-expressing and control cells. This finding was surprising since plasmablast/plasma cell frequencies decreased at day three in both LPS-stimulated and unstimulated Notch2IC-expressing B cells (see Fig. 31), with nearly no plasma cells detectable in cultures of LPS-treated cells. To clarify why on day three Blimp-1 and Irf4 levels were still higher in LPS-treated Notch2IC-expressing cells, whereas in unstimulated Notch2IC-expressing cells they already dropped, we compared the Blimp-1 and Irf4 expression levels of CD138⁺ B220^{low} cells arising in LPS-stimulated control cells with levels of CD138⁻ B220^{high} non-plasma cells of stimulated and unstimulated Notch2IC-expressing and control cells (Fig. 40). These analyses revealed that the majority of non-plasma cells in LPS-treated Notch2IC-expressing cells had nearly similar Irf4^{high} levels as typical plasma cells arising in LPS-treated control cells (Fig. 40). Furthermore, non-plasma cells of LPS-treated controls had higher Irf4 levels than non-plasma cells of unstimulated Notch2IC-expressing cells (Fig. 40). Hence, in LPS-treated Notch2IC-expressing cells, every cell exhibited Irf4^{high} levels, whereas in unstimulated Notch2IC-expressing cells only plasmablasts/plasma cells - which decreased on day three - were Irf4^{high}. Thus, in Irf4 histogram overlays, the proportion of Irf4^{high} cells decreased in unstimulated Notch2IC-expressing cells, while the bulk of LPS-stimulated cells remained Irf4^{high}, although plasma cells were not detectable anymore. As already described in chapter 3.2.5, α -CD40 stimulation hampered spontaneous plasmablast/plasma

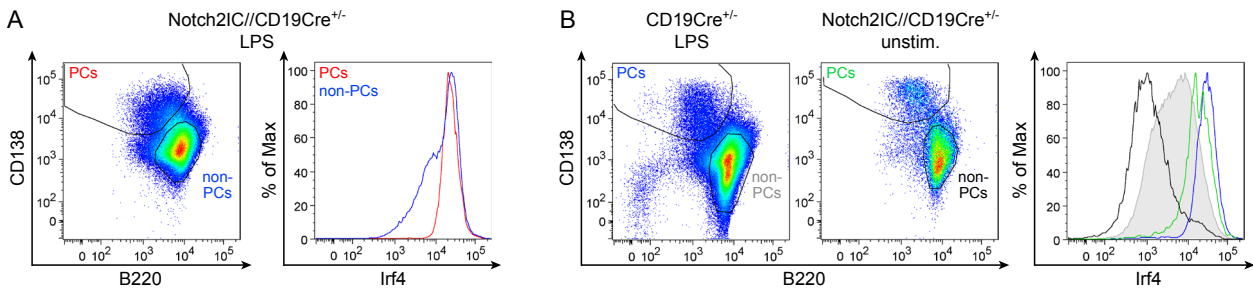


Figure 40: LPS-stimulated non-plasma cells have higher Irf4 levels than unstimulated non-plasma cells. Splenic B cells were isolated from Notch2IC//CD19Cre^{+/-} and CD19Cre^{+/-} mice and cultured with or without LPS. On day three, cells were stained for B220 and CD138, fixed, permeabilised and subsequently stained and analysed for Irf4 by intracellular flow cytometry. **(A)** Exemplary dot plot gated on living cells depicting CD138^{high} B220^{low} plasma cells (PCs) and CD138^{low} B220^{high} non-plasma cells (non-PCs) with respective Irf4 levels (histograms) of LPS-treated Notch2IC-expressing cells. **(B)** Exemplary histograms are gated on living cells and display overlays of the abundance of Irf4 of CD138^{high} B220^{low} control plasma cells (PCs) with CD138^{low} B220^{high} non-plasma cells (non-PCs) (both represented in dot plots) of unstimulated Notch2IC-expressing B cells and LPS-treated control and Notch2IC-expressing B cells. Line colours in histograms correspond to colour codings of the different populations in respective dot plots. Data is representative of two independent experiments.

cell development in Notch2IC-expressing cells. In accordance, among the different *in vitro* cultures of Notch2IC-expressing cells, those treated with α -CD40 had lower Blimp-1 expression levels than unstimulated or LPS-treated cells. However, increases in Irf4 levels could still be detected with α -CD40 stimulation (Fig. 41). These data show that α -CD40 stimulation led to the upregulation of Irf4 but not Blimp-1, which might explain why α -CD40 treatment leads to an inhibition of plasma cell differentiation in cultures of Notch2IC-expressing cells. In summary, the expression strength and the

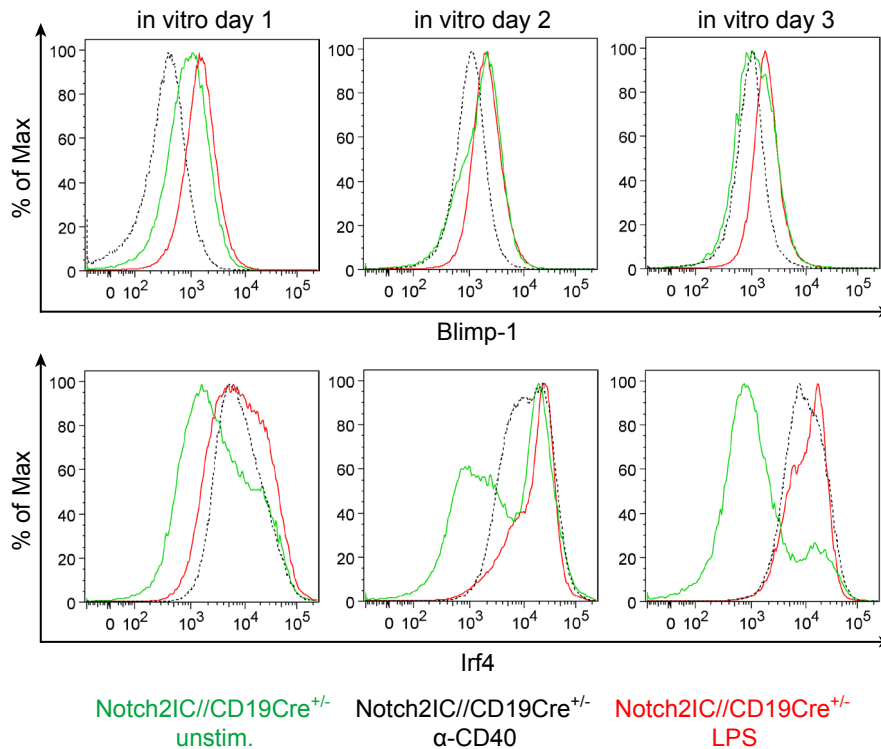


Figure 41: Notch2IC-expressing B cells cultured with α -CD40 have lower Blimp-1 levels than cells cultured with or without LPS. Splenic B cells were isolated from Notch2IC//CD19Cre^{+/-} mice and cultured with or without LPS or α -CD40. On day one to three, cells were stained for B220, fixed, permeabilised and subsequently stained and analysed for the indicated transcription factors by intracellular flow cytometry. Exemplary histograms depict overlays of the abundance of the indicated molecules. They are gated on living, hCD2⁺ cells. Data is representative of two independent experiments.

course of Blimp-1 and Irf4 expression in Notch2IC-expressing cells together with the results from former experiments strongly suggest that fully functional plasmablasts or plasma cells are indeed arising in in vitro cultures of Notch2IC-expressing B cells. Furthermore, probably due to the pre-activated state of Notch2IC-expressing cells, plasmablast/plasma cell development seems accelerated in unstimulated Notch2IC-expressing cells compared to LPS-treated control B cells and even more in LPS-treated Notch2IC-expressing cells.

3.3 The role of Notch2 signalling in immune responses

3.3.1 Notch2IC//CD19Cre^{+/-} mice are impaired in their TI-2 immune response

MZ B cells are known to play a decisive role in the production of natural antibodies (Casali and Schettino, 1996; Cerutti et al., 2013) and in TI immune responses, by rapidly recognising antigens and by secreting low-affinity IgM and IgG3 antibodies (Martin et al., 2001). Notch2IC//CD19Cre^{+/-} mice have increased MZ B cell numbers, yet they exhibit decreased basal IgG3 titers and a disturbed TD immune response, the latter probably due to decreased Fo B cell numbers (Hampel et al., 2011). Still, when taken into in vitro culture, Notch2IC-expressing B cells rapidly develop into antibody-secreting plasmablasts or plasma cells without being stimulated. So, although constitutive Notch2IC-expression together with the positioning of the MZ B cells in the MZ somehow seems to form an inhibitory environment suppressing the intrinsic plasma cell differentiation potential of Notch2IC-expressing MZ B cells, we wanted to investigate whether this in vivo inhibition could possibly also entail defects in TI-2 immune responses (NP-Ficoll) in Notch2IC/CD19Cre^{+/-} mice. To check this, Notch2IC//CD19Cre^{+/-} and control animals were primarily immunised intraperitoneally (i.p.) with 50 µg 4-hydroxy-3-nitrophenylacetyl (NP) conjugated to Ficoll. NP-specific plasma cell numbers as well as serum titers of NP-specific antibodies were determined by ELISPOT and ELISA, respectively, seven and 14 days after immunisations. On day seven as well as on day 14, sera of immunised Notch2IC//CD19Cre^{+/-} mice contained significantly lower levels of NP-specific IgM and IgG3 titers than those of control animals (Fig. 42). Furthermore, in contrast to controls, no NP-specific IgG3-secreting plasma cells could be detected among splenic cells of immunised Notch2IC//CD19Cre^{+/-} mice (Fig. 43), which was in accordance with the decreased NP-specific IgG3 antibody titers in sera

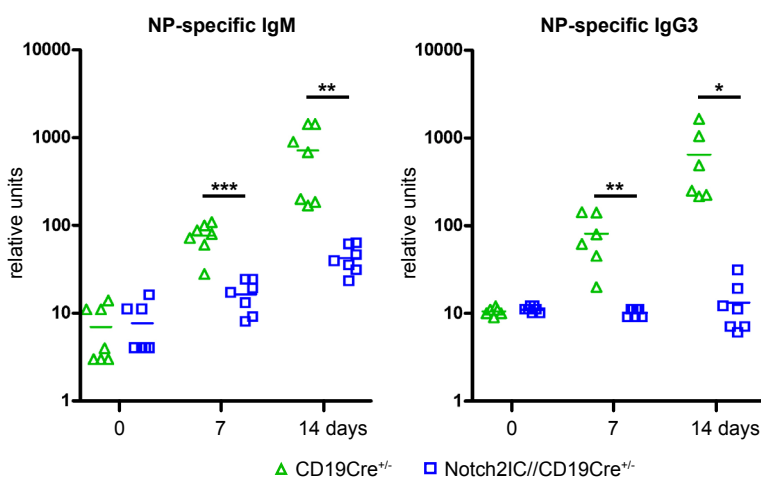


Figure 42: Notch2IC//CD19Cre^{+/-} have reduced antigen-specific IgM and IgG3 serum titers after TI-2 immunisation. Notch2IC//CD19Cre^{+/-} and CD19Cre^{+/-} control mice were injected intraperitoneally with 50 µg NP-Ficoll. NP-specific IgM and IgG3 concentrations were measured by ELISA of blood serum taken seven and 14 days after injection. Points represent data from individual animals and horizontal bars mark the mean value. CD19Cre^{+/-} controls (Ctrl, green triangles); Notch2IC//CD19Cre^{+/-} (blue squares); * p < 0.05; ** p < 0.01; *** p < 0.001 in comparison to controls.

of Notch2IC//CD19Cre^{+/-} mice after immunisation with NP-Ficoll. However, in comparison to controls, Notch2IC//CD19Cre^{+/-} mice exhibited an extremely high density of IgM-secreting plasma cells independent of the immunisation status of the animals (Fig. 43). Even control wells only coated with bovine serum albumin (BSA) revealed high numbers of these IgM-secreting plasma cells (data not shown). Similar results were obtained with ELISPOT analyses on day 14 after immunisation (data not shown). Yet, both, immunised and unimmunised Notch2IC-expressing MZ B cells exhibited a very high amount of NP-IgM-secreting antibodies able to recognise NP-BSA. This indicates that Notch2IC-expressing MZ B cells differentiate to plasma cells, secreting immunisation-independent polyreactive antibodies as soon as they are taken into culture. In summary, these data suggest that in spite of the enlarged MZ B cell population, Notch2IC//CD19Cre^{+/-} mice are unable to mount a normal immune response to the TI-2 antigen NP-Ficoll. However, after ex vivo isolation, B cells rapidly develop to plasmablasts/plasma cells secreting polyreactive antibodies.

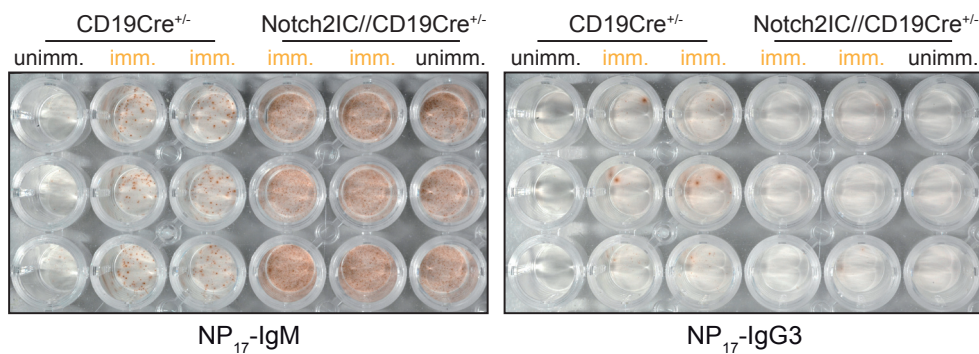


Figure 43: Notch2IC//CD19Cre^{+/-} splenic B cells do not develop into antigen-specific IgG3-secreting plasma cells after TI-2 immunisation, yet they seem to carry polyreactive IgM receptors. Notch2IC//CD19Cre^{+/-} and control mice were injected intraperitoneally with 50 µg NP-Ficoll. Seven days after injection, splenic cells were isolated and transferred in triplicates for 1.5 - 2 days onto ELISPOT plates (1x10⁶ cells/well). NP-specific IgM- and IgG3-secreting plasma cells were visualised and determined. Experiment was performed with three animals for each genotype and treatment.

3.3.2 Notch2IC//CD19Cre^{+/-} mice are impaired in their immune response to the TI-1 antigen NP-LPS

MZ B cells are equipped with polyreactive BCRs and high levels of TLRs for a quick recognition of conserved microbial patterns such as LPS (Bendelac et al., 2001; Martin and Kearney, 2002; Trembl et al., 2007) and they are known to rapidly differentiate to antibody-secreting plasma cells after LPS stimulation (Oliver et al., 1999b). Since Notch2IC//CD19Cre^{+/-} mice are hampered in their TI-2 immune response to NP-Ficoll, we wanted to know if they are also inhibited in their TI-1 immune response to NP-LPS. Preliminary ELISA data using sera of two Notch2IC//CD19Cre^{+/-} and two control mice analysed seven days after immunisation with 50 µg NP-LPS suggest that Notch2IC-expressing mice could also have slight defects in their response to TI-1 antigens, as NP-specific IgG3, but not IgM titers were decreased (data not shown). However, LPS - in contrast to NP-Ficoll - activates B cells in a polyclonal way irrespective of the BCR specificity. Thus, it is possible that defects in TI-1 immune responses could be masked by the strong activation of all MZ B cells in these immunisation experiments with 50 µg NP-LPS. So we asked whether lower NP-LPS concentrations would lead to immune reactions

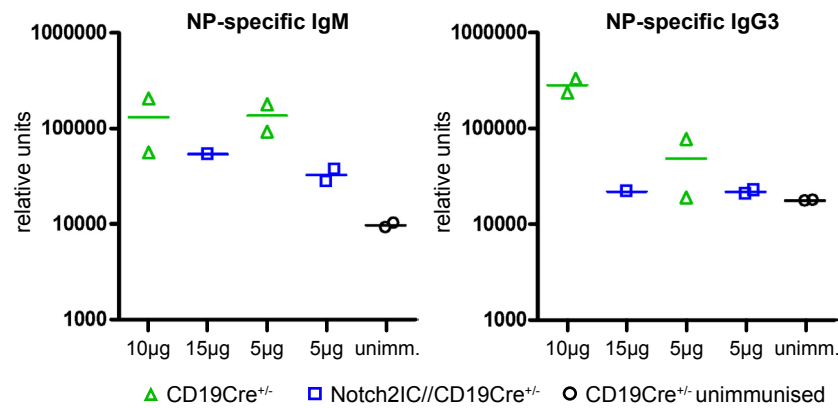


Figure 44: Notch2IC//CD19Cre^{+/-} mice are impaired in their TI-1 immune response to low NP-LPS concentrations. Notch2IC//CD19Cre^{+/-} and control mice were immunised intraperitoneally with 5 - 15 µg NP-LPS. Concentrations of NP-specific antibody titers of the indicated isotypes were measured by ELISA of blood serum taken seven days after injection. Points represent data from individual animals and horizontal bars mark the mean value. CD19Cre^{+/-} controls (green triangles); Notch2IC//CD19Cre^{+/-} (blue squares); unimmunised CD19Cre^{+/-} control mice (white circles).

resembling those with NP-Ficoll and thus reveal significant defects also in TI-1 immune reactions in Notch2IC-expressing animals. To this end, Notch2IC//CD19Cre^{+/-} and CD19Cre^{+/-} control mice were immunised with lower NP-LPS concentrations (5-15 µg) per animal and analysed after seven days. On the day of analysis, blood sera were taken and serum titers of NP-specific IgM and IgG3 were determined by ELISA. Measurements of antigen-specific antibody titers revealed that Notch2IC//CD19Cre^{+/-} mice had diminished NP-IgM and NP-IgG3 titers (Fig. 44). Furthermore, the Notch2IC//CD19Cre^{+/-} mouse immunised with 15 µg NP-LPS still exhibited decreased NP-specific antibody titers in comparison to control mice immunised with only 10 µg. Moreover, determination of NP-specific antibody-secreting plasma cells by ELISPOT revealed that among B cells of control mice immunised with 10 µg NP-LPS, increased amounts of NP-IgG3- and NP-IgM-secreting plasma

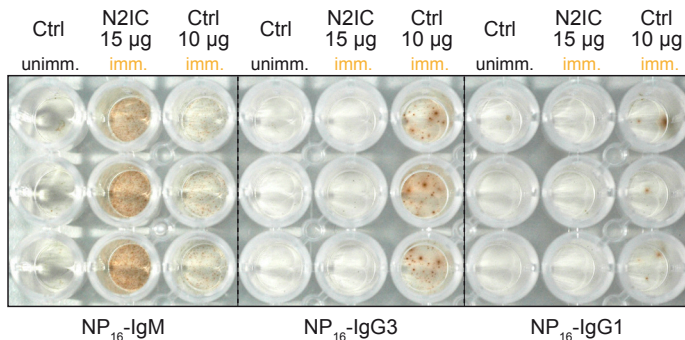


Figure 45: Notch2IC-expressing splenic B cells do not develop into antigen-specific IgG1- or IgG3-secreting plasma cells after TI-1 immunisation, yet they seem to be polyreactive. Notch2IC//CD19Cre^{+/-} (N2IC) and control (Ctrl) mice were immunised intraperitoneally with 10-15 µg NP-LPS. Seven days after injection, splenic cells were isolated and transferred in triplicates for 1.5-2 days onto ELISPOT plates (1×10^6 cells/well). Subsequently, NP-specific IgM-, IgG3- and IgG1-secreting plasma cells were visualised and determined. Experiment was performed with two animals for each genotype and treatment, except the 15 µg treatment in the Notch2IC//CD19Cre^{+/-} mouse, which was only performed once.

cells could be detected in comparison to unimmunised animals (Fig. 45). In contrast, irrespective of the NP-LPS concentrations, in wells with Notch2IC-expressing cells no NP-IgG3 or NP-IgG1 spots could be detected (Fig. 45 and data not shown). ELISPOT wells for NP-IgM exhibited again a very high, most likely also in part unspecific background staining (Fig. 45) as already seen in unimmunised and NP-Ficoll immunised mice (see 3.3.1, Fig. 43). Although experiments need to be repeated with more animals and with varying NP-LPS concentrations, these first results suggest that Notch2IC//CD19Cre^{+/-} mice indeed are also impaired

in their TI-1 immune response. With respect to the role of Notch2 in immune responses and plasma cell differentiation, we could show so far that Notch2IC-expressing MZ B cells are spontaneously and rapidly able to develop to antibody-secreting plasmablasts or plasma cells *in vitro*. On the other hand, *in vivo* plasma cell frequencies among cells of the spleen and bone marrow were not increased compared to controls and TI immune responses were drastically reduced. Only highly polyreactive IgM antibodies were detected irrespective of the immunisation state and immunisations did not induce any class switching. We hypothesise that Notch2IC-expression forces MZ B cells to stay in the MZ, so that MZ B cells cannot move into the follicle and hence cannot develop to plasma cells. As a first attempt to reveal potential defects in the migration capacity of Notch2IC-expressing MZ B cells, we performed so called “marginal zone clearance” experiments. It is known that LPS injections in mice lead to a clearance of the MZ as all MZ B cells migrate into the follicle after LPS stimulation (Martin and Kearney, 2002). To investigate whether this LPS-triggered relocalisation of Notch2IC-expressing B cells could still be induced, we treated control and Notch2IC//CD19Cre^{+/-} mice with different NP-LPS concentrations and assessed the clearance of the MZ by immunohistochemistry. Notch2IC//CD19Cre^{+/-} as well as control mice were treated with 2.5-50 µg NP-LPS. After five to six hours post injection, spleens were isolated and frozen in Tissue-Tek® for later cryosections and subsequent immunohistochemistry. Splenic sections were stained with α-IgM to detect B cells, α-CD3 for T cells and α-MOMA-1 for metallophilic macrophages lining the marginal sinus. In control mice marginal zone clearance could be induced down to NP-LPS concentrations as low as 5 µg. In spleens from mice treated with only 2.5 µg NP-LPS a thin line of MZ B cells located within the MZ was still visible (Fig. 46, upper row), suggesting that this concentration was too low to induce complete migration into the follicle. In Notch2IC//CD19Cre^{+/-} mice an injection with 50 µg NP-LPS led to an almost complete migration of MZ B cells into the follicle, making splenic sections resemble those of an untreated wild type mouse (Fig. 46, lower row, left picture). In Notch2IC-expressing mice treated with 20 µg NP-LPS, a great proportion of MZ B cells could still be detected within the follicle, however already to a lesser extent than with 50 µg. The fraction of Notch2IC-expressing cells relocating to the follicle diminished with decreasing NP-LPS concentrations, so that at a concentration of 5 µg no difference could be observed between treated and untreated mice (Fig. 46, lower row). Experiments investigating the LPS-induced MZ clearance suggest that Notch2IC-expressing MZ B cells are still able to migrate into the follicle, if they are activated by a sufficiently strong stimulus, such as high NP-LPS concentrations (~50-20 µg). However, in response to weaker stimulation, such as low NP-LPS concentrations or NP-Ficoll, they remain within the MZ. This implicates that the migration potential of Notch2IC-expressing MZ B cells is not completely disturbed, but impaired after immunisation with lower NP-LPS concentrations. To unravel other potential factors affecting TI immune responses in Notch2IC//CD19Cre^{+/-} mice, we took a closer look at antigen capturing and transport after immunisations with the TI-2 antigen 2,4,6-trinitrophenyl (TNP) conjugated to Ficoll.

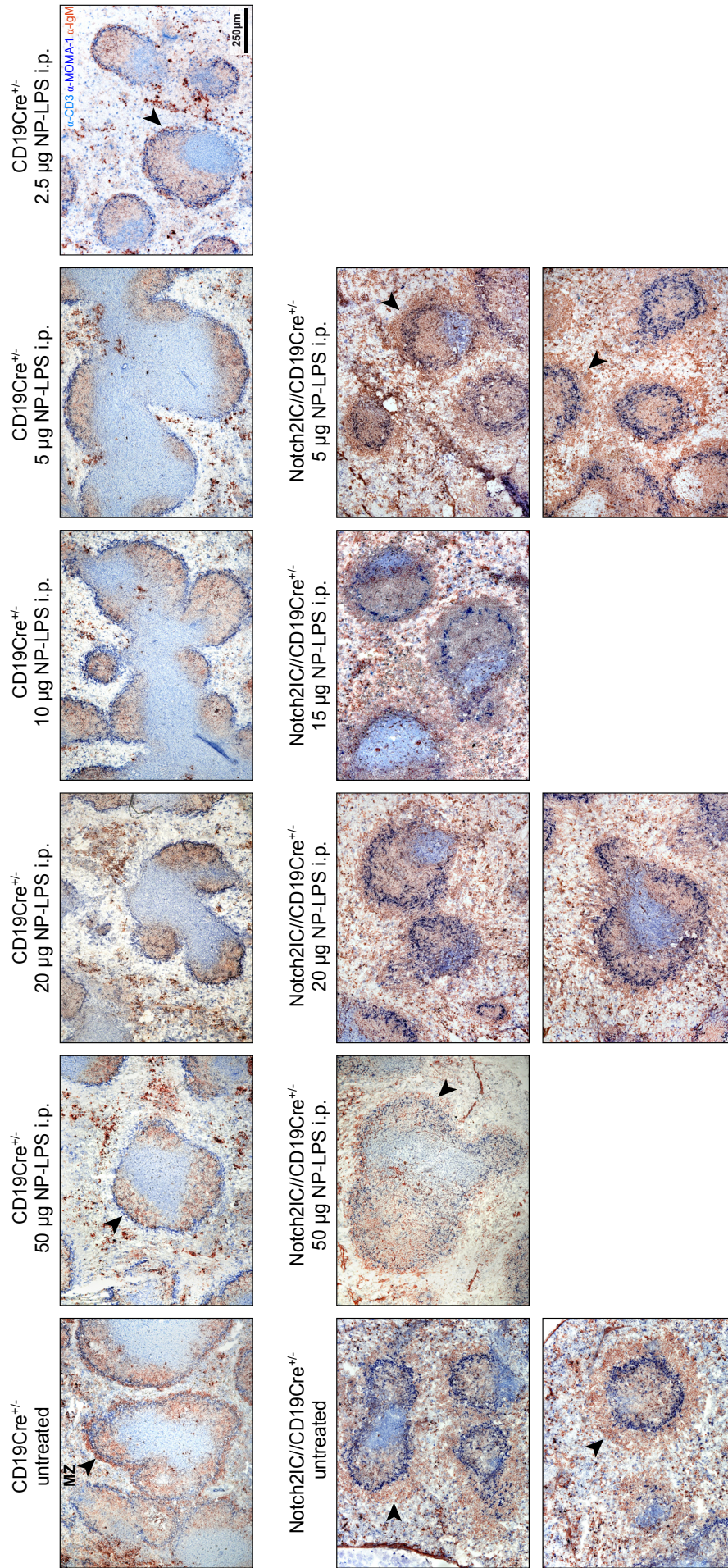


Figure 46: Marginal zone clearance after treatment with different NP-LPS concentrations. Immunohistochemical analyses of splenic cryosections of Notch2/CD19Cre^{+/-} and CD19Cre^{+/-} mice five to six hours after intraperitoneal injections of the indicated NP-LPS concentrations. Sections (8 μm) were stained for MOMA-1⁺ metallophilic macrophages (α-MOMA-1, dark blue), lining the MZ at the sinus, for IgM⁺ B cells (α-IgM, red) and for CD3⁺ T cells (α-CD3, blue). The MZ is indicated by arrowheads. As follicle outlines are more difficult to distinguish in Notch2/CD19Cre^{+/-} mice, two representative pictures were depicted for further clarification. Scale bar: 250 μm.

3.3.3 Notch2IC//CD19Cre^{+/-} mice exhibit defects in their SIGN-R1⁺ macrophage population and in antigen capturing

Next to the MZ B cells, the splenic MZ comprises different types of macrophages. Marginal metallophilic macrophages (MOMA-1⁺) lining the marginal sinus and marginal zone macrophages (MARCO⁺), which are located within the MZ interspersed between the MZ B cells (Mebius and Kraal, 2005). A subset of MARCO⁺ macrophages also expresses the SIGN-R1 receptor. SIGN-R1⁺ macrophages have been shown to capture antigens out of the circulation, engulf and process them for the subsequent presentation to MZ B cells, which in turn are essential for the subsequent transport of the antigens into the follicle (Arnon et al., 2013; Cinamon et al., 2008; Ferguson et al., 2004). Mice with defects in SIGN-R1⁺ macrophages underpin the important role of SIGN-R1⁺ macrophages in antigen capturing and presentation (Koppel et al., 2008; Kang et al., 2006). Hence, we were interested whether this cell population was still present and normally distributed in Notch2IC//CD19Cre^{+/-} mice. Splenic cryosections of Notch2IC//CD19Cre^{+/-} and control mice were analysed by immunofluorescent or immunohistochemical stainings for the presence and distribution of SIGN-R1⁺ macrophages. In

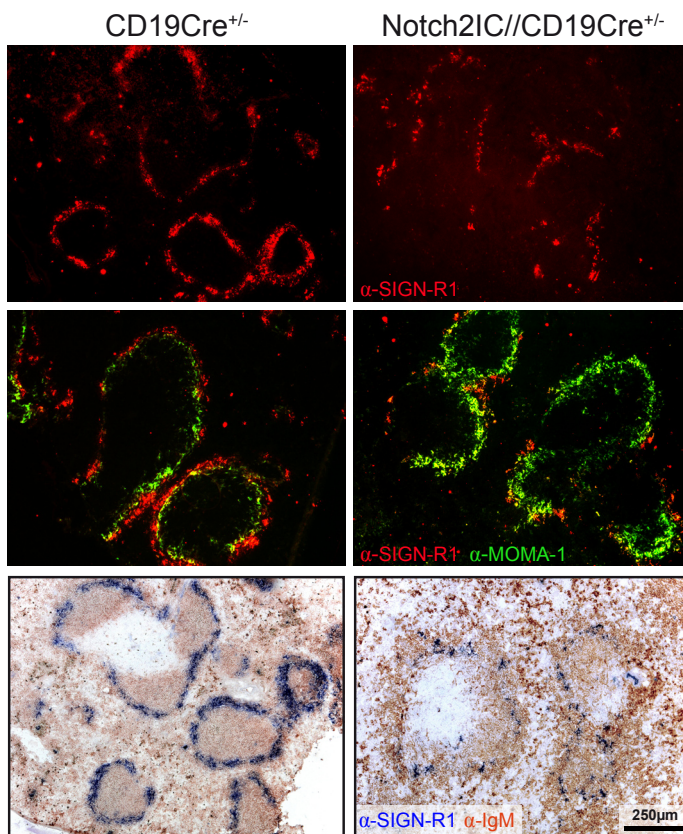


Figure 47: SIGN-R1⁺ macrophages seem reduced in Notch2IC//CD19Cre^{+/-} mice. Immunofluorescent and immunohistochemical stainings of splenic cryosections (8 μ m) of Notch2IC//CD19Cre^{+/-} and CD19Cre^{+/-} mice for SIGN-R1⁺ macrophages (α -SIGN-R1, red or blue) located within the MZ, MOMA-1⁺ metallophilic macrophages (α -MOMA-1, green) lining the marginal sinus and IgM⁺ B cells (α -IgM, red). Depicted photomicrographs are representative for two independent experiments. Scale bar: 250 μ m.

sections of control mice, SIGN-R1⁺ macrophages were detectable as a nearly closed ring, positioned within the MZ and lying clearly outside of the marginal sinus, which is lined by MOMA-1⁺ macrophages (Fig. 47, left column). In Notch2IC//CD19Cre^{+/-} mice, on the other hand, SIGN-R1⁺ macrophages were scarce and more scattered, however still correctly localised within the MZ (Fig. 47, right column). So it seems that constitutive Notch2 signalling is either directly or indirectly - by increasing MZ B cell numbers - influencing the frequency and/or positioning of SIGN-R1⁺ macrophages. To be able to track antigen capturing as well as the transport into the follicle and to check if this could still be induced in Notch2IC-expressing animals, Notch2IC//CD19Cre^{+/-} and control mice were treated with 50 μ g TNP-Ficoll. Mice were taken down after one or five hours and the presence and localisation of TNP⁺ cells was assessed by immunohistochemistry and

immunofluorescence on splenic cryosections. In control mice, one hour post injection, TNP⁺ cells could be detected within the MZ outside of the MOMA-1⁺ ring of macrophages lining the marginal sinus (Fig. 48A+B, left panels). Five hours after injection, TNP⁺ cells had clearly migrated into the follicle in control animals (Fig. 48C+D, left panels). In great contrast to this, fewer, scattered TNP⁺ cells could be detected in the marginal zones of Notch2IC//CD19Cre^{+/-} mice after one hour (Fig. 48A+B, right panels) and nearly no TNP⁺ cells were visible within the follicle five hours post injections (Fig. 48C+D, right panels). In summary, this indicates that antigen capturing is impaired in Notch2IC-expressing mice and no antigen transport into the follicle takes place.

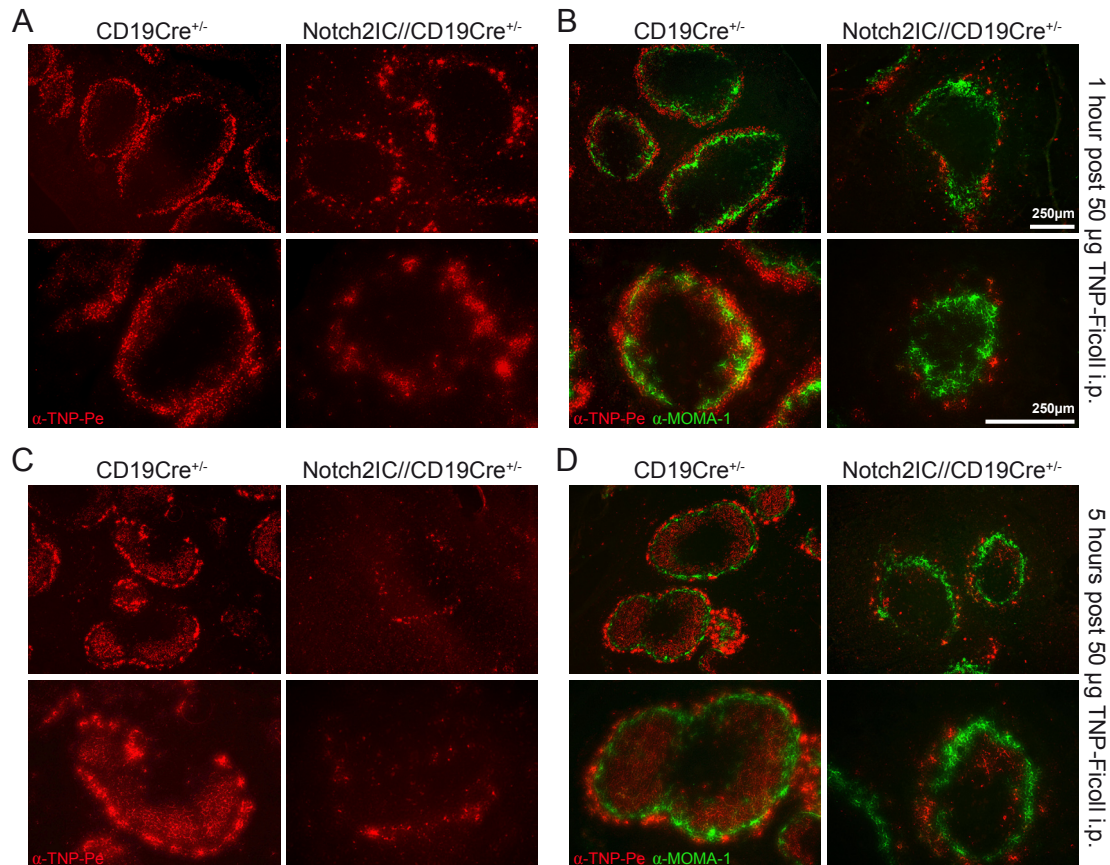


Figure 48: Notch2IC//CD19Cre^{+/-} mice exhibit defects in antigen capturing and transport into the follicle. Immunofluorescent stainings of splenic cryosections of Notch2IC//CD19Cre^{+/-} and CD19Cre^{+/-} mice one (A-B) and five hours (C-D) after intraperitoneal injections (i.p.) of 50 µg TNP-Ficoll. Sections (8 µm) were stained for TNP⁺ cells (α-TNP-Pe, red) and MOMA-1⁺ metallophilic macrophages (α-MOMA-1, green) lining the marginal sinus. Depicted photomicrographs are representative for two independent experiments. Scale bars: 250 µm.

3.3.4 Notch2^{fl/fl}//CD19Cre^{+/-} mice have a reduced TI-2 immune reponse, but functional antigen capturing and transport into the splenic follicle

As already mentioned in preceding chapters, SIGN-R1⁺ MZ macrophages are implicated in antigen capturing and presentation (Aichele et al., 2003; Koppel et al., 2008). Under normal circumstances they are localised outside of the marginal sinus, interspersed within the MZ (Koppel et al., 2008). However, MZ B cells have been shown to be the key B cell population responsible for transporting antigen from the MZ into the follicle (Arnon et al., 2013; Ferguson et al., 2004; Cinamon et al., 2008). In Notch2IC//

CD19Cre^{+/-} mice, SIGN-R1⁺ macrophages are reduced, however, these remaining macrophages seem to fulfill their role in capturing TNP-Ficoll. Still, no transport of antigen into the follicle could be detected, implicating that MZ B cells are possibly not able to migrate into the follicle when activated by the antigen TNP-Ficoll. To investigate whether antigen transport into the follicle can also take place in the absence of MZ B cells, we analysed antigen capturing and transport in Notch2-deficient mice, which are devoid of MZ B cells (Fig. 49). Firstly we checked whether Notch2^{fl/fl}//CD19Cre^{+/-} mice still had normal positioned and normal frequencies of SIGN-R1⁺ macrophages, although

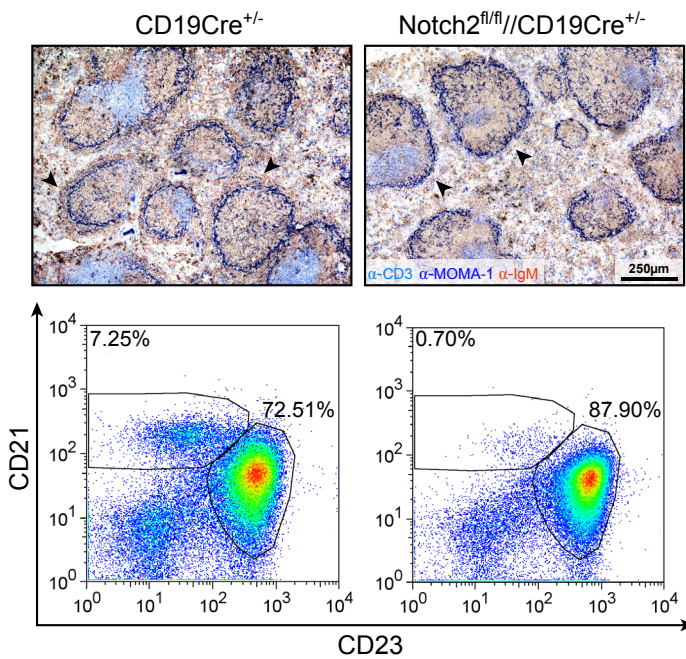


Figure 49: Notch2^{fl/fl}//CD19Cre^{+/-} mice are devoid of MZ B cells. The upper row displays immunohistochemical stainings of splenic cryosections (8 μ m) of Notch2^{fl/fl}//CD19Cre^{+/-} and CD19Cre^{+/-} mice for MOMA-1⁺ metallophilic macrophages (α -MOMA-1, dark blue) lining the marginal sinus, for IgM⁺ B cells (α -IgM, red) and for CD3⁺ T cells (α -CD3, blue). Arrowheads indicate marginal zone. The lower row displays flow cytometrical analyses of control and Notch2-deficient splenic cells for their CD21 and CD23 expression. Exemplary dot plots are gated on B220⁺ lymphocytes. Data is representative of three independent experiments. Scale bar: 250 μ m.

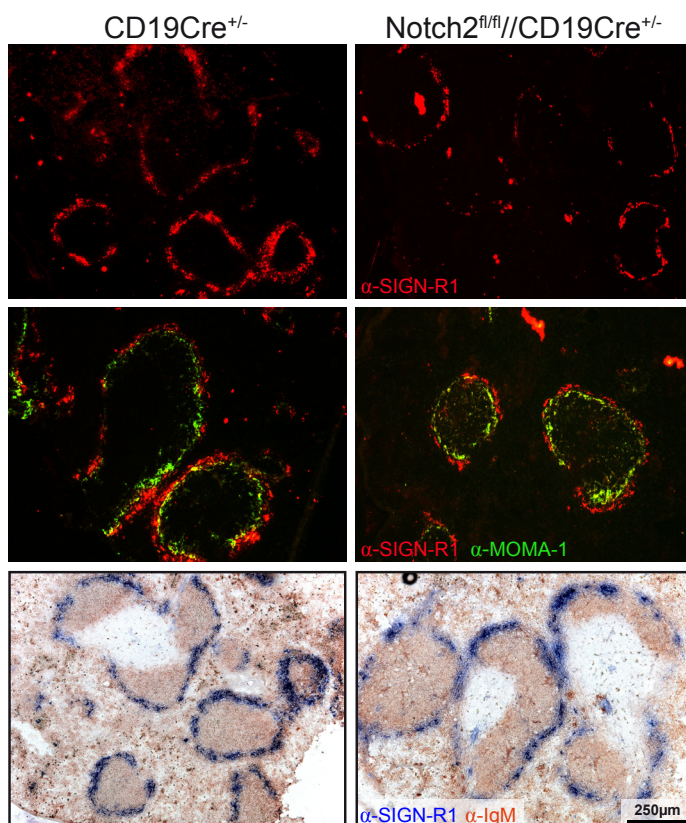


Figure 50: SIGN-R1⁺ macrophages are slightly reduced, but present in Notch2^{fl/fl}//CD19Cre^{+/-} mice. Immunofluorescent and immunohistochemical stainings of splenic cryosections (8 μ m) of Notch2^{fl/fl}//CD19Cre^{+/-} and CD19Cre^{+/-} mice for SIGN-R1⁺ macrophages (α -SIGN-R1, red or blue) located within the MZ, MOMA-1⁺ metallophilic macrophages (α -MOMA-1, green) lining the marginal sinus and IgM⁺ B cells (α -IgM, red). Depicted photomicrographs are representative of two independent experiments. Scale bar: 250 μ m.

they are devoid of MZ B cells. Analysis of this macrophage population by immunofluorescent or immunohistochemical stainings on splenic cryosections of $\text{Notch2}^{\text{fl/fl}}//\text{CD19Cre}^{+/-}$ and control mice revealed that there is only a faint reduction in the frequency and localisation of these cells in Notch2 -deficient mice (Fig. 50). To further analyse if antigen capturing and especially transport was still functional in these mice, $\text{Notch2}^{\text{fl/fl}}//\text{CD19Cre}^{+/-}$ and control animals were treated with $50 \mu\text{g}$ TNP-Ficoll. Spleens were isolated one and five hours after injection and cryosections were analysed by immunofluorescent stainings with $\alpha\text{-TNP-Pe}$ for cells bearing TNP-Ficoll on their surface. In control animals, one hour after injection TNP⁺ cells were clearly located within the MZ, whereas after five hours TNP⁺ cells could be detected within the splenic follicle (Fig. 51A-D, left panels). Surprisingly, similar antigen capturing and transport could be seen in Notch2 -deficient mice (Fig. 51A-D, right panels). These results show that SIGN-R1⁺ macrophages, which are important for antigen capturing and presentation, are still present and functional in Notch2 -deficient mice and that the antigen transport into the follicle is still warranted, although MZ B cells are missing.

Mouse models with defects in their MZ B cell population have been shown to exhibit alterations in their TI immune responses (reviewed in Martin and Kearney, 2002). However, from our previous results we inferred that immune responses to TI antigens would be normal in $\text{Notch2}^{\text{fl/fl}}//\text{CD19Cre}^{+/-}$ mice, although they lack MZ B cells. In line with this is the publication of Tanigaki and colleagues, showing

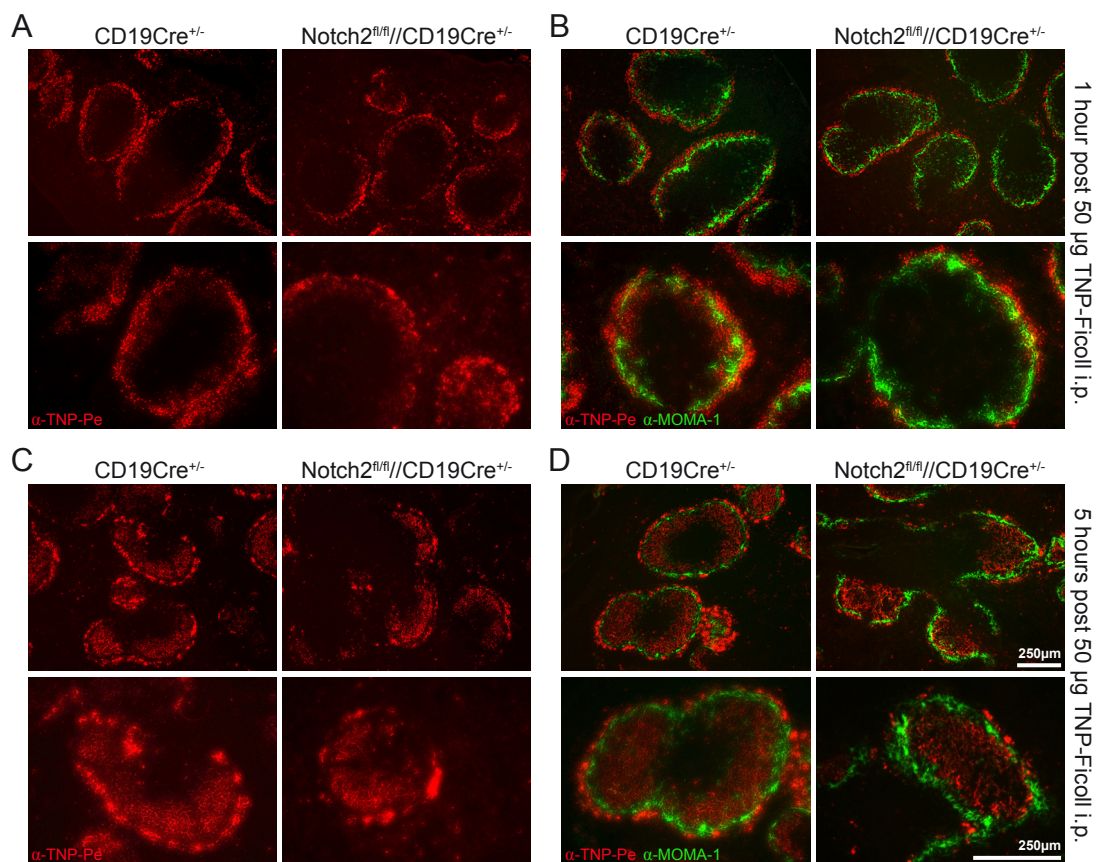


Figure 51: Antigen capturing and transport into the follicle is similar in control and $\text{Notch2}^{\text{fl/fl}}//\text{CD19Cre}^{+/-}$ mice. Immunofluorescent stainings of splenic cryosections of $\text{Notch2}^{\text{fl/fl}}//\text{CD19Cre}^{+/-}$ and $\text{CD19Cre}^{+/-}$ mice one (A-B) and five hours (C-D) after intraperitoneal (i.p.) injection of $50 \mu\text{g}$ TNP-Ficoll. Sections ($8 \mu\text{m}$) were stained for TNP⁺ cells ($\alpha\text{-TNP-Pe}$, red) and MOMA-1⁺ metallophilic macrophages ($\alpha\text{-MOMA-1}$, green) lining the marginal sinus. Depicted photomicrographs are representative of two independent experiments. Scale bars: $250 \mu\text{m}$.

that mice with a B cell-specific RBP-J μ knockout in which Notch signalling is completely abrogated and hence MZ B cell development abolished, exhibit a normal TI-2 response (Tanigaki et al., 2002). To examine the TI immune response in the absence of Notch2 signalling, Notch2^{fl/fl}//CD19Cre^{+/-} and CD19Cre^{+/-} control mice were immunised with NP-Ficoll. NP-specific plasma cells as well as serum titers of NP-specific antibodies were determined by ELISPOT and ELISA, respectively seven days after immunisation. Sera of immunised Notch2^{fl/fl}//CD19Cre^{+/-} mice contained significantly lower levels of NP-specific IgM and IgG3 titers than those of control animals (Fig. 52). In addition, in comparison to controls, no NP-specific IgG3- and reduced numbers of NP-specific IgM-secreting plasma cells could be detected among splenic cells of immunised Notch2^{fl/fl}//CD19Cre^{+/-} mice (Fig. 53). These analyses indicate that Notch2^{fl/fl}//CD19Cre^{+/-} mice are hampered in their TI-2 immune

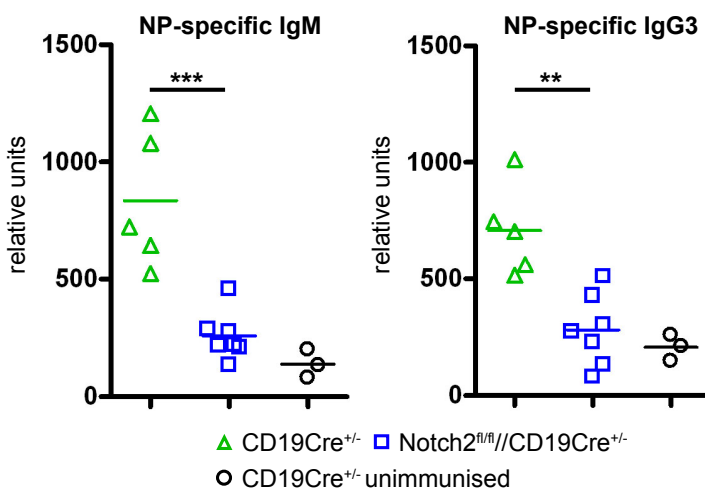


Figure 52: Notch2^{fl/fl}//CD19Cre^{+/-} have reduced antigen-specific IgM and IgG3 serum titers after TI-2 immunisation. Notch2^{fl/fl}//CD19Cre^{+/-} and control mice were injected intraperitoneally with 50 μ g NP-Ficoll. NP-specific IgM and IgG3 concentrations were measured by ELISA in serum taken seven days after injection. Points represent data from individual animals and horizontal bars mark the mean value. Controls (green triangles); Notch2^{fl/fl}//CD19Cre^{+/-} (blue squares); unimmunised controls (white circles); ** p < 0.01; *** p < 0.001 in comparison to immunised controls.

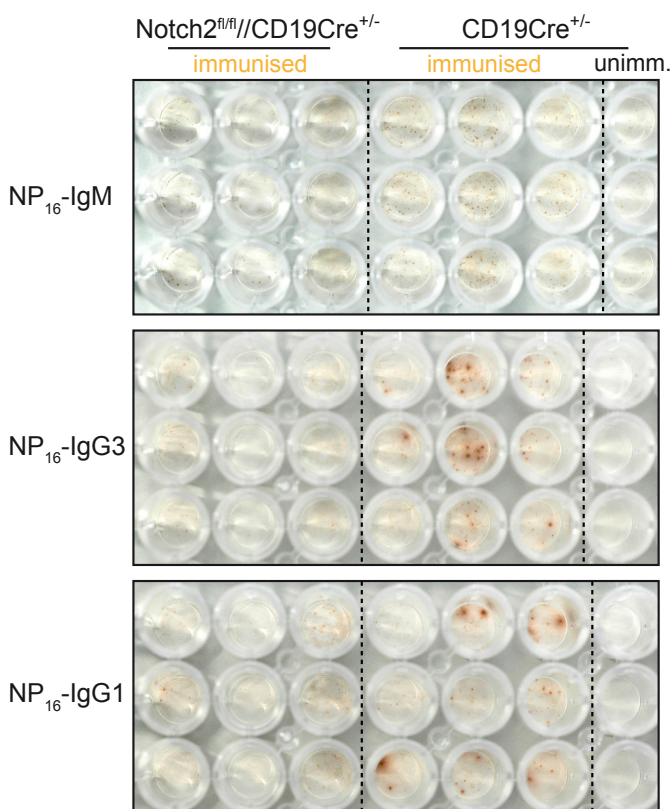


Figure 53: Notch2^{fl/fl}//CD19Cre^{+/-} mice have reduced numbers of antigen-specific IgM-, IgG1- and IgG3-secreting plasma cells after TI-2 immunisation. Notch2^{fl/fl}//CD19Cre^{+/-} and control mice were injected intraperitoneally with 50 μ g NP-Ficoll. Seven days after injection, splenic cells were isolated and transferred in triplicates for 1.5-2 days onto ELISPOT plates (1 \times 10⁶ cells/well). Subsequently, NP-specific IgM-, IgG3- and IgG1-secreting plasma cells were visualised and determined as brown spots. Experiment was performed with three animals for each genotype and treatment.

response to NP-Ficoll. In summary, *Notch2^{fl/fl}//CD19Cre^{+/-}* are impaired or delayed in their TI-2 immune response to NP-Ficoll, probably due to the lack of MZ B cells. Yet, antigen capturing by SIGN-R1⁺ macrophages and antigen transport into the follicle is still functional in these mice.

3.4 The role of Notch2 in lymphomagenesis

3.4.1 Constitutive, B cell-specific Notch2 expression seems not to be sufficient to strongly drive B cell lymphomagenesis

Mutations in the *notch* genes predominantly resulting in constitutively active Notch signalling have been shown to be implicated in various disease including B cell malignancies. Of special interest for us were recent publications showing that mutations in the *notch2* gene were specific for SMZL (Troen et al., 2008; Kiel et al., 2012; Rossi et al., 2012). Young *Notch2IC//CD19Cre^{+/-}* mice display a slight splenomegaly and elevated levels of the proto-oncogene *c-myc*, which is known to be implicated in cell growth, proliferation and apoptosis (Wade and Wahl, 2006). Furthermore, due to their MZ B cell phenotype, *Notch2IC*-expressing cells exhibit increased proliferation, especially in response to LPS and α -CD40 stimulation (Hampel et al., 2011). To explore whether constitutive Notch2 signalling would lead to an earlier onset of lymphoma development in *Notch2IC//CD19Cre^{+/-}* mice compared to lymphoma spontaneously arising in old wild type mice (older than 19 months), we assembled cohorts of 26 *Notch2IC//CD19Cre^{+/-}* and 19 *CD19Cre^{+/-}* animals and let them age. Animals were euthanised when exhibiting first signs of morbidity or when a maximum age of 22 months was reached. Table 5 is

Table 5: Overview of all analysed aged *Notch2IC//CD19Cre^{+/-}* and control mice.

Mouse number	GT	Age (months)	Sp weight (mg)	Sp cells (counts)	IgM ⁺ B cells (counts)	CD3 ⁺ /Thy1.2 ⁺ T cells (counts)	IgM ⁺ hCD2 ⁺ B cells (counts)
663	CD19	3,0	116	8,7E+07	4,2E+07	3,1E+07	n.a.
652	CD19	4,0	98	4,2E+07	1,5E+07	1,5E+07	n.a.
485	CD19	6,0	95	8,3E+07	3,7E+07	2,8E+07	n.a.
515	CD19	6,0	n.d.	1,3E+08	6,1E+07	4,3E+07	n.a.
516	CD19	6,0	n.d.	7,9E+07	3,5E+07	2,8E+07	n.a.
2610	CD19	12,0	147	6,0E+07	3,4E+07	1,7E+07	n.a.
69	Ctrl	12,0	83	2,7E+07	1,3E+07	9,8E+06	n.a.
80	Ctrl	13,0	110	3,8E+07	2,1E+07	1,2E+07	n.a.
2612	CD19	14,0	85	3,4E+07	1,5E+07	9,8E+06	n.a.
7638	CD19	15,0	n.d.	1,1E+08	6,1E+07	3,8E+07	n.a.
292	CD19	16,0	125	2,2E+08	1,1E+08	8,1E+07	n.a.
7891	CD19	17,0	165	7,6E+07	4,6E+07	2,0E+07	n.a.
24	Ctrl	17,0	102	3,9E+07	2,9E+07	5,3E+06	n.a.
7745	CD19	17,5	211	1,0E+08	3,3E+07	1,8E+07	n.a.
353	CD19	18,0	200	8,1E+07	4,8E+07	1,7E+07	n.a.
7461	CD19	19,0	83	4,3E+07	2,4E+07	1,5E+07	n.a.
7576	CD19	19,0	120	1,8E+08	9,6E+07	6,4E+07	n.a.
7640	CD19	19,0	89	2,5E+07	n.d.	n.d.	n.a.
7578	CD19	19,5	97	1,8E+08	9,8E+07	4,9E+07	n.a.

Table 5 continued:

Mouse number	GT	Age (months)	Sp weight (mg)	Sp cells (counts)	IgM ⁺ B cells (counts)	CD3 ⁺ /Thy1.2 ⁺ T cells (counts)	IgM ⁺ hCD2 ⁺ B cells (counts)
653	N2IC	4,0	150	7,2E+07	3,5E+07	2,3E+07	3,0E+07
7890	N2IC	4,0	711	2,8E+08	1,2E+08	4,5E+07	9,1E+07
621	N2IC	6,0	167	6,3E+07	3,9E+07	1,1E+07	3,0E+07
498	N2IC	6,0	n.d.	1,8E+08	8,9E+07	5,9E+07	6,7E+07
499	N2IC	6,0	n.d.	7,0E+07	2,8E+07	2,8E+07	2,2E+07
961	N2IC	12,0	354	1,0E+08	4,5E+07	3,8E+07	3,6E+07
948	N2IC	12,0	616	1,2E+08	3,5E+07	5,2E+07	2,4E+07
7592	N2IC	13,0	2524	2,7E+09	1,3E+09	2,8E+08	1,3E+09
968	N2IC	13,0	312	1,2E+08	6,3E+07	2,6E+07	4,5E+07
952	N2IC	14,0	171	1,8E+08	6,9E+07	6,1E+07	5,7E+07
7594	N2IC	15,0	n.d.	8,8E+07	5,3E+07	3,6E+07	4,1E+07
297	N2IC	16,0	250	1,8E+08	7,3E+07	8,6E+07	3,2E+07
959	N2IC	16,0	123	2,1E+07	8,8E+06	5,7E+06	6,2E+06
7595	N2IC	18,5	n.d.	1,8E+08	7,0E+07	7,5E+07	6,1E+07
374	N2IC	18,5	629	7,7E+07	1,9E+07	2,0E+07	1,6E+07
341	N2IC	19,0	211	4,5E+07	2,5E+07	1,3E+07	2,4E+07
302	N2IC	19,0	771	1,6E+08	4,8E+07	2,5E+07	3,9E+07
7596	N2IC	19,0	535	7,4E+07	3,0E+07	1,8E+07	2,6E+07
293	N2IC	19,5	390	5,7E+07	2,6E+07	1,8E+07	2,2E+07
7577	N2IC	19,5	108	1,8E+07	8,1E+06	5,3E+06	5,2E+06
373	N2IC	20,0	818	2,8E+08	7,0E+07	5,0E+07	5,7E+07
335	N2IC	20,5	2200	1,8E+08	5,7E+07	2,1E+07	5,5E+07
342	N2IC	20,5	911	2,8E+08	1,2E+08	6,5E+07	1,1E+08
343	N2IC	22,0	422	1,0E+08	7,8E+07	3,2E+07	7,0E+07
344	N2IC	22,0	614	1,8E+08	6,6E+07	3,8E+07	5,7E+07
380	N2IC	22,0	139	2,2E+07	6,8E+06	8,8E+06	5,4E+06

Cohorts of Notch2IC//CD19Cre^{+/-} (N2IC) and control mice (CD19Cre^{+/-} or wildtype) were aged up to 22 months. Mice were analysed when showing first signs of illness. Table summarises the genotype (GT), age, splenic (Sp) weight, total splenic cell numbers, IgM⁺ splenic B cell numbers, splenic T cell numbers and numbers of IgM⁺ hCD2⁺ splenic cells of all analysed mice. Ctrl (wildtype mice), n.a. (not applicable).

giving an overview of all analysed mice, including genotype, age, splenic weight, total splenic cell numbers as well as cell numbers of IgM⁺ and IgM⁺ hCD2⁺ cells as well as CD3⁺ or Thy1.2⁺ T cells. Due to the expansion of MZ B cells, which are larger than Fo B cells, spleens of Notch2IC//CD19Cre^{+/-} mice were on average 1.5-fold heavier than spleens of control mice (Hampel et al., 2011). Examining spleens of aged mice (4 to 22 months) now revealed that in addition to this initial difference, old Notch2IC//CD19Cre^{+/-} mice had on average even bigger spleens than young Notch2IC//CD19Cre^{+/-} mice and the respective old control mice (Fig. 54). In comparison, in control mice no big difference could be detected between splenic weights of young and old mice. Still, plotting splenic weight against the age of the mice, uncovered the huge variation among splenic weight data of old Notch2IC//CD19Cre^{+/-} mice (Fig. 55). In these graphs it again seemed as if there was a slight positive correlation between the splenic weight and older age of Notch2IC//CD19Cre^{+/-} mice, yet, due to the great variation, statistical correlation analysis didn't reveal

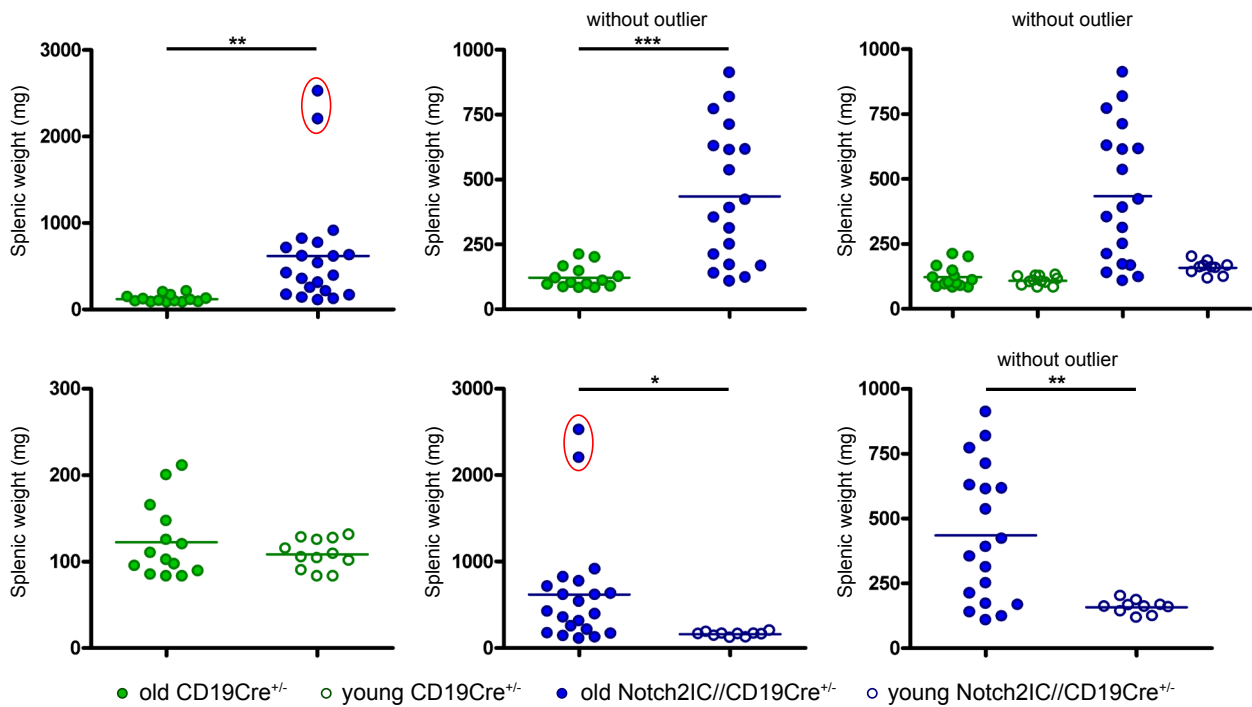


Figure 54: Splenic weight of aged and young Notch2IC//CD19Cre^{+/-} and control mice. Cohorts of Notch2IC//CD19Cre^{+/-} and control mice were aged up four to 22 months. Mice were analysed when showing first signs of illness and splenic weights were determined. Points represent data from individual animals and horizontal bars mark the mean value. Outliers (red circles), old control mice (filled green circles); old Notch2IC//CD19Cre^{+/-} mice (filled blue circles); young control mice (blank green circles); old Notch2IC//CD19Cre^{+/-} mice (blank blue circles). * $p < 0.05$; ** $p < 0.01$; *** $p < 0.001$ in comparison to respective controls.

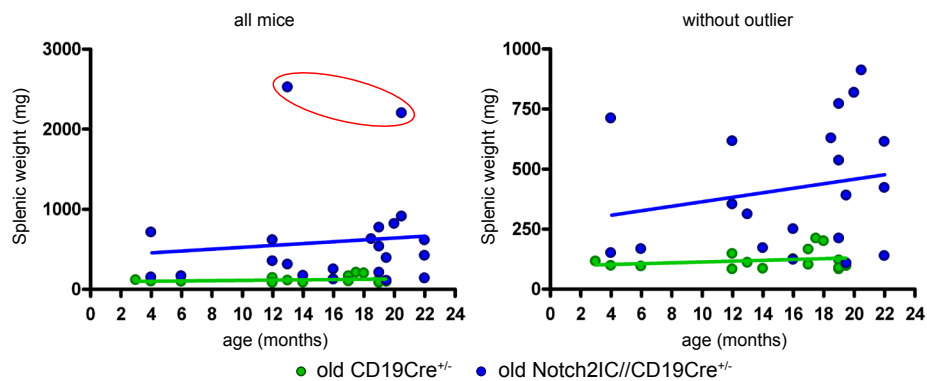


Figure 55: Correlation of splenic weight with age in Notch2IC//CD19Cre^{+/-} and control mice. Cohorts of Notch2IC//CD19Cre^{+/-} and control mice were aged up to 22 months. Mice were analysed when showing first signs of illness and splenic weights were determined. The graph on the left shows the correlation of splenic weights with age of all analysed mice, whereas the graph on the right depicts the same without the two outliers in the red circle. Points represent data from individual animals and trendlines of linear regression analyses are included in diagrams. Control mice (green); Notch2IC//CD19Cre^{+/-} mice (blue).

any significance (Fig. 55). Despite this increase in splenic size in aging Notch2IC//CD19Cre^{+/-} mice, no difference could be detected regarding total splenic cell numbers (Fig. 56A). To assess whether an expansion of one or more B cell clones (mono- or polyclonality) took place in old mice - which would confirm lymphomagenesis - a first Southern blot analysis was undertaken with DNA probes from total splenocytes of eleven Notch2IC//CD19Cre^{+/-} and seven CD19Cre^{+/-} mice. Tested animals were aged between 12 and 20.5 months. Unfortunately two CD19Cre^{+/-} probes dropped out and couldn't be analysed later on. With a radioactively-labeled IgH-probe on membrane-bound DNA, one could either detect

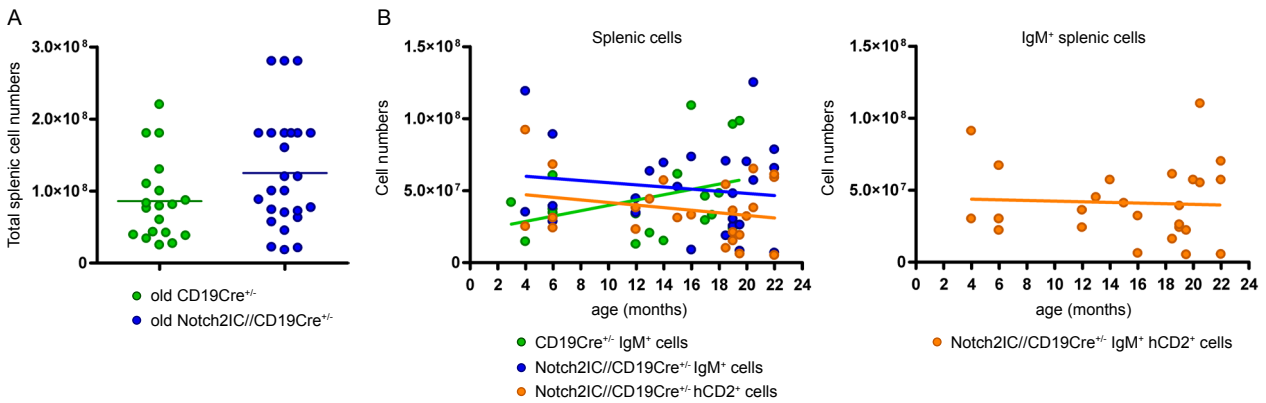


Figure 56: Total splenic cells as well as IgM⁺ and IgM⁺ hCD2⁺ splenic cell populations of aged Notch2IC//CD19Cre^{+/-} and control mice. Cohorts of Notch2IC//CD19Cre^{+/-} and control mice were aged up to 22 months. Mice were analysed when showing first signs of illness. **(A)** Graph shows total splenic cell numbers of old Notch2IC//CD19Cre^{+/-} (blue) and control mice (green). Points represent data from individual animals and horizontal bars mark the mean value. **(B)** Graphs show numbers of IgM⁺ and hCD2⁺ splenic cells (left) and IgM⁺ hCD2⁺ splenic cells (right) of old Notch2IC//CD19Cre^{+/-} (blue, orange) and control mice (green) correlated to age. Points represent data from individual animals and trendlines of linear regression analyses are included in diagrams. Values of mouse #7592 were extrem outliers (see table 5) and were therefore not included in (B).

and visualise the native, germline configuration of the IgH-locus or one or more other distinct bands representing the expansion of one or more B cell clones equipped with the same BCR rearrangement. Two (#7461 and #353) out of five (40 %) control mice showed additional bands at the age of 18 and 19 months. In Notch2IC//CD19Cre^{+/-} mice, seven (#7592, #373, #7577, #7595, #293, #302, #342) out of eleven (64 %) animals clearly showed mono- or polyclonality. Two animals (#374 and #7596) showed faint bands. Further analyses with mice aged about 19 months will be necessary to be able to determine a significant difference in lymphoma development between Notch2IC//CD19Cre^{+/-} and control mice. In addition, Southern blot analyses of younger Notch2IC//CD19Cre^{+/-} mice are planned in the near future to clarify whether lymphoma also develop at earlier time points. Tumor development not always correlated with an increase in splenic size (Fig. 57, table 5) or with stronger forms of morbidity in mice and until now it looks as if its onset was relatively late. These results suggest that constitutive Notch2 signalling drives the development of indolent lymphoma, however, with a late onset and a long latency.

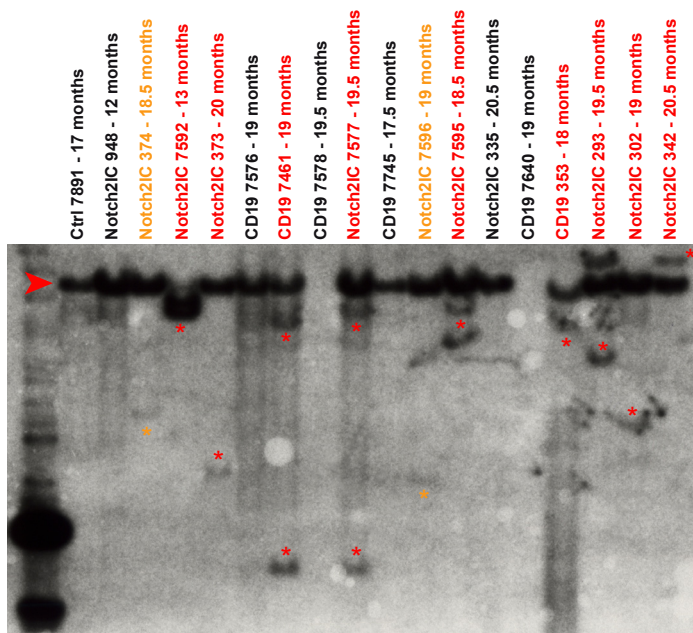


Figure 57: Southern blot analysis of aged Notch2IC//CD19Cre^{+/-} and control mice. Southern blot of *EcoRI*-digested DNA isolated from total splenocyte preparations. A radioactively-labeled IgH-probe was used to check the configurations of the IgH-locus in B cells of depicted animals. The arrow points to the band indicating the germline configuration of the respective sample as found in B cells and in any other cell type. Additional bands representing changes in the IgH-locus and hence mono- or polyclonality of the analysed B cell population are indicated by asterisks. B cells of following mice exhibited mono- or polyclonality: Control animals #7461 and #353 as well as Notch2IC-expressing animals #7592, #373, #7577, #7595, #293, #302 and #342 (red). Mice #374 and #7596 exhibited only faint additional bands (orange).

3.4.2 Constitutive Notch2IC expression alters the phenotype of B cells in aging mice irrespective of tumor development

To investigate whether possible tumor development and aging would induce changes in splenic cell populations of Notch2IC//CD19Cre^{+/-} and control animals with regard to frequency or cell numbers, extensive FACS analyses were performed. As most important differences could be detected in CD21, CD23, IgM, IgD as well as in B220 and hCD2 expression in the spleen, bone marrow and lymph nodes, these stainings will be described and discussed in detail. In our first Southern blot analysis, mouse #7592 (13 months) exhibited the most distinct and biggest band clearly pointing at a monoclonal tumor population (Fig. 57), which was also clearly distinguishable by flow cytometry. In contrast to young Notch2IC//CD19Cre^{+/-} animals harbouring almost only CD21^{high} CD23^{low} IgM^{high} IgD^{low} MZ B cells in their spleens, all lymphocytes of this tumor mouse had shifted to a B220^{low} CD21^{low} CD23^{low} IgM^{low-Int} hCD2⁺ phenotype with most of them being IgD^{high} (Fig. 58A, upper rows). The fact that all B cells were hCD2⁺ implies that only Notch2IC-expressing B cells had expanded. Lymphocytes within BM and LN exhibited a similar phenotype (Fig. 58A), indicating that the tumor cell population had infiltrated other lymphoid organs. However, none of the other Notch2IC//CD19Cre^{+/-} animals displaying additional bands in Southern blot analysis exhibited this special, distinct kind of “tumor phenotype”. B cell populations of the majority of aged Notch2IC-expressing animals resembled each other regardless if an additional band was present in Southern blot analysis or not, suggesting that alterations in surface marker expression were rather induced by aging than by tumor formation. Figure 58 depicts exemplary Notch2IC-expressing and control mice representing and summarising major phenotypes observed in flow cytometrical analyses of all analysed aged animals. Splenic lymphocytes of aged Notch2IC-expressing mice exhibited reduced percentages of IgM⁺ and hCD2⁺ (Fig. 56B) as well as of B220⁺ cells (Fig. 58). Gating on IgM⁺ cells, however, revealed that remaining IgM⁺ B cells were all hCD2⁺ and frequencies of IgM⁺ hCD2⁺ cells were not significantly reduced (Fig. 56B), indicating that reductions in percentages of hCD2⁺ cells were caused by a general decrease in IgM⁺ total B cell numbers. Furthermore, among IgM⁺ and among hCD2⁺ cell populations, the percentage of B220^{low} cells increased with age, implying that B220 expression is downregulated in IgM⁺ B cells. Beyond that, IgM⁺ hCD2⁺ showed downregulation of CD21 and although hCD2⁺ cells were those exhibiting still highest CD21 expression, these higher levels did not reach original levels expressed by MZ B cells in young Notch2IC//CD19Cre^{+/-} mice. Almost no IgD⁺ cells could be detected among lymphocytes, whereas there were still populations of IgM^{high} cells, which were all hCD2⁺ in accordance with their MZ B cell phenotype. In most Notch2IC//CD19Cre^{+/-} mice, lymphocytes of the lymph nodes and bone marrow exhibited a similar CD21 downregulation and IgM, IgD expression as in splenic cells (data not shown). Quite similar alterations in surface marker expressions could be detected among other aged Notch2IC//CD19Cre^{+/-} mice, not yet tested for tumor development by Southern blot analysis, starting at 15-16 months and aggravating with age (data not shown). In contrast to Notch2IC//CD19Cre^{+/-} animals, control mice showed no drastic aging-induced changes in CD21, CD23, IgM, IgD or B220 expression (Fig. 58B, #7576 as example). Only the two mice (#353 and #7461), which developed tumors, exhibited clear alterations (Fig. 58B, #7461 as example). Both mice

Results

exhibited an expansion of an IgM^{high} IgD^{low} B cell population in the spleen. In addition the typical CD21^{high} CD23^{low} MZ B cells could not be detected anymore. Fo B cells, however, could be detected at normal frequencies and expressed normal CD21, CD23, IgM, IgD levels in these two animals. The expanded IgM^{high} IgD^{low} population was also detectable in the bone marrow of these two mice (Fig. 58B, #7461), suggesting that tumor cells had spread into other organs. In summary, present results from our analyses indicate that constitutive Notch2IC expression might drive lymphoma development, but only with a late onset and long latency. It further seems that B cells of Notch2IC-expressing mice aged 15 months and older exhibit changes (especially downregulation) in their surface marker expression irrespective of tumor development. This fact together with the observation that tumor development was not always correlated with increased splenic weight or stronger signs of sickness in mice, suggest that Southern blot analyses are necessary to be able to judge possible tumor development. Collectively, our data indicates that constitutive Notch2IC-expression is not a strong oncogen in B cells.

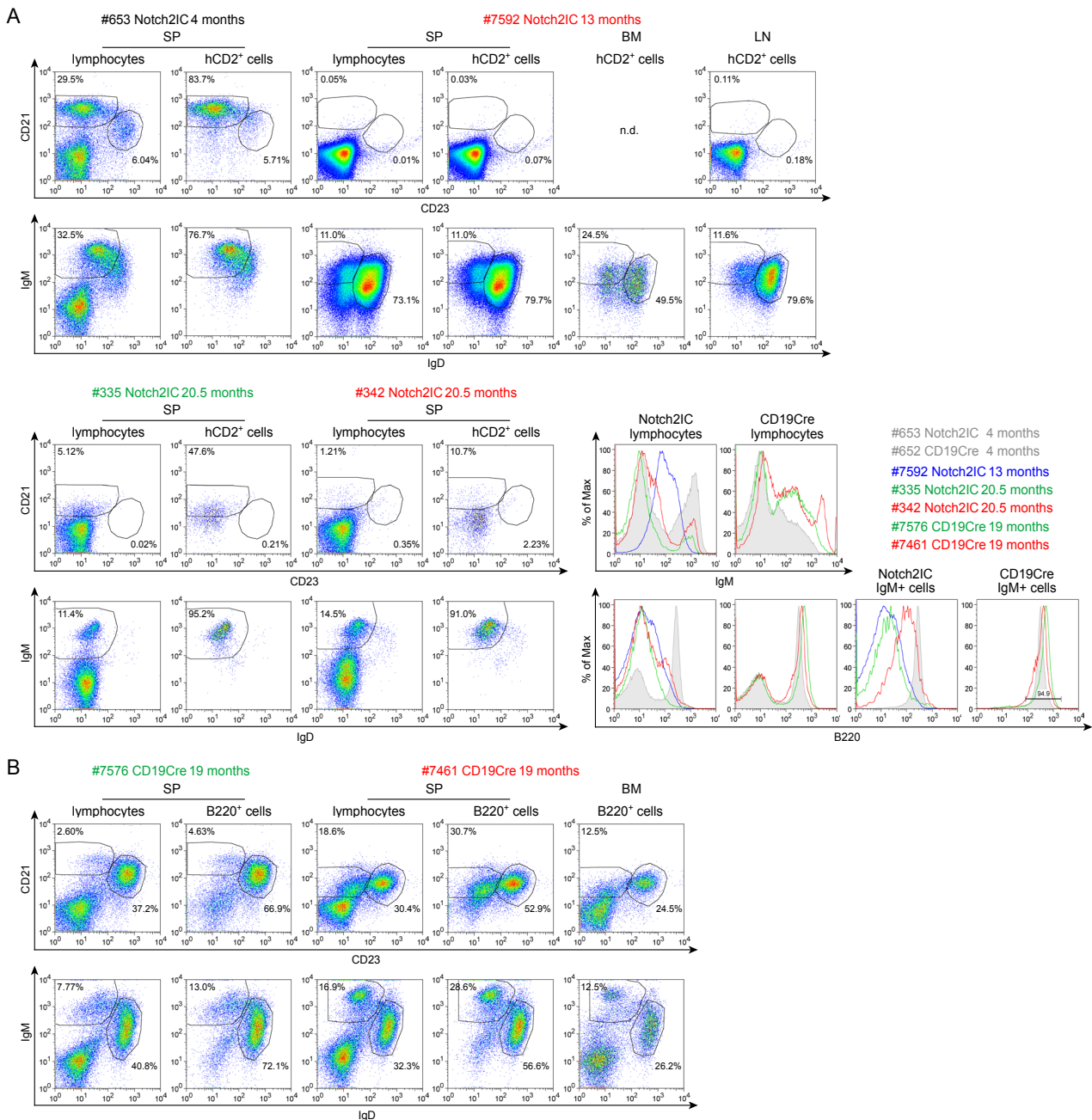


Figure 58 (depicted on previous page): Results of representative FACS analyses, depicting splenic cells of aged Notch2IC//CD19Cre^{+/-} and control mice. Cohorts of Notch2IC//CD19Cre^{+/-} (Notch2IC) and control mice (CD19Cre) were aged up to 22 months. Mice were analysed when showing first signs of illness. Splenic cells were subsequently isolated and analysed via FACS analyses for their CD21, CD23, IgM, IgD and B220 expression. Depicted dot plots are gated as indicated on lymphocytes, B220⁺ (in controls) or hCD2⁺ cells (in Notch2IC//CD19Cre^{+/-}). Animals marked in red displayed additional bands, animals marked in green no additional bands in Southern blot analysis. Mice marked in black were not tested by Southern blot. **(A)** Dot plots display results of FACS analyses of four exemplary animals representing results of all analysed Notch2IC//CD19Cre^{+/-} mice aged up to 22 months. Histograms show overlays of B220 levels of splenic lymphocytes and IgM⁺ splenic cells of old and young Notch2IC//CD19Cre^{+/-} and control mice with and without additional bands in Southern blot analysis. **(B)** Results of FACS analyses of two exemplary control animals representing results of all analysed control mice aged up to 19 months. Sp (spleen), BM (bone marrow), LN (lymph nodes), n.d. (not determined).

4. Discussion

Notch receptors play crucial roles during various developmental steps in many different tissues. In lymphocytes mainly Notch1 and 2 are expressed, with Notch1 being necessary for T cell development (Han et al., 2002; Radtke et al., 1999; Pui et al., 1999), while Notch2 is essential for MZ B cell differentiation (Saito et al., 2003). Mutations concerning the Notch receptors in general have been shown to be implicated in the development of various tumors. Constitutive active Notch1 is especially transforming for T cells, but also Notch2 and 3 signalling have been shown to induce T cell leukemias (Tzoneva and Ferrando, 2012; Pui et al., 1999; Bellavia et al., 2000; Rohn et al., 1996). However, Notch mutations have recurrently also been found in several B cell lymphomas. Especially, alterations in the *notch2* gene, resulting in an enhancement of the corresponding signalling pathway, are the most frequent ones found in splenic marginal zone lymphomas (SMZL) (Troen et al., 2008; Kiel et al., 2012; Rossi et al., 2012) as well as diffuse large B cell lymphoma (DLBCL) (Lee et al., 2009) and seem to be relatively specific for these type of tumor as they are absent from other B cell lymphomas. To investigate the role of Notch2 signalling in B cell activation and immune responses as well as the role of a constitutively active Notch2 signal on lymphoma development, two conditional transgenic mouse strains, allowing a *Cre/loxP*-dependent expression of a truncated Notch2 receptor (Besseyrias et al., 2007) or the ligand-independent expression of the intracellular part of Notch2 (Notch2IC) (Hampel et al., 2011) were used. In addition, I attempted at distinguishing direct Notch2 effects on the MZ B cell phenotype from those supplied by the marginal zone.

4.1 Gene expression profiles of Notch2IC-expressing MZ B and Notch2-deficient Fo B cells resemble their wild type counterparts, yet still exhibiting clear differences

Notch2 deficiency such as in *Notch2^{fl/fl}/CD19Cre^{+/-}* mice leads specifically to the absence of MZ B cells, while a constitutively active Notch2 pathway results in an expansion of this cell population within the MZ even in the absence of the BCR co-receptor CD19, normally important in MZ B cell development (Besseyrias et al., 2007; Hampel et al., 2011). Furthermore, Notch2 could directly or indirectly also be implicated in providing MZ B cells with localisation and retention signals for the MZ (Tan et al., 2009; Simonetti et al., 2013). In previous experiments we could already show that Notch2-deficient Fo B cells as well as Notch2IC-expressing MZ B cells resemble their respective wild type counterparts with respect to their localisation and known typical surface marker expression. In addition, Notch2IC-expressing B cells also exhibited a pre-activated state, characterised by enhanced proliferation and the expression of activation markers (Hampel et al., 2011). To dissect in detail the differences in gene expression profiles between Notch2-deficient and wild type Fo B cells as well as between Notch2IC-expressing and wild type MZ B cells, and to possibly differentiate between Notch2 target genes and those induced by the respective environment, we performed whole mouse-genome gene expression profiling using Illumina BeadChip microarrays. Hierarchical clustering analysis revealed that independent of constitutive Notch2 expression or ablation, MZ B cells and Fo B cells primarily

grouped according to their cell-type identity. Yet, already on the next subsequent clustering level, four clusters could be separated from each other: one cluster comprising wild type MZ B cells clearly separated from the one containing Notch2IC-expressing MZ B cells, in addition, a wild type Fo B cell cluster and a cluster containing Notch2-deficient Fo B cells. Several aspects of these observations demonstrate the good quality of our microarray results. Firstly, we could not observe any further outliers apart from the two, which already completely dropped out during quality controls, hence before further data analyses. Secondly, the appearance of three instead of two clusters among Fo B cell populations could clearly be attributed to a mild amplification bias, which was considered in all subsequent analyses. And finally, gene expression profiles of Notch2IC-expressing and wild type MZ B cells strongly resembled each other, which is in accordance with the previously discovered similarities among both cell types (Hampel et al., 2011). Accordingly, obtained lists containing differentially regulated genes reflect “real”, technically unbiased differences in expression. Apart from the quality control, hierarchical clustering in line with PCA and Volcano plot analyses revealed that Fo B and MZ B cells greatly differ in their gene expression profiles. Furthermore, wild type and Notch2-deficient Fo B cells are more closely related to each other compared to wild type and Notch2IC-expressing MZ B cells. Still, constitutive Notch2IC-expression or Notch2 ablation resulted in clear differences in gene expression profiles of these cells compared to their respective wild type counterparts. In PCA, wild type MZ B cell samples in fact seemed slightly more scattered than the other groups. This might be due to mild, negligible contaminations with dead cells or other cell populations. Those contaminations become more noticeable and hence carry more weight in data of small, sort-purified populations, such as 5 % of total B cells for wild type MZ B cells, in comparison to data from sort-purifications of big populations. Accordingly, this could result in a greater variance among wild type MZ B cell data, appearing as if Notch2IC-expressing and wild type MZ B cells are less similar than wt and Notch2-deficient Fo B cell populations. However, we think that these possible, slight contaminations only affect comparisons of wild type MZ B cell samples among each other, than the relation to the other analysed cell populations. The fact that wild type MZ B cells are still clearly a group on their own underpins this argument. Results from hierarchical clustering, PCA and Volcano plot analyses suggest that in contrast to Notch2-deficient Fo B cells, wild type Fo B cells apparently still get some Notch2 signal, as some markers typical for MZ B cells and thus possibly Notch2 target genes were upregulated in wild type versus Notch2-deficient Fo B cells. So, it could either be that all Fo B cells get a very weak Notch2 signal or that only few Fo B cells get a normal Notch2 signal. We think that the second scenario is more likely, as CD21 is a Notch2 target (Strobl et al., 2000) and only few wild type Fo B cells are CD21^{high} and hence receive most likely a Notch2 signal. The just mentioned CD21^{high} population could also represent Fo II B cells (pre-MZ B cells) (Cariappa et al., 2007a), which consequently have Notch2 signalling. Yet, as this CD21^{high} wild type Fo B cell population is very small only genes strongly regulated by Notch2 signalling emerge in our microarray gene lists. On the other hand it seems that even wild type MZ B cells do not permanently get a strong Notch2 signal as it is the case for Notch2IC-expressing B cells. However, the number of differentially regulated genes suggested that wild type Fo B and Notch2-deficient Fo B cells are more closely related to each other than those of Notch2IC-expressing and wild type MZ B cells. One reason accounting for differences

among the MZ B cell populations might be that in Notch2IC//CD19Cre^{+/-} mice Notch2 expression is independent of Dll1 binding, while wild type MZ B cells have to compete for Dll1, as its expression is quite restricted in wild type spleens (Sheng et al., 2008; Tan et al., 2009). Another possibility could be that Notch2 signalling is much stronger in Notch2IC-expressing cells than in wild type MZ B cells as the Notch2IC transgene is placed under the very strong CAGGS promoter. The fact that known MZ B or Fo B cell markers were clearly up- or downregulated in the respective analysed populations again affirmed the good quality of our microarrays. Among those were the characteristic MZ B cell surface and activation markers CD9, CD1d, CD21, CD86 and CD38 as well as CD23, which is a typical marker for Fo B cells. Known direct Notch2 targets such as members of the Hes, Hey and Deltex family were clearly upregulated in Notch2IC-expressing MZ B cells versus wild type ones. Many MZ B cell markers were further upregulated by Notch2IC expression and some of them were downregulated in Notch2-deficient compared to wild type Fo B cells. All these findings led us to the assumption that our gene lists are a quite promising source to identify further currently still unknown candidate genes that are regulated by Notch2 signalling and not by the MZ environment. Thus, these gene lists can be used to get deeper insights into Notch2 target genes implicated in MZ B cell differentiation and immune responses.

4.2 Notch2IC-expressing B cells show enhanced proliferation mainly due to their MZ B cell phenotype

Cell cycle analyses of directly ex vivo isolated splenic B cells revealed that more Notch2IC-expressing B cells were in S or G2/M phase compared to control B cells from CD19Cre^{+/-} mice (Hampel et al., 2011). However, these differences were only small. No differences could be detected among survival curves of unstimulated Notch2IC-expressing and control B cells over three days of in vitro culture and in accordance with this, proliferation experiments using carboxyfluorescein succinimidyl ester (CFSE) performed on day three of unstimulated in vitro cultures also displayed only slightly increased proliferation rates in Notch2IC-expressing versus control B cells (Hampel et al., 2011). On the other hand, similar CFSE experiments with LPS- and α -CD40-treated, in vitro cultured B cells clearly demonstrated that, compared to control B cells, proliferation was much stronger in Notch2IC-expressing cells after stimulation. MZ B cells are well-known to have a pre-activated phenotype and to rapidly start proliferating after LPS stimulation or CD40 ligation (Gunn and Brewer, 2006; Oliver et al., 1999b; Thomas et al., 2007; Hampel et al., 2011). Hence, since in these previous experiments Notch2IC-expressing B cell populations - including ~80 % MZ B cells - were always compared to total splenic B cells from control mice with only ~5 % MZ B cells, it was not clear whether the investigated strong increase in proliferation was only a typical, natural MZ B cell phenotype or an additional effect of constitutive Notch2 signalling. By performing CFSE proliferation experiments using sort-purified wild type and Notch2IC-expressing MZ B cells, which were cultured with LPS or α -CD40 for 2.5 days, I could show that stimulated Notch2IC-expressing MZ B cells had quite similar or marginally enhanced proliferation potentials than similarly treated control MZ B cells. These results indicated that the strongly enhanced cell division rate specifically after stimulation is indeed mainly a typical

MZ B cell phenotype. Moreover, the experiment showed that Notch2IC expression has reinforcing effects on cell proliferation. The enhanced proliferation potential detectable when comparing LPS- or α -CD40-stimulated wild type and Notch2IC-expressing MZ B cells is in agreement to data analysis of our Illumina BeadChip arrays. Annotation cluster analyses comparing differentially regulated genes between wild type and Notch2IC-expressing MZ B cells revealed enriched biological terms such as “positive regulation of B cell/lymphocyte proliferation” indicating that constitutive Notch2 signalling might additionally slightly enhance intrinsic, natural proliferation potentials of MZ B cells. The reason why in CFSE experiments we could only detect small increases in proliferation rates of Notch2IC-expressing compared to control MZ B cells could stem from the fact that Notch2 is not only inducing proliferation, but at the same time also apoptosis. Hence, the biggest part of Notch2IC-expressing cells was already dead when proliferation experiments were performed so that possible differences were underestimated. In line with this theory, annotation cluster analyses performed on our microarray data, provided enriched terms such as “cell death” or “apoptosis” for the comparison of MZ B and Fo B cells in general but also for wild type versus Notch2IC-expressing MZ B cells. Furthermore, previous data of our group, showing that Notch2IC indeed drives EBV-transformed B cell lines into cell cycle, but at the same time also induces the expression of pro-apoptotic genes, is also in agreement with the proposed model (Kohlhof et al., 2009). **In addition, cell cycle experiments undertaken by A. Draeseke, another former member of our group, showed that until day two of in vitro culture unstimulated Notch2IC-expressing B cells had a distinctly greater cell division rate than control B cells. However, on day three most of the Notch2IC-expressing cells were dead, suggesting again that B cells constitutively expressing Notch2IC proliferate faster but also attain an apoptotic state more rapidly. When these experiments were performed with B cells expressing not only constitutive Notch2, but additionally also a ligand-independent, constitutively active CD40 receptor, this premature induction of apoptosis could be inhibited, while at the same time enhanced proliferation rates were maintained (A. Draeseke, PhD thesis). And last but not least, in vitro cultured Notch2IC-expressing cells were apparently more rapidly consuming nutrients within cell culture media (identified by means of yellow coloured medium) possibly due to this higher rate of proliferation, implicating that the maximum division rate achievable in vitro was possibly already reached (personal observation). Accordingly, it could be that in vivo, Notch2IC-expressing B cells only have slightly elevated cell division rates, but that these rates further increase as soon as co-stimulatory factors such as CD40 or BAFF are present or when Notch2IC-expressing cells are taken out of their natural environment. Hence, it could well be that CFSE proliferation analyses of LPS- or α -CD40-stimulated MZ B cells performed already after one or two days in vitro would result in an even stronger difference in the proportion of cell divisions in stimulated Notch2IC-expressing compared to control MZ B cells. And finally, this data could also indicate that Notch2 induced proliferation is in large part somehow contained in vivo, possibly by the MZ environment.**

4.3 Increased Erk, Jnk, Akt levels in Notch2IC-expressing MZ B cells in vivo

In former experiments we could already clearly show that Notch2 is instructive for MZ B cell development even in the absence of the BCR co-receptor CD19 (Hampel et al., 2011), which has been shown to impact on MZ B cell differentiation (Engel et al., 1995; Rickert et al., 1995; Martin and Kearney, 2000). Thus, Notch2IC//CD19Cre^{+/+} mice, whose CD19 locus is disrupted due to the insertion of the *Cre* recombinase into both alleles, displayed a similar phenotype as Notch2IC//CD19Cre^{+/-} animals, including increased activation of the MAP kinases Erk and Jnk (Hampel et al., 2011). In this work we additionally demonstrated that constitutive Notch2 signalling could not only overcome the MZ B cell deficiency induced by a CD19 knockout, but that B cells of Notch2IC//CD19Cre^{+/+} mice exhibited enhanced PI3K/Akt signalling in comparison to respective control B cells. This was surprising as CD19 is known to be a major trigger of this signalling pathway (Buhl et al., 1997; Carter et al., 1997; Otero et al., 2001) and CD19-deficient mouse splenic B cells display reductions in Akt signalling (Otero et al., 2001). In B cells of Notch2IC//CD19Cre^{+/-} animals, levels of pAkt and its targets pp70 (pS6K) and pGSK-3 were higher compared to control cells, while FoxO1 protein levels, which are negatively regulated by Akt signalling were decreased. All of these findings clearly pointed at an enhanced PI3K/Akt signalling in Notch2IC-expressing cells. In addition greater amounts of Tcl1B, a co-activator of Akt, could also be detected. However, expression levels of PTEN, known to negatively regulate the PI3K/Akt pathway, were also enhanced by constitutive Notch2 signalling. Most likely the overall turnover of the whole PI3K/Akt pathway is amplified in MZ B cells and thus, also the amounts of members of counterregulatory mechanisms are increased ensuring that PI3K signalling is not continuously active and thus overshooting. pAkt, pp70 (pS6K) and pGSK-3 levels in B cells of Notch2IC//CD19Cre^{+/+} mice were also clearly increased compared to cells of CD19Cre^{+/+} controls, suggesting that Notch2IC expression fully rescues defects in PI3K signalling of CD19-deficient cells. Yet, expression levels of FoxO1 and PTEN show that the rescue is only partial. It is not clear how PI3K/Akt signalling is induced by constitutive Notch2 signalling in the absence of a CD19 receptor. One possibility could be that Notch2 is somehow directly exerting influence on members of this pathway, as ligand-dependent activated NotchIC has already been shown to induce phosphorylation of Akt via the mTOR-RICTOR complex (Perumalsamy et al., 2009). Another possibility could be that it increases the expression of G-protein coupled receptors and/or integrins on the surface of MZ B cells, which then in turn could take over the downstream activation of PI3K/Akt activation. One candidate mediating PI3K signalling might be the S1PR3 receptor, which was clearly upregulated by Notch2 in our microarray when comparing wild type and Notch2IC-expressing MZ B cells and which has been shown to be able to induce PI3K (Takuwa et al., 2011). As integrins are also known to act upstream of the CD19 co-receptor and to activate PI3K signalling (discussed in Pillai and Cariappa, 2009), we checked for genes encoding integrins that exhibited upregulation by Notch2 in our microarrays. Preliminary analysis already revealed a couple of candidates such as Itga10 and Itgae on our gene list comparing wild type and Notch2IC-expressing MZ B cells. Not only the phosphorylated forms of Akt and the Akt targets p70 and GSK-3 were increased but also

their basal protein levels. Since we did not find enhanced levels of PI3K members, such as Akt and Akt target genes in our microarray experiments, we suggest that these proteins are regulated on a posttranscriptional level. Apart from these findings, we could also demonstrate that pErk, pJnk and pAkt levels of ex vivo isolated Notch2IC-expressing cells were similar to those found in ex vivo isolated wild type MZ B cells and that both expressed increased levels compared to Fo B cells. It has already been shown that MZ B cells exhibit increased Akt phosphorylation (Meyer-Bahlburg et al., 2009). We could add to this finding that also the MAPK Erk and Jnk display increased phosphorylation in MZ B cells further underlining their hyper-activated state. By cultivating Notch2IC-expressing and control B cells in vitro, we tested whether the expression of MZ B cell surface markers and the increased activity of signalling pathways is mediated by the expression of Notch2IC or the MZ environment. Although in vitro cultured Notch2IC-expressing B cells were able to maintain the expression of typical MZ B cell surface markers, they rapidly lost enhanced Erk, Jnk and PI3K/Akt levels, with greatest reductions in Erk and Jnk, suggesting that the natural environment of the MZ is providing additional signals resulting in greater amounts of the MAP kinases Erk and Jnk as well as Akt.

4.4 Notch2IC-expressing MZ B cells spontaneously differentiate to functional, antibody-secreting plasmablasts/plasma cells in vitro, but not in vivo

Next to their established important role in T cell-independent immune responses and their characteristic property to rapidly differentiate to antibody-secreting plasma cells (Martin et al., 2001), MZ B cells represent a major source of natural, mostly IgM antibodies (Holodick et al., 2014; Casali and Schettino, 1996; Cerutti et al., 2013). Yet, although Notch2IC//CD19Cre^{+/-} mice have highly increased numbers of MZ B cells, no increased frequencies of plasma cells could be detected in vivo in unimmunised animals. This was in accordance with previous already published experiments of our group, illustrating that basal antibody titers of unimmunised Notch2IC//CD19Cre^{+/-} mice were similar to those in control animals, except IgG3 titers which were surprisingly even reduced (Hampel et al., 2011). However, when taken into in vitro culture without any stimulation, Notch2IC-expressing cells spontaneously started to differentiate into antibody-secreting plasmablasts or plasma cells with highest frequencies reaching up to 30 % in unstimulated cells at day two. LPS stimulation did not further enhance this differentiation, but frequencies were still a lot larger than in LPS-treated control B cells. We found that when LPS-stimulated control and Notch2IC-expressing B cells as well as unstimulated Notch2IC-expressing cells were additionally treated with α -CD40, no or reduced plasmablast/plasma cell formation could be detected. This is in line with a previous observation demonstrating that ligation of the TNF receptors CD40 and CD27 inhibits terminal differentiation of plasma cells via Jnk and in part also via Erk (Satpathy et al., 2010). Secreted IgM titers found within cell culture supernatants and the amount of antibody-secreting cells detected by ELISPOT analyses largely correlated with the amount of CD138⁺ B220^{low} cells detected by flow cytometry, confirming their plasmablastic/plasma cell phenotype. The reason why secreted IgM titers in supernatants seemed lower than the amount expected from the great number of IgM-secreting cells detected by ELISPOTs, could be rooted in the

fact that CD138⁺ B220^{low} cells possibly contain many pre-plasmablasts, which are IgM⁺, but do not yet secrete large amounts of antibodies. MZ B cells are known to carry polyreactive BCRs (Bendelac et al., 2001). So, as **these strong signals in IgM-specific ELISPOT analyses were obtained in immunised as well as in unimmunised Notch2IC-expressing mice**, this could be a typical feature of MZ B cells, which remains unnoticed in analyses with wild type B cells, as MZ B cell populations are underrepresented. Another possibility is that the induction of constitutive Notch2 signalling already in late stages of B cell development in the BM, leads to a slightly premature migration of MZ B cells out of the BM and into the MZ, thereby possibly skipping terminal V(D)J recombination events, thus leading to MZ B cells which carry a BCR which exhibits even stronger polyreactivity than a normal MZ B cell BCR would do. To clarify this, ELISPOT analyses need to be performed with sorted wild type MZ B cells and Notch2IC-expressing cells. In summary, **these first experiments indicate that Notch2IC-expressing MZ B cell have an intrinsic potential to spontaneously differentiate to functional, antibody-secreting plasmablasts or plasma cells as soon as they are taken out of their natural MZ environment**. The fact that Notch2IC-expressing B cells do not spontaneously differentiate to plasma cells *in vivo*, but exhibit enhanced plasmablast/plasma cell differentiation after *ex vivo* isolation even in the absence of stimulation suggests that the MZ forms an inhibitory environment for plasma cell differentiation. This is in accordance with observations that after antigen encounter, activated MZ B cells can only develop to fully mature plasma cells when they are able to migrate into the follicle and subsequently out into the red pulp (Shapiro-Shelef and Calame, 2005; Sze et al., 2000). MZ B cells are known to shuttle continuously between the MZ and the follicle. The key mechanism underlying this shuttling is the alternating up- and downregulation of the S1PR1, another important signal mediating the correct localisation of MZ B cells (Arnon et al., 2013). **There are indications that Notch2 signalling could be essential for MZ B cells to be able to migrate and to localise within the MZ** (Simonetti et al., 2013). Consequently we think that constitutive Notch2 signalling interferes with the migration capacity of MZ B cells, thereby possibly retaining MZ B cells within the MZ and subsequently inhibiting their spontaneous development into plasma cells. Possible candidates underlying this inhibition could be various integrins, chemokines or other molecules/receptors shown to be implicated in the retention of MZ B cells within the MZ. S1PR3 and CB2 for example could be interesting candidates, because firstly they were among the genes in our microarray differentially upregulated by Notch2 and secondly, S1PR3 and CB2 have been shown to be at least in part involved in the migration of MZ B cells to the MZ and their retention in it (Muppidi et al., 2011; Cinamon et al., 2004). **S1PR3 has in addition been shown to be the key chemotactic receptor in B cells responsible for the migration towards S1P** (Cinamon et al., 2004) and CD27 or CD40 are both TNFR known to inhibit plasma cell development (Satpathy et al., 2010).

Additional experiments using sort-purified MZ B cells indicated that the spontaneous plasmablast/plasma cell differentiation of Notch2IC-expressing MZ B cells *in vitro* is in some way triggered and/or accelerated by constitutive Notch2 expression and not just a natural, intrinsic MZ B cell feature, as unstimulated wild type MZ B cells did not develop into plasma cells unless stimulated with LPS. Nonetheless, as antigen-activated B cells first of all undergo a burst of proliferation, before differentiating into plasma cells (Shapiro-Shelef and Calame, 2005), one could assume that strong

proliferation is a prerequisite for subsequent plasma cell differentiation. Knowing this, one cannot completely rule out that wild type MZ B cells also have the intrinsic potential for spontaneous plasma cell differentiation *in vitro*, but as their proliferation capacity is possibly lower as the one in Notch2IC-expressing MZ B cells, plasmablasts or plasma cells would arise belatedly. Thus, it could be that plasmablast/plasma cell development in unstimulated Notch2IC-expressing B cells is an indirect effect of enhanced proliferation, which in consequence could lead to a premature induction of plasma cell differentiation. In contrast to *in vitro* cultured total B cell populations, sort-purified, LPS-treated Notch2IC-expressing cells exhibited a greater CD138⁺ B220^{low} population on day two of *in vitro* culture than those without stimulation. It could be that the stressful sort procedure is delaying the onset of proliferation and differentiation as it takes some time for the cells to recover. The higher percentage of plasma cells in LPS-treated than in untreated Notch2IC-expressing B cells, might indicate that LPS stimulation further accelerates plasma cell differentiation of Notch2IC-expressing B cells. Hence, the peak of plasma cell development within LPS-treated Notch2IC-expressing B cells might have been missed in previous experiments with unsorted cells. The finding that antibody titers in cell culture supernatants were quite similar between unstimulated and LPS-treated Notch2IC-expressing B cells further confirms this theory. Hence, further experiments are planned in which Notch2IC-expressing B cells are cultured in the presence of LPS and possible plasma cell development is checked at various time points (after 24 h, but before 48 h of culture) via flow cytometry to be able to assess the peak in plasma cell differentiation under these circumstances.

Blimp-1 as well as Irf4 are both transcription factors, which are essential for and strongly upregulated during plasma cell development (Shapiro-Shelef and Calame, 2005). Hence, analyses on the Blimp-1 and Irf4 expression levels during *in vitro* cultures not only additionally underpinned the plasmablast/plasma cell phenotype of the CD138⁺ B220^{low} B cell population arising in Notch2IC-expressing cells, but also gave deeper insights into the course of its development under various conditions. *Ex vivo* isolated Notch2IC-expressing MZ B cells had clearly increased Blimp-1 and Irf4 levels compared to wild type Fo B cells and even higher levels of Irf4 than wild type MZ B cells. Blimp-1 amounts were similar or marginally increased in Notch2IC-expressing cells compared to wild type MZ B cells, which is in accordance with data from Fairfax and colleagues, showing that only a small subset of wild type MZ B cells expresses low but detectable levels of Blimp-1, which are higher than those of splenic Fo B cells (Fairfax et al., 2007). Wild type MZ B cells are known to be in a pre-activated state to be able to rapidly respond to pathogens by quickly differentiating into plasma cells (Martin et al., 2001). The increased levels of Blimp-1 and Irf4 already in *ex vivo* isolated Notch2IC-expressing cells compared to wild type MZ B cells could be an explanation why Notch2IC-expressing cells are so fast at spontaneously differentiating into antibody-secreting plasmablasts/plasma cells *in vitro*. The observation that in those highly pre-activated Notch2IC-expressing MZ B cells, Irf4 levels exhibited stronger increases than Blimp-1 levels compared to wild type MZ B cells, was in accordance with literature showing that the onset of Irf4 expression during B cell activation and subsequent plasma cell development is much earlier than the one of Blimp-1 (Oracki et al., 2010). Furthermore, it could be that Irf4 is directly regulated by Notch2 and hence strongly upregulated in Notch2IC-expressing MZ B cells. In agreement with the fact that Notch2IC-expressing cells differentiate into

plasmablasts/plasma cells more rapidly, an extremely fast upregulation of Blimp-1 and Irf4 could be detected in cultures of unstimulated Notch2IC-expressing cells, peaking at day two concomitant with highest plasma cell/plasmablast frequencies. In control B cells, such a distinct rise in Blimp-1 and Irf4 levels could only be detected in LPS-treated cultures. Here, expression levels peaked at day three, again in accordance with highest percentages of plasma cells. Yet, Notch2IC-expressing cells were faster (highest levels on day two) compared to LPS-treated control cells (highest levels on day three). Although unstimulated Notch2IC-expressing cells always exhibited highest plasma cell or plasmablast frequencies on in vitro day two, the course of Blimp-1 and Irf4 expression levels in LPS-treated cells suggests that Notch2IC-expressing B cells are differentiating even more rapidly to plasma cells/plasmablasts with LPS stimulation and that similar or even greater amounts of plasma cells/plasmablasts than in unstimulated cells would have been detectable after 1.5 days of in vitro cultures, a time point which we did not yet analyse.

To find out which signalling pathways are responsible for driving or inhibiting plasma cell differentiation we analysed Western blot analyses originally performed to investigate MAPK and PI3K signalling in B cells during in vitro culture. We could see that in in vitro cultures of LPS-treated control cells as well as of unstimulated and LPS-stimulated Notch2IC-expressing cells, in which plasmablast/plasma cell populations appeared, pJnk levels - predominantly pJnk2 - were always downregulated compared to ex vivo levels. This indicates that pJnk needs to be downregulated for plasma cell development. pErk levels on the other hand were also strongly downregulated in unstimulated and LPS-stimulated Notch2IC-expressing cells, whereas in LPS-treated control B cells they were upregulated compared to ex vivo levels. However, these seemingly contradictory findings are in accordance with results from other research groups, showing that apparently Erk signalling is differentially regulated in LPS-treated and GC B cells. In GC B cells, which are mainly derived from Fo B cells the activation of Erk1 and 2 after BCR ligation leads to the induction of Blimp-1 and the appearance of plasma cells (Yasuda et al., 2011). Yet, continuous Erk activation via chronic BCR activation for example, possibly mimicking self-reacting B cells, inhibited LPS-induced plasma cell development (Rui et al., 2006; Rui et al., 2003). Hence, it might be that in cultures of control B cells, which mainly consist of Fo B cells with low pErk levels, LPS-stimulation is able to enhance Erk signalling. In contrast, in cultures of Notch2IC-expressing cells, mainly comprising MZ B cells, which already exhibit high pErk levels, LPS treatment leads to a downregulation of Erk signalling. In summary, we suggest that high levels of pErk and pJnk naturally occurring in MZ B cells are inhibitory for plasma cell differentiation and probably need to be downregulated during TI immune responses. α -CD40 stimulation strongly inhibited plasmablast differentiation in Notch2IC-expressing B cells, indicating that TNF receptor signalling could also be involved in the inhibition of plasma cell differentiation occurring in the MZ. By applying different small chemical inhibitors Satpathy and colleagues could already show that CD40 inhibits terminal plasma cell differentiation via Jnk and partially also via Erk. In accordance, we could observe that α -CD40-treated Notch2IC-expressing and control B cells exhibited highest levels of phosphorylated Erk and Jnk again indicating that elevated amounts of pErk and pJnk - in this case induced by α -CD40 treatment - are responsible for the hampered plasmablast development. The contribution of NF κ B signalling in the inhibition or induction of plasma cell differentiation still needs to be determined.

Similar experiments with short-term stimulations of only a few hours are planned to analyse initial changes in signalling pathways as soon as cells are taken out of their environment and treated with different stimuli (Satpathy et al., 2010).

4.5 Notch2IC//CD19Cre^{+/-} mice are impaired in their TI immune response, antigen capturing and the subsequent transport into the follicle

MZ B cells are well established as key players in TI immune responses (Martin et al., 2001). Yet, although Notch2IC-expressing MZ B cells exhibit a pre-activated phenotype and have the intrinsic potential for spontaneous plasmablast development, which is somehow inhibited in vivo, we were quite surprised to discover that after immunisation with the TI-2 antigen NP-Ficoll, or with low concentrations of the TI-1 antigen NP-LPS, Notch2IC//CD19Cre^{+/-} mice had clearly reduced antigen-specific IgM and IgG3 titers, implicating that they were impaired in their TI-2 and partially also in their TI-1 immune response. Immunisation with high amounts of NP-LPS (50 µg) however, revealed no defects in the antigen-specific IgM response, but a reduction in NP-IgG3 titers, pointing at additional, specific problems in isotype switching. We think that one aspect contributing to the hampered TI immune reactions is, that constitutive Notch2 signalling impacts on the migration capacity of Notch2IC-expressing MZ B cells. Treating mice with LPS (i.p.) is known to induce the clearance of the MZ five to six hours post injection (Cinamon et al., 2004). In wild type mice, concentrations as low as 5 µg still led to a complete localisation of all MZ B cells into the follicle. In contrast to this, nearly complete clearance could only be achieved with 50 µg NP-LPS in Notch2IC//CD19Cre^{+/-} mice and diminished with declining amounts of injected LPS. This data clearly points to a defect in stimulation-induced migration of Notch2IC-expressing MZ B cells. In agreement with experiments showing that S1PR1, which is implicated in the positioning of MZ B cells in the MZ, is downregulated in response to LPS (Cinamon et al., 2004), these data suggest that, under normal conditions, TI antigens, which activate MZ B cells induce a downregulation of certain localisation signals so that MZ B cells are able to move into the follicle and then into the red pulp to develop to fully mature plasma cells (Hargreaves et al., 2001). We propose that in Notch2IC//CD19Cre^{+/-} mice, constitutive Notch2 signalling forces MZ B cells to stay within the MZ by inhibiting the downregulation of such localisation signals. Immunisations with the TI-2 antigen NP-Ficoll only activate MZ B cells carrying an antigen-specific BCR. Thus, treating Notch2IC//CD19Cre^{+/-} with this rather “weak” antigen is possibly not strong enough to overcome Notch2IC-induced MZ localisation signals. Consequently, MZ B cells cannot further develop to plasma cells and immunised mice cannot build up a functional response to this sort of antigens. High concentrations of NP-LPS, on the other hand, strongly activate nearly all MZ B cells in a polyclonal fashion as they interact with the BCR and TLRs, irrespective of their antigen-specificity. In addition, as already mentioned before, LPS induces a drastic downregulation of the S1PR1, normally implicated in positioning MZ B cells in the MZ (Cinamon et al., 2004). Hence, it could be that changes induced by high concentrations of “strong” antigens such as NP-LPS are sufficient to overcome localisation signals induced by Notch2IC and that in these circumstances Notch2IC-expressing MZ B cells would

indeed be able to differentiate into plasma cells, although constitutive Notch2IC expression might still interfere with isotype switching. Constitutive Notch2 signalling might also inhibit the natural shuttling of MZ B cells in and out of the MZ, although this still needs to be investigated.

Another explanation for the hampered TI immune responses comes along with our finding that SIGN-R1⁺ macrophages, known to be implicated in antigen capturing and presentation to MZ B cells (Kang et al., 2004; Kang et al., 2006; Lanoue et al., 2004) are reduced and scattered in Notch2IC//CD19Cre^{+/-} mice. Hence, only few TNP-Ficoll antigen is captured within the MZ and in line with the defective migration potential of Notch2IC-expressing MZ B cells, absolutely no transport of antigen into the follicle could be detected five hours post injection. So it could be that reduced antigen capturing due to reduced SIGN-R1⁺ macrophages in combination with a defective antigen-induced MZ B cell migration into the follicle are the cause for the reduced immune response to the TI-2 antigen NP-Ficoll. However, recent publications challenge the contribution of SIGN-R1⁺ macrophages in TI immune responses. Aichele and colleagues could show that no antigen capturing was taking place when they depleted the MZ of its macrophages. Even so, a protective T cell response was induced in these animals (Aichele et al., 2003). Moreover, Kraal and colleagues could prove that the depletion of MZ macrophages did not impact on the immune response to NP-Ficoll (Kraal et al., 1989). These results indicate that the defective migration capacity of Notch2IC-expressing B cells possibly has a greater impact on the defective TI-2 immune response than the reduction in SIGN-R1⁺ macrophages. As LPS seems more suitable to overcome the forced MZ localisation, it would be interesting to investigate, whether the transport of TNP-LPS antigen is still possible in Notch2IC//CD19Cre^{+/-} mice. However, the reason how and why constitutive Notch2 expression in B cells impacts on SIGN-R1⁺ macrophages remains to be elucidated. So in summary, we propose that Notch2 signalling needs to be downregulated - at least for a short term - enabling antigen triggered MZ B cells to migrate into the follicle and subsequently into the red pulp to be able to fully differentiate into mature antibody-secreting plasma cells. Additional experiments using the S1PR1 inhibitor FTY720 are planned to test whether MZ B cells can be relocated to the follicle without being triggered by antigens and, if this is the case, to test whether spontaneous plasma cell differentiation can be triggered also in vivo when “unactivated” MZ B cells are just forced out of their natural MZ environment.

4.6 Notch2^{fl/fl}//CD19Cre^{+/-} mice show reduced TI-2 immune response, despite intact antigen capturing and transport into the follicle

As already discussed before, MZM and MZ B cells seem to cooperate during immune responses. SIGN-R1⁺ macrophages are key players in antigen capturing and presentation within the MZ (Batista and Harwood, 2009) and MZ B cells play a decisive role in transporting antigens from the MZ to the follicle (Arnon et al., 2013). You and colleagues could show by means of immunofluorescent stainings on splenic cryosections that in mice devoid of MZ B cells, such as in CD19 knockout or Notch2-deficient mouse strains, or in animals where MZ B cells were forced out of the MZ, SIGN-R1⁺ macrophages are drastically reduced or missing. Thus, they claimed that the correct localisation of

SIGN-R1⁺ macrophages in the MZ is dependent on the concomitant presence of MZ B cells within this splenic compartment. They also showed that in mice with missing or not correctly located SIGN-R1⁺ macrophages, TNP-Ficoll capturing was not detectable by immunofluorescent stainings anymore and thus deduced that it is not taking place (You et al., 2011; You et al., 2009). Therefore, we were surprised to see that populations of SIGN-R1⁺ macrophages were only slightly - if at all - reduced on splenic cryosections of Notch2-deficient mice. Besides, antigen capture and transport assays using TNP-Ficoll showed that in MZ B cell-deficient Notch2^{fl/fl}//CD19Cre^{+/-} mice, trapping of TNP-Ficoll within the MZ and transporting it into the follicle was still possible to the same extent as in wild type animals. The discrepancy between our and the published results are currently unclear. However, the still functional TNP-Ficoll trapping in Notch2^{fl/fl}//CD19Cre^{+/-} mice strongly implies that SIGN-R1⁺ signals visible on our splenic cryosections are specific and indeed depict functional SIGN-R1⁺ macrophages as otherwise capturing would not be taking place. In accordance with our observations were experiments performed by Cinamon and colleagues, which showed that BM chimeras reconstituted with S1PR1-deficient fetal liver cells have normal frequencies of MZ macrophages, although MZ B cells are localised within the follicle (Cinamon et al., 2004). You and colleagues also mention the fact that when CD19 knockout mice age beyond 10 to 12 weeks, some animals begin to accumulate MZ B cells and thereby recover their SIGN-R1⁺ cell population. However, such a rescue of MZ B cells could not be detected in our analysed Notch2-deficient mice. So, altogether we think that Notch2-deficient mice still have SIGN-R1⁺ macrophages and that antigen capturing and transport is still functional in these mice. These findings implicate that despite the absence of MZ B cells, TNP-Ficoll is captured and probably transferred from macrophages in the MZ to Fo B cells positioned within the follicle. Nevertheless, Notch2^{fl/fl}//CD19Cre^{+/-} mice exhibited reduced antigen-specific IgM and IgG3 plasma cell numbers and hence antibody titers in response to TI-2 immunisations with NP-Ficoll. This finding is in line with experiments obtained from various mouse models exhibiting defects in their MZ B cell population and hence in their TI immune response, thereby underpinning the important role that MZ B cells adopt in this type of immune response (Guinamard et al., 2000; Tanigaki et al., 2002; Sha et al., 1995). Yet, on the other hand RBP-J κ knockout mice, in which the MZ B cell population is also absent, display a normal immune response to the TI-2 antigen NP-Ficoll (Tanigaki et al., 2002). In these mice neither Notch1IC nor Notch2IC can bind to the transcription factor RBP-J κ and thus no transcription of Notch target genes takes place. This finding together with recent results of experiments performed in our group (not shown in this work) point at potential different roles of Notch1 and Notch2 during immune responses, especially plasma cell differentiation. Further investigations are currently being performed to unravel these different mechanisms. Apart from that, we also want to investigate if Fo B cells in Notch2^{fl/fl}//CD19Cre^{+/-} mice are perhaps after all able to take over the role of MZ B cells in response to NP-Ficoll immunisations, but that reactions are delayed, as Fo B cells are not designated to rapidly react to TI antigens. This would explain why antigen-specific titers are so low on day seven after immunisation. Currently, immunisation experiments analysing antibody titers 14 days post NP-Ficoll immunisation are planned to investigate whether the reaction of Fo B cells to NP-Ficoll in these mice is only retarded or indeed permanently reduced due to the lack of MZ B cells.

4.7 Constitutive Notch2 signalling is not acting as a strong oncogene in B cells, yet it alters the characteristic phenotype of B cells in aging mice

Notch genes belong to the rare gene group that exhibit haploinsufficiency, implicating that organisms are quite sensitive to changes in *notch* gene dosage. So it is not surprising that most Notch-associated malignancies are based on activating mutations of the corresponding genes. These sort of mutations have also been found in various B cell lymphomas. Since we are working on the role of Notch2 signalling in MZ B cell development and lymphomagenesis the following facts were of special interest for us: 30 % of SMZL exhibit recurrent mutations in the Notch signalling pathway, with the most frequent ones being localised in the PEST domain of the *notch2* gene, thereby leading to an increased stability of the receptor and thus to enhanced Notch2 signalling. Hence, we were especially interested in whether aging Notch2IC//CD19Cre^{+/-} mice would at some point exhibit signs of splenic lymphoma. From the data we have at the moment, we can say that although young Notch2IC-expressing B cells clearly exhibit increased levels of the proto-oncogene *c-myc*, a slight splenomegaly, and an increased proliferative potential, constitutive Notch2 signalling alone is not acting as a strong oncogene in B cells. First analyses on the B cell populations of old mice by Southern blot revealed that more Notch2IC//CD19Cre^{+/-} than control mice carried B cell populations exhibiting mono- or polyclonality, indicating that constitutive Notch2 signalling has mild oncogenic effects. However, the fact that most of these animals were already relatively old and that a large fraction of our mouse cohort aged without showing any signs of morbidity although at the time point of analysis, some had quite obvious signs of splenomegaly exceeding the one already seen in young Notch2IC//CD19Cre^{+/-} mice, suggests the development of indolent lymphomas with a long latency and a late onset. The probability of natural, Notch2IC unrelated tumor development increases with age. In line with this, two control mice also developed tumors at the age of 18 and 19 months. Therefore, further experiments are planned to prove that Notch2IC-expressing mice develop significantly more lymphomas than control animals and to determine the onset of lymphoma development in Notch2IC//CD19Cre^{+/-} animals. To this end, small cohorts of mice will systematically be analysed at different time points between six and 19 months. One possible reason why constitutive Notch2 signalling is not a strong oncogene could be that Notch2IC-expressing cells not only proliferate better but also go into apoptosis more rapidly. So an additional survival signal would be needed to drive lymphomagenesis. CD40 is a promising candidate as preliminary proliferation experiments and lymphoma analyses of mice expressing Notch2IC together with a ligand-independent, constitutive active CD40 receptor specifically in B cells, indicate that these mice develop lymphomas at younger age and in in vitro cultures, cells not only proliferate better, but also survive longer than cells with a Notch2IC alone.

In old Notch2IC-expressing mice, frequencies of splenic IgM⁺ B cells were slightly and B220 levels strongly diminishing with age and in addition B cells were in general losing their characteristic CD21^{high} CD23^{low} MZ B cell phenotype, irrespective of tumor formation. A publication from Birjandi and colleagues comparing MZ B cell and MZ macrophage populations in old mice (18 to 23 months) to those in young mice (two to six months), revealed that in aged mice there was great variability regarding

the appearance and shape of the MZ as well as the frequency and localisation of cells within this zone. While in young mice the MZ was a very distinct ring encircling the white pulp, in old mice it was highly diffuse and difficult to discern. Yet, there were still some individual old mice with a splenic architecture similar to those in young animals (Birjandi et al., 2011). Our finding that CD21 is downregulated in old Notch2^{IC}-expressing mice together with the fact that apparently the microarchitecture of the splenic MZ starts to dissolve when mice are aging, suggests that old Notch2^{IC}-expressing B cells lose their localisation in the MZ and hence their typical MZ B cell phenotype. One possible explanation for this age-related change in surface marker expression could be that due to constitutive Notch2 signalling MZ B cells are in a state of permanent activation. Thus, after some time these cells become kind of exhausted or anergic and as a counterregulatory mechanism start to downregulate their typical surface markers.

5. Summary

Notch2 is pivotal for the generation of MZ B cells. However, it is still unclear whether Notch2 is only a differentiation signal or an additional localisation signal for MZ B cells in the MZ and whether it is only needed for the generation of MZ B cells or for the maintenance of the MZ B cell phenotype. In addition, the regulation and role of Notch2 in antigen-activated MZ B cells during immune responses has not yet been studied in detail. Increased Notch2 signalling has been found in diverse B cell malignancies, but whether its constitutive expression is sufficient to induce lymphomas is not known. To get further insights into these roles of Notch2 signalling, we used two transgenic mouse strains previously established in our group allowing the *Cre/loxP* dependent, B cell-specific expression of a defective Notch2 receptor or a constitutively active, intracellular form of Notch2 (Notch2IC). We could previously show that Notch2IC expression via CD19-*Cre* induces a strong differentiation towards MZ B cells, while mice with a defective Notch2 signal in B cells lack MZ B cells. To find Notch2 regulated genes and distinguish them from those induced by the cell type or the cell's environment, we performed a whole mouse-genome gene expression profiling comparing Notch2IC-expressing MZ B and Notch2-deficient Fo B cells with their corresponding wild type counterparts. These Illumina BeadArrays revealed that cells of the same cell type clustered, apparently being quite similar according to their gene expression profile. Still, Notch2IC-expressing and Notch2-deficient Fo B cells clearly differed from their wild type counterparts, suggesting that not only MZ B but also wild type Fo B cells receive a Notch2 signal and that Notch2 signalling is weaker in wild type MZ B than in Notch2IC-expressing B cells or probably not constitutively active as in Notch2IC-expressing cells. We could also demonstrate that Notch2IC-expressing B cells exhibit similar or possibly slightly increased rates of proliferation, in particular after α -CD40 stimulation and apoptosis than wild type MZ B cells. Notch2IC-expressing B cells displayed similarly enhanced PI3K and MAPK signalling as wild type MZ B cells, even in the absence of the CD19 receptor. However, when taken into in vitro culture, Notch2IC-expressing B cells were not able to sustain these enhanced signalling pathway activity, although typical MZ B cell surface markers were maintained. This suggests that the enforced Erk, Jnk and Akt signalling, but not the expression of typical MZ B cell markers is in great part conferred by the MZ environment.

MZ B cells are believed to contribute to the pool of natural antibodies and to be key players in T cell-independent (TI) immune responses. Still, despite the high number of MZ B cells, Notch2IC//CD19Cre^{+/-} mice exhibited no rise in plasma cell frequencies in vivo, although Notch2IC-expressing cells were able to spontaneously and rapidly differentiate to antibody-secreting plasma cells in vitro. Immune responses to the TI-2 antigen NP-Ficoll and to the TI-1 antigen LPS - here especially to low concentrations - were hampered, correlating with a reduced migration of Notch2IC-expressing cells into the follicle. In addition, SIGN-R1⁺ macrophages, important players in antigen capturing and subsequent presentation to MZ B cells were scarce, but apparently still functional in Notch2IC//CD19Cre^{+/-} mice. These results suggest that Notch2 signalling drives plasma cell development, but their differentiation is inhibited as long as Notch2IC-expressing B cells are localised in the MZ. We think that a persistent localisation in the MZ due to a potential misregulation of the migration capacity

of Notch2IC-expressing cells could be the main underlying cause for the suppression of spontaneous plasma cell development *in vivo*, the defective TNP-Ficolin antigen transport into the follicle and the impaired reaction to TI antigens. This consequently implies that Notch2 signalling has to be switched off, when MZ B cells encounter antigen, so that they can migrate into the follicle to differentiate to plasma cells.

Furthermore, we studied TI immune responses in mice with B cell-specific Notch2 ablation. These mice exhibited normal frequencies of SIGN-R1⁺ macrophages and, consequently, intact antigen capturing. Surprisingly, antibody titers after TI-2 immunisation were reduced, but antigen transport into the follicle was still functional, although MZ B cells are missing in these animals. These findings suggest that antigen transport into the follicle can be performed by other cell types than MZ B cells, but that the presence of MZ B cells is essential for an adequate, quick response to TI-2 antigens.

A proportion of aged Notch2IC//CD19Cre^{+/-} mice developed lymphoma, however, not before reaching an advanced age and with mostly mild or no symptoms of morbidity. These data suggest that Notch2IC alone is not a strong oncogene in B cells, but may drive the development of indolent lymphoma with long latency and late onset.

6. Zusammenfassung

Notch2 Signale sind essentiell für die Entwicklung von Marginalzonen (MZ) B-Zellen. Dennoch ist immer noch nicht ganz klar, ob Notch2 nur ein Differenzierungssignal für MZ B-Zellen ist oder zusätzlich noch als Signal zur Lokalisation in der MZ dient. Des Weiteren ist nicht bekannt, ob es nur zur Bildung der MZ B-Zellen beiträgt oder auch benötigt wird, um den typischen MZ B-Zellphänotyp aufrecht zu erhalten. Auch die Rolle von Notch2 und dessen Regulierung in Antigen-aktivierten MZ B-Zellen während der Immunantwort wurde bisher noch nicht genauer untersucht. Verstärkte Notch2 Signale konnten in verschiedenen B-Zelltumoren identifiziert werden, aber ob eine alleinige, dauerhafte verstärkte Expression ausreicht, um zur Lymphomentstehung zu führen ist noch unklar. Um mehr Einblicke in all diese Funktionen des Notch2 Signalweges zu erhalten, haben wir uns zwei, in unserem Labor etablierte transgene Mauslinien zu Nutze gemacht. Diese Mauslinien exprimieren abhängig vom *Cre/loxP* System entweder einen defekten Notch2 Rezeptor oder eine konstitutiv aktive, intrazelluläre Form des Notch2 Rezeptors (Notch2IC) spezifisch in B-Zellen. Wir konnten bereits zeigen, dass eine Notch2IC Expression mittels *CD19-Cre* zu einer Verschiebung der B-Zell-differenzierung hin zu MZ B-Zellen führt, wohingegen Tieren mit einem defekten Notch2 Rezeptor die MZ B-Zellen fehlen. Um Notch2 regulierte Gene zu finden und diese von Genen unterscheiden zu können, welche vom Zelltyp oder der Umgebung der Zelle induziert werden, haben wir eine Mausgenom Genexpressionsanalyse durchgeführt. In dieser haben wir Notch2IC-exprimierende MZ B-Zellen und Notch2-defiziente folliculäre (Fo) B-Zellen mit den entsprechenden Wildtyp Populationen verglichen. Die Auswertung dieser Illumina Microarrays zeigte, dass Zellen vom gleichen Zelltyp ein recht ähnliches Genexpressionsprofil haben und demzufolge „clustern“. Dennoch unterschieden sich Notch2IC-exprimierende und Notch2-defiziente Zellen deutlich von ihren entsprechenden Wildtyp Populationen. Dies deutet zum einen darauf hin, dass nicht nur MZ B-, sondern auch Wildtyp Fo B-Zellen ein Notch2 Signal erhalten, zum anderen, dass das Notch2 Signal in Wildtyp MZ B-Zellen entweder schwächer ist, als in Notch2IC-exprimierenden Zellen oder nicht konstitutiv aktiv, wie dies bei Notch2IC-exprimierenden Zellen der Fall ist.

Notch2IC-exprimierende Zellen zeigten im Vergleich zu Wildtyp MZ B-Zellen eine ähnliche oder leicht erhöhte Apoptoserate und Proliferation, Letzteres insbesondere nach α -CD40 Stimulation. Darüberhinaus wiesen Notch2IC-exprimierende Zellen - auch in Abwesenheit des CD19 Rezeptors - und Wildtyp MZ B-Zellen eine ähnlich erhöhte Aktivität der PI3K und MAPK Signalwege auf. Jedoch waren Notch2IC-exprimierende B-Zellen nicht in der Lage diese verstärkten Signale *in vitro* aufrecht zu erhalten, obwohl sie die Expression typischer MZ B-Zellmarker beibehalten konnten. Dies könnte bedeuten, dass großteils die MZ zur Erhaltung der verstärkten Erk, Jnk und Akt Signale, jedoch nicht zur Expression der MZ B-Zellmarker beiträgt.

MZ B-Zellen tragen zum Pool der natürlichen Antikörper bei und spielen eine entscheidende Rolle bei der T-Zellunabhängigen (TI) Immunantwort. Jedoch wiesen Notch2IC//CD19Cre^{+/-} Mäuse trotz der hohen Anzahl an MZ B-Zellen, *in vivo* keine erhöhte Anzahl an Plasmazellen auf, obwohl Notch2IC-exprimierende Zellen *in vitro* spontan und schnell zu Antikörper-sekretierenden Plasmazellen differenzieren konnten. Darüberhinaus war die Immunantwort auf das TI-2 Antigen NP-Ficoll, sowie

die Reaktion auf das TI-1 Antigen NP-LPS - hier vor allem niedrige Konzentrationen - gehemmt, was mit einer verminderten Wanderung von Notch2IC-exprimierenden Zellen in den Follikel korreliert war. Nur wenige, allerdings noch funktionale SIGN-R1⁺ Makrophagen, welche beim „Antigen-capturing“ und der darauffolgenden Antigenpresentation eine wichtige Rolle spielen, waren in diesen Mäusen detektierbar. Diese Ergebnisse legen nahe, dass Notch2 Signale die Plasmazellentwicklung treiben, aber dass die Differenzierung gehemmt ist, solange Notch2IC-exprimierende Zellen in der MZ sind. Wir denken, dass eine dauerhafte Lokalisation in der MZ, aufgrund einer möglichen Deregulation des Migrationspotentials Notch2IC-exprimierender Zellen, der Hauptgrund sein könnte, welcher der spontanen Plasmazellbildung *in vivo*, dem defekten Antigentransport von TNP-Ficoll in den Follikel und der verminderten Immunreaktion auf TI Antigene zugrunde liegt. Folglich muss das Notch2 Signal abgeschaltet werden, sobald MZ B-Zellen auf ein Antigen treffen, damit die Migration in den Follikel und somit die Entwicklung zu Plasmazellen stattfinden kann.

Wir haben zudem die TI Immunantwort in Mäusen mit B-Zell-spezifischer Notch2-Defizienz analysiert. Diese Tiere wiesen eine normale Anzahl an SIGN-R1⁺ Makrophagen, sowie intaktes „Antigen-capturing“ auf. Die TI-2-spezifischen Antikörpertiter waren jedoch vermindert, wobei der Antigentransport in den Follikel noch statt fand, obwohl die MZ B-Zellen in diesen Tieren fehlen. Dies könnte darauf hinweisen, dass der Antigentransport nicht unbedingt durch MZ B-Zellen erfolgen muss, aber dass MZ B-Zellen für eine adequate, schnelle Antwort auf TI-2 Antigene benötigt werden.

Ein Teil der alten Notch2IC//CD19Cre^{+/-} Mäuse entwickelte in fortgeschrittenem Alter B-Zelllymphome, wobei die meisten dabei nur leichte oder keine Krankheitszeichen aufwiesen. Dies deutet darauf hin, dass Notch2IC alleine in B-Zellen nicht als starkes Onkogen wirkt, aber höchstwahrscheinlich in fortgeschrittenem Alter zur Entstehung indolenter Lymphomen mit langer Latenzzeit beiträgt.

7. Material

7.1 Mouse strains

I) CD19-*Cre* (Rickert et al., 1997)

BALB/c or C57BL/6 mouse strain with the *Cre* recombinase gene placed into the *cd19* locus, thereby disrupting the *cd19* gene. The expression of the *Cre* gene is regulated by the CD19 promoter.

II) Notch2IC^{#STOP} (Hampel et al., 2011)

BALB/c mouse strain that is conditional transgenic for the *notch2IC* and *human CD2* gene placed into the *rosa26*-locus. A loxP sites-flanked STOP cassette upstream of the *notch2IC* and *human CD2* gene prevents transgene expression. Only in the presence of *Cre*, the STOP cassette is excised and *notch2IC* and *human CD2* are expressed under the control of the very strong CAGGS promoter and an IRES element, respectively.

III) Notch2^{fl/fl} (Besseyrias et al., 2007)

BALB/c mouse strain in which the exons d and e (coding for the C-terminal part of the RAM23 domain and nuclear localisation sequence) of the endogenous *notch2* gene are flanked by loxP sites. Only in the presence of *Cre*, the functional, intracellular part of the endogenous *notch2* gene is excised.

IV) BALB/c

These mice were used to keep the Notch2IC-expressing and Notch2-deficient mouse strains on a pure BALB/c background. If needed BALB/c mice were purchased from The Jackson Laboratory.

7.2 Primer, enzymes and Southern blot DNA probe

Oligonucleotides were all synthesised by Metabion, Martinsried.

Primers for PCR and sequencing reactions:

Primer name	Primer sequence (5' to 3')
CD19c	AACCAGTCAACACCCTTCC
CD19d	CCAGACTAGATACAGACCAG
Cre7	TCAGCTACACCAGAGACGG
Notch2 sense	GAGAAGCAGAGATGAGCAGATA
Notch2 antisense	GTGAGATGTGACACTTCTGAGC
Notch2IC 25 rev	ATCCCGGTCTCCGTATAGTG
Notch2IC 33 fw	CCCTTGCCCTCTATGTACCA
Rosa fw1 (60)	CTCTCCCAAAGTCGCTCTG
Rosa rev2 (62)	TACTCCGAGGCGGATCACAAGC

Restriction endonucleases were purchased from New England BioLabs and MBI Fermentas GmbH. Taq DNA polymerase was purchased from Life Technologies™. Proteinase K was purchased from Sigma-Aldrich.

The DNA probe for Southern blotting binds to a sequence between the J4- and E μ -segment of the mouse IgH locus. It was isolated from the mouse IgH by digestion with the restriction enzymes NaeI and EcoRI. The fragment was cloned into a bluescript-vector and can now be isolated via restriction digest with EcoRI and HindIII from the plasmid (kindly provided by Stefano Casola).

7.3 Antibodies

I) Primary Antibodies for immunoblotting

Antigen	Manufacturer	Source	kDa	Dilution	Diluent
Akt	Cell Signaling	Rabbit	60	1:1000	TBST, 5 % (w/v) BSA
Erk	Cell Signaling	Rabbit	42, 44	1:1000	TBST, 5 % (w/v) BSA
FoxO1	Cell Signaling	Rabbit	78-82	1:1000	TBST, 5 % (w/v) BSA
GAPDH	Calbiochem	Mouse	40	1:10000	TBST, 5 % (w/v) BSA
GSK-3	Cell Signaling	Rabbit	46-51	1:1000	TBST, 5 % (w/v) BSA
Jnk	Cell Signaling	Rabbit	46, 54	1:1000	TBST, 5 % (w/v) BSA
p70	Cell Signaling	Rabbit	70-85	1:1000	TBST, 5 % (w/v) BSA
pAkt (Ser)	Cell Signaling	Rabbit	60	1:1000	TBST, 5 % (w/v) BSA
pErk	Cell Signaling	Rabbit	42, 44	1:1000	TBST, 5 % (w/v) BSA
pGSK-3	Cell Signaling	Rabbit	46-51	1:1000	TBST, 5 % (w/v) BSA
pJnk	Abcam	Rabbit	46, 54	1:500	TBST, 5 % (w/v) BSA
pp70	Cell Signaling	Rabbit	70-85	1:1000	TBST, 5 % (w/v) BSA
PTEN	Cell Signaling	Rabbit	54	1:1000	TBST, 5 % (w/v) BSA
Tcl1B 1/5	Santa Cruz	Goat	14	1:1000	TBST, 5 % (w/v) BSA
Tubulin	Cell Signaling	Mouse	55	1:1000	TBST, 5 % (w/v) BSA

II) Secondary Antibodies for immunoblotting

Antigen	Manufacturer	Source	Dilution	Diluent
Anti-rabbit IgG	Cell Signaling	Goat	1:2000	TBST, 5 % (w/v) milk powder
Anti-mouse IgG	Cell Signaling	Horse	1:2000	TBST, 5 % (w/v) milk powder
Anti-goat/sheep IgG	Sigma-Aldrich	Mouse	1:20000	TBST, 5 % (w/v) milk powder

All secondary antibodies were coupled to horseradish peroxidase.

III) Antibodies for immunohistochemistry and immunofluorescence

Antigen	Manufacturer	Source	Coupled to	Dilution
Mouse CD3	By courtesy of E. Kremmer	Rat	/	1:2
Mouse IgM	Sigma-Aldrich	Goat	Peroxidase	1:100
Mouse MOMA-1	BMA Biomedicals	Rat	/	1:100
Anti-rat IgG2	Jackson Laboratories	Mouse	Biotin	1:250
Anti-rat	Jackson Laboratories	Goat	Alexa Fluor 488	1:100
Mouse SIGN-R1	BMA Biomedicals	Rat	Biotin	1:200
Streptavidin	Life Technologies™	/	Alexa Fluor 594	1:200
Streptavidin	Sigma-Aldrich	/	Alkaline phosphatase	1:400
Anti-TNP	BD Bioscience	Hamster	Pe	1:100

IV) Antibodies for ELISA and ELISPOT

Primary antibodies for ELISAs and ELISPOTs:

IgM, II/41; IgG1, A85-3; IgG3, R2-38 (BD Bioscience).

Concentrations: 0.5 mg/ml

Capture antigen for NP-specific ELISAs and ELISPOTs:

NP_{17/16}-BSA (Biosearch Technologies)

Biotinylated secondary antibodies:

IgM-Bio, R6-60.2; IgG1-Bio, A85-1; IgG3-Bio, R40-82 (BD Bioscience)

Concentrations: 0.5 mg/ml

Detection with Horseradish Peroxidase (HRP) Avidin D (Vector Laboratories)

Isotype controls for ELISAs:

Purified mouse IgM, IgG1 or IgG3 κ isotype control

Concentrations: 0.5 mg/ml

7.4 Software

Adobe Illustrator CS3

Adobe Photoshop CS3

Adobe InDesign CS3

GraphPad Prism 4

Epson Scanner program

Microsoft Excel

Microsoft Word

FlowJo

ImageJ

Axio Vision Zeiss

Glucore Omix Explorer

Pathway Studio

Bead Studio R

8. Methods

8.1 Mice-associated methods

8.1.1 Mouse breeding

Mice carrying the *notch2IC^{ΔSTOP}* allele were crossed to the CD19-*Cre* mouse strain (on a BALB/c or C57BL/6 background) to generate mice (Notch2IC//CD19Cre^{+/-}) expressing the transgene from the pro-B cell stage with a gradual increase in *Cre*-mediated recombination during proceeding B cell differentiation (Rickert et al., 1997). Notch2IC//CD19Cre^{+/+} mice were generated by crossing Notch2IC//CD19Cre^{+/-} to CD19-*Cre* mice. Analyses of the PI3K pathway, of potential lymphoma development in aging mice and in vitro proliferation assays (CFSE) were performed on a mixed background. All other experiments were performed on a pure BALB/c background. Mice carrying the *notch2^{Δin}* allele were crossed to the CD19-*Cre* mouse strain to generate mice with a truncated Notch2 receptor lacking the intracellular signalling domain from the pro-B cell stage on (Notch2^{Δin}//CD19Cre^{+/-}). All analyses with these mice were performed on a pure BALB/c background.

Mice were analysed at eight to 20 weeks of age, unless stated otherwise. Mice that were monitored for the development of lymphomas or leukemic disease were kept under special observation. They were analysed as soon as first signs of illness became noticeable or at the age of 22 months as from this timepoint on the incidence of unspecific, spontaneous tumors increases exponentially. All mice were bred and maintained in specific pathogen-free conditions. All experiments were performed in compliance with the German animal welfare law and have been approved by the Institutional Committee on Animal Experimentation and the government of Upper Bavaria.

8.1.2 Isolation of primary lymphocytes

Mice were euthanised by CO₂ gassing for 5 min and were subsequently dissected. Peritoneal cells were harvested by rinsing the peritoneal cavity with ~8 ml 1 % B cell medium (BCM) (1x RPMI 1640 (Gibco), containing 1 % (v/v) heat-inactivated fetal calf serum (FCS) (PAA Cell culture Company), 1 % (v/v) penicillin streptomycin, 1 % (v/v) sodium pyruvate, 1 % (v/v) L-glutamine, and 52 μM β-mercaptoethanol (all purchased from Gibco)) and aspirating it with a syringe. Spleen and inguinal lymph nodes were taken out as whole organs and were maintained in 1 % BCM on ice until further procedures. To isolate cells from the bone marrow, tibia bones were dissected and cut and the cavity was rinsed with 1 % BCM. To receive single cell suspensions, spleen and lymph nodes were passed through a 70 μm capillary cell strainer (Corning). Single cell suspensions from spleen and bone marrow were depleted from erythrocytes by lysis with the hypotonic 1x RBC lysis buffer (eBioscience) for 3 min at room temperature (RT). Bloody cell suspensions from the peritoneal cavity were discarded completely to ensure that only cells from the peritoneum were analysed. Cells were kept on ice during the entire procedures and were generally centrifuged for 10 min at 300 x g at 4°C in a Rotanta 460 R centrifuge (Hettich Zentrifugen). Isolation of splenic B cells was performed by depletion of CD43⁺ non-B cells by magnetic cell separation (MACS), using α-CD43 beads and LS columns according to the manufacturer's specifications (Miltenyi Biotec). This resulted in a purity of 85 to 95 % B cells.

For subsequent CFSE proliferation assays (8.1.5.2) with sort-purified wild type MZ B cells, splenic cell suspension were not only subjected to depletions of CD43⁺ non-B cells, but in addition also to depletions of the majority of CD23⁺ Fo B cells by using simultaneously α -CD23 beads. By this means, MZ B cells were already pre-purified and enriched prior to sorting, hence leading to a reduction of sorting time as direct sorting was not feasible, as it would have taken too long and hence stressed the cells so that their survival and proliferation in subsequent in vitro cultures and especially CFSE proliferation experiments would have been affected.

8.1.3 Determination of cell numbers

A “Neubauer” counting chamber was used to determine the cell density of obtained cell suspensions from different organs via light microscopy (Zeiss Axio Vert.A1 with phase contrast filter). To this end 10 μ l cell suspension were pre-diluted adequately in 1 % BCM. 10 μ l of this dilution were pipetted into the counting chamber and cells within two to four of the chambers’ big squares were counted. Only cells that appeared round and bright were included. Cell suspension densities were calculated as follows: Mean of counted cells x dilution factor x 10⁴ (counting chamber factor). For cell number determination using trypan blue, cell suspensions were diluted 1:2 in trypan blue (Gibco). 10 μ l of this dilution were then immediately pipetted into the counting chamber and unstained (living) cells were counted.

8.1.4 Freezing of cells

For cell storage for subsequent Southern blot or Western blot analyses, cell pellets containing at least 1x10⁷ cells were washed twice with PBS (Gibco). After discarding PBS, cell pellets were shortly vortexed to loosen cells to avoid clogging in subsequent analyses. Cell pellets were stored at -80°C.

8.1.5 In vitro culture of primary splenic mouse lymphocytes

8.1.5.1 In vitro culture with different stimuli

Cell culture was performed under sterile conditions in a laminar flow (BDK). Cells were grown in an incubator (Binder) at 37°C, 5 % CO₂ and 95 % air humidity. Splenic cells in total or MACS- purified splenic B cells were cultured up to eight days in 10 % BCM (containing 10 % (v/v) FCS) with or without stimuli in 96-well round-bottom (5x10⁵-1x10⁶ cells/well) (Corning) or conical-bottom (1,25x10⁵-4x10⁵ cells/well) plates (Neolab) unless stated otherwise. Stimuli included LPS (50 μ g/ml; E. coli 055:B5; Sigma-Aldrich), IL-4 (10 ng/ml; mouse recombinant; Sigma-Aldrich), α -CD40 antibody (2.5 μ g/ml; eBioscience (HM40-3)). At different time points, cells were subjected to flow cytometrical analyses (see 8.1.6) or to protein isolation for subsequent Western blot analyses (see 8.4).

8.1.5.2 In vitro proliferation (CFSE) assay

For proliferation assays, sort-purified cell populations or MACS-purified splenic B cells were washed with RPMI 1640 and subsequently labeled with RPMI 1640 containing 5- (and 6)-carboxyfluorescein

diacetate N-succinimidyl ester (CFSE, Molecular Probes, final concentration 5 μ M) for 5 min at 37°C (incubator) in a concentration of 5x10⁶ cells/ml. For this, cell pellets were first resuspended with pre-warmed (37°C) RPMI 1640 without CFSE (utilising half of the final volume used for labeling). Then the cell suspension was mixed with a similar volume of RPMI 1640 containing CFSE (double concentrated) and placed into the incubator. CFSE binds to proteins on the inner cell membrane and is consequently transferred equally to each daughter cell upon cell division, leading to declining fluorescence intensity. To stop the labeling reaction, cells were twice abundantly washed with ice-cold 10 % BCM, before resuspending them in 1 ml 10 % BCM. CFSE-labeled cells were cultured for up to five days in 96-well plates (1.25x10⁵ - 5x10⁵ cells/well) in 200 μ l 10 % BCM/well and were analysed by flow cytometry every day. Percents of divided cells (% divided), the proliferation index (number of divisions of cells that underwent at least one division) and division index (average number of cell divisions in total, including cells that never divided) were calculated using the “proliferation platform” of the FlowJo software (BD Biosciences) according to the FlowJo manual.

8.1.6 Flow Cytometry

8.1.6.1 Analysis of murine lymphocytes by flow cytometry

Single cell suspensions prepared from various lymphoid organs or in vitro cultured splenic cells were surface-stained (20 min on ice, protected from light) with a combination of Fitc-, Pe-, PerCP-, APC-, Alexa Fluor 700-, Horizon V450- and Brilliant Violet 421-conjugated monoclonal antibodies, diluted in MACS buffer (Miltenyi Biotec). Antibodies specific for B220, Blimp-1, CD1d, CD2 (human), CD19, CD21, CD23, CD25, CD38, CD80, CD86, CD138, ICAM-1, IgD, IgM, Irf4, S1PR1, Thy1.2-Bio were purchased from BD Biosciences. Prior and after staining, cells were washed with MACS buffer. Measurement on the LSRFortessa™ required filtering of cell suspensions into a FACS tube equipped with a nylon mesh (Corning) before flow cytometrical analyses. Data were analysed from viable, lymphocyte-gated cells as determined from forward and side scatter as well as from TO-PRO-3 iodide, 4',6-Diamidin-2-phenylindol (DAPI), propidiumiodide (PI) or the LIVE/DEAD® Fixable Blue Dead Cell Stain kit (all Life Technologies™), which are all intercalating fluorescent dyes that bind DNA and thus only stain dead cells that are permeable for the dye to diffuse into the nucleus. All analyses were performed on a LSRFortessa™ or a FACSCalibur™ flow cytometer (both from BD Biosciences) and results were analysed using FlowJo software.

8.1.6.2 Intracellular analysis of murine lymphocytes by flow cytometry

Freshly isolated splenic cell suspensions or cells from in vitro cultures were washed with PBS and stained for 30 min at RT or on ice with 1 μ l/ml LIVE/DEAD® Fixable Blue Dead Cell Stain Kit diluted in PBS. This dye ensured that in spite of the subsequent permeabilisation and fixation steps, living and dead cells could still be discriminated from each other later on in the analysis. After a washing step in MACS buffer, surface-staining of cells with a combination of different antibodies (as in 8.1.6.1) was performed. After an additional washing step, cell suspensions were fixed for 15 min at RT with 4 % paraformaldehyde (PFA) (Carl Roth), again followed by two washing steps. Cells were

now either kept in MACS buffer at 4°C light-protected over night and further processed the next day or directly permeabilised by washing them with PBS containing 1 % bovine serum albumin (BSA) (AppliChem) and 0.5 % Saponin (VWR). Staining reactions using antibodies against intracellularly measured factors was performed at RT for 30 to 60 min. These antibodies were conjugated to Fitc, Pe or APC and diluted in PBS/1 % BSA/0.5 % Saponin. Before filtering, cells were washed and resuspended in MACS buffer. Flow cytometrical analyses were done on a LSRFortessa™. All staining steps were performed in darkness.

8.1.6.3 Fluorescence-associated cell sorting (FACS)

The day prior to sorting, 15 ml falcons were filled with pure heat-inactivated FCS and kept at 4°C over night. On the day of the experiment, FCS was tilted, replaced by 1 ml 1 % BCM and falcons were placed in a cooled (4°C) holder of the cell sorter. This procedure assured that cells were collected in cooled 1 % BCM directly after sorting to minimise unspecific cell activation or apoptosis due to stress from a prolonged contact to PBS (sheath fluid of the sorter) and the sorting procedure itself. Single cell suspension from spleens were washed with MACS buffer, surface-stained with a combination of Fitc-, Pe-, PerCP-, APC-conjugated monoclonal antibodies, diluted in MACS buffer. Subsequently, cells were washed and resuspended in 700 - 1500 µl MACS buffer. Prior to sorting, cells were filtered into a FACS tube equipped with a nylon mesh (Corning) to avoid clogging of the cell sorter. Cell sorting procedures were performed in the “purity mode” using a 70 µm nozzle. Only lymphocyte-gated cells as determined from forward and side scatter were sorted. Sorted cell populations were rechecked for their purity by normal flow cytometry analysis on the sorter. In general, a purity between 97 to 98 % of lymphocyte-gated cells was obtained. All cell sorting experiments were performed on a FACS AriaIIIu™ (BD Biosciences). For sort-purifications of wild type and Notch2IC-expressing MZ B cells for subsequent CFSE proliferation experiments, splenic cell suspensions of 12 wild type and three Notch2IC//CD19Cre^{+/±} mice on average were pooled to be able to gain enough MZ B cells for in vitro cultures.

8.1.7 T cell-independent immunisation of mice

Mice at the age of eight to 16 weeks were immunised with 2.5 - 50 µg NP-LPS or 50 µg TNP-/NP-Ficoll (all Biosearch Technologies). NP-LPS antigen stocks were quickly centrifuged before usage and the supernatant was transferred to a new tube to remove any precipitation. Finally, desired amounts of each antigen was resuspended in 200 or 100 µl sterile PBS for intraperitoneal or intravenous injections.

8.1.8 Enzyme-linked immunosorbent assay (ELISA)

To determine concentrations of secreted antibodies in sera or cell culture supernatants with a certain antigen specificity and/or a certain immunoglobulin isotype, blood serum or cell culture supernatants were collected and ELISAs were performed.

8.1.8.1 Preparation of serum from murine blood

On living mice, blood was collected from the caudal mouse vein using a glass capillary (Hirschmann-Laborgeräte). When dissecting mice seven or 14 days after immunisation or in regular analyses without immunisation, blood was directly collected from the heart with a pipette. The blood was incubated on ice for at least three hours and subsequently centrifuged at 9.000 x g and 4°C for 10 min in a microcentrifuge (Eppendorf, 5417 R). The supernatant was transferred to a new reaction tube and the procedure was repeated once to guarantee pure serum. Serum was rapidly frozen at -80°C to avoid any antibody degradation.

8.1.8.2 Preparation of cell culture supernatant for ELISA

After four to eight days of cell culture, cells were centrifuged for 10 min at 4°C and 300 x g. Supernatants were carefully transferred into a new reaction tube and subsequently immediately frozen at -80°C to avoid any antibody degradation.

8.1.8.3 Detection of specific standard immunoglobulin titers

Maxisorb 96-well plates (Nunc) were coated over night at 4°C with 5 µg/ml of immunoglobulin isotype-specific rat α -mouse antibodies (depending on the isotype: IgM, II/41; IgG1, A85-3; IgG3, R2-38, all from BD Bioscience), diluted in 0.1 M NaHCO₃ (pH 9.2). All the following procedures were performed at RT. Wells were blocked with PBS, 1 % (w/v) milk powder (Carl Roth) solution for 60 min. Subsequently, cell culture supernatant (always diluted 1:2) or different dilutions of serum (both diluted in 1 % (w/v) milk powder solution) were applied to the wells and incubated for 60 min, then incubated 30 min with 1 µg/ml biotin-conjugated secondary antibodies specific for the different antibody isotypes (depending on the isotype: IgM-Bio, R6-60.2; IgG1-Bio, A85-1; IgG3-Bio, R40-82, all from BD Bioscience), followed by a 60 min incubation with 2.5 µg/ml Horseradish Peroxidase (HRP) Avidin D (Vector Laboratories), diluted in 0.1 M NaHCO₃ (pH 9.2). The amount of bound HRP was detected by incubation with o-phenylenediamine dihydrochloride (Sigma-Aldrich) in 0.1 M citric acid buffer (0.1 M citric acid, 0.1 M Tris) containing 0.015 % (v/v) H₂O₂ that serves as substrate for the reaction. Following each incubation step, plates were washed three times with PBS. The absorbance was determined at 405 nm, using a microplate reader (Photometer Sunrise RC, Tecan) and antibody concentrations were determined by comparing them with isotype-specific standards (IgM, G155-228; IgG1, MOPC-31-C; IgG3, A112-3).

8.1.8.4 Detection of NP-specific immunoglobulin titers

NP-specific immunoglobulin titers of different isotypes were determined by NP-specific ELISA with the same procedure as described above, but using NP₁₇-BSA as capture antigen. Plates were therefore coated over night at 4°C with 5 µg/ml NP₁₇-BSA (Biosearch Technologies) to detect NP-specific IgG1, IgM and IgG3 antibodies, respectively.

8.1.9 Enzyme-linked immunosorbent spot (ELISPOT) assay

ELISPOT assays were performed to visualise and enumerate small numbers of B cells secreting antigen-specific antibodies. Until the day of ELISPOT development, all steps were undertaken under sterile conditions using a laminar flow. Membranes of ELISPOT plates (Merck Millipore) were either coated with 5 µg/ml immunoglobulin isotype-specific antibodies (as in 8.1.8.3) or with 25 µg/ml NP₁₇-BSA as capture antigen (see 8.1.8.4) or with PBS containing sterile 25 µg/ml BSA (NEB) as control at 4°C over night. The next day plates were washed three times with sterile PBS and incubated for at least 2 h at 37°C with 10 % BCM. Blocking solution was tilted and cells were disseminated in different densities into the wells and cultured for 1.5 - 2 days at 37°C in 200 µl 10 % BCM. Antibodies that are being produced during these days are now directly captured and immobilised on the ELISPOT membrane after being secreted by the activated B cell. At the desired timepoint, cells were discarded, ELISPOT plates were washed six times with PBST (PBS containing 0.025 % Tween20 (Carl Roth) and incubated for 2 h at 37°C with 1 µg/ml biotin-conjugated secondary antibodies specific for the different antibody isotypes (as in 8.1.8.3) diluted in PBS with 1 % BSA (AppliChem). Plates were again washed six times with PBST and subsequently incubated with 2.5 µg/ml Horseradish Peroxidase (HRP) Avidin D diluted in PBS with 1 % BSA for 45 min (max. 1 h) at RT and light-protected. Prior to development plates were washed three times with PBST and three times with PBS. DAB (3,3'-diaminobenzidine) solution (highly cancerogenic!) was prepared by dissolving one tablet (Sigma-Aldrich) in 5 ml bidest. water. Plates were then incubated with DAB solution for ~5 min until brown spots were visible. DAB solution was carefully discarded, plates were thoroughly rinsed with bidest. water and finally air-dried. Now, each spot that developed during the assay represents a single antibody-secreting cell. Hence, ELISPOT assays yield qualitative (type of immune protein) as well as quantitative (number of responding cells) information.

8.1.10 Immunohistochemistry and Immunofluorescence

Spleens were embedded in O.C.T. Tissue Tek (Sakura) and were frozen on dry-ice. Embedded organs were stored at -20°C, wrapped in aluminum foil to avoid air contact. Sections of 8 µm in thickness were cut, using a cryostat (Leica Microsystems) and were air-dried over night. Sections were fixed for 10 min in 100 % (v/v) acetone. Subsequently, slides were dried for ~5 min at RT again, excessive Tissue Tek was removed with a scalpel and sections were surrounded with a Pap-Pen to keep buffers and antibody solutions on the tissue later on. Sections were incubated with PBS for 5 min, with quenching buffer (PBS containing 10 % (v/v) goat serum, 1 % (w/v) BSA) for 20 min to block non-specific binding sites. Afterwards, sections were incubated for each 15 min in two different blocking buffers (Avidin/Biotin Blocking Kit; Vector Laboratories). Between procedures for blocking, sections were washed for 5 min in PBS, whereas before and after labeling procedures, sections were washed with PBS, each three times for 5 min. Subsequently, labeling was performed by incubating sections with different antibodies and streptavidin-conjugated alkaline phosphatase (SA-AP) (Sigma-Aldrich), diluted in PBS/1 % BSA, each for 1 h. Antibodies conjugated to streptavidin were detected in blue using Blue Alkaline Phosphatase Substrate Kit III (Vector Laboratories). Antibodies conjugated to peroxidase were stained in red due

to a reaction with 3-amino-9-ethylcarbazole (AEC) after treatment with the Peroxidase Substrate Kit AEC (Vector Laboratories). Staining reactions were stopped submerging sections in PBS. All incubation and washing steps were performed at RT in a wet chamber. Sections were air-dried and subsequently embedded in gelatin or ProLong® Gold antifade reagent (Life Technologies™) before a coverslip was put on top. Slides were inspected and pictures were obtained using light (Axioskop equipped with an AxioCam Mrc5, Zeiss) or fluorescent microscopy (Axiovert 200 M equipped with an AxioCam MRm, Zeiss). Pictures were edited using Adobe Photoshop software.

8.2 DNA-related techniques

8.2.1 DNA isolation

8.2.1.1 Isolation of genomic DNA from murine tails

DNA was isolated from each analysed mouse for subsequent genotyping to be able to differentiate between control and transgenic mice. For this, DNA from small pieces of murine tails was isolated according to a slightly modified procedure derived from Laird (Laird et al., 1991). A small piece of murine tail was incubated shaking either over night (o.n.) or for 3 h at 56°C in 500 µl lysis buffer (100 mM Tris/HCl pH 8, 5 mM EDTA, 0.2 % (w/v) SDS, 200 mM NaCl) with 100 µg/ml (o.n.) or 200 µg/ml (3 h) proteinase K. 170 µl of a saturated (> 5 M) NaCl solution were added to the samples to precipitate proteins, followed by a centrifugation step (10 min, 4°C, 10.000 x g). The supernatant was transferred into a new reaction tube. DNA was then precipitated by adding 600 µl 100 % (v/v) isopropyl alcohol and inverting reaction tubes. Samples were again centrifuged as described above. Subsequently, the supernatant was removed and the DNA was washed once by adding 1 ml 70 % (v/v) ethanol, air-dried afterwards, and ultimately dissolved in 100 µl TE (10 mM Tris/HCl pH 8, 1 mM EDTA pH 8) by shaking for several hours at 37°C.

8.2.1.2 Isolation of genomic DNA from primary murine lymphocytes

Frozen cell pellets containing $\sim 1 \times 10^7$ cells were thawed and shortly vortexed subsequently to loosen cells. Cells were then incubated shaking over night at 56°C in 1 ml lysis buffer (see 8.2.1.1) containing 200 µg/ml proteinase K. Precipitation of proteins with NaCl was performed as in 8.2.1.1. Subsequently, the 1 ml supernatant was transferred into a new reaction. 500 µl of it were mixed with 500 µl 100 % isopropyl alcohol respectively and successively centrifuged (see 8.2.1.1) within the same tube to precipitate the DNA. Supernatant was discarded, DNA pellets were washed with 1 ml 70 % (v/v) ethanol, air-dried afterwards and dissolved in 50 µl TE by shaking for several hours at 37°C.

8.2.2 DNA analysis

8.2.2.1 Polymerase Chain Reaction (PCR)

For genotyping of transgenic mice, PCR (Saiki et al., 1985; Saiki et al., 1988) was applied to amplify and to detect specific regions in the DNA obtained from their tail DNA. PCRs were always performed

in thermal cyclers (Biometra). Following reaction mixture (primers from Metabion, DMSO from Carl Roth, residual components from Thermo Scientific) was used in different variations:

Reaction batch	1x	Reaction cycle
Taq (10x) buffer	2.5 μ l	Starting temperature 95°C 5'
MgCl ₂ (50 mM)	1 or 1.5 μ l	Cyclic denaturation 95°C 45"
dNTP mixture (10 mM)	0.5 μ l	Cyclic annealing 55-63°C 45"
Primer sense	0.1 or 0.25 μ l	Cyclic elongation 72°C 1-2'
Primer antisense	0.1 or 0.25 μ l	Final elongation 72°C 10'
TaqPol (5 U/ μ l)	0.15 μ l	Cooling to 10°C
DNA (about 5 ng)	1-1.5 μ l	# cycles 30-35
DMSO (100 %)	0.25 μ l	
H ₂ O	to 25 μ l	

8.2.2.2 Agarose gel electrophoresis of DNA

Agarose gel electrophoresis was performed according to (Sambrook and Russell, 2000), to determine the yield of a DNA isolation or PCR reaction. Gels contained 1x TAE (40 mM Tris/HCl, 20 mM acetic acid, 1 mM EDTA pH 8.5), 5 μ g/ml ethidium bromide, and 1.5 - 2 % (w/v) agarose (Biozym). Electrophoresis was performed in a gel electrophoresis chamber (PEQLAB Biotechnologie GmbH) with 1x TAE buffer at 90 to 100 V for one to two hours.

8.2.3 Southern blotting (Southern et al., 1997)

This method was used for the identification of mono- or polyclonality of potential tumor cells. Thereby, electrophoretically separated DNA is transferred from an agarose gel to a nitrocellulose membrane, and the hybridisation of a radioactively labeled DNA probe to the denatured DNA on the membrane allows the detection of specific DNA fragments as definite bands on the membrane.

8.2.3.1 Restriction digest of genomic DNA

Genomic DNA from primary splenic lymphocytes was digested by specific enzymes for the subsequent performance of a Southern blot. The restriction buffer mix (1 mM Spermidin, 1 mM DTT, 100 μ g/ml BSA, 50 μ g/ml RNase, enzyme specific buffer, 50 U of the respective enzyme) was added to DNA from primary lymphocytes dissolved in TE buffer. Digestion took place at 37°C for 16 hours.

8.2.3.2 Gelelectrophoresis and blotting

After digestion as described in 8.2.3.1, the samples were electrophoretically separated on a 0.8 % (w/v) agarose gel together with a standard 1 kb DNA ladder (Life Technologies™) overnight. Having recorded the separated DNA and standard in the gel on a UV luminescent screen together with a ruler, the gel was incubated in 0.25 M HCl for 25 min to fragment the DNA. To equilibrate the gel

for the following DNA transfer, the gel was shortly rinsed in water and subsequently incubated for 40 min in alkaline transfer buffer (0.4 M NaOH, 0.6 M NaCl) to denature the DNA. Afterwards, the DNA was blotted from the gel to a nylon membrane (Immobilon™ Ny+ membrane, Millipore) o.n. from top to bottom by capillary pressure of the transfer buffer. After transfer, the slots of the gel were marked on the membrane with a soft pencil and the membrane was rinsed shortly in 2x SSC (0.3 M NaCl, 0.03 M NaCitrate, pH 6.5) for neutralisation. Then, DNA was cross-linked to the membrane by baking for one hour at 80°C.

8.2.3.3 Hybridisation & detection

In order to prevent unspecific binding, the 2x SSC-wetted membrane was pre-hybridised in pre-heated hybridisation solution (1 M NaCl, 50 mM Tris, pH 7.5, 10 % (w/v) dextran sulfate, 1 % (w/v) SDS, 250 µg salmon sperm DNA/ml) for at least six hours at 65°C, before incubation with the radioactively labeled probe. Applying Random Prime Labeling Kit (GE Healthcare) according to manufacturer's instructions, 50 ng DNA probe were labeled with 50 µCi α^{32} -dCTP (Hartmann Analytic). Subsequently, the labeled probe fraction was separated from the non-incorporated nucleotides using a G50 sephadex column (GE Healthcare) according to manufacturer's specifications. For denaturation, the probe was incubated for five minutes at 100°C and was quenched for 2 min on ice. The membrane was incubated over night at 65°C in the hybridisation solution, containing pre-hybridisation buffer with labeled probe. Afterwards, the membrane was rinsed three times each for 10 min in pre-heated washing buffer (0.5x SSC, 0.5 % (w/v) SDS) at 60°C to wash off unbound probe. Washing was stopped when radioactivity reached 150 counts. Radioactivity was visualised by autoradiography, using radiosensitive films (Biomax MS PE Applied Biosystems 35x43 cm, KODAK), exposed for one day at -80°C in a Biomax cassette.

8.3 RNA-related techniques

8.3.1 Isolation & quantification of total RNA

Total RNA from sort-purified B cell populations of interest (see 8.1.6.3) was isolated directly after sorting using the peqGOLD Trifast™ reagent according to manufacturer's specifications (PEQLAB Biotechnologie GmbH). Briefly, up to 1×10^6 sort-purified, splenic cells were centrifuged (10 min at $300 \times g$ at 4°C) and the supernatant was removed. As resuspension of cell pellets before lysis with the peqGOLD Trifast™ reagent was critical for subsequent RNA isolation, a small amount (~50 µl) of supernatant (not more than 10 % of the reagent's volume) was spared and used for cell pellet resuspension. Subsequently, cells were lysed by applying 1 ml peqGOLD Trifast™ reagent, followed by quick and vigorous mixing by pipetting. Probes were incubated for 5 min at RT. Chloroform (200 µl/1 ml reagent) was added and probes were shaken for 15 sec, followed by an additional incubation step of 6 min at RT. After separating the aqueous phase (RNA) from the phenol-chloroform phase (proteins) and interphase (DNA) by centrifugation (5 min, $12.000 \times g$, RT), the aqueous phase was transferred into a new reaction tube. RNA was precipitated by applying 100 % (w/v) isopropyl alcohol (500 µl/1 ml reagent). Probes were inverted and incubated for 10 min on ice, followed by

centrifugation at 12.000 x g for 10 min at 4°C. RNA pellets were washed two times with 75 % (w/v) ethanol (10 min, 12.000 x g, 4°C) and then air-dried. As complete drying drastically reduces the solubility of RNA, pellets were monitored during drying and nuclease-free water (Ambion[®]) was added as soon as no ethanol residues were visible anymore. RNA was dissolved by passing the solution several times through a pipette tip and incubating it for 10 min at 56 to 60°C. After an immediate first determination of the RNA quantity using a nanophotometer (see paragraph below), aliquots (~2 µl) of each RNA sample - needed for later Bioanalyzer analyses - were transferred into new reaction tubes. Subsequently, original RNA samples and respective aliquots were stored at -80°C. As repeated freeze-thaw cycles would affect RNA integrity, the generation of specific aliquots for later Bioanalyzer analyses assured that original RNA samples would only have to be thawed once on the day of cRNA amplification.

To determine and calculate RNA concentration, its absorbance at 260 nm was measured utilising a nanophotometer (Nanodrop 2000, Thermo Fisher Scientific). The ratio of the readings at 260 and 280 nm (OD260/OD280) provides an estimation of the purity of the RNA preparation, with respect to contaminants that absorb UV, such as proteins. Pure RNA has an OD260/OD280 ratio of ~1.8. RNA that was prepared for subsequent microarray experiments was additionally controlled for its quantity, quality and integrity by capillary gel electrophoresis using the RNA 6000 Nano Kit (Agilent Technologies) on an Agilent 2100 Bioanalyzer (Agilent Technologies) according to the manufacturer's specifications. Only RNA samples with a RNA integrity number (RIN) greater than seven and with a graph clearly pointing to an intact, not contaminated RNA (see 3.1.1, Fig. 12) were further utilised.

8.3.2 cRNA synthesis

Total RNA of the B cell populations of interest was labeled and linearly amplified to cRNA in a commercial form of the classical procedure by Eberwine (Van Gelder et al., 1990). cRNA was synthesised using the Illumina[®] TotalPrep[™] RNA Amplification Kit according to manufacturer's specifications (Life Technologies[™]). All kit reagents (except enzymes) were thawed at RT and mixed thoroughly before use. RNA and kit reagents were kept on ice during the whole procedure unless stated otherwise. All centrifugation steps undertaken during purification were performed at 10,000 x g at RT.

First strand cDNA synthesis by reverse transcription

A maximum volume of 11 µl total RNA (50 to 500 ng) was transferred into a nonstick, sterile, RNase-free, 0.5 ml microcentrifuge tube (Life Technologies[™]). If necessary nuclease-free water was added to bring all samples to 11 µl. 9 µl of Reverse Transcription Master Mix was added to each RNA sample. Samples were mixed thoroughly by pipetting up and down, placed in a thermal cycler (Biometra) and incubated for 2 h at 42°C. Samples were then immediately placed on ice.

Reverse Transcription Master Mix (for a single 20 µl reaction)	
Amount	Component
1 µl	T7 Oligo(dT) Primer
2 µl	10x First Strand Buffer
4 µl	dNTP Mix
1 µl	RNase Inhibitor
1 µl	ArrayScript (reverse transcriptase)

Second strand cDNA synthesis

80 µl of well mixed Second Strand Master Mix were added to each sample. Samples were mixed thoroughly and placed for 2 h into a thermal cycler at 16°C. The lid of the thermal cycler was disabled before and was not completely closed as a lid temperature over RT would inhibit the reaction. Samples were subsequently immediately placed on ice again.

Second Strand Master Mix (for a single 100 µl reaction)	
Amount	Component
63 µl	Nuclease-free water
10 µl	10x Second Strand Buffer
4 µl	dNTP Mix
2 µl	DNA polymerase
1 µl	RNase H

cDNA purification

Nuclease-free water (Life Technologies™) (at least 20 µl/sample) was preheated to 55°C before starting with the purification. 250 µl cDNA Binding Buffer were added to each sample. Samples were mixed, transferred to the center of the cDNA Filter Cartridges (placed within a washing tube) and centrifuged for 1 min. Flow-through was discarded and each filter was replaced into its washing tube. 500 µl of Washing Buffer was added to the filters followed by a centrifugation step of 1 min again. Flow-through was tilted and filters including their washing tube were additionally centrifuged for 1 min. Filters were then transferred to cDNA Elution Tubes and 20 µl of preheated, nuclease-free water were applied to the center of the filters. Samples were now left at RT for 2 min and finally centrifuged for 1 min to obtain the double-stranded cDNA within the eluate.

cRNA synthesis by in vitro transcription

cDNA probes (~17.5 µl) were again transferred into nonstick, sterile, RNase-free, 0.5 ml microcentrifuge tubes and 7.5 µl of the well mixed In Vitro Transcription (IVT) Master Mix was pipetted to each sample. Probes were mixed and incubated for 14 h at 37°C within a thermal cycler (lid temperature 100°C). Subsequently samples were placed on ice and mixed with 75 µl nuclease-free water.

IVT Master Mix (for a single 25 µl reaction)	
Amount	Component
2.5 µl	T7 10x Reaction Buffer
2.5 µl	T7 Enzyme Mix
2.5 µl	Biotin-NTP Mix

cRNA purification

Nuclease-free water (at least 200 µl/sample) was preheated to 55°C before starting with the purification. 350 µl cRNA Binding Buffer were intermixed with each cRNA sample. Afterwards 250 µl 100 % (v/v) ethanol were mixed by pipetting (NOT vortexing!) with the samples until a homogenous, clear solution was achieved. Each probe was directly transferred to a cRNA Filter Cartridge within a cRNA Collection Tube and centrifuged for 1 min. Flow-through was discarded, filters replaced in their collection tubes and 650 µl Wash Buffer were applied to them. After two additional centrifugation steps for 1 min, filters were placed into a new collection tube. 200 µl of preheated, nuclease-free water were applied to the center of the filters, which were then incubated for 10 min at 55°C in a heat block. In the end, filters were centrifuged for 2 min to obtain the cRNA within 200 µl of eluate. As for total RNA, quantity and quality of cRNA was determined by measuring its absorbance at 260 nm with a nanophotometer (Nanodrop 2000, Thermo Fisher Scientific) and by capillary gel electrophoresis using the RNA 6000 Nano Kit (Agilent Technologies) on an Agilent 2100 Bioanalyzer (Agilent Technologies) according to the manufacturer's specifications. As only 1.5 µg cRNA in a maximum volume of 10 µl RNA-free water (Ambion[®]) can be loaded onto an Illumina array, cRNA sample volumes were if necessary downsized by evaporation using a vacuum centrifuge (Eppendorf).

8.3.3 Micoarray-based gene expression profiling

Samples containing 1.5 µg labeled cRNA were hybridised onto the whole mouse genome gene expression microarray "Illumina MouseWG-6 v2.0 Expression BeadChip Kit". These BeadChips consist of oligonucleotides immobilised to beads held in microwells on the surface of an array substrate. The labelled RNA strand is hybridised to these beads on the BeadChip containing the complementary gene-specific sequence. The following hybridisation, washing and signal detection steps were performed in cooperation with Dr. Peter Weber from the MPI of Psychiatry and according to the Illumina "WGGEX Direct Hybridization Assay Guide 11322355A". Utilised buffers and BeadChip-specific devices were purchased from Illumina unless stated otherwise. Sample randomisation and alternate processing between the experimental groups was applied in order to avoid technical bias to be correlated with group comparisons.

Hybridisation

The hybridisation oven was set to 58°C. HYB and HCB buffers were heated to 58°C for 10 min in this oven, cooled down to RT and thoroughly mixed before use. BeadChips were removed from cold storage and equilibrated to RT for 10 min. 200 µl of HCB buffer were pipetted into the humidifying buffer reservoirs of the Hyb Chamber. Only reservoirs containing BeadChips later on were filled with buffer. cRNA probes were brought to a volume of 10 µl either by adding nuclease-free water or by vacuum centrifugation (see 8.3.2 cRNA purification). They were incubated for 5 min at 65°C, shortly vortexed, pulse centrifuged at 250 x g and allowed to cool to RT. Subsequently 20 µl of HYB buffer were added to the probes. BeadChips were unpacked and placed into the Hyb Chambers. cRNA probes (now 30 µl) were carefully pipetted onto the center of each inlet port of the BeadChips

thereby avoiding air bubbles. The Hyb Chamber was then placed into the hybridisation oven (58°C with rocking platform inside) according to Illumina instructions and incubated rocking slowly (speed 5) at least 14 h but not more than 20 h. 500 ml 1x High-Temp Wash Buffer were added to a Hybex Waterbath insert sitting within a Hybex Heating Base and warmed to 55°C over night.

Washing steps

The next day, BeadChips were removed from the Hyb Chamber and submerged face up at the bottom of a Pyrex No. 3140 beaker containing 1 liter of Wash E1BC buffer. Within the buffer BeadChips were consecutively freed from their coverseals and transitionally placed into a slide rack within a glass jar containing 250 ml Wash E1BC buffer. Subsequently the slide rack containing all BeadChips was transferred into the preheated (55°C) Hybex Waterbath containing the 1x High-Temp Wash Buffer and incubated for 10 min. Afterwards BeadChips were thoroughly washed by plunging them 5 to 10 times into fresh Wash E1BC buffer (250 ml) and shaking them for 5 min at RT on an orbital-shaker at medium speed. The rack was now plunged 5 to 10 times into 250 ml 100 % (v/v) ethanol and shaken for 10 min at RT on an orbital-shaker at medium speed. BeadChips were placed back into the glass jar with the Wash E1BC buffer and shaken for 2 min at RT again.

Blocking

BeadChip Wash Trays containing 4 ml Block E1 buffer were placed on a rocker mixer. BeadChips were transferred face up into the wash trays thereby ensuring that they are completely covered with buffer and rocked at medium speed for 10 min at RT.

Signal detection

Cy3-Streptavidin (1 mg/ml) was removed from cold storage and equilibrated to RT for 10 min. 2 ml of Block E1 buffer containing Cy3-Streptavidin (dilution 1:1000) were prepared for each BeadChip and were poured into BeadChip Wash Trays. BeadChips were now transferred into the Block E1 buffer with Cy3-Streptavidin ensuring that BeadChips are covered in it. Wash trays were covered with a lid and rocked at medium speed for 10 min at RT. BeadChips were then submerged in a rack placed in 250 ml Wash E1BC buffer and shaken for 5 min at RT on an orbital-shaker at medium speed. Afterwards the rack with the BeadChips was immediately centrifuged at 1.400 rpm for 4 min at RT. Once BeadChips were dry they were stored in darkness and scanned within one hour of the final RT washing step.

BeadChip imaging (performed by Dr. Peter Weber, MPI of Psychiatry)

Microrrays were scanned and intensity extractions were computed using a BeadArray Reader (Illumina) via the BeadScan Software (Version 3.7.9) with activated internal outlier detection and a scan factor of 1 (PMT = 478; PMTFactor = 1). The extracted bead summary data provides gene expression levels from 45281 array features per sample. Quality control (QC) of microarray data was based on visual inspection of scan images, data distributions, internal Illumina controls, pairwise scatterplots and statistical outlier detection of samples.

Microarray data processing and statistical analysis (in cooperation with Dr. Peter Weber, MPI of Psychiatry)

For the samples fulfilling QC criteria, bead summary scan data were filtered (background removal) for detected probes with p-detection < 0.05 in at least three samples in the whole data set. 20242 variables remained and were VSN (Variance Stabilising Normalisation) transformed and normalised using the bioconductor R package “beadarray” (The R Project for Statistical Computing, R version 2.15.1, (Dunning et al., 2007)). Hierarchical clustering was also performed in R using the “stats” package. Volcano plots were also generated in R. Normalised and filtered data were imported into Qlucore Omics Explorer 2.3 (Qlucore) for exploration of batch effects and for inference testing. Principal component analysis (PCA) was used to identify batch effects and artefacts according to correlations of the sample structure with putative confounders. PCA is a common multivariate technique for finding patterns in data sets comprising high dimensions. The central idea is to reduce the dimensionality of a data set consisting of a large number of interrelated variables (in our case genes), while retaining as much as possible of the existing variation. This is achieved by transforming to a new set of variables, the so called principal components, which are uncorrelated, and which are ordered so that the first few (in our case the first three principal components) retain most of the variation present in all of the original variables (Jolliffe, 2002). So by this means most of the information is extracted from the data set and represented by the principal components. In PCA graphs each point represents one sample and its distance to other points reflects its similarity or difference to the other samples (Abdi and Williams, 2010). For inference testing and the subsequent generation of lists with differentially regulated genes, variables (individual microarray probes) were further filtered for variance (variance > 0.05). Subsequent, statistical tests of microarray data are based on two group comparisons using ANOVA. A mild technical bias was removed by using bead chip-id amplification rounds as co-variate in ANOVA. For comparisons among CD19Cre[±] samples paired tests were applied, whereas for the other comparisons unpaired tests were performed. To control for false positive rates due to multiple testing the Benjamini-Hochberg procedure was used for correction of the p-values, thereby obtaining the Benjamini-Hochberg based FDR-analogue q-values. Annotation of microarray probes was done by using the manufacturer’s annotation file (MouseWG-6_V2_0_R2_11278593_A.bgx).

Microarray data analysis - Functional Annotation

For functional annotation of the differentially regulated genes the “Functional Annotation Clustering” tool of the DAVID (**D**atabase for **A**nnotation, **V**isualization and **I**ntegrated **D**iscovery) Bioinformatics Resources 6.7 was used. Gene lists of interests were submitted to DAVID by using the Illumina_ID as identifier and the “MouseWG-6_V2_0_R2_11278593_A” as background (provided by DAVID software). Subsequently the “Functional Annotation Clustering” tool was selected and performed. Classification stringencies were set to “high” unless stated otherwise.

8.4 Protein detection

8.4.1 Protein isolation & quantification

Following MACS purification, ex vivo isolated B cells were rested for one hour in 1 % BCM at 37°C before proteins were isolated. In vitro cultured B cells were directly subjected to the protein isolation procedure. Cells were washed twice with ice-cold PBS before protein extraction. To prepare whole-cell extracts, 20 µl of 2x NP40 lysis buffer (100 mM Tris pH 7.4, 300 mM NaCl, 4 mM EDTA, 2 % (v/v) NP40) containing freshly added phosphatase inhibitors (Halt phosphatase inhibitor cocktail, Pierce) and protease inhibitors (Mini Complete, Roche Diagnostics) were added to a pellet of 5x10⁶ B cells without resuspension and reaction tubes were mixed on a vortexer at 4°C for 20 min. Cell debris and DNA was separated from the protein supernatant by centrifugation at maximum speed for 15 min at 4°C. Protein samples were subsequently frozen at -80°C. Protein concentration of protein samples was measured by using a Bradford reagent (DC protein assay; Bio-Rad) according to manufacturer's instructions and a BSA in standard slope.

8.4.2 SDS polyacrylamide gel electrophoresis (PAGE)

Protein mixtures were separated by discontinuous SDS PAGE (Laemmli, 1970). In discontinuous PAGE, the acrylamide gel is composed of a stacking gel (5 % (v/v) acrylamide, 0.625 mM Tris pH 6.8, 0.1 % (w/v) SDS, 0.1 % (w/v) APS, 0.006 % (w/v) TEMED), in which negatively charged proteins are focused at the separation line, and a resolving gel (10 to 12 % (v/v) acrylamide, 3.75 mM Tris pH 6.8, 0.1 % (w/v) SDS, 0.1 % (w/v) APS, 0.004 % (w/v) TEMED), in which proteins are separated according to molecular weight. 5x Laemmli buffer (300 mM Tris pH 6.8, 7.5 % (w/v) SDS, 50 % (v/v) glycerin, 0.01 % (v/v) bromphenol blue, 1 % (v/v) β-mercaptoethanol) was added to the samples to a concentration of 1x before heating the samples at 70°C for 10 min and loading denatured proteins onto a SDS polyacrylamide gel together with a protein standard (Benchmark™, Invitrogen). Electrophoresis was accomplished in Laemmli running buffer (25 mM Tris base, 0.2 M glycine, 0.1 % (v/v) SDS) for at least 30 min at 30 V (stacking gel) and after that at up to 100 V (resolving gel), using a Bio-Rad electrophoresis chamber.

8.4.3 Western blotting

After having separated proteins by SDS PAGE, proteins were transferred onto a polyvinylidene-fluoride (PVDF) membrane by using electrical current (Western blotting, (Towbin et al., 1979). Proteins were blotted to the PVDF membrane (Immobilon™ P membrane, Millipore) by wet transfer over night at 80 mA per gel in transfer buffer (25 mM Tris base, 0.2 M glycine, 20 % (v/v) methanol), utilising a Bio-Rad mini tank blotting chamber on a magnetic stirrer in the cold room. To verify protein transfer and equal loading, the membrane was incubated for 5 min in Ponceau S solution (Sigma-Aldrich) to stain proteins non-specifically.

8.4.4 Immunostaining

Non-specific binding sites were blocked by incubating membranes at RT in TBST (0.1 M Tris/HCl pH 7.5, 0.1 M NaCl, 0.02 % (v/v) Tween20), containing 5 % (w/v) BSA, for several hours with slight shaking. Incubation with the primary antibody was performed over night at 4°C in TBST, containing 5 % (w/v) BSA, unless stated otherwise. The membrane was incubated with the secondary antibody, conjugated to HRP, diluted in TBST, containing 1 - 5 % (w/v) milk powder, for two hours at RT. Antibody incubation was always performed on a roller and the membranes were washed three times in between and afterwards with TBST for 7 min with vigorous shaking. Proteins were visualised using Enhanced Chemiluminescence ECLTM (GE Healthcare) according to manufacturer's instructions. Signals were detected by the exposition of photosensitive films (CEA RP new) using a Cawomat 2000 IR processor (both ErnstChristiansen). For reprobing with further antibodies, bound antibodies were stripped from the membrane by incubating in stripping buffer (62.5 mM Tris/HCl pH 6.8, 2 % (w/v) SDS, 100 mM β -mercaptoethanol) at 56°C for 30 min slightly shaking.

8.4.5 Western blot quantification

Films (Agfa Healthcare) were scanned with an Epson Expression-1680Pro scanner. For Western blot quantification by densitometry, films were scanned in transmission mode with off-switched automatic gain control. A reference film was generated by creating an exposure series with the use of defined light quantities. All films (including reference film) were scanned using identical scanning conditions. The reference film ensured that only Western blot bands within the dynamic range of the film and scanner were quantified. Thus, this reference assured that only films on which signals of the respective proteins were not overexposed were used for densitometry. Images were quantified with ImageJ 1.43 (NIH) according to the tutorial on www.lukemiller.org "Analyzing gels and Western blots with ImageJ" using the "area under the curve" values. The ration between the "area" of the analysed protein and the "area" of the reference protein (in this work GSK-3) were generated and used for further calculations.

8.5 Statistics

Two-tailed Student *t*-test was calculated using GraphPad Prism 4 software and was applied to determine the significance of splenic weight values, cell numbers, antibody titers, percentages and absolute numbers of flow cytometrically analysed cell populations and ratios of signal intensities from immunoblotting.

9. References

- Abdi H, Williams L, 2010. Principal component analysis. *Wiley Interdisciplinary Reviews: Computational Statistics* 2: 433-459.
- Aichele P, Zinke J, Grode L, Schwendener RA, Kaufmann SH, Seiler P, 2003. Macrophages of the splenic marginal zone are essential for trapping of blood-borne particulate antigen but dispensable for induction of specific T cell responses. *J. Immunol.* 171: 1148-1155.
- Alberi L, Hoey SE, Brai E, Scotti AL, Marathe S, 2013. Notch signaling in the brain: in good and bad times. *Ageing Res. Rev.* 12: 801-814.
- Allman D, Calamito M, 2009. Instructing B cell fates on the fringe. *Immunity.* 30: 175-177.
- Allman D, Karnell FG, Punt JA, Bakkour S, Xu L, Myung P, Koretzky GA, Pui JC, Aster JC, Pear WS, 2001a. Separation of Notch1 promoted lineage commitment and expansion/transformation in developing T cells. *J. Exp. Med.* 194: 99-106.
- Allman D, Lindsley RC, DeMuth W, Rudd K, Shinton SA, Hardy RR, 2001b. Resolution of three nonproliferative immature splenic B cell subsets reveals multiple selection points during peripheral B cell maturation. *J. Immunol.* 167: 6834-6840.
- Allman D, Pillai S, 2008. Peripheral B cell subsets. *Curr. Opin. Immunol.* 20: 149-157.
- Alugupalli KR, Leong JM, Woodland RT, Muramatsu M, Honjo T, Gerstein RM, 2004. B1b lymphocytes confer T cell-independent long-lasting immunity. *Immunity.* 21: 379-390.
- Arnon TI, Horton RM, Grigorova IL, Cyster JG, 2013. Visualization of splenic marginal zone B-cell shuttling and follicular B-cell egress. *Nature* 493: 684-688.
- Aster JC, Pear WS, Blacklow SC, 2008. Notch signaling in leukemia. *Annu. Rev. Pathol.* 3: 587-613.
- Auguin D, Barthe P, Royer C, Stern MH, Noguchi M, Arold ST, Roumestand C, 2004. Structural basis for the co-activation of protein kinase B by T-cell leukemia-1 (TCL1) family proto-oncoproteins. *J. Biol. Chem.* 279: 35890-35902.
- Avalos AM, Ploegh HL, 2014. Early BCR Events and Antigen Capture, Processing, and Loading on MHC Class II on B Cells. *Front Immunol.* 5: 92.
- Balazs M, Martin F, Zhou T, Kearney J, 2002. Blood dendritic cells interact with splenic marginal zone B cells to initiate T-independent immune responses. *Immunity.* 17: 341-352.
- Basso K, Klein U, Niu H, Stolovitzky GA, Tu Y, Califano A, Cattoretti G, la-Favera R, 2004. Tracking CD40 signaling during germinal center development. *Blood* 104: 4088-4096.
- Batista FD, Harwood NE, 2009. The who, how and where of antigen presentation to B cells. *Nat. Rev. Immunol.* 9: 15-27.
- Batten M, Groom J, Cachero TG, Qian F, Schneider P, Tschopp J, Browning JL, Mackay F, 2000. BAFF mediates survival of peripheral immature B lymphocytes. *J. Exp. Med.* 192: 1453-1466.
- Bekeredjian-Ding I, Jegu G, 2009. Toll-like receptors--sentries in the B-cell response. *Immunology* 128: 311-323.

References

- Bellavia D, Campese AF, Alesse E, Vacca A, Felli MP, Balestri A, Stoppacciaro A, Tiveron C, Tatangelo L, Giovarelli M, Gaetano C, Ruco L, Hoffman ES, Hayday AC, Lendahl U, Frati L, Gulino A, Screpanti I, 2000. Constitutive activation of NF-kappaB and T-cell leukemia/lymphoma in Notch3 transgenic mice. *EMBO J.* 19: 3337-3348.
- Bendelac A, Bonneville M, Kearney JF, 2001. Autoreactivity by design: innate B and T lymphocytes. *Nat. Rev. Immunol.* 1: 177-186.
- Bergtold A, Desai DD, Gavhane A, Clynes R, 2005. Cell surface recycling of internalized antigen permits dendritic cell priming of B cells. *Immunity.* 23: 503-514.
- Besseyrias V, Fiorini E, Strobl LJ, Zimmer-Strobl U, Dumortier A, Koch U, Arcangeli ML, Ezine S, MacDonald HR, Radtke F, 2007. Hierarchy of Notch-Delta interactions promoting T cell lineage commitment and maturation. *J. Exp. Med.* 204: 331-343.
- Birjandi SZ, Ippolito JA, Ramadorai AK, Witte PL, 2011. Alterations in marginal zone macrophages and marginal zone B cells in old mice. *J. Immunol.* 186: 3441-3451.
- Blaumueller CM, Qi H, Zagouras P, rtavanis-Tsakonas S, 1997. Intracellular cleavage of Notch leads to a heterodimeric receptor on the plasma membrane. *Cell* 90: 281-291.
- Bolos V, Grego-Bessa J, de la Pompa JL, 2007. Notch signaling in development and cancer. *Endocr. Rev.* 28: 339-363.
- Bray SJ, 2006. Notch signalling: a simple pathway becomes complex. *Nat. Rev. Mol. Cell Biol.* 7: 678-689.
- Buhl AM, Pleiman CM, Rickert RC, Cambier JC, 1997. Qualitative regulation of B cell antigen receptor signaling by CD19: selective requirement for PI3-kinase activation, inositol-1,4,5-trisphosphate production and Ca²⁺ mobilization. *J. Exp. Med.* 186: 1897-1910.
- Cancro MP, 2009. Signalling crosstalk in B cells: managing worth and need. *Nat. Rev. Immunol.* 9: 657-661.
- Cariappa A, Boboila C, Moran ST, Liu H, Shi HN, Pillai S, 2007a. The recirculating B cell pool contains two functionally distinct, long-lived, posttransitional, follicular B cell populations. *J. Immunol.* 179: 2270-2281.
- Cariappa A, Chase C, Liu H, Russell P, Pillai S, 2007b. Naive recirculating B cells mature simultaneously in the spleen and bone marrow. *Blood* 109: 2339-2345.
- Cariappa A, Liou HC, Horwitz BH, Pillai S, 2000. Nuclear factor kappa B is required for the development of marginal zone B lymphocytes. *J. Exp. Med.* 192: 1175-1182.
- Cariappa A, Tang M, Parnig C, Nebelitskiy E, Carroll M, Georgopoulos K, Pillai S, 2001. The follicular versus marginal zone B lymphocyte cell fate decision is regulated by Aiolos, Btk, and CD21. *Immunity.* 14: 603-615.
- Carrasco YR, Batista FD, 2007. B cells acquire particulate antigen in a macrophage-rich area at the boundary between the follicle and the subcapsular sinus of the lymph node. *Immunity.* 27: 160-171.
- Carter RH, Doody GM, Bolen JB, Fearon DT, 1997. Membrane IgM-induced tyrosine phosphorylation of CD19 requires a CD19 domain that mediates association with components of the B cell antigen receptor complex. *J. Immunol.* 158: 3062-3069.

- Casali P, Schettino EW, 1996. Structure and function of natural antibodies. *Curr. Top. Microbiol. Immunol.* 210: 167-179.
- Cerutti A, Cols M, Puga I, 2013. Marginal zone B cells: virtues of innate-like antibody-producing lymphocytes. *Nat. Rev. Immunol.* 13: 118-132.
- Cesta MF, 2006. Normal structure, function, and histology of the spleen. *Toxicol. Pathol.* 34: 455-465.
- Chen Y, Pikkarainen T, Elomaa O, Soininen R, Kodama T, Kraal G, Tryggvason K, 2005. Defective microarchitecture of the spleen marginal zone and impaired response to a thymus-independent type 2 antigen in mice lacking scavenger receptors MARCO and SR-A. *J. Immunol.* 175: 8173-8180.
- Chopin M, Quemeneur L, Ripich T, Jessberger R, 2010. SWAP-70 controls formation of the splenic marginal zone through regulating T1B-cell differentiation. *Eur. J. Immunol.* 40: 3544-3556.
- Chorny A, Puga I, Cerutti A, 2012. Regulation of frontline antibody responses by innate immune signals. *Immunol. Res.* 54: 4-13.
- Chung JB, Silverman M, Monroe JG, 2003. Transitional B cells: step by step towards immune competence. *Trends Immunol.* 24: 343-349.
- Cinamon G, Matloubian M, Lesneski MJ, Xu Y, Low C, Lu T, Proia RL, Cyster JG, 2004. Sphingosine 1-phosphate receptor 1 promotes B cell localization in the splenic marginal zone. *Nat. Immunol.* 5: 713-720.
- Cinamon G, Zachariah MA, Lam OM, Foss FW, Jr., Cyster JG, 2008. Follicular shuttling of marginal zone B cells facilitates antigen transport. *Nat. Immunol.* 9: 54-62.
- Ciofani M, Knowles GC, Wiest DL, von BH, Zuniga-Pflucker JC, 2006. Stage-specific and differential notch dependency at the alphabeta and gammadelta T lineage bifurcation. *Immunity.* 25: 105-116.
- Clayton E, Bardi G, Bell SE, Chantry D, Downes CP, Gray A, Humphries LA, Rawlings D, Reynolds H, Vigorito E, Turner M, 2002. A crucial role for the p110delta subunit of phosphatidylinositol 3-kinase in B cell development and activation. *J. Exp. Med.* 196: 753-763.
- Cyster JG, 2010. B cell follicles and antigen encounters of the third kind. *Nat. Immunol.* 11: 989-996.
- Dammers PM, de Boer NK, Deenen GJ, Nieuwenhuis P, Kroese FG, 1999. The origin of marginal zone B cells in the rat. *Eur. J. Immunol.* 29: 1522-1531.
- Deimling J, Thompson K, Tseu I, Wang J, Keijzer R, Tanswell AK, Post M, 2007. Mesenchymal maintenance of distal epithelial cell phenotype during late fetal lung development. *Am. J. Physiol Lung Cell Mol. Physiol* 292: L725-L741.
- Dorshkind K, Montecino-Rodriguez E, 2007. Fetal B-cell lymphopoiesis and the emergence of B-1-cell potential. *Nat. Rev. Immunol.* 7: 213-219.
- Duchez S, Rodrigues M, Bertrand F, Valitutti S, 2011. Reciprocal polarization of T and B cells at the immunological synapse. *J. Immunol.* 187: 4571-4580.

References

- Dunning MJ, Smith ML, Ritchie ME, Tavare S, 2007. beadarray: R classes and methods for Illumina bead-based data. *Bioinformatics*. 23: 2183-2184.
- Edry E, Melamed D, 2004. Receptor editing in positive and negative selection of B lymphopoiesis. *J. Immunol*. 173: 4265-4271.
- Elgert KD, 2009. *Immunology: Understanding The Immune System*. Wiley-Blackwell.
- Ellisen LW, Bird J, West DC, Soreng AL, Reynolds TC, Smith SD, Sklar J, 1991. TAN-1, the human homolog of the Drosophila notch gene, is broken by chromosomal translocations in T lymphoblastic neoplasms. *Cell* 66: 649-661.
- Ellyard JI, Avery DT, Mackay CR, Tangye SG, 2005. Contribution of stromal cells to the migration, function and retention of plasma cells in human spleen: potential roles of CXCL12, IL-6 and CD54. *Eur. J. Immunol*. 35: 699-708.
- Engel P, Zhou LJ, Ord DC, Sato S, Koller B, Tedder TF, 1995. Abnormal B lymphocyte development, activation, and differentiation in mice that lack or overexpress the CD19 signal transduction molecule. *Immunity*. 3: 39-50.
- Fairfax KA, Corcoran LM, Pridans C, Huntington ND, Kallies A, Nutt SL, Tarlinton DM, 2007. Different kinetics of blimp-1 induction in B cell subsets revealed by reporter gene. *J. Immunol*. 178: 4104-4111.
- Fairfax KA, Kallies A, Nutt SL, Tarlinton DM, 2008. Plasma cell development: from B-cell subsets to long-term survival niches. *Semin. Immunol*. 20: 49-58.
- Ferguson AR, Youd ME, Corley RB, 2004. Marginal zone B cells transport and deposit IgM-containing immune complexes onto follicular dendritic cells. *Int. Immunol*. 16: 1411-1422.
- Fortini C, Cesselli D, Beltrami AP, Bergamin N, Caragnano A, Moretti L, Cecaro F, Aquila G, Rizzo P, Riberti C, Tavazzi L, Fucili A, Beltrami CA, Ferrari R, 2014. Alteration of Notch signaling and functionality of adipose tissue derived mesenchymal stem cells in heart failure. *Int. J. Cardiol*. 174: 119-126.
- Fouillade C, Monet-Lepretre M, Baron-Menguy C, Joutel A, 2012. Notch signalling in smooth muscle cells during development and disease. *Cardiovasc. Res*. 95: 138-146.
- Garcia d, V, Gulbranson-Judge A, Khan M, O'Leary P, Cascalho M, Wabl M, Klaus GG, Owen MJ, MacLennan IC, 1999a. Dendritic cells associated with plasmablast survival. *Eur. J. Immunol*. 29: 3712-3721.
- Garcia d, V, O'Leary P, Sze DM, Toellner KM, MacLennan IC, 1999b. T-independent type 2 antigens induce B cell proliferation in multiple splenic sites, but exponential growth is confined to extrafollicular foci. *Eur. J. Immunol*. 29: 1314-1323.
- Garg V, Muth AN, Ransom JF, Schluterman MK, Barnes R, King IN, Grossfeld PD, Srivastava D, 2005. Mutations in NOTCH1 cause aortic valve disease. *Nature* 437: 270-274.
- Gianfelici V, 2012. Activation of the NOTCH1 pathway in chronic lymphocytic leukemia. *Haematologica* 97: 328-330.

- Gibb DR, El SM, Kang DJ, Rowe WJ, El SR, Cichy J, Yagita H, Tew JG, Dempsey PJ, Crawford HC, Conrad DH, 2010. ADAM10 is essential for Notch2-dependent marginal zone B cell development and CD23 cleavage in vivo. *J. Exp. Med.* 207: 623-635.
- Goodnow CC, Crosbie J, Adelstein S, Lavoie TB, Smith-Gill SJ, Brink RA, Pritchard-Briscoe H, Wotherspoon JS, Loblay RH, Raphael K, ., 1988. Altered immunoglobulin expression and functional silencing of self-reactive B lymphocytes in transgenic mice. *Nature* 334: 676-682.
- Gordon WR, Arnett KL, Blacklow SC, 2008. The molecular logic of Notch signaling--a structural and biochemical perspective. *J. Cell Sci.* 121: 3109-3119.
- Gross JA, Dillon SR, Mudri S, Johnston J, Littau A, Roque R, Rixon M, Schou O, Foley KP, Haugen H, McMillen S, Waggle K, Schreckhise RW, Shoemaker K, Vu T, Moore M, Grossman A, Clegg CH, 2001. TACI-Ig neutralizes molecules critical for B cell development and autoimmune disease. impaired B cell maturation in mice lacking BLyS. *Immunity.* 15: 289-302.
- Guinamard R, Okigaki M, Schlessinger J, Ravetch JV, 2000. Absence of marginal zone B cells in Pyk-2-deficient mice defines their role in the humoral response. *Nat. Immunol.* 1: 31-36.
- Gunn KE, Brewer JW, 2006. Evidence that marginal zone B cells possess an enhanced secretory apparatus and exhibit superior secretory activity. *J. Immunol.* 177: 3791-3798.
- Gururajan M, Jacob J, Pulendran B, 2007. Toll-like receptor expression and responsiveness of distinct murine splenic and mucosal B-cell subsets. *PLoS. One.* 2: e863.
- Haas KM, Poe JC, Steeber DA, Tedder TF, 2005. B-1a and B-1b cells exhibit distinct developmental requirements and have unique functional roles in innate and adaptive immunity to *S. pneumoniae*. *Immunity.* 23: 7-18.
- Haines N, Irvine KD, 2003. Glycosylation regulates Notch signalling. *Nat. Rev. Mol. Cell Biol.* 4: 786-797.
- Hamada Y, Kadokawa Y, Okabe M, Ikawa M, Coleman JR, Tsujimoto Y, 1999. Mutation in ankyrin repeats of the mouse Notch2 gene induces early embryonic lethality. *Development* 126: 3415-3424.
- Hamidi H, Gustafson D, Pellegrini M, Gasson J, 2011. Identification of novel targets of CSL-dependent Notch signaling in hematopoiesis. *PLoS. One.* 6: e20022.
- Hampel F, Ehrenberg S, Hojer C, Draeseke A, Marschall-Schroter G, Kuhn R, Mack B, Gires O, Vahl CJ, Schmidt-Supprian M, Strobl LJ, Zimmer-Strobl U, 2011. CD19-independent instruction of murine marginal zone B-cell development by constitutive Notch2 signaling. *Blood* 118: 6321-6331.
- Han H, Tanigaki K, Yamamoto N, Kuroda K, Yoshimoto M, Nakahata T, Ikuta K, Honjo T, 2002. Inducible gene knockout of transcription factor recombination signal binding protein-J reveals its essential role in T versus B lineage decision. *Int. Immunol.* 14: 637-645.
- Hao Z, Rajewsky K, 2001. Homeostasis of peripheral B cells in the absence of B cell influx from the bone marrow. *J. Exp. Med.* 194: 1151-1164.
- Hardy RR, Hayakawa K, Parks DR, Herzenberg LA, 1983. Demonstration of B-cell maturation in X-linked immunodeficient mice by simultaneous three-colour immunofluorescence. *Nature* 306: 270-272.

References

- Hargreaves DC, Hyman PL, Lu TT, Ngo VN, Bidgol A, Suzuki G, Zou YR, Littman DR, Cyster JG, 2001. A coordinated change in chemokine responsiveness guides plasma cell movements. *J. Exp. Med.* 194: 45-56.
- Hase H, Kanno Y, Kojima M, Hasegawa K, Sakurai D, Kojima H, Tsuchiya N, Tokunaga K, Masawa N, Azuma M, Okumura K, Kobata T, 2004. BAFF/BLyS can potentiate B-cell selection with the B-cell coreceptor complex. *Blood* 103: 2257-2265.
- Haynes NM, Allen CD, Lesley R, Ansel KM, Killeen N, Cyster JG, 2007. Role of CXCR5 and CCR7 in follicular Th cell positioning and appearance of a programmed cell death gene-1high germinal center-associated subpopulation. *J. Immunol.* 179: 5099-5108.
- Helgason CD, Damen JE, Rosten P, Grewal R, Sorensen P, Chappel SM, Borowski A, Jirik F, Krystal G, Humphries RK, 1998. Targeted disruption of SHIP leads to hemopoietic perturbations, lung pathology, and a shortened life span. *Genes Dev.* 12: 1610-1620.
- Hikida M, Johmura S, Hashimoto A, Takezaki M, Kurosaki T, 2003. Coupling between B cell receptor and phospholipase C-gamma2 is essential for mature B cell development. *J. Exp. Med.* 198: 581-589.
- Holodick NE, Vizconde T, Rothstein TL, 2014. Splenic B-1a Cells Expressing CD138 Spontaneously Secrete Large Amounts of Immunoglobulin in Naive Mice. *Front Immunol.* 5: 129.
- Honjo T, Kinoshita K, Muramatsu M, 2002. Molecular mechanism of class switch recombination: linkage with somatic hypermutation. *Annu. Rev. Immunol.* 20: 165-196.
- Hopfer O, Zwahlen D, Fey MF, Aebi S, 2005. The Notch pathway in ovarian carcinomas and adenomas. *Br. J. Cancer* 93: 709-718.
- Hozumi K, Negishi N, Suzuki D, Abe N, Sotomaru Y, Tamaoki N, Mailhos C, Ish-Horowicz D, Habu S, Owen MJ, 2004. Delta-like 1 is necessary for the generation of marginal zone B cells but not T cells in vivo. *Nat. Immunol.* 5: 638-644.
- Hsu MC, Toellner KM, Vinuesa CG, MacLennan IC, 2006. B cell clones that sustain long-term plasmablast growth in T-independent extrafollicular antibody responses. *Proc. Natl. Acad. Sci. U. S. A* 103: 5905-5910.
- Huang NN, Han SB, Hwang IY, Kehrl JH, 2005. B cells productively engage soluble antigen-pulsed dendritic cells: visualization of live-cell dynamics of B cell-dendritic cell interactions. *J. Immunol.* 175: 7125-7134.
- Hubmann R, Schwarzmeier JD, Shehata M, Hilgarth M, Duechler M, Dettke M, Berger R, 2002. Notch2 is involved in the overexpression of CD23 in B-cell chronic lymphocytic leukemia. *Blood* 99: 3742-3747.
- Iwanami A, Cloughesy TF, Mischel PS, 2009. Striking the balance between PTEN and PDK1: it all depends on the cell context. *Genes Dev.* 23: 1699-1704.
- Janeway C, Murphy K, Walport MJ, Travers P, 2012. *Janeway's Immunobiology*. Garland Science, Taylor & Francis Group, LLC.
- Jolliffe IT, 2002. *Principal Component Analysis*.

- Jou ST, Carpino N, Takahashi Y, Piekorz R, Chao JR, Carpino N, Wang D, Ihle JN, 2002. Essential, nonredundant role for the phosphoinositide 3-kinase p110delta in signaling by the B-cell receptor complex. *Mol. Cell Biol.* 22: 8580-8591.
- Jundt F, Anagnostopoulos I, Forster R, Mathas S, Stein H, Dorken B, 2002. Activated Notch1 signaling promotes tumor cell proliferation and survival in Hodgkin and anaplastic large cell lymphoma. *Blood* 99: 3398-3403.
- Jundt F, Probsting KS, Anagnostopoulos I, Muehlinghaus G, Chatterjee M, Mathas S, Bargou RC, Manz R, Stein H, Dorken B, 2004. Jagged1-induced Notch signaling drives proliferation of multiple myeloma cells. *Blood* 103: 3511-3515.
- Jung D, Giallourakis C, Mostoslavsky R, Alt FW, 2006. Mechanism and control of V(D)J recombination at the immunoglobulin heavy chain locus. *Annu. Rev. Immunol.* 24: 541-570.
- Kallies A, Hasbold J, Fairfax K, Pridans C, Emslie D, McKenzie BS, Lew AM, Corcoran LM, Hodgkin PD, Tarlinton DM, Nutt SL, 2007. Initiation of plasma-cell differentiation is independent of the transcription factor Blimp-1. *Immunity.* 26: 555-566.
- Kallies A, Hasbold J, Tarlinton DM, Dietrich W, Corcoran LM, Hodgkin PD, Nutt SL, 2004. Plasma cell ontogeny defined by quantitative changes in blimp-1 expression. *J. Exp. Med.* 200: 967-977.
- Kang YS, Do Y, Lee HK, Park SH, Cheong C, Lynch RM, Loeffler JM, Steinman RM, Park CG, 2006. A dominant complement fixation pathway for pneumococcal polysaccharides initiated by SIGN-R1 interacting with C1q. *Cell* 125: 47-58.
- Kang YS, Kim JY, Bruening SA, Pack M, Charalambous A, Pritsker A, Moran TM, Loeffler JM, Steinman RM, Park CG, 2004. The C-type lectin SIGN-R1 mediates uptake of the capsular polysaccharide of *Streptococcus pneumoniae* in the marginal zone of mouse spleen. *Proc. Natl. Acad. Sci. U. S. A* 101: 215-220.
- Karlsson MC, Guinamard R, Bolland S, Sankala M, Steinman RM, Ravetch JV, 2003. Macrophages control the retention and trafficking of B lymphocytes in the splenic marginal zone. *J. Exp. Med.* 198: 333-340.
- Kidd S, Kelley MR, Young MW, 1986. Sequence of the notch locus of *Drosophila melanogaster*: relationship of the encoded protein to mammalian clotting and growth factors. *Mol. Cell Biol.* 6: 3094-3108.
- Kiel MJ, Velusamy T, Betz BL, Zhao L, Weigelin HG, Chiang MY, Huebner-Chan DR, Bailey NG, Yang DT, Bhagat G, Miranda RN, Bahler DW, Medeiros LJ, Lim MS, Elenitoba-Johnson KS, 2012. Whole-genome sequencing identifies recurrent somatic NOTCH2 mutations in splenic marginal zone lymphoma. *J. Exp. Med.* 209: 1553-1565.
- Klein U, Casola S, Cattoretti G, Shen Q, Lia M, Mo T, Ludwig T, Rajewsky K, la-Favera R, 2006. Transcription factor IRF4 controls plasma cell differentiation and class-switch recombination. *Nat. Immunol.* 7: 773-782.
- Koch U, Lehal R, Radtke F, 2013. Stem cells living with a Notch. *Development* 140: 689-704.
- Koch U, Radtke F, 2007. Notch and cancer: a double-edged sword. *Cell Mol. Life Sci.* 64: 2746-2762.

References

- Kohlhof H, Hampel F, Hoffmann R, Burtscher H, Weidle UH, Holzels M, Eick D, Zimmer-Strobl U, Strobl LJ, 2009. Notch1, Notch2, and Epstein-Barr virus-encoded nuclear antigen 2 signaling differentially affects proliferation and survival of Epstein-Barr virus-infected B cells. *Blood* 113: 5506-5515.
- Kopan R, Ilagan MX, 2009. The canonical Notch signaling pathway: unfolding the activation mechanism. *Cell* 137: 216-233.
- Koppel EA, Litjens M, van dB, V, van KY, Geijtenbeek TB, 2008. Interaction of SIGNR1 expressed by marginal zone macrophages with marginal zone B cells is essential to early IgM responses against *Streptococcus pneumoniae*. *Mol. Immunol.* 45: 2881-2887.
- Koppel EA, van Gisbergen KP, Geijtenbeek TB, van KY, 2005. Distinct functions of DC-SIGN and its homologues L-SIGN (DC-SIGNR) and mSIGNR1 in pathogen recognition and immune regulation. *Cell Microbiol.* 7: 157-165.
- Kraal G, ter HH, Meelhuizen C, Venneker G, Claassen E, 1989. Marginal zone macrophages and their role in the immune response against T-independent type 2 antigens: modulation of the cells with specific antibody. *Eur. J. Immunol.* 19: 675-680.
- Kraus M, Alimzhanov MB, Rajewsky N, Rajewsky K, 2004. Survival of resting mature B lymphocytes depends on BCR signaling via the Igalphabeta heterodimer. *Cell* 117: 787-800.
- Kridel R, Meissner B, Rogic S, Boyle M, Telenius A, Woolcock B, Gunawardana J, Jenkins C, Cochrane C, Ben-Neriah S, Tan K, Morin RD, Opat S, Sehn LH, Connors JM, Marra MA, Weng AP, Steidl C, Gascoyne RD, 2012. Whole transcriptome sequencing reveals recurrent NOTCH1 mutations in mantle cell lymphoma. *Blood* 119: 1963-1971.
- Kuroda K, Han H, Tani S, Tanigaki K, Tun T, Furukawa T, Taniguchi Y, Kurooka H, Hamada Y, Toyokuni S, Honjo T, 2003. Regulation of marginal zone B cell development by MINT, a suppressor of Notch/RBP-J signaling pathway. *Immunity.* 18: 301-312.
- Laemmli UK, 1970. Cleavage of structural proteins during the assembly of the head of bacteriophage T4. *Nature* 227: 680-685.
- Laine J, Kunstle G, Obata T, Sha M, Noguchi M, 2000. The protooncogene TCL1 is an Akt kinase coactivator. *Mol. Cell* 6: 395-407.
- Laird PW, Zijderveld A, Linders K, Rudnicki MA, Jaenisch R, Berns A, 1991. Simplified mammalian DNA isolation procedure. *Nucleic Acids Res.* 19: 4293.
- Lalor PA, Nossal GJ, Sanderson RD, Heyzer-Williams MG, 1992. Functional and molecular characterization of single, (4-hydroxy-3-nitrophenyl)acetyl (NP)-specific, IgG1+ B cells from antibody-secreting and memory B cell pathways in the C57BL/6 immune response to NP. *Eur. J. Immunol.* 22: 3001-3011.
- Lam KP, Kuhn R, Rajewsky K, 1997. In vivo ablation of surface immunoglobulin on mature B cells by inducible gene targeting results in rapid cell death. *Cell* 90: 1073-1083.
- Lanoue A, Clatworthy MR, Smith P, Green S, Townsend MJ, Jolin HE, Smith KG, Fallon PG, McKenzie AN, 2004. SIGN-R1 contributes to protection against lethal pneumococcal infection in mice. *J. Exp. Med.* 200: 1383-1393.

- Lanzavecchia A, 1990. Receptor-mediated antigen uptake and its effect on antigen presentation to class II-restricted T lymphocytes. *Annu. Rev. Immunol.* 8: 773-793.
- Lee SY, Kumano K, Nakazaki K, Sanada M, Matsumoto A, Yamamoto G, Nannya Y, Suzuki R, Ota S, Ota Y, Izutsu K, Sakata-Yanagimoto M, Hangaishi A, Yagita H, Fukayama M, Seto M, Kurokawa M, Ogawa S, Chiba S, 2009. Gain-of-function mutations and copy number increases of Notch2 in diffuse large B-cell lymphoma. *Cancer Sci.* 100: 920-926.
- Leek JT, Scharpf RB, Bravo HC, Simcha D, Langmead B, Johnson WE, Geman D, Baggerly K, Irizarry RA, 2010. Tackling the widespread and critical impact of batch effects in high-throughput data. *Nat. Rev. Genet.* 11: 733-739.
- Lin KI, ngelin-Duclos C, Kuo TC, Calame K, 2002. Blimp-1-dependent repression of Pax-5 is required for differentiation of B cells to immunoglobulin M-secreting plasma cells. *Mol. Cell Biol.* 22: 4771-4780.
- Lin L, Gerth AJ, Peng SL, 2004. Active inhibition of plasma cell development in resting B cells by microphthalmia-associated transcription factor. *J. Exp. Med.* 200: 115-122.
- Lin Y, Wong K, Calame K, 1997. Repression of c-myc transcription by Blimp-1, an inducer of terminal B cell differentiation. *Science* 276: 596-599.
- Lindsley RC, Thomas M, Srivastava B, Allman D, 2007. Generation of peripheral B cells occurs via two spatially and temporally distinct pathways. *Blood* 109: 2521-2528.
- Liubchenko GA, Appleberry HC, Holers VM, Banda NK, Willis VC, Lyubchenko T, 2012. Potentially autoreactive naturally occurring transitional T3 B lymphocytes exhibit a unique signaling profile. *J. Autoimmun.* 38: 293-303.
- Lo CG, Lu TT, Cyster JG, 2003. Integrin-dependence of lymphocyte entry into the splenic white pulp. *J. Exp. Med.* 197: 353-361.
- Logeat F, Bessia C, Brou C, LeBail O, Jarriault S, Seidah NG, Israel A, 1998. The Notch1 receptor is cleaved constitutively by a furin-like convertase. *Proc. Natl. Acad. Sci. U. S. A* 95: 8108-8112.
- Lu TT, Cyster JG, 2002. Integrin-mediated long-term B cell retention in the splenic marginal zone. *Science* 297: 409-412.
- MacLennan IC, Toellner KM, Cunningham AF, Serre K, Sze DM, Zuniga E, Cook MC, Vinuesa CG, 2003. Extrafollicular antibody responses. *Immunol. Rev.* 194: 8-18.
- Maillard I, Tu L, Sambandam A, Yashiro-Ohtani Y, Millholland J, Keeshan K, Shestova O, Xu L, Bhandoola A, Pear WS, 2006. The requirement for Notch signaling at the beta-selection checkpoint in vivo is absolute and independent of the pre-T cell receptor. *J. Exp. Med.* 203: 2239-2245.
- Mak TW, Shahinian A, Yoshinaga SK, Wakeham A, Boucher LM, Pantić M, Duncan G, Gajewska BU, Gronski M, Eriksson U, Odermatt B, Ho A, Bouchard D, Whorisky JS, Jordana M, Ohashi PS, Pawson T, Bladt F, Tafuri A, 2003. Costimulation through the inducible costimulator ligand is essential for both T helper and B cell functions in T cell-dependent B cell responses. *Nat. Immunol.* 4: 765-772.
- Martin F, Kearney JF, 2000. Positive selection from newly formed to marginal zone B cells depends on the rate of clonal production, CD19, and btk. *Immunity.* 12: 39-49.

References

- Martin F, Kearney JF, 2002. Marginal-zone B cells. *Nat. Rev. Immunol.* 2: 323-335.
- Martin F, Oliver AM, Kearney JF, 2001. Marginal zone and B1 B cells unite in the early response against T-independent blood-borne particulate antigens. *Immunity.* 14: 617-629.
- Martins G, Calame K, 2008. Regulation and functions of Blimp-1 in T and B lymphocytes. *Annu. Rev. Immunol.* 26: 133-169.
- McDaniell R, Warthen DM, Sanchez-Lara PA, Pai A, Krantz ID, Piccoli DA, Spinner NB, 2006. NOTCH2 mutations cause Alagille syndrome, a heterogeneous disorder of the notch signaling pathway. *Am. J. Hum. Genet.* 79: 169-173.
- Mebius RE, Kraal G, 2005. Structure and function of the spleen. *Nat. Rev. Immunol.* 5: 606-616.
- Meyer-Bahlburg A, Bandaranayake AD, Andrews SF, Rawlings DJ, 2009. Reduced c-myc expression levels limit follicular mature B cell cycling in response to TLR signals. *J. Immunol.* 182: 4065-4075.
- Minguet S, Dopfer EP, Pollmer C, Freudenberg MA, Galanos C, Reth M, Huber M, Schamel WW, 2008. Enhanced B-cell activation mediated by TLR4 and BCR crosstalk. *Eur. J. Immunol.* 38: 2475-2487.
- Moloney DJ, Panin VM, Johnston SH, Chen J, Shao L, Wilson R, Wang Y, Stanley P, Irvine KD, Haltiwanger RS, Vogt TF, 2000. Fringe is a glycosyltransferase that modifies Notch. *Nature* 406: 369-375.
- Mond JJ, Lees A, Snapper CM, 1995. T cell-independent antigens type 2. *Annu. Rev. Immunol.* 13: 655-692.
- Morgan TH, 1917. The theory of the gene. *The American Naturalist* 51: 527-529.
- Muppidi JR, Arnon TI, Bronevetsky Y, Veerapen N, Tanaka M, Besra GS, Cyster JG, 2011. Cannabinoid receptor 2 positions and retains marginal zone B cells within the splenic marginal zone. *J. Exp. Med.* 208: 1941-1948.
- Nelms K, Keegan AD, Zamorano J, Ryan JJ, Paul WE, 1999. The IL-4 receptor: signaling mechanisms and biologic functions. *Annu. Rev. Immunol.* 17: 701-738.
- Nera KP, Lassila O, 2006. Pax5--a critical inhibitor of plasma cell fate. *Scand. J. Immunol.* 64: 190-199.
- Nicolas M, Wolfer A, Raj K, Kummer JA, Mill P, van NM, Hui CC, Clevers H, Dotto GP, Radtke F, 2003. Notch1 functions as a tumor suppressor in mouse skin. *Nat. Genet.* 33: 416-421.
- Noah TK, Shroyer NF, 2013. Notch in the intestine: regulation of homeostasis and pathogenesis. *Annu. Rev. Physiol* 75: 263-288.
- Northrup DL, Allman D, 2008. Transcriptional regulation of early B cell development. *Immunol. Res.* 42: 106-117.
- Nutt SL, Eberhard D, Horcher M, Rolink AG, Busslinger M, 2001. Pax5 determines the identity of B cells from the beginning to the end of B-lymphopoiesis. *Int. Rev. Immunol.* 20: 65-82.
- O'Neil J, Look AT, 2007. Mechanisms of transcription factor deregulation in lymphoid cell transformation. *Oncogene* 26: 6838-6849.

- Ochiai K, Maienschein-Cline M, Simonetti G, Chen J, Rosenthal R, Brink R, Chong AS, Klein U, Dinner AR, Singh H, Sciammas R, 2013. Transcriptional regulation of germinal center B and plasma cell fates by dynamical control of IRF4. *Immunity*. 38: 918-929.
- Oda T, Elkahoulou AG, Pike BL, Okajima K, Krantz ID, Genin A, Piccoli DA, Meltzer PS, Spinner NB, Collins FS, Chandrasekharappa SC, 1997. Mutations in the human Jagged1 gene are responsible for Alagille syndrome. *Nat. Genet.* 16: 235-242.
- Okkenhaug K, Bilancio A, Farjot G, Priddle H, Sancho S, Peskett E, Pearce W, Meek SE, Salpekar A, Waterfield MD, Smith AJ, Vanhaesebroeck B, 2002. Impaired B and T cell antigen receptor signaling in p110delta PI 3-kinase mutant mice. *Science* 297: 1031-1034.
- Oliver AM, Grimaldi JC, Howard MC, Kearney JF, 1999a. Independently ligating CD38 and Fc gammaRIIB relays a dominant negative signal to B cells. *Hybridoma* 18: 113-119.
- Oliver AM, Martin F, Kearney JF, 1999b. IgM^{high}CD21^{high} lymphocytes enriched in the splenic marginal zone generate effector cells more rapidly than the bulk of follicular B cells. *J. Immunol.* 162: 7198-7207.
- Oracki SA, Walker JA, Hibbs ML, Corcoran LM, Tarlinton DM, 2010. Plasma cell development and survival. *Immunol. Rev.* 237: 140-159.
- Otero DC, Omori SA, Rickert RC, 2001. Cd19-dependent activation of Akt kinase in B-lymphocytes. *J. Biol. Chem.* 276: 1474-1478.
- Oyama T, Harigaya K, Muradil A, Hozumi K, Habu S, Oguro H, Iwama A, Matsuno K, Sakamoto R, Sato M, Yoshida N, Kitagawa M, 2007. Mastermind-1 is required for Notch signal-dependent steps in lymphocyte development in vivo. *Proc. Natl. Acad. Sci. U. S. A* 104: 9764-9769.
- Palomero T, Lim WK, Odom DT, Sulis ML, Real PJ, Margolin A, Barnes KC, O'Neil J, Neuberg D, Weng AP, Aster JC, Sigaux F, Soulier J, Look AT, Young RA, Califano A, Ferrando AA, 2006. NOTCH1 directly regulates c-MYC and activates a feed-forward-loop transcriptional network promoting leukemic cell growth. *Proc. Natl. Acad. Sci. U. S. A* 103: 18261-18266.
- Pape KA, Catron DM, Itano AA, Jenkins MK, 2007. The humoral immune response is initiated in lymph nodes by B cells that acquire soluble antigen directly in the follicles. *Immunity*. 26: 491-502.
- Paus D, Phan TG, Chan TD, Gardam S, Basten A, Brink R, 2006. Antigen recognition strength regulates the choice between extrafollicular plasma cell and germinal center B cell differentiation. *J. Exp. Med.* 203: 1081-1091.
- Pear WS, Aster JC, Scott ML, Hasserjian RP, Soffer B, Sklar J, Baltimore D, 1996. Exclusive development of T cell neoplasms in mice transplanted with bone marrow expressing activated Notch alleles. *J. Exp. Med.* 183: 2283-2291.
- Peng SL, 2005. Signaling in B cells via Toll-like receptors. *Curr. Opin. Immunol.* 17: 230-236.
- Pereira JP, Kelly LM, Cyster JG, 2010. Finding the right niche: B-cell migration in the early phases of T-dependent antibody responses. *Int. Immunol.* 22: 413-419.
- Perrimon N, Pitsouli C, Shilo BZ, 2012. Signaling mechanisms controlling cell fate and embryonic patterning. *Cold Spring Harb. Perspect. Biol.* 4: a005975.

References

- Perumalsamy LR, Nagala M, Banerjee P, Sarin A, 2009. A hierarchical cascade activated by non-canonical Notch signaling and the mTOR-Rictor complex regulates neglect-induced death in mammalian cells. *Cell Death. Differ.* 16: 879-889.
- Pezzutto A, Dorken B, Rabinovitch PS, Ledbetter JA, Moldenhauer G, Clark EA, 1987. CD19 monoclonal antibody HD37 inhibits anti-immunoglobulin-induced B cell activation and proliferation. *J. Immunol.* 138: 2793-2799.
- Phan TG, Grigorova I, Okada T, Cyster JG, 2007. Subcapsular encounter and complement-dependent transport of immune complexes by lymph node B cells. *Nat. Immunol.* 8: 992-1000.
- Pillai S, Cariappa A, 2009. The follicular versus marginal zone B lymphocyte cell fate decision. *Nat. Rev. Immunol.* 9: 767-777.
- Pillai S, Cariappa A, Moran ST, 2005. Marginal zone B cells. *Annu. Rev. Immunol.* 23: 161-196.
- Porta C, Paglino C, Mosca A, 2014. Targeting PI3K/Akt/mTOR Signaling in Cancer. *Front Oncol.* 4: 64.
- Puga I, Cols M, Barra CM, He B, Cassis L, Gentile M, Comerma L, Chorny A, Shan M, Xu W, Magri G, Knowles DM, Tam W, Chiu A, Bussel JB, Serrano S, Lorente JA, Bellosillo B, Lloreta J, Juanpere N, Alameda F, Baro T, de Heredia CD, Toran N, Catala A, Torrebadell M, Fortuny C, Cusi V, Carreras C, Diaz GA, Blander JM, Farber CM, Silvestri G, Cunningham-Rundles C, Calvillo M, Dufour C, Notarangelo LD, Lougaris V, Plebani A, Casanova JL, Ganal SC, Diefenbach A, Arostegui JI, Juan M, Yague J, Mahlaoui N, Donadieu J, Chen K, Cerutti A, 2012. B cell-helper neutrophils stimulate the diversification and production of immunoglobulin in the marginal zone of the spleen. *Nat. Immunol.* 13: 170-180.
- Pui JC, Allman D, Xu L, DeRocco S, Karnell FG, Bakkour S, Lee JY, Kadesch T, Hardy RR, Aster JC, Pear WS, 1999. Notch1 expression in early lymphopoiesis influences B versus T lineage determination. *Immunity.* 11: 299-308.
- Qi H, Egen JG, Huang AY, Germain RN, 2006. Extrafollicular activation of lymph node B cells by antigen-bearing dendritic cells. *Science* 312: 1672-1676.
- Radbruch A, Muehlinghaus G, Luger EO, Inamine A, Smith KG, Dorner T, Hiepe F, 2006. Competence and competition: the challenge of becoming a long-lived plasma cell. *Nat. Rev. Immunol.* 6: 741-750.
- Radtke F, Fasnacht N, MacDonald HR, 2010. Notch signaling in the immune system. *Immunity.* 32: 14-27.
- Radtke F, Wilson A, Mancini SJ, MacDonald HR, 2004. Notch regulation of lymphocyte development and function. *Nat. Immunol.* 5: 247-253.
- Radtke F, Wilson A, Stark G, Bauer M, van MJ, MacDonald HR, Aguet M, 1999. Deficient T cell fate specification in mice with an induced inactivation of Notch1. *Immunity.* 10: 547-558.
- Ramirez J, Lukin K, Hagman J, 2010. From hematopoietic progenitors to B cells: mechanisms of lineage restriction and commitment. *Curr. Opin. Immunol.* 22: 177-184.
- Randall TD, Heath AW, Santos-Argumedo L, Howard MC, Weissman IL, Lund FE, 1998. Arrest of B lymphocyte terminal differentiation by CD40 signaling: mechanism for lack of antibody-secreting cells in germinal centers. *Immunity.* 8: 733-742.

- Reif K, Ekland EH, Ohl L, Nakano H, Lipp M, Forster R, Cyster JG, 2002. Balanced responsiveness to chemoattractants from adjacent zones determines B-cell position. *Nature* 416: 94-99.
- Reljic R, Wagner SD, Peakman LJ, Fearon DT, 2000. Suppression of signal transducer and activator of transcription 3-dependent B lymphocyte terminal differentiation by BCL-6. *J. Exp. Med.* 192: 1841-1848.
- Rickert RC, Rajewsky K, Roes J, 1995. Impairment of T-cell-dependent B-cell responses and B-1 cell development in CD19-deficient mice. *Nature* 376: 352-355.
- Rickert RC, Roes J, Rajewsky K, 1997. B lymphocyte-specific, Cre-mediated mutagenesis in mice. *Nucleic Acids Res.* 25: 1317-1318.
- Rohn JL, Luring AS, Linenberger ML, Overbaugh J, 1996. Transduction of Notch2 in feline leukemia virus-induced thymic lymphoma. *J. Virol.* 70: 8071-8080.
- Rosati E, Sabatini R, Rampino G, Tabilio A, Di IM, Fettucciari K, Bartoli A, Coaccioli S, Screpanti I, Marconi P, 2009. Constitutively activated Notch signaling is involved in survival and apoptosis resistance of B-CLL cells. *Blood* 113: 856-865.
- Rossi D, Trifonov V, Fangazio M, Brusca A, Rasi S, Spina V, Monti S, Vaisitti T, Arruga F, Fama R, Ciardullo C, Greco M, Cresta S, Piranda D, Holmes A, Fabbri G, Messina M, Rinaldi A, Wang J, Agostinelli C, Piccaluga PP, Lucioni M, Tabbo F, Serra R, Franceschetti S, Deambrogi C, Daniele G, Gattei V, Marasca R, Facchetti F, Arcaini L, Inghirami G, Bertoni F, Pileri SA, Deaglio S, Foa R, la-Favera R, Pasqualucci L, Rabadan R, Gaidano G, 2012. The coding genome of splenic marginal zone lymphoma: activation of NOTCH2 and other pathways regulating marginal zone development. *J. Exp. Med.* 209: 1537-1551.
- Roy M, Pear WS, Aster JC, 2007. The multifaceted role of Notch in cancer. *Curr. Opin. Genet. Dev.* 17: 52-59.
- Rui L, Healy JI, Blasioli J, Goodnow CC, 2006. ERK signaling is a molecular switch integrating opposing inputs from B cell receptor and T cell cytokines to control TLR4-driven plasma cell differentiation. *J. Immunol.* 177: 5337-5346.
- Rui L, Vinuesa CG, Blasioli J, Goodnow CC, 2003. Resistance to CpG DNA-induced autoimmunity through tolerogenic B cell antigen receptor ERK signaling. *Nat. Immunol.* 4: 594-600.
- Saiki RK, Gelfand DH, Stoffel S, Scharf SJ, Higuchi R, Horn GT, Mullis KB, Erlich HA, 1988. Primer-directed enzymatic amplification of DNA with a thermostable DNA polymerase. *Science* 239: 487-491.
- Saiki RK, Scharf S, Faloona F, Mullis KB, Horn GT, Erlich HA, Arnheim N, 1985. Enzymatic amplification of beta-globin genomic sequences and restriction site analysis for diagnosis of sickle cell anemia. *Science* 230: 1350-1354.
- Saito T, Chiba S, Ichikawa M, Kunisato A, Asai T, Shimizu K, Yamaguchi T, Yamamoto G, Seo S, Kumano K, Nakagami-Yamaguchi E, Hamada Y, Aizawa S, Hirai H, 2003. Notch2 is preferentially expressed in mature B cells and indispensable for marginal zone B lineage development. *Immunity.* 18: 675-685.
- Samardzic T, Gerlach J, Muller K, Marinkovic D, Hess J, Nitschke L, Wirth T, 2002. CD22 regulates early B cell development in BOB.1/OBF.1-deficient mice. *Eur. J. Immunol.* 32: 2481-2489.

References

- Sambrook J, Russell DW, 2000. *Molecular Cloning: A Laboratory Manual*, 3rd ed., vol. 3. Cold Spring Harbour Laboratory Press, New York.
- Santos MA, Sarmiento LM, Rebelo M, Doce AA, Maillard I, Dumortier A, Neves H, Radtke F, Pear WS, Parreira L, Demengeot J, 2007. Notch1 engagement by Delta-like-1 promotes differentiation of B lymphocytes to antibody-secreting cells. *Proc. Natl. Acad. Sci. U. S. A* 104: 15454-15459.
- Sasaki Y, Derudder E, Hobeika E, Pelanda R, Reth M, Rajewsky K, Schmidt-Supprian M, 2006. Canonical NF-kappaB activity, dispensable for B cell development, replaces BAFF-receptor signals and promotes B cell proliferation upon activation. *Immunity*. 24: 729-739.
- Satpathy S, Shenoy GN, Kaw S, Vaidya T, Bal V, Rath S, George A, 2010. Inhibition of terminal differentiation of B cells mediated by CD27 and CD40 involves signaling through JNK. *J. Immunol.* 185: 6499-6507.
- Schebesta A, McManus S, Salvaggio G, Delogu A, Busslinger GA, Busslinger M, 2007. Transcription factor Pax5 activates the chromatin of key genes involved in B cell signaling, adhesion, migration, and immune function. *Immunity*. 27: 49-63.
- Schiemann B, Gommerman JL, Vora K, Cachero TG, Shulga-Morskaya S, Dobles M, Frew E, Scott ML, 2001. An essential role for BAFF in the normal development of B cells through a BCMA-independent pathway. *Science* 293: 2111-2114.
- Sciammas R, Davis MM, 2004. Modular nature of Blimp-1 in the regulation of gene expression during B cell maturation. *J. Immunol.* 172: 5427-5440.
- Sciammas R, Shaffer AL, Schatz JH, Zhao H, Staudt LM, Singh H, 2006. Graded expression of interferon regulatory factor-4 coordinates isotype switching with plasma cell differentiation. *Immunity*. 25: 225-236.
- Sha WC, Liou HC, Tuomanen EI, Baltimore D, 1995. Targeted disruption of the p50 subunit of NF-kappa B leads to multifocal defects in immune responses. *Cell* 80: 321-330.
- Shaffer AL, Lin KI, Kuo TC, Yu X, Hurt EM, Rosenwald A, Giltnane JM, Yang L, Zhao H, Calame K, Staudt LM, 2002. Blimp-1 orchestrates plasma cell differentiation by extinguishing the mature B cell gene expression program. *Immunity*. 17: 51-62.
- Shaffer AL, Shapiro-Shelef M, Iwakoshi NN, Lee AH, Qian SB, Zhao H, Yu X, Yang L, Tan BK, Rosenwald A, Hurt EM, Petroulakis E, Sonenberg N, Yewdell JW, Calame K, Glimcher LH, Staudt LM, 2004. XBP1, downstream of Blimp-1, expands the secretory apparatus and other organelles, and increases protein synthesis in plasma cell differentiation. *Immunity*. 21: 81-93.
- Shaffer AL, Yu X, He Y, Boldrick J, Chan EP, Staudt LM, 2000. BCL-6 represses genes that function in lymphocyte differentiation, inflammation, and cell cycle control. *Immunity*. 13: 199-212.
- Shapiro-Shelef M, Calame K, 2005. Regulation of plasma-cell development. *Nat. Rev. Immunol.* 5: 230-242.
- Sheng Y, Yahata T, Negishi N, Nakano Y, Habu S, Hozumi K, Ando K, 2008. Expression of Delta-like 1 in the splenic non-hematopoietic cells is essential for marginal zone B cell development. *Immunol. Lett.* 121: 33-37.
- Shlomchik MJ, Weisel F, 2012. Germinal centers. *Immunol. Rev.* 247: 5-10.

- Simonetti G, Carette A, Silva K, Wang H, De Silva NS, Heise N, Siebel CW, Shlomchik MJ, Klein U, 2013. IRF4 controls the positioning of mature B cells in the lymphoid microenvironments by regulating NOTCH2 expression and activity. *J. Exp. Med.* 210: 2887-2902.
- Smith KG, Hewitson TD, Nossal GJ, Tarlinton DM, 1996. The phenotype and fate of the antibody-forming cells of the splenic foci. *Eur. J. Immunol.* 26: 444-448.
- Song R, Kim YW, Koo BK, Jeong HW, Yoon MJ, Yoon KJ, Jun DJ, Im SK, Shin J, Kong MP, Kim KT, Yoon K, Kong YY, 2008. Mind bomb 1 in the lymphopoietic niches is essential for T and marginal zone B cell development. *J. Exp. Med.* 205: 2525-2536.
- South AP, Cho RJ, Aster JC, 2012. The double-edged sword of Notch signaling in cancer. *Semin. Cell Dev. Biol.* 23: 458-464.
- Southern EM, Milner N, Mir KU, 1997. Discovering antisense reagents by hybridization of RNA to oligonucleotide arrays. *Ciba Found. Symp.* 209: 38-44.
- Srivastava B, Quinn WJ, III, Hazard K, Erikson J, Allman D, 2005. Characterization of marginal zone B cell precursors. *J. Exp. Med.* 202: 1225-1234.
- Stein KE, 1992. Thymus-independent and thymus-dependent responses to polysaccharide antigens. *J. Infect. Dis.* 165 Suppl 1: S49-S52.
- Strobl LJ, Hofelmayr H, Marschall G, Brielmeier M, Bornkamm GW, Zimmer-Strobl U, 2000. Activated Notch1 modulates gene expression in B cells similarly to Epstein-Barr viral nuclear antigen 2. *J. Virol.* 74: 1727-1735.
- Suzuki A, Kaisho T, Ohishi M, Tsukio-Yamaguchi M, Tsubata T, Koni PA, Sasaki T, Mak TW, Nakano T, 2003. Critical roles of Pten in B cell homeostasis and immunoglobulin class switch recombination. *J. Exp. Med.* 197: 657-667.
- Suzuki K, Grigorova I, Phan TG, Kelly LM, Cyster JG, 2009. Visualizing B cell capture of cognate antigen from follicular dendritic cells. *J. Exp. Med.* 206: 1485-1493.
- Suzuki K, Maruya M, Kawamoto S, Sitnik K, Kitamura H, Agace WW, Fagarasan S, 2010. The sensing of environmental stimuli by follicular dendritic cells promotes immunoglobulin A generation in the gut. *Immunity.* 33: 71-83.
- Swanson CL, Wilson TJ, Strauch P, Colonna M, Pelanda R, Torres RM, 2010. Type I IFN enhances follicular B cell contribution to the T cell-independent antibody response. *J. Exp. Med.* 207: 1485-1500.
- Sze DM, Toellner KM, Garcia d, V, Taylor DR, MacLennan IC, 2000. Intrinsic constraint on plasmablast growth and extrinsic limits of plasma cell survival. *J. Exp. Med.* 192: 813-821.
- Tafuri A, Shahinian A, Bladt F, Yoshinaga SK, Jordana M, Wakeham A, Boucher LM, Bouchard D, Chan VS, Duncan G, Odermatt B, Ho A, Itie A, Horan T, Whoriskey JS, Pawson T, Penninger JM, Ohashi PS, Mak TW, 2001. ICOS is essential for effective T-helper-cell responses. *Nature* 409: 105-109.
- Takuwa N, Du W, Kaneko E, Okamoto Y, Yoshioka K, Takuwa Y, 2011. Tumor-suppressive sphingosine-1-phosphate receptor-2 counteracting tumor-promoting sphingosine-1-phosphate receptor-1 and sphingosine kinase 1 - Jekyll Hidden behind Hyde. *Am. J. Cancer Res.* 1: 460-481.

References

- Tan JB, Xu K, Cretegnny K, Visan I, Yuan JS, Egan SE, Guidos CJ, 2009. Lunatic and manic fringe cooperatively enhance marginal zone B cell precursor competition for delta-like 1 in splenic endothelial niches. *Immunity*. 30: 254-263.
- Tanigaki K, Han H, Yamamoto N, Tashiro K, Ikegawa M, Kuroda K, Suzuki A, Nakano T, Honjo T, 2002. Notch-RBP-J signaling is involved in cell fate determination of marginal zone B cells. *Nat. Immunol.* 3: 443-450.
- Tarakhovsky A, 1997. Antigen receptor signalling in B cells. *Res. Immunol.* 148: 457-460.
- Teague BN, Pan Y, Mudd PA, Nakken B, Zhang Q, Szodoray P, Kim-Howard X, Wilson PC, Farris AD, 2007. Cutting edge: Transitional T3 B cells do not give rise to mature B cells, have undergone selection, and are reduced in murine lupus. *J. Immunol.* 178: 7511-7515.
- Thomas M, Calamito M, Srivastava B, Maillard I, Pear WS, Allman D, 2007. Notch activity synergizes with B-cell-receptor and CD40 signaling to enhance B-cell activation. *Blood* 109: 3342-3350.
- Thrasher AJ, 2002. WASp in immune-system organization and function. *Nat. Rev. Immunol.* 2: 635-646.
- Towbin H, Staehelin T, Gordon J, 1979. Electrophoretic transfer of proteins from polyacrylamide gels to nitrocellulose sheets: procedure and some applications. *Proc. Natl. Acad. Sci. U. S. A* 76: 4350-4354.
- Trembl LS, Carlesso G, Hoek KL, Stadanlick JE, Kambayashi T, Bram RJ, Cancro MP, Khan WN, 2007. TLR stimulation modifies BlyS receptor expression in follicular and marginal zone B cells. *J. Immunol.* 178: 7531-7539.
- Troen G, Wlodarska I, Warsame A, Hernandez LS, De Wolf-Peeters C, Delabie J, 2008. NOTCH2 mutations in marginal zone lymphoma. *Haematologica* 93: 1107-1109.
- Tze LE, Schram BR, Lam KP, Hogquist KA, Hippen KL, Liu J, Shinton SA, Otipoby KL, Rodine PR, Vegoe AL, Kraus M, Hardy RR, Schlissel MS, Rajewsky K, Behrens TW, 2005. Basal immunoglobulin signaling actively maintains developmental stage in immature B cells. *PLoS. Biol.* 3: e82.
- Tzivion G, Dobson M, Ramakrishnan G, 2011. FoxO transcription factors; Regulation by AKT and 14-3-3 proteins. *Biochim. Biophys. Acta* 1813: 1938-1945.
- Tzoneva G, Ferrando AA, 2012. Recent advances on NOTCH signaling in T-ALL. *Curr. Top. Microbiol. Immunol.* 360: 163-182.
- Van Gelder RN, von Zastrow ME, Yool A, Dement WC, Barchas JD, Eberwine JH, 1990. Amplified RNA synthesized from limited quantities of heterogeneous cDNA. *Proc. Natl. Acad. Sci. U. S. A* 87: 1663-1667.
- van KC, Banchereau J, 2000. CD40-CD40 ligand. *J. Leukoc. Biol.* 67: 2-17.
- Vences-Catalan F, Santos-Argumedo L, 2011. CD38 through the life of a murine B lymphocyte. *IUBMB. Life* 63: 840-846.
- Wade M, Wahl GM, 2006. c-Myc, genome instability, and tumorigenesis: the devil is in the details. *Curr. Top. Microbiol. Immunol.* 302: 169-203.
- Walker L, Carlson A, Tan-Pertel HT, Weinmaster G, Gasson J, 2001. The notch receptor and its ligands are selectively expressed during hematopoietic development in the mouse. *Stem Cells* 19: 543-552.

- Wehrli N, Legler DF, Finke D, Toellner KM, Loetscher P, Baggiolini M, MacLennan IC, Cha-Orbea H, 2001. Changing responsiveness to chemokines allows medullary plasmablasts to leave lymph nodes. *Eur. J. Immunol.* 31: 609-616.
- Weih DS, Yilmaz ZB, Weih F, 2001. Essential role of RelB in germinal center and marginal zone formation and proper expression of homing chemokines. *J. Immunol.* 167: 1909-1919.
- Wen R, Chen Y, Xue L, Schuman J, Yang S, Morris SW, Wang D, 2003. Phospholipase Cgamma2 provides survival signals via Bcl2 and A1 in different subpopulations of B cells. *J. Biol. Chem.* 278: 43654-43662.
- Weng AP, Millholland JM, Yashiro-Ohtani Y, Arcangeli ML, Lau A, Wai C, Del BC, Rodriguez CG, Sai H, Tobias J, Li Y, Wolfe MS, Shachaf C, Felsher D, Blacklow SC, Pear WS, Aster JC, 2006. c-Myc is an important direct target of Notch1 in T-cell acute lymphoblastic leukemia/lymphoma. *Genes Dev.* 20: 2096-2109.
- Westerberg LS, de la Fuente MA, Wermeling F, Ochs HD, Karlsson MC, Snapper SB, Notarangelo LD, 2008. WASP confers selective advantage for specific hematopoietic cell populations and serves a unique role in marginal zone B-cell homeostasis and function. *Blood* 112: 4139-4147.
- Wharton KA, Johansen KM, Xu T, Katsanis-Tsakonas S, 1985. Nucleotide sequence from the neurogenic locus notch implies a gene product that shares homology with proteins containing EGF-like repeats. *Cell* 43: 567-581.
- Witt CM, Won WJ, Hurez V, Klug CA, 2003. Notch2 haploinsufficiency results in diminished B1 B cells and a severe reduction in marginal zone B cells. *J. Immunol.* 171: 2783-2788.
- Wolfer A, Wilson A, Nemir M, MacDonald HR, Radtke F, 2002. Inactivation of Notch1 impairs VDJbeta rearrangement and allows pre-TCR-independent survival of early alpha beta lineage thymocytes. *Immunity.* 16: 869-879.
- Wu L, Maillard I, Nakamura M, Pear WS, Griffin JD, 2007. The transcriptional coactivator Maml1 is required for Notch2-mediated marginal zone B-cell development. *Blood* 110: 3618-3623.
- Yasuda T, Kometani K, Takahashi N, Imai Y, Aiba Y, Kurosaki T, 2011. ERKs induce expression of the transcriptional repressor Blimp-1 and subsequent plasma cell differentiation. *Sci. Signal.* 4: ra25.
- Yeramilli VA, Knight KL, 2011. Somatic diversification and proliferating transitional B cells: implications for peripheral B cell homeostasis. *J. Immunol.* 186: 6437-6444.
- You Y, Myers RC, Freeberg L, Foote J, Kearney JF, Justement LB, Carter RH, 2011. Marginal zone B cells regulate antigen capture by marginal zone macrophages. *J. Immunol.* 186: 2172-2181.
- You Y, Zhao H, Wang Y, Carter RH, 2009. Cutting edge: Primary and secondary effects of CD19 deficiency on cells of the marginal zone. *J. Immunol.* 182: 7343-7347.
- Zandvoort A, Timens W, 2002. The dual function of the splenic marginal zone: essential for initiation of anti-TI-2 responses but also vital in the general first-line defense against blood-borne antigens. *Clin. Exp. Immunol.* 130: 4-11.
- Zanotti S, Canalis E, 2013. Notch signaling in skeletal health and disease. *Eur. J. Endocrinol.* 168: R95-103.

10. Appendix

Supplementary Data

Table S1: Top 100 regulated genes between wild type MZ B and Fo B cells.

Probe_ID	Gene symbol	Accession	q-value	Relat. expression	Fold change
ILMN_2765759	Asb2	NM_023049.1	9.85E-05	28.3245	28.3245
ILMN_2747923	Slc40a1	NM_016917.2	1.15E-03	14.7752	14.7752
ILMN_1227577	Rap1gap	NM_001081155.1	1.38E-04	12.7579	12.7579
ILMN_2756046	Ffar2	NM_146187.3	1.84E-04	12.7011	12.7011
ILMN_2878071	Lyz	NM_013590.2	2.86E-04	12.3668	12.3668
ILMN_1246808	Serpine2	AK045954	2.86E-04	12.0890	12.0890
ILMN_2778655	Vcam1	NM_011693.2	1.31E-03	10.6918	10.6918
ILMN_1223416	Fer1f3	XM_001480162.1	2.86E-04	9.7781	9.7781
ILMN_2651715	Axl	NM_009465.3	2.25E-03	8.7607	8.7607
ILMN_2699531	Rgs10	NM_026418.2	9.04E-05	7.3290	7.3290
ILMN_2975312	Fcgr2a (CD23)	NM_013517.1	3.02E-04	0.1368	-7.3074
ILMN_2650557	Ccbp2	NM_021609.3	3.41E-04	7.2927	7.2927
ILMN_1237406	Itgad (CD11d)	NM_001029872.1	1.57E-03	7.2887	7.2887
ILMN_2718589	Fcna	NM_007995.3	1.12E-03	6.8123	6.8123
ILMN_1214608	Plxnd1	NM_026376.3	2.33E-04	6.4647	6.4647
ILMN_2432550	Trib2	NM_144551.3	8.41E-04	0.1711	-5.8450
ILMN_3092056	Itgad (CD11d)	NM_001029872.1	1.82E-03	5.6914	5.6914
ILMN_1256771	Adrbk2	NM_001035531.1	3.02E-04	5.3235	5.3235
ILMN_2722996	Sirpa	NM_007547.2	1.60E-03	5.2973	5.2973
ILMN_2725414	Cd9	NM_007657.2	3.94E-04	5.2842	5.2842
ILMN_2652877	Fcgr2a (CD23)	NM_013517.3	4.32E-04	0.1899	-5.2667
ILMN_1256817	Sipi	NM_011414.2	1.73E-03	5.2381	5.2381
ILMN_2652875	Fcgr2a (CD23)	NM_013517.1	6.55E-04	0.1911	-5.2328
ILMN_2641793	Dtx1	NM_008052.3	8.65E-04	5.0124	5.0124
ILMN_2925653	Ear2	NM_007895.2	9.80E-04	5.0116	5.0116
ILMN_2604029	Klf2	NM_008452.1	9.61E-04	0.2007	-4.9818
ILMN_3124528	Hvcn1	NM_001042489.1	9.05E-04	0.2031	-4.9232
ILMN_2631161	Fcgr4	NM_144559.1	9.80E-04	4.9071	4.9071
ILMN_1228942	Cd59a	NM_007652.2	4.96E-04	4.8092	4.8092
ILMN_1252076	Lyz2	NM_017372.3	9.20E-04	4.7926	4.7926
ILMN_2635272	Igh-VJ558	XM_001472091.1	8.84E-03	4.7819	4.7819
ILMN_2939681	Lyzs	NM_017372.2	9.04E-05	4.7193	4.7193
ILMN_2790357	Sema7a	NM_011352.2	1.07E-03	4.6383	4.6383
ILMN_1235456	Icosl	AK041320	4.99E-03	0.2185	-4.5773
ILMN_2734212	Cd1d1	NM_007639.2	1.90E-04	4.4784	4.4784
ILMN_1243451	Hvcn1	NM_001042489.1	9.13E-04	0.2237	-4.4705
ILMN_1252005	B230334f05Rik	AK046024	5.30E-04	4.4704	4.4704
ILMN_1256142	Marcks	NM_008538.2	3.17E-04	4.3772	4.3772
ILMN_2903945	Gadd45g	NM_011817.1	8.66E-04	0.2290	-4.3675
ILMN_2678127	Rnf144a	NM_080563.3	3.41E-04	0.2309	-4.3300
ILMN_1253387	Klf5	NM_009769.4	6.55E-04	4.2957	4.2957
ILMN_1224754	Ckb	NM_021273.3	9.55E-04	4.2489	4.2489
ILMN_1214783	A530050E01Rik	AK040949	2.72E-04	0.2361	-4.2362

Table S1 continued:

Probe_ID	Gene symbol	Accession	q-value	Relat. expression	Fold change
ILMN_1258908	A630008H02Rik	AK041423	6.42E-04	0.2399	-4.1680
ILMN_2731735	Ear2	NM_007895.2	1.23E-03	4.1603	4.1603
ILMN_2716622	Mapk11	NM_011161.4	5.90E-04	0.2417	-4.1374
ILMN_2644587	Bzw2	NM_025840.2	1.38E-04	4.0998	4.0998
ILMN_2485323	Trf	NM_133977.2	1.47E-03	4.0838	4.0839
ILMN_1220975	Ptpn22	NM_008979.1	1.63E-03	4.0757	4.0757
ILMN_2813830	Nt5e	NM_011851.2	3.56E-04	4.0480	4.0481
ILMN_2619620	C1qb	NM_009777.2	1.94E-03	4.0340	4.0340
ILMN_2729252	5830431A10Rik	XR_002313.1	8.24E-06	0.2487	-4.0209
ILMN_2819558	Bach2	NM_007521.2	1.66E-03	0.2487	-4.0205
ILMN_2595973	Grn	NM_008175.3	1.07E-03	3.9967	3.9967
ILMN_2703329	AI324046	NM_198640.1	1.07E-03	3.9649	3.9649
ILMN_1231884	Tmem121	NM_153776.2	2.27E-03	3.9454	3.9454
ILMN_1229449	B930008G09Rik	AK046968	1.31E-04	0.2548	-3.9253
ILMN_2982781	Kcnk5	NM_021542.2	5.52E-04	3.9241	3.9241
ILMN_1252514	C920016N10Rik	AK083355	2.26E-04	3.9092	3.9092
ILMN_2658501	Ifitm3	NM_025378.2	1.09E-03	3.8847	3.8847
ILMN_2858200	Klk4	NM_019928.1	1.29E-03	3.8793	3.8793
ILMN_2593994	5033430I15Rik	XM_001473131.1	7.00E-04	3.8783	3.8783
ILMN_2721198	Ggnbp1	NM_027544.1	3.18E-04	3.8592	3.8592
ILMN_3162075	Fcrl5	NM_183222.2	8.41E-04	3.8235	3.8235
ILMN_2819586	Gpr156	NM_153394.2	4.32E-04	3.8025	3.8025
ILMN_2523841	AI324046	NM_198640.1	1.01E-03	3.7954	3.7954
ILMN_1226073	Trps1	AK036590	4.96E-04	3.7904	3.7904
ILMN_1250135	A930005H10Rik		1.07E-03	3.7854	3.7854
ILMN_2988143	Plac8	NM_139198.1	3.34E-04	3.7721	3.7721
ILMN_2657828	Rhbdf1	NM_010117.1	1.16E-03	3.7299	3.7299
ILMN_2715840	C1qc	NM_007574.2	1.79E-03	3.7179	3.7179
ILMN_1248714	Cd55	NM_010016.2	4.97E-04	0.2705	-3.6963
ILMN_1244272	Epb4.1l3	NM_013813.1	1.59E-03	3.6443	3.6443
ILMN_1248890	AW011738	XM_489070	3.27E-04	3.6175	3.6175
ILMN_2749364	LOC382646	XM_356604.1	2.33E-04	0.2768	-3.6124
ILMN_2749363	LOC382646	XM_356604.1	1.38E-04	0.2779	-3.5978
ILMN_2883164	Serpine2	NM_009255.2	2.44E-03	3.5904	3.5904
ILMN_2721439	Csrp2	NM_007792.3	6.44E-03	0.2798	-3.5746
ILMN_1250195	Ndrp1	NM_008681.2	1.09E-03	0.2798	-3.5735
ILMN_1234988	Gad1	NM_008077.4	3.09E-04	0.2817	-3.5494
ILMN_1217527	Ly108	AK089750	6.56E-04	0.2839	-3.5219
ILMN_2576568	D130062J21Rik	AK051661	3.09E-04	0.2846	-3.5134
ILMN_1259764	1500005K14Rik	XM_203453	9.80E-04	0.2855	-3.5024
ILMN_3112011	Dusp16	NM_130447.2	8.73E-04	3.4977	3.4977
ILMN_1239430	Mrc1	NM_008625.1	2.49E-03	3.4964	3.4964
ILMN_2692615	Tgm2	NM_009373.3	1.68E-03	3.4824	3.4824
ILMN_3005873	Sort1	NM_019972.2	1.98E-03	3.4797	3.4797
ILMN_2792485	Ube2e2	NM_144839.1	5.27E-04	3.4572	3.4572
ILMN_1254409	Atxn1	NM_009124.4	4.29E-04	3.4526	3.4526
ILMN_1258272	LOC382646	XM_356604.1	4.96E-04	0.2907	-3.4404

Table S1 continued:

Probe_ID	Gene symbol	Accession	q-value	Relat. expression	Fold change
ILMN_2550095	6230425C21Rik	AK012678	3.25E-04	3.4337	3.4337
ILMN_1237978	9930005O13Rik	AK036773	1.07E-03	0.2915	-3.4303
ILMN_1228320	Cfp	NM_008823.3	4.97E-04	3.4050	3.4050
ILMN_2710819	Csf1r	NM_001037859.2	2.37E-03	3.3507	3.3507
ILMN_2619707	Slco2b1	NM_175316.3	3.75E-03	3.3233	3.3233
ILMN_2901626	Tnfrsf21	NM_178589.2	8.03E-04	3.3072	3.3072
ILMN_1253182	Hs3st1	NM_010474.1	1.54E-03	3.3009	3.3009
ILMN_2721571	Slamf1	NM_013730.4	3.41E-04	0.3078	-3.2491
ILMN_1234020	scl0002007.1_97		5.90E-04	3.2469	3.2469
ILMN_3091003	Ms4a7	NM_027836.5	6.10E-04	3.2372	3.2372

Final gene lists from the comparison wild type MZ B vs. Fo B cells were sorted by q-value and only genes with a q-value < 0.05 were chosen. Remaining genes were sorted according to their absolute fold change (regardless of up- or downregulation) and the top 100 most strongly regulated genes were chosen for this table. Genes upregulated in MZ B have positive fold change values, genes upregulated in Fo B cells negative values. Illumina internal identifier (Probe_ID).

Table S2: Top 100 regulated genes between Notch2-deficient Fo B and Notch2IC-expressing MZ B cells.

Probe_ID	Gene symbol	Accession	q-value	Relat. expression	Fold change
ILMN_2765759	Asb2	NM_023049.1	8.04E-06	0.0328	-30.4901
ILMN_2756046	Ffar2	NM_146187.3	1.76E-05	0.0378	-26.4380
ILMN_2975312	Fcer2a (CD23)	NM_013517.1	8.04E-06	25.7955	25.7955
ILMN_1214608	Plxnd1	NM_026376.3	7.50E-06	0.0456	-21.9239
ILMN_2699531	Rgs10	NM_026418.2	8.04E-06	0.0467	-21.3948
ILMN_1223416	Fer1l3	XM_001480162.1	1.61E-05	0.0483	-20.6941
ILMN_2792485	Ube2e2	NM_144839.1	8.04E-06	0.0514	-19.4489
ILMN_1227577	Rap1gap	NM_001081155.1	2.98E-05	0.0552	-18.1162
ILMN_1256771	Adrbk2	NM_001035531.1	7.73E-05	0.0712	-14.0538
ILMN_2725414	Cd9	NM_007657.2	1.20E-05	0.0723	-13.8279
ILMN_2641793	Dtx1	NM_008052.3	7.50E-06	0.0737	-13.5603
ILMN_1243451	Hvcn1	NM_001042489.1	1.90E-05	12.8988	12.8988
ILMN_2604029	Klf2	NM_008452.1	2.78E-05	12.6686	12.6686
ILMN_2550095	6230425C21Rik	AK012678	1.59E-05	0.0873	-11.4513
ILMN_3124528	Hvcn1	NM_001042489.1	2.26E-05	10.8238	10.8238
ILMN_2759207	Kcne1	NM_008424.2	3.53E-05	0.0926	-10.8045
ILMN_2790357	Sema7a	NM_011352.2	3.99E-05	0.0936	-10.6794
ILMN_2652875	Fcer2a (CD23)	NM_013517.1	2.35E-05	10.2966	10.2966
ILMN_2652877	Fcer2a (CD23)	NM_013517.3	5.38E-05	9.5545	9.5545
ILMN_2716622	Mapk11	NM_011161.4	1.91E-05	8.2945	8.2945
ILMN_1253182	Hs3st1	NM_010474.1	6.92E-05	0.1207	-8.2869
ILMN_1227434	Itgb7	NM_013566.1	2.51E-05	8.2575	8.2575
ILMN_2692615	Tgm2	NM_009373.3	1.88E-05	0.1224	-8.1727
ILMN_2856926	Gpr114	NM_001033468.1	1.42E-05	0.1280	-7.8121
ILMN_2819586	Gpr156	NM_153394.2	1.92E-05	0.1310	-7.6320
ILMN_2467596	Dusp16	NM_001048054.1	1.59E-05	0.1356	-7.3756
ILMN_2988143	Plac8	NM_139198.1	2.51E-05	0.1365	-7.3269
ILMN_1259339	Cdk5r1	NM_009871.2	2.27E-05	0.1378	-7.2581
ILMN_2644587	Bzw2	NM_025840.2	2.51E-05	0.1442	-6.9355
ILMN_1248714	Cd55	NM_010016.2	3.65E-05	6.5238	6.5238

Table S2 continued:

Probe_ID	Gene symbol	Accession	q-value	Relat. expression	Fold change
ILMN_1252005	B230334I05Rik	AK046024	2.79E-04	0.1605	-6.2310
ILMN_2749363	LOC382646	XM_356604.1	1.32E-04	6.2302	6.2302
ILMN_2724570	Mapk12	NM_013871.2	1.98E-05	6.2168	6.2168
ILMN_2749364	LOC382646	XM_356604.1	8.00E-05	6.1651	6.1651
ILMN_1258272	LOC382646	XM_356604.1	8.36E-05	6.1639	6.1639
ILMN_2903945	Gadd45g	NM_011817.1	2.43E-05	6.1586	6.1586
ILMN_1220124	Gpr156	NM_153394.2	7.50E-06	0.1632	-6.1289
ILMN_2432550	Trib2	NM_144551.3	1.90E-04	6.0388	6.0388
ILMN_2645780	Osgin1	NM_027950.1	1.48E-05	0.1699	-5.8864
ILMN_1219878	9930022F21Rik	AK036897	1.47E-05	0.1753	-5.7043
ILMN_1248890	AW011738	XM_489070	1.59E-05	0.1754	-5.7010
ILMN_2798086	Fchs2	NM_199012.1	1.95E-05	5.6693	5.6693
ILMN_2683316	Ctsb	NM_007798.2	1.84E-05	0.1767	-5.6586
ILMN_1228942	Cd59a	NM_007652.2	3.17E-04	0.1787	-5.5963
ILMN_3112011	Dusp16	NM_130447.2	7.50E-06	0.1808	-5.5302
ILMN_1221819	Fcgrt	NM_010189	6.04E-04	5.4677	5.4677
ILMN_3150811	Tsc22d3	NM_001077364.1	2.28E-03	5.4559	5.4559
ILMN_2650557	Ccbp2	NM_021609.3	8.04E-06	0.1834	-5.4530
ILMN_2958099	Adssl1	NM_007421.1	2.20E-05	0.1836	-5.4481
ILMN_2661340	Slco4a1	NM_148933.1	3.48E-05	0.1868	-5.3529
ILMN_1253414	Hes5	NM_010419.2	7.43E-05	0.1877	-5.3283
ILMN_1256142	Marcks	NM_008538.2	7.50E-06	0.1888	-5.2970
ILMN_1229449	B930008G09Rik	AK046968	9.86E-05	5.1300	5.1300
ILMN_2593994	5033430I15Rik	XM_001473131.1	8.04E-06	0.1969	-5.0794
ILMN_2982781	Kcnk5	NM_021542.2	2.45E-04	0.1988	-5.0300
ILMN_2592486	Pglyrp1	NM_009402.1	9.87E-05	5.0035	5.0035
ILMN_1246808	Serpine2	AK045954	4.15E-04	0.2008	-4.9790
ILMN_2729252	5830431A10Rik	XR_002313.1	1.84E-05	4.9626	4.9626
ILMN_2593787	Kcnk13	NM_146037.1	3.45E-05	0.2033	-4.9184
ILMN_2451022	Vim	NM_011701.3	2.16E-04	4.9042	4.9042
ILMN_2595973	Grn	NM_008175.3	4.42E-05	0.2047	-4.8863
ILMN_1252514	C920016N10Rik	AK083355	2.43E-05	0.2069	-4.8333
ILMN_2819558	Bach2	NM_007521.2	7.37E-04	4.7991	4.7991
ILMN_2583351	D930042A21Rik	AK086621	2.82E-05	0.2090	-4.7836
ILMN_1247691	Hes1	NM_008235.2	4.87E-05	0.2097	-4.7678
ILMN_2734212	Cd1d1	NM_007639.2	1.90E-04	0.2099	-4.7642
ILMN_2667994	Dnase1l3	NM_007870.2	2.43E-05	0.2107	-4.7472
ILMN_2733356	Endod1	NM_028013.2	6.14E-05	0.2121	-4.7149
ILMN_2984744	Emp3	NM_010129.1	1.07E-04	4.6659	4.6659
ILMN_1231851	Enpp1	NM_008813.3	7.50E-06	4.5977	4.5977
ILMN_1223317	Lgals3	NM_010705.2	3.35E-04	4.5963	4.5963
ILMN_2743902	Matk	NM_010768.1	7.16E-05	0.2226	-4.4927
ILMN_2624153	Hes5	NM_010419.4	1.89E-04	0.2250	-4.4450
ILMN_2818246	Cpne4	NM_028719.1	1.04E-04	4.4216	4.4216
ILMN_1212982	Zfp318	NM_207671.2	1.99E-04	4.3960	4.3960
ILMN_1216368	B3gnt5	NM_054052.2	1.18E-04	4.3648	4.3648
ILMN_1247704	Hmgn3	NM_175074.1	3.35E-05	0.2298	-4.3523

Table S2 continued:

Probe_ID	Gene symbol	Accession	q-value	Relat. expression	Fold change
ILMN_2678127	Rnf144a	NM_080563.3	8.39E-05	4.3147	4.3147
ILMN_2754148	Dusp16	NM_001048054.1	8.04E-06	0.2331	-4.2893
ILMN_2506039	A130090K04Rik		3.47E-04	0.2345	-4.2651
ILMN_2843782	Tpst2	NM_009419.2	1.20E-04	0.2374	-4.2129
ILMN_2914010	Dmwd	NM_010058.1	1.60E-05	4.2018	4.2018
ILMN_2645208	Arhgef3	NM_027871.1	2.17E-05	4.1699	4.1699
ILMN_3128992	Cd27	NM_001033126.2	6.58E-05	0.2400	-4.1666
ILMN_2674367	Agrn	NM_021604.2	3.09E-05	0.2411	-4.1480
ILMN_2675785	Myo18b	XM_912851.3	2.45E-04	0.2413	-4.1443
ILMN_2508910	Tpst2	NM_009419	1.19E-04	0.2428	-4.1182
ILMN_2878071	Lyz	NM_013590.2	9.68E-03	0.2436	-4.1059
ILMN_2644719	Hmgn3	NM_026122.3	1.71E-05	0.2444	-4.0918
ILMN_1248028	Emp3	NM_010129.1	1.20E-05	4.0509	4.0509
ILMN_2502471	BC023892	XM_994662.1	2.31E-05	4.0467	4.0467
ILMN_2782964	Enpp1	NM_008813.2	1.15E-04	4.0394	4.0394
ILMN_3091003	Ms4a7	NM_027836.5	1.32E-04	0.2479	-4.0339
ILMN_2917497	Fcgrt	NM_010189.1	1.28E-04	4.0308	4.0308
ILMN_2767605	Lmo2	NM_008505.3	8.04E-06	4.0263	4.0263
ILMN_2458765	Ahnak	NM_009643.1	1.24E-03	4.0209	4.0209
ILMN_2744846	Guca2b	NM_008191.1	8.04E-06	0.2494	-4.0104
ILMN_2772582	Smad3	NM_016769	7.36E-05	0.2515	-3.9758
ILMN_2629191	Cpm	XM_994613.1	2.07E-04	3.9512	3.9512
ILMN_1226766	B430320J11Rik	AK046714	2.45E-04	0.2536	-3.9434

Final gene lists from the comparison Notch2-deficient Fo B vs. Notch2IC-expressing MZ B cells were sorted by q-value and only genes with a q-value < 0.05 were chosen. Remaining genes were sorted according to their absolute fold change (regardless of up- or downregulation) and the top 100 most strongly regulated genes were chosen for this table. Genes upregulated in Notch2-deficient cells have positive fold change values, genes upregulated in Notch2IC-expressing cells negative values. Illumina internal identifier (Probe_ID).

Table S3: Top 100 regulated genes between wild type and Notch2IC-expressing MZ B cells.

Probe_ID	Gene symbol	Accession	q-value	Relat. expression	Fold change
ILMN_2759207	Kcne1	NM_008424.2	8.11E-05	0.0844	-11.8446
ILMN_2792485	Ube2e2	NM_144839.1	4.31E-04	0.1410	-7.0915
ILMN_2467596	Dusp16	NM_001048054.1	1.51E-04	0.1711	-5.8452
ILMN_1253414	Hes5	NM_010419.2	1.51E-04	0.1874	-5.3363
ILMN_2661340	Slco4a1	NM_148933.1	2.81E-04	0.1930	-5.1818
ILMN_1377919	Tubb2b	NM_023716.2	4.42E-04	0.2017	-4.9576
ILMN_2856926	Gpr114	NM_001033468.1	1.51E-04	0.2091	-4.7824
ILMN_1219878	9930022F21Rik	AK036897	8.11E-05	0.2149	-4.6531
ILMN_2747923	Slc40a1	NM_016917.2	3.55E-02	4.4105	4.4105
ILMN_2624153	Hes5	NM_010419.4	3.29E-04	0.2307	-4.3345
ILMN_2778655	Vcam1	NM_011693.2	2.97E-02	4.2022	4.2022
ILMN_1214608	Plxnd1	NM_026376.3	1.40E-03	0.2420	-4.1327
ILMN_2550095	6230425C21Rik	AK012678	1.65E-03	0.2492	-4.0127
ILMN_2645780	Osgin1	NM_027950.1	7.97E-04	0.2630	-3.8024
ILMN_2596979	Nrarp	NM_025980.2	8.54E-04	0.2723	-3.6720
ILMN_2975312	Fcgr2a (CD23)	NM_013517.1	3.55E-03	3.6246	3.6246

Table S3 continued:

Probe_ID	Gene symbol	Accession	q-value	Relat. expression	Fold change
ILMN_1221819	Fcgrt	NM_010189	2.43E-02	3.6220	3.6220
ILMN_1237406	Itgad (CD11d)	NM_001029872.1	1.90E-02	3.5631	3.5631
ILMN_2651715	Axl	NM_009465.3	3.79E-02	3.5387	3.5387
ILMN_2725414	Cd9	NM_007657.2	1.21E-03	0.2964	-3.3740
ILMN_2958099	Adssl1	NM_007421.1	3.69E-04	0.2990	-3.3446
ILMN_1243451	Hvcn1	NM_001042489.1	6.51E-03	3.3340	3.3340
ILMN_2780247	Lta	NM_010735.1	3.80E-03	3.2637	3.2637
ILMN_1256817	Slpi	NM_011414.2	2.30E-02	3.2626	3.2626
ILMN_1256771	Adrbk2	NM_001035531.1	4.26E-03	0.3143	-3.1814
ILMN_2740869	Rims2	NM_053271.1	3.66E-03	0.3147	-3.1778
ILMN_2604029	Klf2	NM_008452.1	3.84E-03	3.1291	3.1291
ILMN_1236799	Tfll2	NM_001098267.1	2.77E-04	0.3202	-3.1228
ILMN_2657980	Faah	NM_010173.3	1.65E-03	3.0948	3.0948
ILMN_3092056	Itgad (CD11d)	NM_001029872.1	2.24E-02	3.0924	3.0924
ILMN_2718589	Fcna	NM_007995.3	2.75E-02	3.0922	3.0922
ILMN_2595918	Gimap7	NM_146167.3	8.51E-03	3.0058	3.0058
ILMN_2638509	LOC639715	XM_916269.3	1.39E-03	0.3416	-2.9271
ILMN_2657175	Anxa2	NM_007585.3	1.59E-02	2.9255	2.9255
ILMN_2790357	Sema7a	NM_011352.2	4.59E-04	0.3426	-2.9186
ILMN_2699531	Rgs10	NM_026418.2	4.59E-04	0.3469	-2.8823
ILMN_3128992	Cd27	NM_001033126.2	5.27E-03	0.3480	-2.8733
ILMN_1245079	Adssl1	NM_007421.1	6.29E-04	0.3564	-2.8062
ILMN_3124528	Hvcn1	NM_001042489.1	1.84E-02	2.7792	2.7792
ILMN_1227434	Irgb7	NM_013566.1	7.60E-04	2.7397	2.7397
ILMN_2756046	Ffar2	NM_146187.3	8.26E-03	0.3663	-2.7304
ILMN_2917497	Fcgrt	NM_010189.1	7.61E-03	2.6365	2.6365
ILMN_1252601	Bcl7a	NM_029850.2	1.02E-03	0.3805	-2.6284
ILMN_2593787	Kcnk13	NM_146037.1	1.07E-03	0.3827	-2.6131
ILMN_2495896	IGKV1-88_AJ231206 Igxvariable1-88_289		8.31E-03	2.6004	2.6004
ILMN_2675785	Myo18b	XM_912851.3	2.35E-03	0.3847	-2.5994
ILMN_2592486	Pglyrp1	NM_009402.1	2.77E-03	2.5918	2.5918
ILMN_2692615	Tgm2	NM_009373.3	1.47E-02	0.3868	-2.5854
ILMN_1213139	Heyl	NM_013905.3	4.42E-04	0.3918	-2.5520
ILMN_2596932	Rapgef2	NM_001099624.1	8.32E-05	0.4069	-2.4579
ILMN_2919786	Erh	NM_007951.1	3.62E-02	0.4077	-2.4528
ILMN_2715840	C1qc	NM_007574.2	1.56E-02	2.4276	2.4276
ILMN_1220124	Gpr156	NM_153394.2	3.80E-03	0.4128	-2.4222
ILMN_2819586	Gpr156	NM_153394.2	8.42E-03	0.4165	-2.4012
ILMN_2619620	C1qb	NM_009777.2	3.34E-02	2.3785	2.3785
ILMN_1217879	LOC100042777	XM_001478939.1	3.45E-02	0.4220	-2.3698
ILMN_2485323	Trf	NM_133977.2	3.68E-02	2.3441	2.3441
ILMN_2458765	Ahnak	NM_009643.1	2.79E-03	2.3150	2.3150
ILMN_2682162	Bcl2	NM_177410.2	3.55E-03	2.3137	2.3137
ILMN_1223317	Lgals3	NM_010705.2	1.16E-02	2.3002	2.3002
ILMN_2766930	Faah	NM_010173.3	3.80E-03	2.2839	2.2839
ILMN_2619707	Slco2b1	NM_175316.3	4.05E-02	2.2666	2.2666

Table S3 continued:

Probe_ID	Gene symbol	Accession	q-value	Relat. expression	Fold change
ILMN_2440634	3526401B18Rik		4.42E-04	2.2616	2.2616
ILMN_2770119	Zbtb32	NM_021397.2	5.22E-02	2.2580	2.2580
ILMN_1231915	LOC633273	XM_919047.2	5.73E-03	0.4430	-2.2573
ILMN_1216880	Emr1	NM_010130.3	1.34E-02	2.2525	2.2525
ILMN_2742840	Gpr34	NM_011823.4	3.29E-04	2.2508	2.2508
ILMN_3005873	Sort1	NM_019972.2	3.26E-02	2.2253	2.2253
ILMN_1231884	Tmem121	NM_153776.2	5.05E-02	2.2198	2.2198
ILMN_2743902	Matk	NM_010768.1	2.31E-04	0.4510	-2.2172
ILMN_2467151	Cyp11a1	NM_019779	3.46E-03	0.4513	-2.2157
ILMN_2925653	Ear2	NM_007895.2	5.02E-02	2.2150	2.2150
ILMN_1239430	Mrc1	NM_008625.1	3.89E-02	2.1936	2.1936
ILMN_2658501	Ifitm3	NM_025378.2	2.39E-02	2.1835	2.1835
ILMN_2716622	Mapk11	NM_011161.4	7.80E-03	2.1777	2.1777
ILMN_2742152	Gadd45a	NM_007836.1	3.60E-03	0.4596	-2.1760
ILMN_1255207	LOC100047749	XM_001478817.1	1.65E-03	2.1474	2.1474
ILMN_3158919	Prkcz	NM_001039079.1	1.77E-03	2.1360	2.1360
ILMN_1217032	D230048P18Rik	AK052127	2.24E-02	0.4689	-2.1325
ILMN_1238725	C130086J11Rik	AK081910	3.65E-02	2.1207	2.1207
ILMN_2697002	Tlr3	NM_126166.4	1.02E-03	0.4719	-2.1191
ILMN_1249975	Ighg	XM_001001076.2	1.56E-02	0.4729	-2.1146
ILMN_1244272	Epb4.1l3	NM_013813.1	3.67E-02	2.1036	2.1036
ILMN_2903945	Gadd45g	NM_011817.1	3.67E-02	2.0957	2.0957
ILMN_2826881	Mybl2	NM_008652.2	7.60E-04	0.4780	-2.0919
ILMN_1226607	Cort	NM_007745.3	7.40E-03	2.0916	2.0916
ILMN_2522460	3010031K01Rik		5.23E-03	0.4811	-2.0784
ILMN_2657828	Rhbdf1	NM_010117.1	3.79E-03	2.0671	2.0671
ILMN_1236107	Ogfr1	XM_973033.1	7.40E-03	0.4849	-2.0622
ILMN_2684205	4930431B09Rik	XR_002338.2	5.46E-03	0.4873	-2.0522
ILMN_3112011	Dusp16	NM_130447.2	2.73E-02	0.4891	-2.0446
ILMN_1227836	Arpc1b	NM_023142.1	1.67E-02	0.4901	-2.0402
ILMN_3162125	Grm6	NM_173372.1	2.24E-02	2.0377	2.0377
ILMN_2795791	Tmem38b	NM_028053.1	3.60E-03	0.4911	-2.0362
ILMN_2744846	Guca2b	NM_008191.1	8.11E-05	0.4912	-2.0360
ILMN_1233809	Cmtm7	NM_133978.1	7.79E-03	2.0324	2.0324
ILMN_2715042	Sdc3	NM_011520.3	4.45E-02	2.0316	2.0316
ILMN_1218799	Emb	NM_010330.3	2.35E-03	2.0246	2.0246
ILMN_2960114	Cyp27a1	NM_024264.3	6.29E-04	0.4944	-2.0225
ILMN_2631143	Sox5	NM_011444.1	2.57E-03	2.0208	2.0208

Final gene lists from the comparison wild type MZ B vs. Notch2IC-expressing MZ B cells were sorted by q-value and only genes with a q-value < 0.05 were chosen. Remaining genes were sorted according to their absolute fold change (regardless of up- or downregulation) and the top 100 most strongly regulated genes were chosen for this table. Genes upregulated in wild type MZ B cells have positive fold change values, genes upregulated in Notch2IC-expressing cells negative values. Illumina internal identifier (Probe_ID).

Table S4: Top 100 regulated genes between wild type and Notch2-deficient Fo B cells.

Probe_ID	Gene symbol	Accession	q-value	Relat. expression	Fold change
ILMN_1256699	Sfi1	NM_030207.2	1.17E-03	0.2882	-3.4696
ILMN_1260218	Sfi1	NM_030207.2	1.81E-04	0.2930	-3.4130
ILMN_2655015	Alad	NM_008525.3	9.42E-04	2.4674	2.4674
ILMN_1259339	Cdk5r1	NM_009871.2	1.41E-03	2.4265	2.4265
ILMN_2944601	4933439C20Rik	NM_001004146.1	1.41E-03	0.4442	-2.2512
ILMN_2762380	Enpp4	NM_199016.2	1.81E-04	0.4536	-2.2048
ILMN_2641793	Dtx1	NM_008052.3	3.74E-03	2.1099	2.1099
ILMN_1222071	C920004C08Rik		3.74E-03	0.4843	-2.0647
ILMN_1255287	Mela	NM_008581	2.86E-02	0.5075	-1.9706
ILMN_1228919	St13	NM_133726.2	5.43E-02	1.8862	1.8862
ILMN_2988143	Plac8	NM_139198.1	1.41E-03	1.8375	1.8375
ILMN_1377919	Tubb2b	NM_023716.2	1.45E-02	1.8324	1.8324
ILMN_1253182	Hs3st1	NM_010474.1	4.56E-02	1.7933	1.7933
ILMN_2645333	H60a	NM_010400.2	3.74E-03	1.7921	1.7921
ILMN_2705578	Snx30	NM_172468.2	1.34E-02	1.7879	1.7879
ILMN_2732848	Tagln2	NM_178598.2	2.17E-02	0.5648	-1.7706
ILMN_2583351	D930042A21Rik	AK086621	3.45E-03	1.7331	1.7331
ILMN_2672597	Gng10	NM_025277.3	3.38E-03	1.6775	1.6775
ILMN_2697615	Mapk12	NM_013871.2	3.97E-02	0.6006	-1.6651
ILMN_1214874	LOC386068	XM_359052.1	2.48E-02	0.6032	-1.6579
ILMN_1228093	Arhgap8	NM_028455.2	1.50E-03	0.6173	-1.6200
ILMN_2817714	Tspan17	NM_028841.1	1.25E-02	0.6221	-1.6075
ILMN_1247691	Hes1	NM_008235.2	5.01E-03	1.5835	1.5835
ILMN_2700166	Ccnd2	NM_009829.3	1.75E-02	1.5732	1.5732
ILMN_1228320	Cfp	NM_008823.3	3.14E-02	1.5712	1.5712
ILMN_2967266	Fxyd5	NM_008761.2	5.42E-02	0.6379	-1.5677
ILMN_2733356	Endod1	NM_028013.2	2.71E-02	1.5645	1.5645
ILMN_2657980	Faah	NM_010173.3	4.63E-03	0.6419	-1.5579
ILMN_2965669	Xlr4a	NM_001081642.1	3.97E-02	1.5562	1.5562
ILMN_1252288	2010007H06Rik		2.56E-02	0.6527	-1.5322
ILMN_2421220	Brwd1	NM_145125.2	7.92E-03	1.5295	1.5295
ILMN_2700168	Ccnd2	NM_009829	4.79E-02	1.5203	1.5203
ILMN_1249378	Bhlhb2	NM_011498.4	8.82E-03	1.5200	1.5200
ILMN_2987062	Thyn1	NM_144543.1	4.98E-03	1.5131	1.5131
ILMN_1213448	LOC669658	XM_976371.1	8.82E-03	0.6629	-1.5086
ILMN_1258950	Slc16a6	NM_134038.2	4.99E-02	1.5078	1.5078
ILMN_1257126	9530055J05Rik	AK020610	4.56E-02	1.5024	1.5024
ILMN_1237034	AU040320	NM_133886.2	4.81E-03	0.6661	-1.5013
ILMN_1252496	Wdr9	NM_145125	1.58E-02	1.4983	1.4983
ILMN_1256780	LOC381528	XM_355489.1	3.27E-02	0.6749	-1.4817
ILMN_2833652	Cr2 (CD21)	NM_007758.2	4.43E-02	1.4797	1.4797
ILMN_2742928	Fxyd5	NM_008761.2	2.56E-02	0.6809	-1.4686
ILMN_2834573	Brwd1	NM_145125.1	1.22E-02	1.4611	1.4611
ILMN_2513837	Gng10	NM_025277.3	8.82E-03	1.4605	1.4605
ILMN_2619316	Prnp	NM_011170.1	3.27E-02	0.6880	-1.4535
ILMN_3152380	Flot2	NM_001040403.1	8.82E-03	0.6898	-1.4498
ILMN_2699531	Rgs10	NM_026418.2	1.22E-02	1.4438	1.4438

Table S4 continued:

Probe_ID	Gene symbol	Accession	q-value	Relat. expression	Fold change
ILMN_1234746	AI790298	XM_902445.3	3.38E-02	0.6946	-1.4397
ILMN_1245389	LOC236604	NR_003517.1	2.66E-02	0.6951	-1.4387
ILMN_1217068	Tusc1	NM_026954.1	4.60E-02	1.4367	1.4367
ILMN_2697174	Trrap	NM_001081362.1	3.09E-02	1.4342	1.4342
ILMN_3006911	Cyp4f13	NM_130882.1	4.14E-02	0.7022	-1.4241
ILMN_2766930	Faah	NM_010173.3	2.93E-02	0.7044	-1.4196
ILMN_2833936	Cryl1	NM_030004.2	1.45E-02	0.7049	-1.4186
ILMN_2562789	C730037N04Rik	AK050331	4.24E-02	0.7089	-1.4106
ILMN_3035795	Mllt3	NM_027326.3	3.74E-03	1.4032	1.4032
ILMN_1247862	Rad23b	AK084917	1.72E-02	1.4005	1.4005
ILMN_2747857	Slc27a3	XM_130954.3	4.14E-02	1.4001	1.4001
ILMN_2506039	A130090K04Rik		3.74E-03	1.3971	1.3971
ILMN_2710484	Rufy3	NM_027530.2	3.19E-02	1.3920	1.3920
ILMN_2683316	Ctsb	NM_007798.2	3.27E-02	1.3919	1.3919
ILMN_2457752	Centd1	XM_001001363.1	2.96E-02	1.3916	1.3916
ILMN_2580536	D630016F07Rik	AK085364	5.11E-03	0.7202	-1.3886
ILMN_2692554	9330186A19Rik	NM_178781.2	3.89E-02	0.7211	-1.3867
ILMN_1221598	9330133O14Rik	NM_176948	1.63E-02	1.3795	1.3795
ILMN_2936199	Trim32	NM_053084.1	3.38E-03	1.3750	1.3750
ILMN_2607786	Fads1	NM_146094.1	3.38E-03	1.3746	1.3746
ILMN_1232452	4921528G01Rik	NM_023884	1.00E-02	1.3719	1.3719
ILMN_2762334	Cept1	NM_133869.3	3.97E-02	1.3666	1.3666
ILMN_1216689	Aplp2	NM_009691.2	4.43E-02	1.3650	1.3650
ILMN_1236601	Pole4	NM_025882.3	2.17E-02	1.3618	1.3618
ILMN_2627179	Ell3	NM_145973.2	1.11E-02	1.3578	1.3578
ILMN_2975312	Fcer2a (CD23)	NM_013517.1	5.26E-02	0.7387	-1.3537
ILMN_1250687	EG627022	XM_891654.3	3.15E-02	0.7395	-1.3522
ILMN_2565243	B130018P07Rik	AK045005	2.48E-02	1.3481	1.3481
ILMN_2623983	Egr2	NM_010118.1	4.62E-02	1.3459	1.3459
ILMN_1256142	Marcks	NM_008538.2	2.29E-02	1.3458	1.3458
ILMN_1233293	Gbp1	NM_010259.2	2.93E-02	1.3440	1.3440
ILMN_1239507	Mrpl15	NM_025300.2	1.82E-02	1.3437	1.3437
ILMN_2730425	Ryr1	NM_009109.2	5.00E-02	0.7464	-1.3398
ILMN_1234618	D630004K10Rik		3.15E-02	0.7495	-1.3342
ILMN_1225994	Vav2	NM_009500.1	2.17E-02	1.3321	1.3321
ILMN_2737463	Ccdc88b	NM_001081291.1	3.97E-02	1.3281	1.3281
ILMN_1249366	LOC100046608	XM_001476583.1	3.38E-02	0.7532	-1.3276
ILMN_1253993	A430083F12Rik	AK040286	3.15E-02	0.7554	-1.3239
ILMN_1258094	4933403K19Rik	AK030157	2.56E-02	1.3232	1.3232
ILMN_1235602	D0Kist3		1.33E-02	1.3214	1.3214
ILMN_2859847	Pygl	NM_133198.1	3.27E-02	0.7569	-1.3211
ILMN_2880536	Uck2	NM_030724.1	5.36E-02	1.3207	1.3207
ILMN_1217454	Lamp2	NM_010685.3	1.82E-02	1.3190	1.3190
ILMN_2517041	Uhrf1	NM_010931.2	3.97E-02	1.3184	1.3184
ILMN_2538597	LOC386405	XM_359211.1	5.20E-02	1.3174	1.3174
ILMN_2758070	Rtn1	NM_153457.6	1.82E-02	0.7591	-1.3173
ILMN_2880052	Xlr4c	NM_183094.1	1.85E-02	1.3157	1.3157

Table S4 continued:

Probe_ID	Gene symbol	Accession	q-value	Relat. expression	Fold change
ILMN_2821736	Jmjd5	NM_029842.1	1.05E-02	0.7602	-1.3154
ILMN_2494455	Zfp219	NM_027248	5.42E-02	0.7618	-1.3126
ILMN_2747472	A230050P20Rik	NM_175687.1	3.89E-02	0.7625	-1.3115
ILMN_2455089	LOC100046087	XM_001475552.1	2.17E-02	1.3100	1.3100
ILMN_1222069	Bbx	NM_027444	3.87E-02	1.3076	1.3076
ILMN_2638558	Pes1	NM_022889.3	5.11E-03	1.3042	1.3042

Final gene lists from the comparison wild type Fo B vs. Notch2-deficient Fo B cells were sorted by q-value and only genes with a q-value < 0.05 were chosen. Remaining genes were sorted according to their absolute fold change (regardless of up- or downregulation) and the top 100 most strongly regulated genes were chosen for this table. Genes upregulated in wild type Fo B cells have positive fold change values, genes upregulated in Notch2-deficient cells negative values. Illumina internal identifier (Probe_ID).

Table S5: Some of the most significant functional annotation clusters comparing gene expression profiles of Notch2IC-expressing MZ B and Notch2-deficient Fo B cells.

Cluster number	Enrichment score / Annotation term	Genes (Count)	Genes (%)	p-value
1	12.87			
	Ribosome	70	2.41	6.10E-15
2	9.94			
	Lymphocyte activation	61	2.1	9.12E-10
3	9.42			
	Intracellular organelle lumen	234	8.06	3.52E-10
4	8.99			
	ATP-binding	260	8.96	4.18E-08
5	8.69			
	Phosphorylation	156	5.38	1.69E-07
6	6.68			
	Lysosome	54	1.86	5.45E-08
7	6.12			
	Immune system development	77	2.65	1.70E-07
8	5.12			
	Apoptosis	106	3.65	2.84E-06
9	5.04			
	Positive regulation of lymphocyte activation	32	1.1	1.85E-06
	Positive regulation of T cell activation	24	0.83	2.46E-05
10	4.95			
	Positive regulation of transcription factor activity	16	0.55	5.06E-05
11	4.33			
	Protein amino acid phosphorylation	133	4.58	2.04E-05
	Protein serine/threonine kinase activity	90	3.1	1.97E-04
15	3.68			
	GTP binding	81	2.79	5.61E-05
17	3.55			
	Positive regulation of lymphocyte proliferation	18	0.62	2.33E-04

Table S5 continued:

Cluster number	Enrichment score / Annotation term	Genes (Count)	Genes (%)	p-value
18	3.51			
	Antigen receptor-mediated signalling pathway	15	0.52	1.51E-04
	T cell receptor signalling pathway	11	0.38	4.38E-04
20	3.34			
	Lymphocyte mediated immunity	21	0.72	3.48E-03
21	3.32			
	Mitochondrial inner membrane	63	2.17	6.21E-04
23	3.10			
	Positive regulation of T cell differentiation	14	0.48	4.32E-04
	Positive regulation of lymphocyte differentiation	14	0.48	8.59E-04
24	3.02			
	Positive regulation of alpha-beta T cell differentiation	10	0.34	8.94E-04
	Positive regulation of alpha-beta T cell activation	11	0.38	2.28E-03
25	3.00			
	Regulation of JNK cascade	17	0.59	3.23E-04
	Regulation of MAPKKK cascade	22	0.76	2.59E-02
29	2.44			
	Cytoplasmic membrane-bounded vesicle	81	2.79	2.87E-03
30	2.39			
	Mitotic cell cycle	56	1.93	1.16E-03
34	2.23			
	Ras GTPase	31	1.07	6.26E-03
36	2.15			
	Pattern recognition receptor signalling pathway	7	0.24	1.45E-03
	Activation of innate immune response	8	0.28	2.32E-03
38	2.12			
	ATP biosynthetic process	19	0.65	4.11E-02
39	2.09			
	Protein transport	118	4.07	1.23E-02
40	2.04			
	B cell mediated immunity	17	0.59	1.46E-02
42	2.00			
	T cell selection	9	0.31	6.23E-03
43	1.88			
	Regulation of ARF GTPase activity	9	0.31	8.75E-03
46	1.77			
	Protein tyrosine phosphatase activity	26	0.9	7.51E-03
51	1.66			
	Histone deacetylase activity	8	0.28	5.83E-03
	Chromatin remodeling complex	7	0.24	7.12E-01
52	1.66			
	Transcription regulation	265	9.13	6.18E-03
55	1.63			
	Regulation of protein kinase activity	37	1.27	4.58E-02

Table S5 continued:

Cluster number	Enrichment score / Annotation term	Genes (Count)	Genes (%)	p-value
57	1.61			
	Antigen processing & presentation of peptide or polysaccharide antigen via MHC class II	8	0.28	1.24E-02
	Antigen processing & presentation of exogenous peptide antigen via MHC class II	7	0.24	2.45E-02
58	1.61			
	Guanine-nucleotide dissociation stimulator CDC25	10	0.34	1.63E-02
	Ras guanine nucleotide exchange factor	10	0.34	3.16E-02
59	1.60			
	Class II histocompatibility antigen	5	0.17	3.33E-02
70	1.33			
	Ly-6 antigen / uPA receptor -like	9	0.31	2.99E-02
	CD59 antigen	9	0.31	9.03E-02
86	1.00			
	Ras GTPase-activating protein	5	0.17	1.14E-01
96	0.95			
	Regulation of IFN-beta production	5	0.17	1.50E-01
112	0.80			
	Positive regulation of humoral immune response	3	0.1	1.11E-01
116	0.77			
	PKC-like, phorbol ester/diacylglycerol binding	14	0.48	1.44E-01
117	0.77			
	Rel-related protein	3	0.1	6.01E-02
	NF-kB/Rel/dorsal	4	0.14	1.75E-01
118	0.77			
	TNFR-associated factor TRAF	4	0.14	4.58E-02
121	0.75			
	Positive regulation of PI3-kinase activity	3	0.1	2.27E-01
128	0.73			
	Negative regulation of T-helper cell differentiation	3	0.1	1.67E-01
	Negative regulation of alpha-beta T cell differentiation	3	0.1	2.27E-01
129	0.72			
	Positive regulation of ERK1 and ERK2 cascade	3	0.1	3.47E-01
130	0.72			
	Regulation of actin polymerization / depolymerization	12	0.41	1.25E-01

Highly enriched biological terms found among differentially regulated genes between Notch2IC-expressing MZ B cells and Notch2-deficient Fo B cells (q-value \leq 0.0149). Terms are clustered in groups of similar meaning. Clusters were obtained by using the Functional Annotation Clustering Tool of the DAVID Bioinformatics Resources.

Table S6: Some of the most significant functional annotation clusters comparing gene expression profiles of wild type MZ B and Fo B cells.

Cluster number	Enrichment score / Annotation term	Genes (Count)	Genes (%)	p-value
1	7.64			
	Phosphorylation	133	5.33	2.35E-06
2	Purine ribonucleotide binding	309	12.39	1.24E-09
	ATP binding	241	9.66	1.44E-06
	Adenyl nucleotide binding	249	9.98	8.96E-06
3	5.87			
	Lymphocyte activation	44	1.76	4.66E-05
6	5.67			
	Lysosome	46	1.84	4.78E-07
7	5.02			
	Cell death	101	4.05	4.65E-06
9	4.19			
	Protein kinase, C-terminal	15	0.60	2.48E-04
10	4.19			
	Positive regulation of adaptive immune response	15	0.601	6.80E-06
11	4.15			
	Transcription regulation	252	10.10	1.73E-05
12	4.09			
	Protein amino acid phosphorylation	125	5.01	3.61E-07
	Protein serine/threonine kinase activity	76	3.05	1.01E-03
16	3.60			
	GTP binding	71	2.85	8.78E-05
18	3.38			
	Endocytosis	42	1.68	2.38E-04
20	2.88			
	B cell mediated immunity	17	0.68	3.27E-03
21	2.80			
	Regulation of ARF GTPase activity	10	0.40	6.84E-04
23	2.69			
	Immune system development	55	2.205	1.89E-03
27	2.33			
	Histone core	13	0.52	1.46E-03
	Nucleosome organization	18	0.72	6.94E-03
28	2.32			
	Positive regulation of lymphocyte proliferation	15	0.60	1.50E-03
29	2.29			
	Positive regulation of T cell activation	17	0.68	5.50E-03
36	2.05			
	Immune response-activating signal transduction	13	0.52	1.02E-02
	Immune response-activating cell surface receptor signalling pathway	11	0.44	2.00E-02
	Antigen receptor-mediated signalling pathway	10	0.40	2.13E-02

Table S6 continued:

Cluster number	Enrichment score / Annotation term	Genes (Count)	Genes (%)	p-value
39	1.87			
	Positive regulation of transferase activity	27	1.08	1.52E-02
	Positive regulation of protein kinase activity	25	1.00	1.73E-02
43	1.80			
	Positive regulation of lymphocyte mediated immunity	11	0.44	1.11E-02
44	1.79			
	Positive regulation of phagocytosis	9	0.36	3.33E-03
48	1.74			
	Ribosome	35	1.40	7.11E-03
49	1.73			
	Protein tyrosine/serine/threonine phosphatase activity	11	0.44	1.96E-02
65	1.38			
	Positive regulation of alpha-beta T cell differentiation	7	0.28	2.85E-02
72	1.26			
	Positive regulation of T cell mediated cytotoxicity	5	0.20	2.06E-02
73	1.23			
	Small GTPase binding	14	0.56	3.56E-02
80	1.13			
	Chemokine receptor activity	6	0.24	1.45E-01
	Chemokine binding	6	0.24	1.67E-01
81	1.13			
	Regulation of IFN-beta production	5	0.20	9.69E-02
	Regulation of type I IFN production	5	0.20	1.19E-01
82	1.12			
	T cell proliferation	8	0.32	6.16E-02
90	1.03			
	Ly-6 antigen / uPA receptor -like	8	0.32	3.89E-02
101	0.92			
	Regulation of actin polymerization / depolymerization	12	0.48	5.21E-02
104	0.90			
	Phosphatidylinositol 3- and 4-kinase, conserved site	5	0.20	1.12E-01
108	0.87			
	TNF receptor-associated factor TRAF	4	0.16	3.03E-02
111	0.84			
	Plexin	8	0.32	6.61E-02
113	0.82			
	Positive regulation of NF- κ B transcription factor activity	7	0.28	9.51E-02

Highly enriched biological terms found among differentially regulated genes between wild type MZ B and Fo B cells (q-value ≤ 0.0149). Terms are clustered in groups of similar meaning. Clusters were obtained by using the Functional Annotation Clustering Tool of the DAVID Bioinformatics Resources.

Table S7: Some of the most significant functional annotation clusters comparing gene expression profiles of wild type and Notch2IC-expressing MZ B cells.

Cluster number	Enrichment score / Annotation term	Genes (Counts)	Genes (%)	p-value
1	5.04			
	Cell death	52	5.31	4.81E-06
2	3.91			
	Positive regulation of apoptosis	29	2.96	1.08E-04
3	3.82			
	Ribosomal protein	23	2.35	7.72E-05
6	3.16			
	B cell mediated immunity	11	1.12	1.25E-03
7	3.06			
	Endocytosis	22	2.24	7.85E-04
8	2.93			
	Positive regulation of transcription factor activity	8	0.82	1.90E-03
11	2.5			
	Positive regulation of lymphocyte activation	13	1.33	2.32E-03
13	2.46			
	Lysosome	20	2.04	1.24E-03
14	2.42			
	Translation initiation factor activity	11	1.12	1.13E-03
15	2.4			
	Cytoplasmic membrane-bounded vesicle	36	3.67	1.52E-03
17	2.18			
	Phosphorylation	55	5.61	4.00E-03
19	2			
	ATP binding	95	9.69	6.98E-03
21	1.83			
	Positive regulation of lymphocyte proliferation	8	0.82	1.08E-02
22	1.81			
	Positive regulation of JNK cascade	6	0.61	1.18E-03
	Positive regulation of IL-6 production	5	0.51	1.13E-02
	Regulation of MAPKKK cascade	10	1.02	5.25E-02
23	1.76			
	Apoptosis regulator Bcl-2	5	0.51	2.40E-02
25	1.72			
	Protein serine/threonine kinase activity	31	3.16	3.89E-02
26	1.69			
	Regulator of G protein signalling	6	0.61	1.72E-02
27	1.67			
	Ras guanine nucleotide exchange factor	6	0.61	1.96E-02
28	1.66			
	Hemopoiesis	20	2.04	6.11E-02
30	1.51			
	GTP binding	28	2.86	2.60E-02

Table S7 continued:

Cluster number	Enrichment score / Annotation term	Genes (Counts)	Genes (%)	p-value
31	1.48			
	Ras GTPase binding	7	0.71	7.57E-02
36	1.28			
	Regulation of calcium ion transport	6	0.61	3.39E-02
37	1.27			
	Protein tyrosine kinase activity	14	1.43	8.15E-02
38	1.26			
	Mitochondrial inner membrane	23	2.35	3.16E-02
39	1.18			
	RhoGAP	8	0.82	4.48E-02
40	1.17			
	Myelination	6	0.61	4.21E-02
	Regulation of action potential	6	0.61	1.55E-01
44	1.12			
	CARD domain	5	0.51	1.90E-02
46	1.11			
	Positive regulation of peptidase/caspase activity	6	0.61	4.21E-02
	Positive regulation of hydrolase activity	8	0.82	1.45E-01
47	1.1			
	TNFR binding	4	0.41	1.05E-01
59	0.84			
	Mitochondrial large ribosomal subunit	4	0.41	8.54E-02
61	0.83			
	PKC-like, phorbol ester/diacylglycerol binding	7	0.71	1.09E-01
62	0.83			
	Positive regulation of tyrosine phosphorylation of STAT	3	0.31	8.09E-02
	Positive regulation of JAK-STAT cascade	3	0.31	1.15E-01
63	0.81			
	Regulation of ion transmembrane transporter activity	3	0.31	1.52E-01
65	0.79			
	Thymic T cell selection	3	0.31	1.92E-01
69	0.78			
	Nucleosome/Chromatin assembly	6	0.61	2.92E-01
72	0.75			
	LPS-mediated signalling pathway	4	0.41	2.37E-02
	TLR signalling pathway	3	0.31	5.07E-02
	Activation of innate immune response	3	0.31	1.72E-01
74	0.73			
	Cellular calcium ion homeostasis	8	0.82	2.18E-01
75	0.72			
	Plexin	5	0.51	5.89E-02
	Semaphorin/CD100 antigen	4	0.41	1.97E-01
80	0.69			
	Ly-6 antigen / uPA receptor -like	4	0.41	1.46E-01

Table S7 continued:

Cluster number	Enrichment score / Annotation term	Genes (Counts)	Genes (%)	p-value
	CD59 antigen	4	0.41	2.25E-01
89	0.61			
	Intracellular organelle lumen	62	6.33	2.38E-01
90	0.61			
	Clathrin adaptor, alpha/beta/gamma-adaptin	3	0.31	7.44E-02
	Clathrin coat	4	0.41	2.28E-01
91	0.59			
	Positive regulation of T cell differentiation	4	0.41	2.46E-01
95	0.58			
	Regulation of immunoglobulin production	4	0.41	1.49E-01
	Regulation of isotype switching	3	0.31	1.72E-01
98	0.55			
	Regulation of protein transport	6	0.61	2.40E-01
	Regulation of protein localization	7	0.71	3.17E-01
100	0.54			
	Cation binding	204	20.82	2.56E-01
102	0.51			
	IgG/MHC, conserved site	6	0.61	2.99E-01
105	0.49			
	T cell activation during immune response	3	0.31	1.72E-01
107	0.48			
	Chemokine receptor activity	3	0.31	3.20E-01
111	0.45			
	Antigen processing & presentation	4	0.41	2.76E-01
119	0.41			
	Toll/Interleukin receptor (TIR)	3	0.31	3.51E-01

Highly enriched biological terms found among differentially regulated genes between wild type and Notch2IC-expressing MZ B cells (q-value \leq 0.0549). Terms are clustered in groups of similar meaning. Clusters were obtained by using the Functional Annotation Clustering Tool of the DAVID Bioinformatics Resources.

Table S8: Some of the most significant functional annotation clusters comparing gene expression profiles of wild type and Notch2-deficient Fo B cells.

Cluster number	Enrichment score / Annotation term	Genes (Count)	Genes (%)	p-value
1	2.32			
	Heat shock chaperonin-binding	3	0.90	9.44E-03
2	2.29			
	Intracellular organelle lumen	31	9.28	5.25E-03
3	1.79			
	Transcription regulation	40	11.98	5.65E-03
4	1.78			
	Cation binding	84	25.15	1.27E-02
6	1.65			
	Cellular ion homeostasis	11	3.29	1.25E-02

Table S8 continued:

Cluster number	Enrichment score / Annotation term	Genes (Count)	Genes (%)	p-value
7	1.58			
	PKC-like, phorbol ester/diacylglycerol binding	5	1.50	2.29E-02
8	1.57			
	Lymphocyte activation	9	2.69	1.36E-02
9	1.53			
	Regulation of phosphorylation	11	3.29	2.48E-02
10	1.51			
	Response to DNA damage stimulus	10	2.99	5.84E-02
12	1.35			
	Intracellular protein transport	9	2.69	9.35E-02
13	1.30			
	Proteolysis involved in cellular protein catabolic process	16	4.79	3.89E-02
16	1.17			
	Lysosome	7	2.10	3.49E-02
18	1.12			
	Chromatin modification	9	2.69	5.13E-02
	Chromosome organization	12	3.59	8.34E-02
20	1.03			
	Positive regulation of immune response	6	1.80	7.19E-02
21	0.97			
	Rho / Ras guanyl-nucleotide exchange factor activity	4	1.20	1.23E-01
22	0.97			
	GTPase activator activity	7	2.10	1.17E-01
27	0.91			
	Negative regulation of apoptosis	8	2.40	1.17E-01
29	0.88			
	Membrane fraction	13	3.89	1.32E-01
33	0.81			
	Ras-associating domain	3	0.90	1.26E-01
34	0.79			
	Lymphocyte proliferation	3	0.90	1.59E-01
35	0.78			
	Myofibril	4	1.20	1.85E-01
36	0.77			
	Mitochondrial envelope	10	2.99	1.77E-01
41	0.68			
	Positive regulation of lymphocyte mediated immunity	3	0.90	1.23E-01
42	0.67			
	Protein localization	17	5.09	2.10E-01
	Protein transport	15	4.49	2.15E-01
44	0.60			
	GTP-binding	9	2.69	1.51E-01
46	0.56			
	T cell activation	5	1.50	1.36E-01

Table S8 continued:

Cluster number	Enrichment score / Annotation term	Genes (Count)	Genes (%)	p-value
	T cell differentiation	4	1.20	1.37E-01
	B cell differentiation	3	0.90	1.59E-01
	Hemopoietic or lymphoid organ development	5	1.50	6.90E-01
47	0.55			
	Ribosome	6	1.80	1.92E-01
48	0.55			
	Microtubule motor activity	3	0.90	3.39E-01
49	0.54			
	ATP binding	29	8.68	3.13E-01
50	0.54			
	Sarcoplasmic reticulum	3	0.90	1.04E-01
	Calcium ion transport	3	0.90	6.15E-01
51	0.54			
	Negative regulation of protein kinase activity	3	0.90	2.15E-01
53	0.53			
	Cell growth	3	0.90	1.34E-01
61	0.45			
	Cation channel activity	7	2.10	2.64E-01
62	0.45			
	Positive regulation of protein modification process	4	1.20	1.37E-01
65	0.39			
	Regulation of locomotion	3	0.90	5.51E-01
66	0.38			
	Dual-specific/protein-tyrosine phosphatase, conserved region	3	0.90	4.04E-01
70	0.34			
	Mitosis	5	1.50	4.19E-01

Highly enriched biological terms found among differentially regulated genes between wild type and Notch2-deficient Fo B cells (q -value ≤ 0.0549). Terms are clustered in groups of similar meaning. Clusters were obtained by using the Functional Annotation Clustering Tool of the DAVID Bioinformatics Resources.

Table S9: Some of the most significant functional annotation clusters obtained with genes upregulated in wild type MZB in comparison to Fo B cells.

Cluster number	Enrichment score / Annotation term	Genes (Count)	Genes (%)	p-value
1	5.01			
	Lysosome	26	2.04	5.93E-06
2	4.58			
	Ribosome	25	1.96	1.84E-08
3	3.81			
	Positive regulation of adaptive immune response	11	0.86	1.30E-05
4	3.17			
	Histone core	11	0.86	7.73E-05
	Nucleosome assembly	13	1.02	1.28E-03

Table S9 continued:

Cluster number	Enrichment score / Annotation term	Genes (Count)	Genes (%)	p-value
5	2.87			
	Programmed cell death	46	3.61	4.72E-03
6	2.72			
	Plexin/semaphorin/integrin	10	0.78	1.88E-03
7	2.67			
	ATP binding	117	9.17	2.31E-03
	Nucleoside binding	123	9.64	4.27E-03
9	2.55			
	“Complement activation, classical pathway”	8	0.63	1.83E-03
	Humoral immune response	10	0.78	4.87E-03
10	2.51			
	Ly-6 antigen / uPA receptor -like	8	0.63	9.55E-04
12	2.38			
	Positive regulation of lymphocyte mediated immunity	9	0.71	1.64E-03
13	2.37			
	Adaptive immune response	13	1.02	5.31E-03
	B cell mediated immunity	11	0.86	5.43E-03
17	2.26			
	Mitotic cell cycle	30	2.35	1.36E-03
20	2.13			
	Positive regulation of phagocytosis	7	0.55	1.85E-03
	Positive regulation of endocytosis	7	0.55	1.43E-02
21	2.09			
	Regulation of phosphorylation	30	2.35	1.10E-02
22	1.99			
	Positive regulation of interferon-beta biosynthetic process	4	0.31	8.16E-03
	Regulation of type I interferon production	5	0.39	1.42E-02
26	1.78			
	Protein tyrosine kinase activity	18	1.41	3.02E-02
31	1.57			
	GTP binding	33	2.59	2.44E-02
32	1.56			
	Glycosylation	12	0.94	3.15E-02
33	1.51			
	Positive regulation of T cell mediated immunity	5	0.39	6.04E-03
	Positive regulation of T cell mediated cytotoxicity	4	0.31	1.77E-02
38	1.43			
	Positive regulation of lymphocyte proliferation	9	0.71	9.57E-03
	Positive regulation of lymphocyte activation	12	0.94	2.72E-02
41	1.41			
	Positive regulation of JNK cascade	5	0.39	1.80E-02
	Positive regulation of MAPKKK cascade	6	0.47	1.84E-01
45	1.32			
	Regulation of ARF GTPase activity	5	0.39	4.56E-02

Table S9 continued:

Cluster number	Enrichment score / Annotation term	Genes (Count)	Genes (%)	p-value
52	1.21			
	Immune response-activating signal transduction	7	0.55	7.31E-02
54	1.17			
	Positive regulation of alpha-beta T cell activation	6	0.47	2.16E-02
58	1.12			
	Positive regulation of chemokine biosynthetic process	3	0.24	3.79E-02
63	1.05			
	Positive regulation of inflammatory response	5	0.39	3.89E-02
	Positive regulation of type IIa hypersensitivity	3	0.24	5.44E-02
	Positive regulation of B cell mediated immunity	3	0.24	1.61E-01
74	0.89			
	Positive regulation of I-kappaB kinase/NF-kappaB cascade	6	0.47	5.62E-02
77	0.84			
	MHC class I protein complex	6	0.47	7.05E-02
80	0.83			
	Rho guanyl-nucleotide exchange factor activity	9	0.71	6.78E-02
	Ras guanyl-nucleotide exchange factor activity	9	0.71	1.39E-01
82	0.82			
	Negative regulation of gene-specific transcription	5	0.39	5.29E-02
121	0.51			
	Rho GTPase binding	5	0.39	6.37E-02

Highly enriched biological terms found among genes upregulated in wild type MZ B cells versus wild type Fo B cells (q-value \leq 0.0549). Terms are clustered in groups of similar meaning. Clusters were obtained by using the Functional Annotation Clustering Tool of the DAVID Bioinformatics Resources.

Table S10: Some of the most significant functional annotation clusters obtained with genes upregulated in Notch2IC-expressing MZ B cells in comparison to wild type MZ B cells.

Cluster number	Enrichment score / Annotation term	Genes (count)	Genes (%)	p-value
1	6.88			
	Ribosomal protein	22	4.53	2.35E-09
2	4.26			
	Translation initiation factor activity	10	2.06	2.53E-05
3	3.43			
	Mitochondrial inner membrane	21	4.32	2.56E-05
4	3.12			
	Intracellular organelle lumen	45	9.26	8.76E-04
5	2.59			
	Positive regulation of apoptosis	16	3.29	2.38E-03
6	2.49			
	Cholesterol binding	4	0.82	1.30E-03
	Steroid binding	5	1.03	1.95E-02

Table S10 continued:

Cluster number	Enrichment score / Annotation term	Genes (count)	Genes (%)	p-value
7	2.11			
	Purine ribonucleotide binding	64	13.17	4.19E-03
	ATP binding	52	10.70	8.50E-03
11	1.62			
	Mitochondrial large ribosomal subunit	4	0.82	1.39E-02
12	1.6			
	Positive regulation of caspase/peptidase activity	5	1.03	1.55E-02
13	1.46			
	Myelination	5	1.03	1.55E-02
	Regulation of action potential in neuron	5	1.03	3.02E-02
15	1.36			
	„RNA helicase, ATP-dependent, DEAD-box, conserved site“	5	1.03	6.91E-03
	ATP-dependent helicase activity	7	1.44	2.30E-02
16	1.36			
	Positive regulation of B cell proliferation/activation	4	0.82	1.36E-02
17	1.35			
	Ly-6 antigen / uPA receptor -like	4	0.82	2.58E-02
18	1.3			
	Positive regulation of transcription factor activity	4	0.82	6.27E-02
19	1.18			
	Phosphorylation	27	5.56	5.63E-02
21	1.11			
	GTP binding	15	3.09	7.02E-02
23	1.05			
	Neuron projection	6	1.23	6.99E-01
25	0.98			
	Cellular amino acid catabolic process	5	1.03	5.10E-02
	Carboxylic acid catabolic process	5	1.03	1.64E-01
26	0.9			
	Positive regulation of JNK cascade	3	0.62	6.77E-02
	Positive regulation of stress-activated protein kinase signaling pathway	3	0.62	6.77E-02
	Positive regulation of cytokine biosynthetic process	4	0.82	9.77E-02
	Positive regulation of MAPKKK cascade	3	0.62	3.53E-01
29	0.87			
	„Serine/threonine protein kinase, active site“	14	2.88	9.90E-02
32	0.8			
	Gut morphogenesis	3	0.62	1.17E-01
33	0.77			
	Regulator of G protein signalling	3	0.62	1.70E-01
34	0.75			
	Lysosome	8	1.65	1.38E-01

Table S10 continued:

Cluster number	Enrichment score / Annotation term	Genes (count)	Genes (%)	p-value
35	0.75			
	NADP metabolic process	3	0.62	5.32E-02
	Pyridine nucleotide metabolic process	3	0.62	1.74E-01
36	0.74			
	Purine nucleotide biosynthetic process	7	1.44	1.46E-01
	Nucleotide & nucleic acid biosynthetic process	8	1.65	1.86E-01
39	0.69			
	Glycolysis	3	0.62	3.03E-01
40	0.66			
	Negative regulation of protein kinase activity	4	0.82	1.51E-01
41	0.66			
	hydrogen ion transmembrane transporter activity	5	1.03	1.40E-01
	ATP synthesis coupled proton transport	3	0.62	2.43E-01
	purine ribonucleotide biosynthetic process	5	1.03	3.01E-01
44	0.62			
	Neural tube development	4	0.82	3.66E-01
45	0.61			
	Glutathione transferase activity	3	0.62	1.28E-01
49	0.49			
	Endoplasmic reticulum membrane	6	1.23	3.05E-01
61	0.42			
	Positive regulation of T cell activation	4	0.82	2.41E-01
64	0.39			
	„IgG/MHC, conserved site“	3	0.62	5.29E-01
65	0.39			
	Protein transport	14	2.88	3.62E-01
69	0.37			
	Glycerophospholipid biosynthetic process	3	0.62	3.23E-01
	Phosphoinositide metabolic process	3	0.62	4.83E-01
70	0.37			
	Links between Pyk2 and Map Kinases	3	0.62	2.90E-01
	Angiotensin II med. activation of JNK via Pyk2 dependent signaling	3	0.62	3.05E-01
71	0.37			
	Rho guanyl-nucleotide exchange factor activity	4	0.82	2.59E-01
77	0.31			
	Regulation of actin polymerization or depolymerization	3	0.62	3.92E-01
	Regulation of actin cytoskeleton organization	3	0.62	4.83E-01
79	0.26			
	Ras GTPase binding	3	0.62	4.38E-01
	Small GTPase binding	3	0.62	4.55E-01

Highly enriched biological terms found among genes upregulated in Notch2IC-expressing MZ B versus wild type MZ B cells (q-value ≤ 0.0549). Terms are clustered in groups of similar meaning. Clusters were obtained by using the Functional Annotation Clustering Tool of the DAVID Bioinformatics Resources.

Acknowledgements

In the end I would like to thank all the people that supported me during the last years and that have contributed to the success of my thesis.

First of all I would like to thank my advisor *PD Ursula Zimmer-Strobl*, for letting me perform my PhD thesis in her laboratory on this very interesting project. For her constant support and advice during my work. For granting me freedom and independence in the experimental design and in decision-making regarding my project, which helped me a lot to learn to assume greater responsibility and to really feel comfortable about it. For giving me the opportunity to learn so many different laboratory techniques and for always encouraging me to do so.

PD Josef Mautner, for supervising my PhD thesis as well as for his feedback and scientific support as part of my thesis committee

Prof. Elisabeth Weiß, for evaluating this work as second examiner.

Prof. Wolfgang Hammerschmidt for giving me the opportunity to perform my research in the pleasant environment and atmosphere of his institute.

Prof. Marc Schmidt-Supprian and *Prof. Vigo Heissmeyer* for their willingness to be part of my thesis committee, to discuss my data and for always providing good new scientific input and ideas.

All members of our research group, especially *Franziska Hampel*, for giving me rapid and excellent introductions into all the techniques used in our lab and for giving me the opportunity to continue working on her mouse strain and to finish her paper. *Gabrielle Marschall-Schröter* for technical assistance and encouraging words in stressful times. *Lothar Strobl* for his scientific advice and help with the analysis of ELISA data and any kind of bioinformatics. *Kristina Stojanovic* for helpful advice and discussions even after her time in the lab and for introducing me into her “secret” of a successful and happy living. *Anne Draeseke* especially for helping me with night-time mice dissections and for really funny “series” conversations and *Samantha Feicht*, *Petra Fiedler*, *Sabine Schmidl*, *Samantha Frankenberger*, *Anna Pollithy* and *Stefanie Zapf* for great, constant support, helpful discussions and making my lab life so much more enjoyable!

Dagmar Pich for always answering all of my questions regarding cell sorting and for helping me at any time when problems occurred (not only) regarding the sorter.

Christoph Vahl for performing sorting of my cells in his lab, when I was not yet able to do it on my own and for the data analysis of my first proliferation assays.

Volker Groß for performing intravenous injections to my mice, even if it sometimes was at short notice.

Acknowledgements

The whole *Mautner lab* for treating me almost as if I was also part of their group and for letting me participate in their “cake afternoons”.

The whole second floor of the “Hämatologikum” and in addition also the *Jeremias and Kempkes lab* for the pleasant atmosphere making my life at the institute really enjoyable.

Christoph Hinzen, in particular for motivating conversations during FACS measurements in the middle of the night.

The mouse facility, especially *Jasmin Teutsch*, *Martina Möschter* and *Silke Spallek*, for taking care of my mice, as well as *Michael Hageman* and *Albert Geissbauer* for introducing me to and helping me with many mouse-related techniques.

Peter Weber for introducing me into the art of microarrays, for helping and supporting me with all experiments and data analyses regarding this part of my work. But beyond this, I would like to thank him for his constant privat and job-related support during the last seven years. Most importantly for encouraging and helping me in difficult times and for his patience and willingness to always answering any of my questions at any given time.

And last but not least of course, my *family* and *friends*, especially my *parents* for constant support, patience and understanding.